

UNIVERSITY OF MINES AND TECHNOLOGY, TARKWA



FACULTY OF ENGINEERING

DEPARTMENT OF ELECTRICAL AND ELECTRONIC ENGINEERING

A THESIS REPORT ENTITLED

FAILURE PREDICTION OF INDUCTION MOTORS: A CASE STUDY USING
CSLGH900/6-214, 5.8 MW, 11 KV/3PH/50HZ SAG MILL MOTOR AT GOLDFIELDS
DAMANG MINE

BY

HARRY WARDEN

SUBMITTED IN PARTIAL FULFILMENT OF THE REQUIREMENT FOR THE
AWARD OF THE DEGREE OF MASTER OF PHILOSOPHY IN ELECTRICAL AND
ELECTRONIC ENGINEERING

THESIS SUPERVISOR

.....

ASSOC PROF C. K. AMUZUVI

TARKWA, GHANA

JULY 2020

DECLARATION

I declare that this thesis is my own work. It is being submitted for examination and approval for the Degree of Master of Philosophy in Electrical and Electronic Engineering in the University of Mines and Technology, Tarkwa. It has not been submitted for any degree, examination or approval in any other University.

.....

(Signature of Candidate)

..... day of August, 2020.



ABSTRACT

This research proposes a generalised feed-forward artificial neural network model that fulfils the failure prediction of CSLGH900/6-214, 5.8 MW, 11 kV/3 ph/50 Hz slip ring SAG Mill induction motor at Goldfields Ghana Limited, Damang Mine. It provides a general understanding of three phase induction motors, faults associated with induction motors and also emphasizes the use of intelligent system, particularly artificial neural network, in modern failure prediction technology of induction motors. Site analysis and motor data (Current, Power and winding temperatures) collection were conducted at Goldfields, Damang Mine. Simulation results are presented using MATLAB software (2017a) package to develop the fault prediction model. The proposed feed-forward neural network used the Levenberg-Marquardt and Bayesian Regularisation in training. The research also employed the use of Log sigmoid and Tan sigmoid as the activation functions of the hidden layer, with hidden layer size being kept at 10 neurons. The simulation and calculation were done with real-time on-load measurement from the SAG Mill motor. Analysis of the model's output performance were done using correlation of coefficient of network performance, R and Mean Squared Error, MSE. When the proposed model is implemented, common faults could be prevented from escalating into major breakdowns, thereby reducing the downtime and hence increasing the availability of the motor for general operation. In the absence of major breakdowns, safety of employees and equipment could be assured. It is therefore worthwhile to invest in deploying this model to augment the conditional monitoring needs like temperature, current and vibration of the SAG Mill motor and other such equipment like the Ball Mill motor in the plant.

DEDICATION

Dedicated to my lovely wife, Pat.



ACKNOWLEDGEMENTS

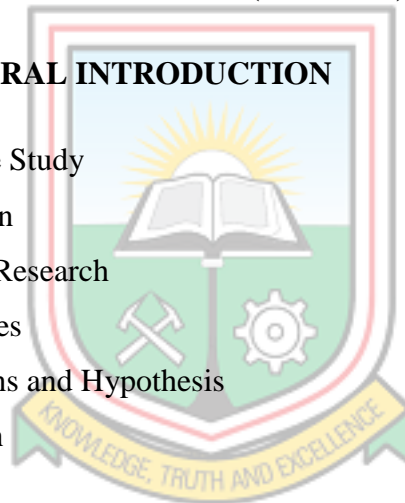
My utmost gratitude goes to the Almighty God for His guidance and protection for making this project a reality. I also extend my profound gratitude to the lecturers of the Electrical and Electronic Engineering Department of the University of Mines and Technology, most especially Assoc. Prof. C. K. Amuzuvi for his guidance, motivation and supervision.

I am also grateful to my many friends, especially Kobina Abakah-Paintsil, for their prayers, support, guidance and inspiration throughout this project work. God richly bless you and maximise your potential everywhere you find yourself. I feel a deep sense of gratitude to my wife, Mrs Patricia Warden, without whose help this work may not have been realised and also to my God mother, Mrs Patience A. Buah, for her love and encouragement. God richly bless you and continue to bless you in all your endeavours.



TABLE OF CONTENTS

Content	Page
DECLARATION	i
ABSTRACT	ii
DEDICATION	iii
ACKNOWLEDGEMENTS	iv
TABLE OF CONTENTS	v
LIST OF FIGURES	ix
LIST OF TABLES	xii
LIST OF ABBREVIATIONS	xiii
LIST OF SYMBOLS	xiv
INTERNATIONAL SYSTEM OF UNITS (SI UNITS)	xv
CHAPTER 1 GENERAL INTRODUCTION	1
1.1 Background to the Study	1
1.2 Problem Definition	1
1.3 Objectives of the Research	3
1.4 Expected Outcomes	3
1.5 Research Questions and Hypothesis	4
1.6 Scope of Research	4
1.7 Methods Used	4
1.8 Significance of Research	4
1.9 Facilities Used	4
1.10 Limitation of Research	5
1.11 Organisation of the Research	5
CHAPTER 2 LITERATURE REVIEW	6
2.1 Introduction	6
2.2 Induction Motor	6
2.2.1 Construction of Induction Motors	7
2.2.2 Principle of Operation	10
2.2.3 Equivalent Circuit	13

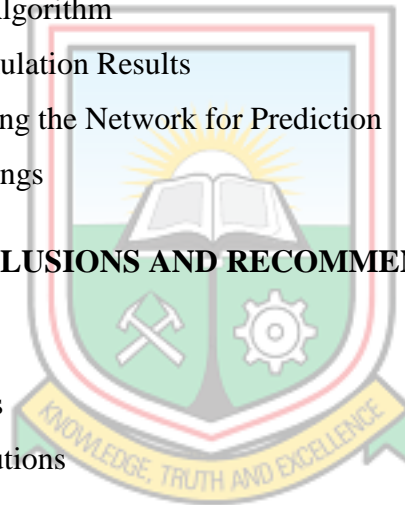


2.2.4	Power Flow Diagram of a Motor	14
2.2.5	Torque Speed Characteristics	14
2.2.6	Starting of Three-Phase Induction Motor	15
2.2.7	Speed Control of Induction Motors	18
2.2.8	Pole Changing Schemes	21
2.2.9	Stator Frequency Control	23
2.3	Induction Motor Failure	25
2.3.1	Broken Rotor Bar Fault	27
2.3.2	Rotor Mass Unbalance	28
2.3.3	Bearing Fault	31
2.3.4	Stator Fault	32
2.3.5	Stator Winding Fault	33
2.3.6	Single Phasing Fault	35
2.3.7	Crawling	36
2.3.8	Over Voltage, Under Voltage, Overload and Blocked Rotor	37
2.4	Condition Monitoring and Its Necessity	38
2.5	Failure Prediction Methods or Techniques	39
2.5.1	Vibration Spectrum Analysis	40
2.5.2	Park Vector Approach and Complex	40
2.5.3	Motor Current Signature Analysis	41
2.5.4	Intelligent Techniques	41
2.6	Artificial Neural Network	42
2.6.1	Development of an ANN Model	43
2.6.2	Architecture of Neural Networks	44
2.6.3	Uses and Applications of Neural Networks	44
2.7	Related Works	47
2.8	Summary of Related Works	50
CHAPTER 3 SAG MILL MOTOR		51
3.1	Introduction	51
3.1.1	The SAG Mill Motor Rating	52
3.2	Main Components of SAG Mill Motor	54
3.2.1	Cooling Fans	54
3.2.2	Carbon Brush and Sliprings	55

3.2.3	Windings	61
3.2.4	Bearings	62
3.3	The Liquid Starter	64
3.3.1	Electrodes	64
3.3.2	Control	65
3.3.3	Electrolyte	66
3.3.4	Enclosures	68
3.3.5	Maintenance	69
3.4	Oil Supply Unit for Motor Bearings	70
3.4.1	Assembly Design of the Oil Supplying System	70
3.4.2	Maintenance and Repairs	72
3.4.3	Operating Faults	73
3.5	Start – up, Operation, Shutdown	73
3.5.1	Start – Up Frequency	73
3.6	Maintenance of SAG Mill Motor	74
3.7	Storage	76
3.7.1	Plain Bearings	76
3.7.2	Rolling Contact Bearings	78
3.7.3	Bare Surfaces	79
3.7.4	Coolers, piping	79
3.7.5	Space Heaters	79
3.7.6	Filters	79
3.7.7	Brushes	79
3.7.8	Openings	79
3.7.9	Inspection, Records	79
3.8	Summary	79
 CHAPTER 4 METHODS USED		 80
4.1	Introduction	80
4.2	Designing and Programming of ANN Models	80
4.3	Data Collection	82
4.4	Data Pre-Processing	84
4.5	Building the Network	86



4.5.1	Feed-Forward Neural Network with Backpropagation Algorithm	86
4.6	Training the Network	88
4.7	Validating and Testing the Network	89
4.8	Programming the Neural Network Model	91
4.9	Implementation of Proposed Methodology	95
CHAPTER 5 RESULTS AND DISCUSSIONS		96
5.1	Introduction	96
5.2	Simulation Results Using Feed-Forward Network	96
5.2.1	Simulation Results of FFNN Using Levenberg-Marquardt Training Algorithm	96
5.2.2	Simulation Results of FFNN Using Bayesian Regularization Training Algorithm	98
5.3	Discussion of Simulation Results	100
5.4	Discussion on Using the Network for Prediction	102
5.5	Summary of Findings	104
CHAPTER 6 CONCLUSIONS AND RECOMMENDATIONS		106
6.1	Conclusions	106
6.2	Recommendations	106
6.3	Research Contributions	106
REFERENCES		107
APPENDICES		111
APPENDIX A	RAW DATA OF SAG MILL MOTOR	111
APPENDIX B	RAW DATA OF MOTOR CHANGE – OUT	133
APPENDIX C	DRAWINGS	141
APPENDIX D	TEST REPORTS	148
APPENDIX E	MATLAB SCRIPTS	154
APPENDIX F	MATLAB RESULTS	160



LIST OF FIGURES

Fig.	Page	Title
1.1		Graph Showing Number of Annual Motor Change - Out 2
1.2		Probability of Occurrence of Faults 2
1.3		Graph Showing Percent Change in Gold Price from 2012 to 2016 3
2.1		Construction and Components of Induction Motor 7
2.2		Single Phase Stator with Windings 8
2.3		Induction Motor Magnetic Circuit Showing Stator and Rotor Slots 8
2.4		Squirrel Cage Rotor Construction 9
2.5		Wound Rotor of a Large Induction Motor 10
2.6		Diagram of the Rotor Circuit 13
2.7		Equivalent Circuit of a Stator 13
2.8		Power Flow Diagram 14
2.9		Torque-Speed Characteristics of an Induction Motor 15
2.10		Rotor Resistance Starting 16
2.11		Direct-on-Line Starting 17
2.12		Star-Delta Starting 17
2.13		Auto-transformer Starting 18
2.14		Speed-Torque Curves: Voltage Variation 19
2.15		Speed-Torque Curves: Rotor Resistance Variation 21
2.16		Pole Arrangement of an Induction Motor 22
2.17		Pole Changing: Various Connections 22
2.18		Torque-Speed Curves with E/F Held Constant 24
2.19		Block Diagram Representation of Internal Faults 25
2.20		Block Diagram Representation of External Faults 25
2.21		Photograph of Rotor and Parts of a Broken Rotor Bars 27
2.22		Rotor with Mass Unbalance Fault 29
2.23		Mass Unbalanced Rotor Fault Types 30
2.24		Ball Bearing 31
2.25		Star-Connected Stator Showing Different Types of Stator Winding Fault 33

2.26	Photograph of Damaged Stator Winding	34
2.27	Torque-Slip Curve Showing Resultant of Fundamental and 7 th Harmonic Torque	37
3.1	Non – Drive Side of the SAG Mill Motor	51
3.2	Drive Side of the SAG Mill Motor	53
3.3	Side View of the SAG Mill Motor	53
3.4	Measurement of the Carbon Brush	57
3.5	Carbon Brush Wear Measurement	57
3.6	Carbon Brush and Holders	59
3.7	Spiral Grooving of Carbon Brush	60
3.8	Positioning of Carbon Brushes on Sliprings	61
3.9	Bearing Lubrication Plate	62
3.10	Electrolyte Resistance (Electrodes)	65
3.11	Electrode Control System	67
3.12	EPM with Heat Exchanger	68
3.13	EPM MV Enclosure	69
3.14	EPM LV Enclosure	70
4.1	General Flow of ANN – Based Fault Classification of Induction Motors	81
4.2	Basic Block Diagram for designing Artificial Neural Network Model	82
4.3	Trends of SAG Mill Motor Current, Power and Temperatures	83
4.4	Graph Showing Trends of SAG Mill Motor Current and Power	83
4.5	Graph Showing Trends of SAG Mill Motor Winding Temperatures	84
4.6	Graph Showing Trends of SAG Mill Motor Current and Power after Normalisation	85
4.7	Graph Showing Trends of SAG Mill Motor Winding Temperatures after Normalisation	85
4.8	Graph Showing Trends of Faulty SAG Mill Motor Current and Power after Normalisation	86
4.9	Architecture of Feed-Forward Network	87
4.10	FFNN Training Window	93
4.11	Flowchart for Developing Feed – Forward Networks Using	94

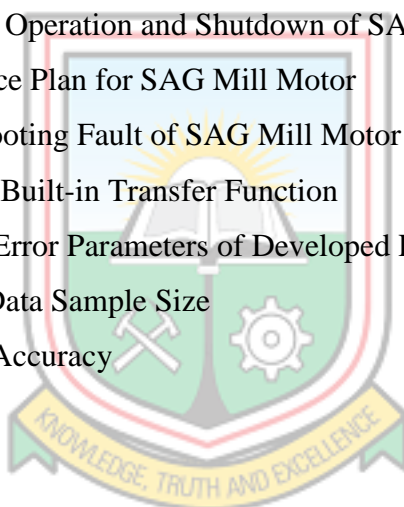
MATLAB

4.12	Overall Block Diagram of Implementation of Proposed Methodology	95
5.1	Correlation Coefficient for Network Performance, R (LM)	96
5.2	Mean Squared Error (MSE) against Epochs (LM)	97
5.3	Error Histogram (LM)	97
5.4	Training State Plot for Model Validation (LM)	98
5.5	Correlation Coefficient for Network Performance, R (BR)	98
5.6	Mean Squared Error (MSE) against Epochs (BR)	99
5.7	Error Histogram (BR)	99
5.8	Training State Plot for Model Validation (BR)	100
5.9	Plot of Confusion Matrix Using Levenberg-Marquardt Algorithm	103
5.10	Plot of Confusion Matrix Using Bayesian Regularization Algorithm	104



LIST OF TABLES

Table	Page	Title
1.1		Gold Price from 2012 to 2016
3.1		SAG Mill Motor Rating
3.2		SAG Mill External Air Circuit Motor Rating
3.3		SAG Mill Internal Air Circuit Motor Rating
3.4		SAG Mill Slipring Compartment Motor Rating
3.5		Maintenance Plan for Bearings
3.6		Liquid Starter Motor Rating
3.7		Liquid Starter Agitator Motor Rating
3.8		Troubleshooting Operating Faults of Oil Supply Unit
3.9		Start – Up, Operation and Shutdown of SAG Mill Motor
3.10		Maintenance Plan for SAG Mill Motor
3.11		Troubleshooting Fault of SAG Mill Motor
4.1		MATLAB Built-in Transfer Function
5.1		Statistical Error Parameters of Developed FFNN Models for Different Data Sample Size
5.2		Detection Accuracy

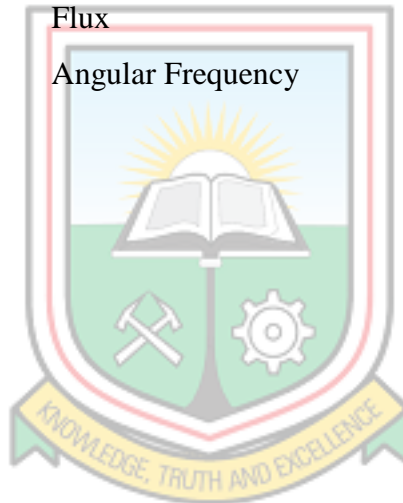


LIST OF ABBREVIATIONS

Abbreviation	Meaning
AC	Alternating Current
ANN	Artificial Neural Networks
BR	Bayesian Regularisation
BRB	Broken Rotor Bar
CIL	Carbon in Leach
DC	Direct Current
DTC	Direct Torque Control
ECG	Electrocardiography
EEG	Electroencephalography
EMF	Electromotive Force
FEMM	Finite Element Modelling
FFNN	Feed-Forward Neural Network
FFT	Fast Fourier Transform
FPGA	Field Programmable Gate Array
GUI	Graphical User Interface
LM	Levenberg-Marquardt Algorithm
MCSA	Motor Current Signature Analysis
MTPA	Metric Tonnes Per Annum
MLP	Multi-Layer Perceptron
MSE	Mean Squared Error
P_{SCL}	Stator Copper Loss
P_{RCL}	Rotor Copper Loss
R	Regression
RAM	Random Access Memory
RPM	Revolution Per Minute
RPI	Rotor Power Input
RUL	Remaining Useful Life
SAG	Semi Autogenous
SCADA	Supervisory Control and Data Analysis

LIST OF SYMBOLS

Symbols	Meaning
B	Flux Density
f	Frequency
f_r	Rotor Frequency
f_s	Slip Frequency
N	Speed
N_r	Rotor Speed
N_s	Synchronous Speed
s	Slip
∞	Infinite
Φ	Flux
ω	Angular Frequency



INTERNATIONAL SYSTEM OF UNITS (SI UNITS)

Quantity	Unit	Symbol
Current	Ampere	A
Mass	kilogram	kg
Power	Watt	W
Temperature	Degree Celsius	°C
Time	second	s
	Minute (60 s)	min
	Hour (3600 s)	h
	Day (86400 s)	d
Voltage	Volt	V



CHAPTER 1

GENERAL INTRODUCTION

1.1 Background to the Study

Damang Gold Mine, a subsidiary of Goldfields International is a world class mining operation consisting of a 25 MTPA open pit mining operation and a 5.2 MTPA Carbon in Leach (CIL) metallurgical plant.

Located in the south western part of Ghana, 300 km by road from the capital of Ghana Accra, the mine exploits oxide and fresh hydrothermal mineralization in addition to Witwatersrand – style transitional paleo placer gold. The plant is designed to treat 5.2 MTPA of gold ore from a blend of approximately 20% oxide ore and 80% fresh ore sourced from various open pit mining operations. Process feed for the 12-month period of 2016 comprised 4.3 Mt at a yield of 1.17 g/t for a 148 koz of gold.

The plant has 2 × 5.8 MW ball mill and sag mill, a 1 × 600 kW primary gyratory crusher, 1 × 375 kW pebble crusher, 8 CIL tanks and a secondary crushing plant with a maximum electric power draw of 17.5 MW at peak times. The mine uses many induction motors at the crushing circuit, milling circuit, CIL circuit, elution circuit, tailings circuit, village, accommodation and dewatering section.

The plant is often faced with issues associated with burnt induction motors. Preliminary cause of the burnt motor is attributed to high temperatures but the root cause is not easily determined.

1.2 Problem Definition

With the mines current maintenance cost of electrical motors on the high, the mine must come up with strategies to bring the overall cost of engineering maintenance down. Fig. 1.1 is a graph showing annual motor change-out from 2012 to 2016. With the current price of gold on the downside, the maintenance department is under intense pressure to efficiently maintain the plant machinery to continue to stay in business. Table 1.1 and Fig. 1.3 shows prices and percentage change in gold price from 2012 to 2016 respectively.

This research work seeks to identify and assess in detail, all the various root causes of induction motor failures in the mine and suggest a means of accurately predicting future failures.

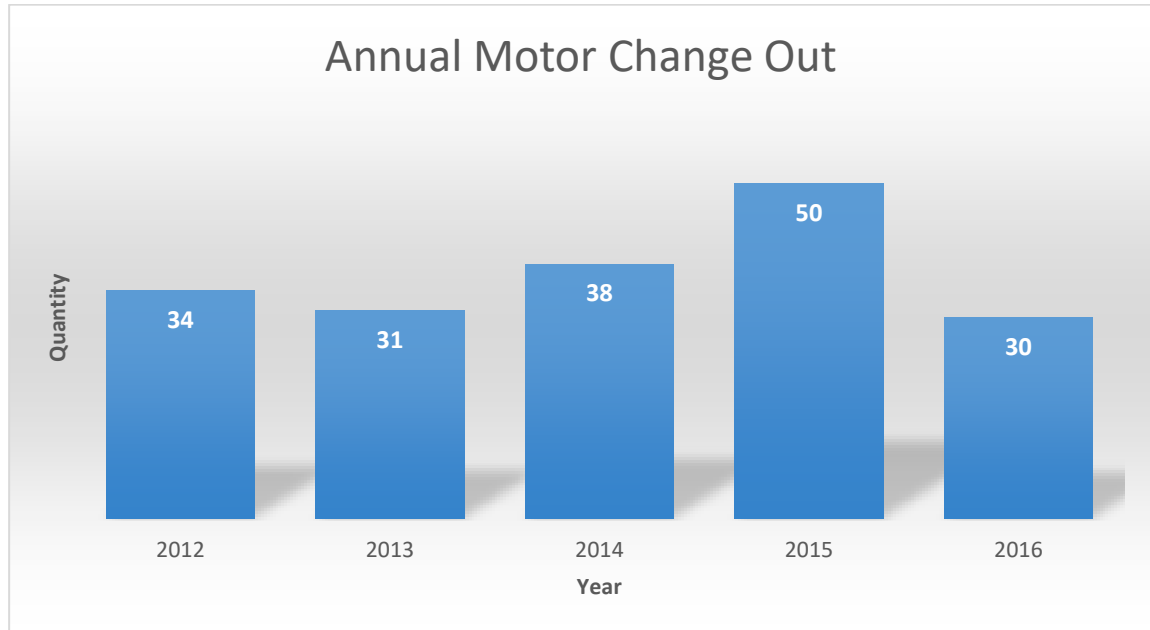


Fig. 1.1 Graph Showing Number of Annual Motor Change - Out

Research has shown that failures associated with induction motors are often caused by rotor, stator, and bearing failures. (Bhowmik *et al*, 2013). Fig. 1.2 (Bhowmik *et al*, 2013) shows the probability of occurrence of faults in an operating induction motor.

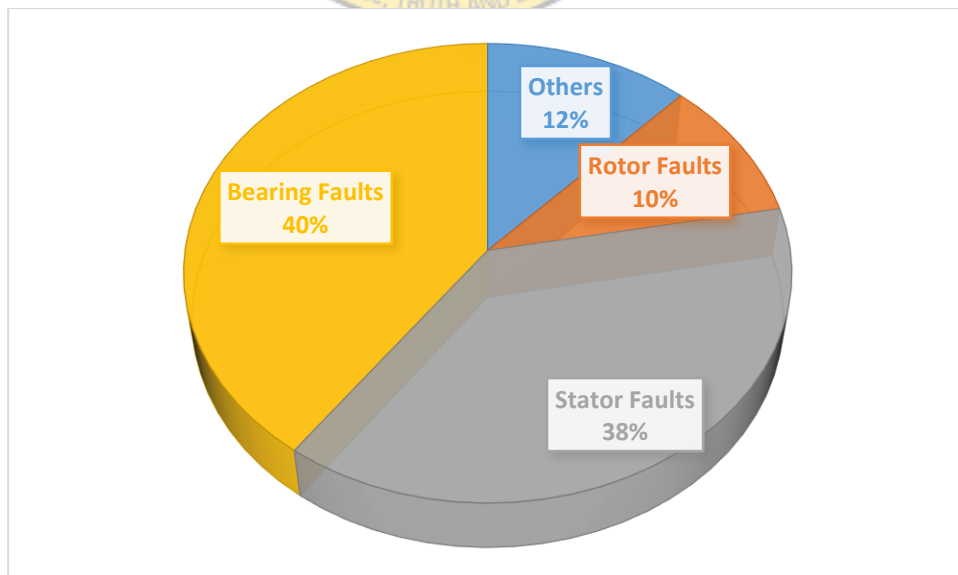


Fig. 1.2 Probability of Occurrence of Faults

Table 1.1 Gold Price from 2012 to 2016 Year

Year	Closing Price	Year Open	Year High	Year Low	Year Close	% Change
2012	\$1,668.86	\$1,590.00	\$1,790.00	\$1,537.50	\$1,664.00	5.68%
2013	\$1,409.51	\$1,681.50	\$1,692.50	\$1,192.75	\$1,201.50	-27.79%
2014	\$1,266.06	\$1,219.75	\$1,379.00	\$1,144.50	\$1,199.25	-0.19%
2015	\$1,158.86	\$1,184.25	\$1,298.00	\$1,049.60	\$1,060.20	-11.59%
2016	\$1,251.92	\$1,075.20	\$1,372.60	\$1,073.60	\$1,151.70	8.63%

(Source: Anon, 2019a)

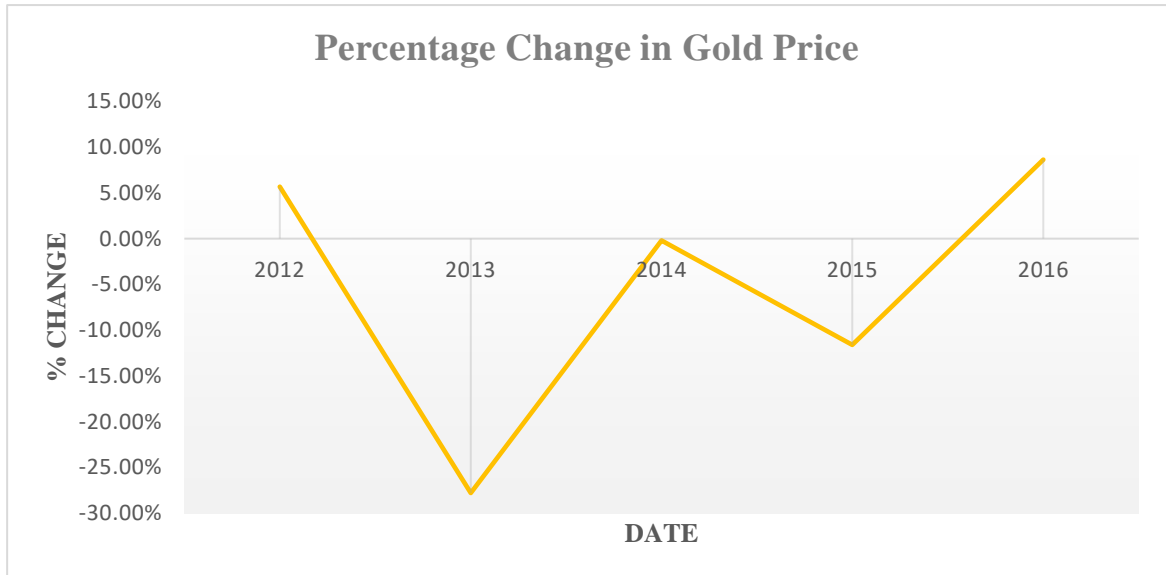


Fig. 1.3 Graph Showing Percent Change in Gold Price from 2012 to 2016

1.3 Objectives of Research

The objectives of this research work are to:

- i. Identify the root causes of induction motor failures at Damang Gold Mine;
- ii. Develop an ANN Model for failure prediction of SAG Mill motor; and
- iii. Suggest methods for implementing ANN aided failure prediction of SAG Mill motors at the Damang Gold Mine.

1.4 Expected Outcomes

At the end of this research, it is expected that:

- i. There shall be integration of all induction motor data into a common programme at the Damang Gold Mine; and

- ii. There shall be cost savings and/or prevention of catastrophic failures of induction motors upon the implementation of findings of this research.

1.5 Research Questions and Hypothesis

The objectives and the expected outcomes of the research give rise to the following research questions:

- i. Is there an efficient and applicable method of using ANN in predicting failure of electrical induction motors at Goldfields, Damang mine?
- ii. What does Goldfields, Damang mine stand to gain from implementing this solution?

The research hypothesis is stated thus:

At the end of this research, there will be an efficient way of using ANN in predicting failure of electrical induction motors at Goldfields, Damang site.

1.6 Scope of Research

This research work was conducted using data samples collected from three phase 5.8 MW, 11 kV slip ring SAG Mill induction motor at Goldfields Ghana Limited, Damang Mine. The data samples collected were current, power and winding temperatures.

1.7 Methods Used

The methods used in the research include the following:

- i. Data collection and analysis of induction motors at the plant;
- ii. Identification of all induction motors and condition monitoring devices; and
- iii. Computer modelling and simulations.

1.8 Significance of Research

Damang Gold Mine upon implementation of this proposed model not only help in increasing SAG Mill motor availability, but also help in cost savings and safety of workers.

1.9 Facilities Used

Facilities used for this research include:

- i. Internet, library and computer facilities at UMaT;
- ii. Induction motors installed at Damang mine;
- iii. Supervisory Control And Data Acquisition (SCADA) system at the processing plant; and
- iv. Condition monitoring and instrumentation devices at Damang mine.

1.10 Limitation of Research

This research work was limited to the use of power, current and winding temperatures of healthy SAG Mill motor to train ANN – Model to assist in predicting faulty conditions of the motor.

1.11 Organisation of the Thesis

This project consists of five chapters. The first chapter defines the problem of failure of electrical induction motors as well as implication of high maintenance cost on Goldfields, Damang mine. The objectives, expected outcome, methods used and facilities used are also provided in this chapter of the project.

The second chapter is based working principles, types and faults associated with induction motors. Intelligent systems for motor failure predictions emphasizing Artificial Neural Networks are discussed. Related works on the use of Artificial Neural Networks for failure predictions of electrical induction motors are also reviewed and summarised.

The third chapter takes a detailed look at the SAG Mill motor, manufacturer, major components and its auxiliary equipment's.

The fourth chapter proposes a design methodology for using Feed-Forward Neural Networks for failure prediction of 5.8 MW 11 kV SAG Mill motor using current, winding temperatures of the motor as input parameters and power as the output parameter.

The fifth chapter provides results and discussion of design and simulation of the proposed Feed-Forward Network using Levenberg-Marquardt and Bayesian Regularisation as the training algorithm. Results shows positive prospects of the network identifying failures. The conclusion and recommendations for further work are detailed in the sixth chapter. References and appendices showing detailed MATLAB Scripts used for simulation of the proposed network are also provided.

CHAPTER 2

LITERATURE REVIEW

2.1 Introduction

Induction motors are the mainstay for every industry. They are widely used in transportation, mining, petrochemical, manufacturing and in almost every other field dealing with electrical power. These motors are simple, efficient, highly robust and rugged thus offering a very high degree of reliability. However, like any other machine, they are susceptible to faults, which if left unmonitored, might lead to catastrophic failure of the machine in the long run especially due to heavy duty cycles, poor working environment alongside with installation and manufacturing factors.

In a bid to detect fault and avoid complete breakdown of induction motors with its concomitant production losses, on-line condition monitoring of the induction motors has been the order of the day for effective operation of these machines. With increasing demands for reliability and efficiency, fault prediction in induction motors has become necessary particularly in industries that make use of these rotary equipment of which the Damang Gold Mine is no exception (Bhowmik *et al.*, 2013). Various fault conditions of induction motors as well as methods of their detection and prediction are presented in this chapter.

2.2 Induction Motor

An induction motor is a type of asynchronous Alternating Current (AC) motor where power is supplied to the rotating device (rotor) by means of electromagnetic induction. There are two types, namely wound or slip-ring induction motor and squirrel-cage induction motor. The wound or wrapped rotor type was invented by Nikola Tesla in 1882 in France though the initial patent was issued in 1888. About a year later, the squirrel-cage induction motor type was invented by Mikhail Dolivo-Dobrovolsky in Europe. The polyphase induction motor is the most widely used motor in industrial and commercial applications. It is sometimes called a rotating transformer because the stationary part (stator) is essentially the primary side of the transformer and the rotating part (rotor) is the secondary side (Anon, 2018a).

Squirrel-cage induction motors are now the preferred choice for industrial motors due to their low cost, high reliability, absence of slip-rings and brushes which eliminate risk of

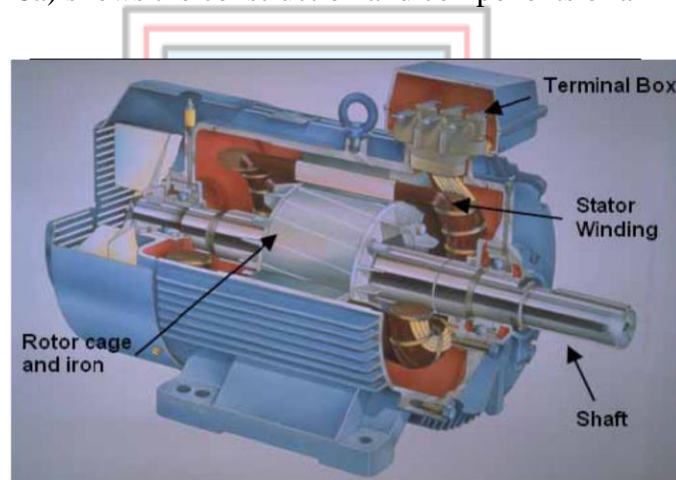
sparking thereby making them explosion proof and high efficiency over a wide range of power outputs. They also have the ability to control their speed. From a constant frequency source, they operate as constant speed drives. For continuous speed control over a wide speed range, a solid-state variable-frequency converter provides an indirect source of supply (Anon, 2018a).

2.2.1 Construction of Induction Motors

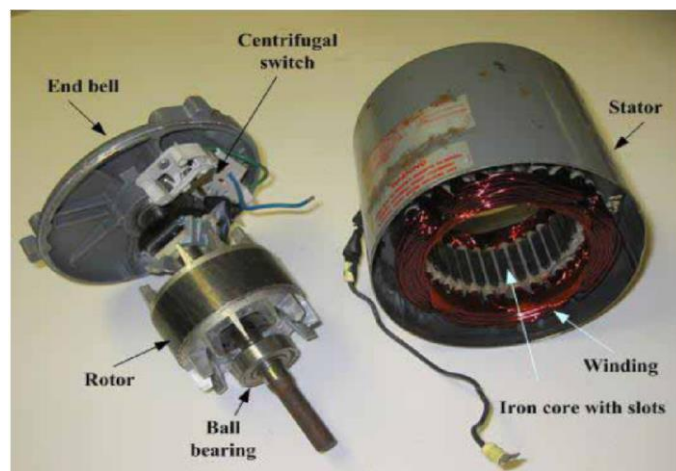
A typical induction motor consists of two parts, namely:

- i. An outside stationary stator having coils supplied with AC current to produce a rotating magnetic field; and
- ii. An inside revolving rotor attached to the output shaft that is given a torque by the rotating field.

Fig. 2.1 (Anon, 2018a) shows the construction and components of an induction motor.



(a)



(b)

Fig. 2.1 (a) Construction and (b) Components of Induction Motor

The rotor is separated from the stator by a small air-gap which ranges from 0.4 mm to 4 mm depending on the power rating of the motor.

Stator construction

The stator of an induction motor consists of a steel frame which encloses or houses a hollow, cylindrical iron core made up of stacked laminations. A number of slots are punched uniformly round the gap surface of the core. Coils are placed in the slots to form a single or three phase winding. Fig. 2.2 and Fig. 2.3 (Anon, 2018a) show the construction of the stator.



Fig. 2.2 Single Phase Stator with Windings

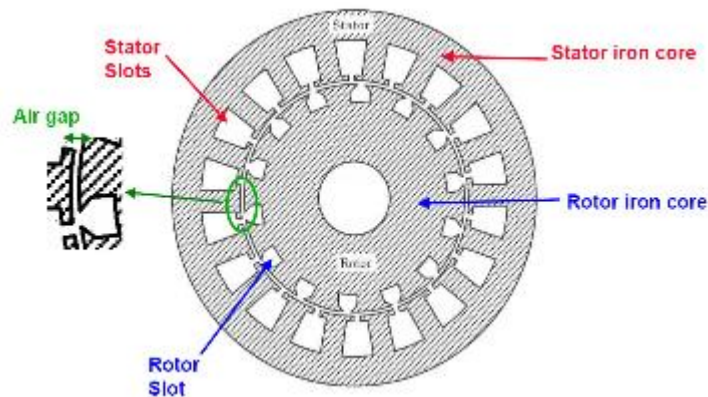


Fig. 2.3 Induction Motor Magnetic Circuit Showing Stator and Rotor Slots

Rotor construction

The rotor is also composed of punched laminations which are carefully stacked to create a series of rotor slots or spaces for the rotor winding. Two types of rotor windings are used. These are:

- i. Squirrel cage rotor; and
- ii. Wound rotor.

The type of winding gives rise to the two main classes of motors: squirrel-cage induction motors and wound-rotor or slip-ring induction motors.

Squirrel-cage rotor: In this type of rotor, the rotor winding consists of single copper or aluminium bars placed in the slots and short-circuited by end-rings on both sides of the rotor. One or two fans are attached to the sides of the shaft to cool the rotor.

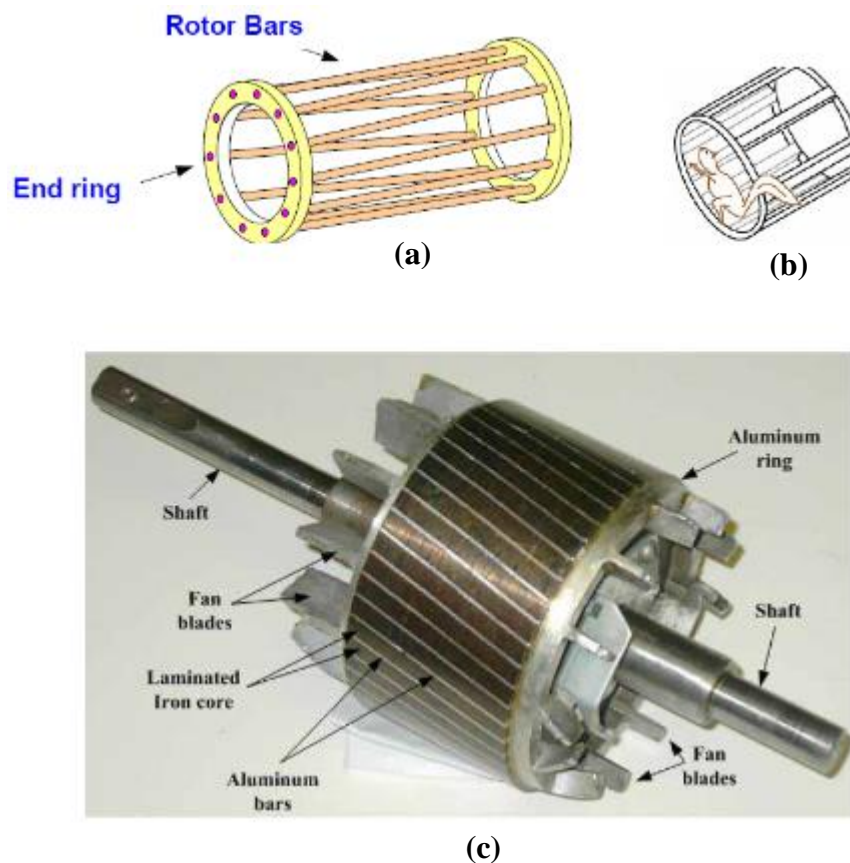


Fig. 2.4 Squirrel Cage Rotor Construction

Fig. 2.4(a) (Anon, 2018a) shows a cage representing rotor bars and end rings similar to squirrel in a cage as shown in (b); suggesting the name of this commonly used type of rotor (squirrel-cage rotor). Fig. 2.4(c) provides the construction of the squirrel-cage rotor with shaft and cooling fan blades.

Wound or slip-ring rotor: This type of rotor contains revolving slip rings and stationary brushes. An insulated three-phase winding similar to the stator winding, wound for the same number of poles as stator, is placed in the rotor slots. The ends of the star-connected rotor

winding are brought to three slip rings on the shaft so that a connection can be made to it for starting or speed control. This connection is made via brushes. The revolving slip-rings and associated stationary brushes enable series connection of external resistors with the rotor windings.

This rotor type is usually for large three-phase induction motor. The rotor has a winding the same as stator and the end of each phase is connected to a slip-ring. Relative to squirrel-cage rotors, wound rotors are expensive and require maintenance of the slip-rings and brushes. They are therefore not so common in industry applications. The rotor can be wound for a number of phases different from that for the stator. Fig. 2.5 (Anon, 2018a) shows the wound rotor of a large induction motor.



Fig. 2.5 Wound Rotor of a Large Induction Motor

2.2.2 Principle of Operation

A rotating magnetic field is generated in the stator magnetic circuit when a three-phase voltage is applied to the stator of an induction motor. The rotating field or flux induces a voltage or electromotive force (EMF) in all the rotor conductors or conducting bars as they cut across them (rotor conductors). According to Faraday's law of electromagnetic induction, the magnitude of this emf is proportional to the rate of change of the rotating magnetic flux linking the rotor circuit.

Large currents flow in the rotor circuit due to the induced emf which in turn, interact with the stator magnetic flux to produce a torque as an output. The torque, according to Lenz's law, drags the rotor along in the direction of the rotating field.

Thus, in a three-phase induction motor, the three-phase currents are of equal magnitude but differ in phase by 120° . There is also a physical 120° shift between each magnetic flux produced by each of the three-phase currents. The sum of the three fluxes gives a total rotating magnetic flux or field in the machine which turns with constant speed (synchronous speed) and has constant amplitude. The existence of a rotating magnetic field is an essential condition for the operation of an induction motor.

If stator is energized by an AC current, a rotating flux is generated due to the applied current to the stator winding. This flux produces magnetic field which revolves in the air gap between stator and rotor. Consequently, the emf or voltage, induced by the magnetic field in the short-circuited bars of the squirrel-cage rotor, drives current through the rotor bars. The interaction of the stator rotating flux and the rotor current generates a force that drives the motor and a torque is developed immediately as explained earlier. The torque (F) is proportional to the flux density (B) and the rotor bar current (I) with bar length L ($F = BIL$). The motor speed is less than the synchronous speed. The direction of the rotation of the rotor is the same as the direction of the rotation of the revolving magnetic field in the air gap.

However, for these currents to be induced, the speed of the physical rotor and the speed of the rotating magnetic field in the stator must be different to effect a relative movement between the magnetic field and the rotor conductors. In such cases, the rotor typically slows slightly until a current is re-induced and then the rotor continues as before. This difference between the speed of the rotor and speed of the rotating magnetic field in the stator is called slip. It is unitless and is the ratio between the relative speed of the magnetic field as seen by the rotor the (slip speed) to the speed of the rotating stator field. Due to this an induction motor may sometimes be referred to as an asynchronous machine.

Slip

The relationship between the supply frequency, f , the number of poles, p , and the synchronous speed (speed of rotating field), n_s is given by:

$$n_s = 120 \frac{f}{p} \quad (2.1)$$

The rotating or stator magnetic field rotates at a synchronous speed, n_s . If, n = speed of the rotor, the slip, s for an induction motor is defined as:

$$s = \frac{(n_s - n)}{n_s} \quad (2.2)$$

At stand still, rotor does not rotate, $n = 0$, so $s = 1$. At synchronous speed, $n = n_s$, $s = 0$. The mechanical speed of the rotor, in terms of slip and synchronous speed is given by:

$$n = (1-s)n_s \quad (2.3)$$

As the motor picks up speed, the relative velocity of the field with respect to the rotor diminishes progressively. As a result, both the magnitude and the frequency of the rotor induced voltage decrease as the rotor conductors are cut more slowly. This causes the rotor current, very large at first, to decrease rapidly as the motor picks up speed.

The speed continues to increase but never catches up with the synchronous speed of the rotating field. However, if the rotor turns at the same speed as the field, there will be no induced voltage and current as the rotating field no longer cuts the rotor conductors. Under these conditions, the force acting on the rotor conductors also becomes zero and friction and windage immediately cause the rotor to decelerate or slow down.

To overcome the braking torque, sufficiently large current must be produced in the rotor bars. This is achieved when the rotor speed is always slightly less than the synchronous speed. At no load, the difference in speed between the rotor and field is very small, usually less than 0.1% of synchronous speed.

Frequency of rotor current and voltage

With the rotor at stand-still, the frequency of the induced voltages and currents is the same as that of the stator (supply) frequency, f_e . If the rotor rotates at speed of n , then the relative speed is the slip speed: $n_{slip} = n_s - n$ and n_{slip} is responsible for induction. Hence, the frequency of the induced voltages and currents in the rotor is, $f_r = sf_e$. Thus, the frequency of the voltage induced in the rotor depends upon the slip.

2.2.3 Equivalent Circuit

The induction motor consists of a two magnetically connected systems namely, stator and rotor. This is similar to a transformer that also has two magnetically connected systems namely primary and secondary windings. Hence, the equivalent circuit of an induction motor is arrived at in the same way as for a transformer. In view of this, the induction motor may sometimes also be called a rotating transformer. Circuits are normally drawn on single-phase basis of the induction motor. The rotor circuit and the equivalent circuit of the induction motor with the secondary rotor referred to the primary stator are shown in Fig. 2.6 and Fig. 2.7 (Anon, 2018a) respectively.

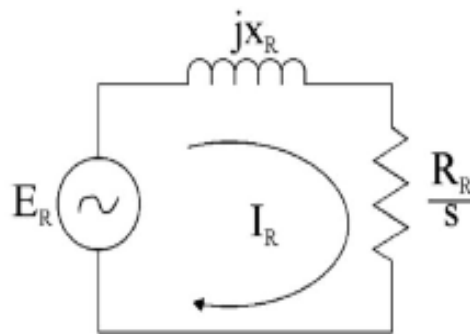


Fig. 2.6 Diagram of the Rotor Circuit

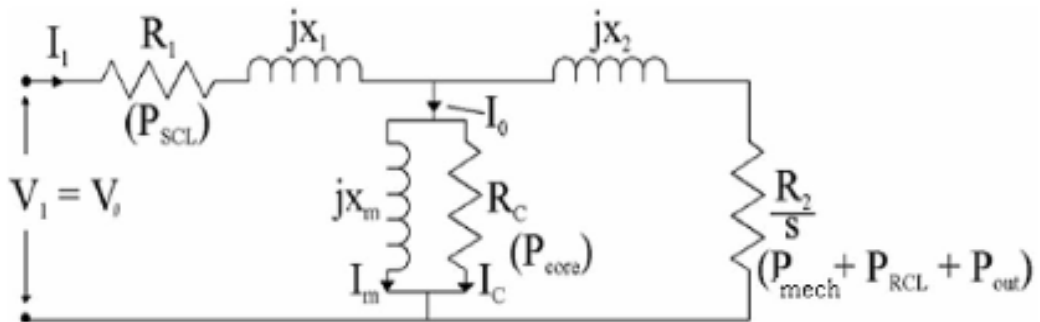


Fig. 2.7 Equivalent Circuit of a Stator

where, I_1 = stator current/phase

R_1 and R_2 or R_R = stator and rotor winding resistance/phase

X_1 and X_2 or X_R = stator and rotor winding reactance/phase

R_R = stator winding resistance/phase

s = slip/phase

I_R = rotor current

V_1 = applied voltage to the stator/phase

$I_o = I_c + I_m$ (I_o – core current; I_m -magnetising component; I_c -core loss component)

P_{mech} , P_{core} and P_{RCL} = mechanical-, core- and rotor copper losses

P_{out} = output or power

The actual rotor impedance and the ratio by which it is transferred to the stator are of interest mainly to the designer, not the analyst. The study of the motor performance is based on the value of impedances of the equivalent circuit and other parameters or impedances obtained from experimental test results.

2.2.4 Power Flow Diagram of a Motor

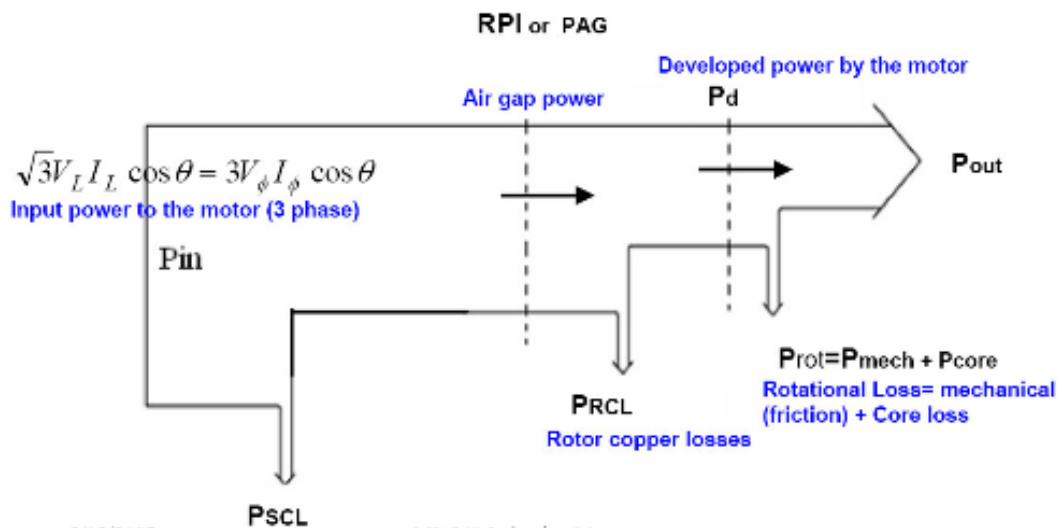


Fig. 2.8 Power Flow Diagram of a Motor

Fig. 2.8 (Anon, 2018a) shows the power flow diagram of a Motor with such parameters as stator copper losses (P_{SCL}), rotor copper losses (P_{RCL}) and rotor power input (P_{RPI}).

The efficiency increases as the speed of the motor increases. Hence, an induction machine should always be operated at low values of slip to ensure efficient (and a high power factor) operation.

2.2.5 Torque-Speed Characteristics

For small values of slip s , the torque is directly proportional to s . For large values of slip s , the torque is inversely proportional to s . Fig. 2.9 (Anon, 2018a) shows the torque-speed characteristics of the induction motor.

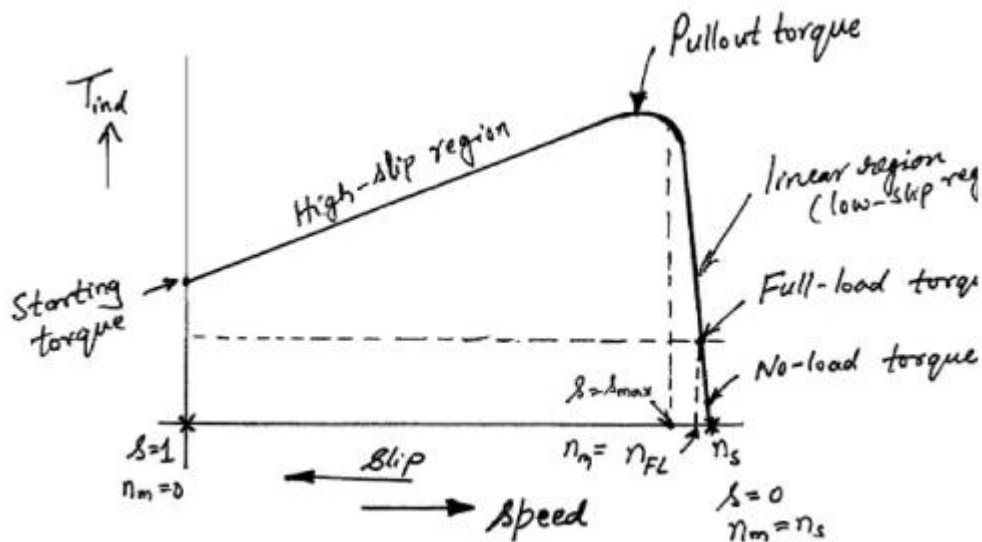


Fig. 2.9 Torque-Speed Characteristics of Induction Motor

2.2.6 Starting of Three-Phase Induction Motors

There are two important factors to be considered in starting of induction motors. These are:

- i. The starting current drawn from the supply; and
- ii. The starting torque.

The starting current should be kept low to avoid overheating of motor and excessive voltage drops in the supply network. The starting torque must be about 50 to 100% more than the expected load torque to ensure that the motor runs up in a reasonably short time. Also the motor:

- i. At synchronous speed, $s = 0$, and therefore, $R_2/s = \infty$, so $I_2' = 0$;
- ii. The stator current therefore comprises only the magnetizing current i.e. $I_1 = I_m$ and is quite therefore quite small;
- iii. At low speeds, $R_2'/s + jX_2 = \infty$ is small, and therefore I_2' is quite high and consequently I_1 is quite large; and
- iv. Actually, the typical starting currents for an induction machine are five to eight times the normal running current.

Hence the starting currents should be reduced. The most usual methods of starting three-phase induction motors are rotor resistance starting (for slip-ring motors) and direct-on-line starting, star-delta starting and autotransformer starting (for squirrel-cage motors).

Rotor resistance starting

By adding external resistance to the rotor circuit, any starting torque up to the maximum torque can be achieved; and by gradually cutting out the resistance, a high torque can be maintained throughout the starting period. Fig. 2.10 (Anon, 2018a) shows a rotor resistance starting of a three-phase induction motor. The added resistance also reduces the starting current, so that a starting torque in the range of 2 to 2.5 times the full load torque can be obtained at a starting current of 1 to 1.5 times the full load current.

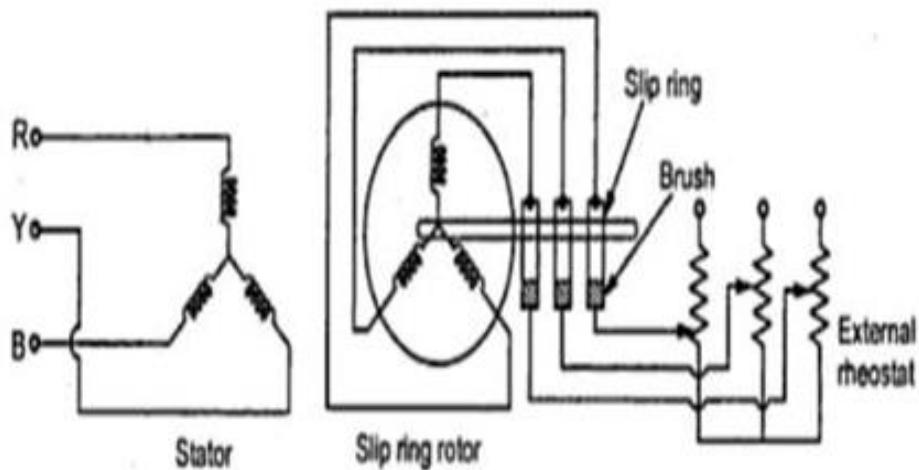


Fig. 2.10 Rotor Resistance Starting

Direct-on-line starting

This is the most simple and inexpensive method of starting a squirrel cage induction motor. The motor is switched on directly to full supply voltage. The initial starting current is large, normally about five to seven times the rated current but the starting torque is likely to be 0.75 to 2 times the full load torque. To avoid excessive supply voltage drops because of large starting currents the method is restricted to small motors only.

To decrease the starting current, cage motors of medium and larger sizes are started at a reduced supply voltage. The reduced supply voltage starting is applied in the next two methods. Fig. 2.11 (Anon, 2018a) shows the direct-on-line starting of an induction motor.

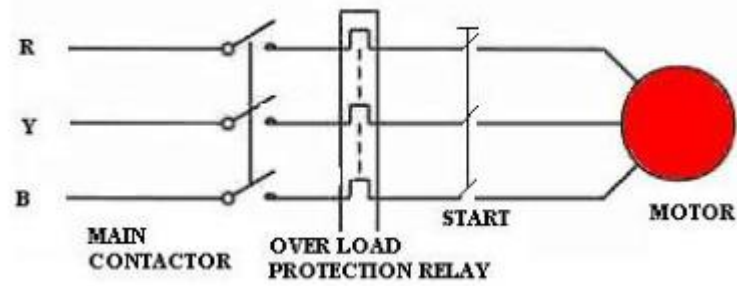


Fig. 2.11 Direct-on-Line Starting

Star-delta starting

This is applicable to motors designed for delta connection in normal running conditions. Both ends of each phase of the stator winding are brought out and connected to a three-phase change-over switch.

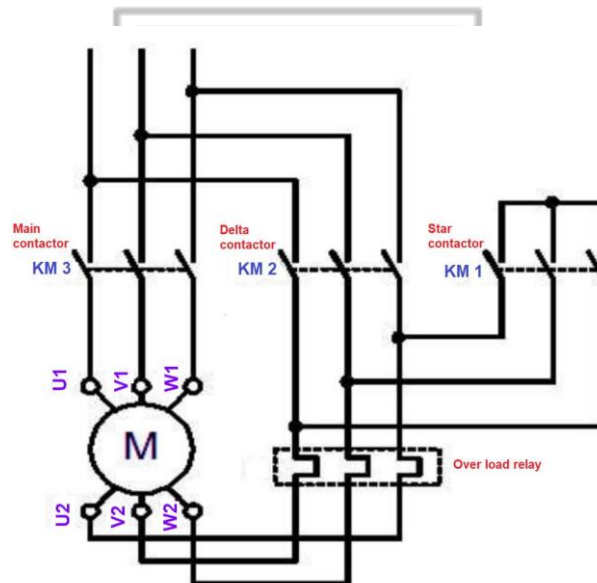


Fig. 2.12 Star-Delta Starting

For starting, the stator windings are connected in star and when the machine is running the switch is thrown quickly to the running position, thus connecting the motor in delta for normal operation. The phase voltages and the phase currents of the motor in star connection are reduced to $1/\sqrt{3}$ of the direct-on-line values in delta. The line current is $1/3$ of the value in delta. Fig. 2.12 (Anon, 2018a) shows the star-delta starting of the induction motor.

A disadvantage of this method is that the starting torque (which is proportional to the square of the applied voltage) is also reduced to $1/3$ of its delta value.

Auto-transformer starting

This method also reduces the initial voltage applied to the motor and therefore the starting current and torque. The motor, which can be connected permanently in delta or in star, is switched first on reduced voltage from a three-phase tapped auto-transformer and when it has accelerated sufficiently, it is switched to the running (full voltage) position. The principle is similar to star/delta starting and has similar limitations. The advantage of the method is that the current and torque can be adjusted to the required value, by taking the correct tapping on the autotransformer. This method is more expensive because of the additional autotransformer. Fig. 2.13 (Anon, 2018a) shows the auto-transformer starting of the induction motor.

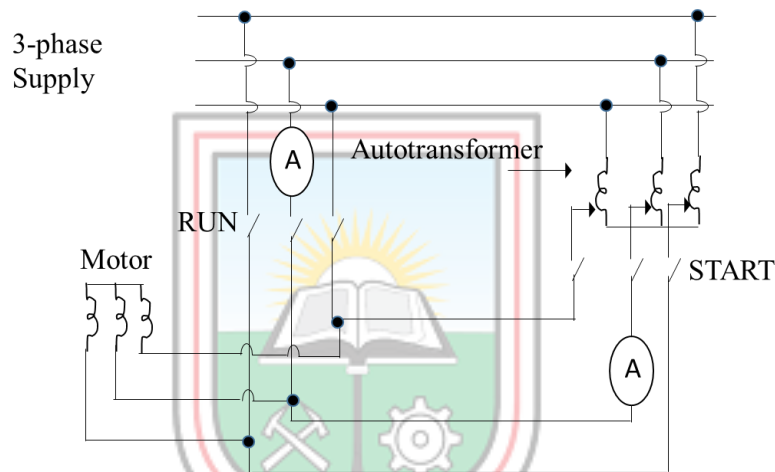


Fig. 2.13 Auto-Transformer Starting

2.2.7 Speed Control of Induction Machines

In the stable region of operation in the motoring mode, the curve is rather steep and goes from zero torque at synchronous speed to the stall torque at a value of slip $s = \hat{s}$. Normally, \hat{s} may be such that stall torque is about three times that of the rated operating torque of the machine, and hence may be about 0.3 or less. This means that in the entire loading range of the machine, the speed change is quite small. The machine speed is quite stiff with respect to load changes. The entire speed variation is only in the range n_s to $(1-s)n_s$, n_s being dependent on supply frequency and the number of poles.

The foregoing discussion shows that the induction machine, when operating from mains is essentially a constant speed machine. Many industrial drives, typically for fan or pump applications, have typically constant speed requirements and hence the induction machine

is ideally suited for these. However, the induction machine, especially the squirrel cage type, is quite rugged and has a simple construction. Therefore, it is good candidate for variable speed applications if it can be achieved.

Speed control by changing applied voltage

The torque equation of the induction machine reveals that the torque depends on the square of the applied voltage. The variation of speed torque curves with respect to the applied voltage is shown in Fig. 2.14 (Anon, 2018a). These curves show that the slip at maximum torque remains same, while the value of stall torque comes down with decrease in applied voltage. The speed range for stable operation remains the same.

Further, we also note that the starting torque is also lower at lower voltages. Thus, even if a given voltage level is sufficient for achieving the running torque, the machine may not start. This method of trying to control the speed is best suited for loads that require very little starting torque, but their torque requirement may increase with speed.

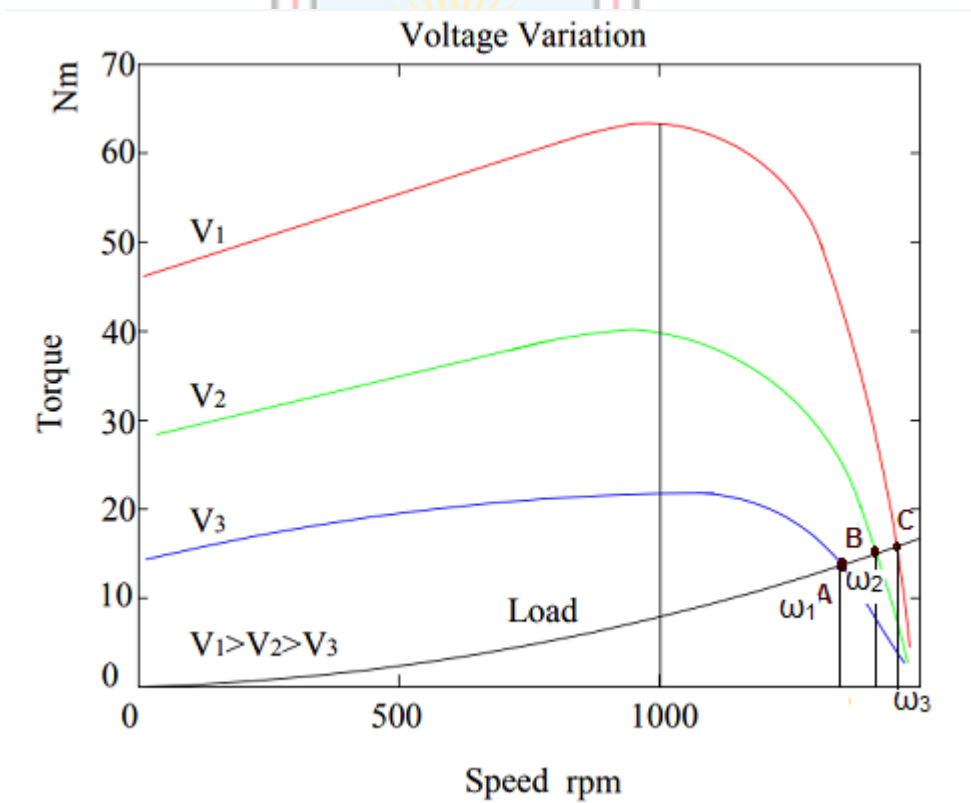


Fig. 2.14 Speed-Torque Curves: Voltage Variation

Fig. 2.14 shows a load torque characteristic, one that is typical of a fan type of load. In a fan (blower) type of load, the variation of torque with speed is such that $T \propto \omega^2$. It may then be

possible to run the motor to lower speeds within the range n_s to $(1-s)n_s$. Further, since the load torque at zero speed is zero, the machine can start even at reduced voltages. This will not be possible with constant torque type of loads. One may note that if the applied voltage is reduced, the voltage across the magnetizing branch also comes down. This in turn means that the magnetizing current and hence flux level are reduced. Reduction in the flux level in the machine impairs torque production, which is primarily the explanation for Fig. 2.14.

If, however, the machine is running under lightly loaded conditions, then operating under rated flux levels is not required. Under such conditions, reduction in magnetizing current improves the power factor of operation. Some amount of energy saving may also be achieved. Voltage control may be achieved by adding series resistors (a lossy, inefficient proposition), or a series inductor/autotransformer (a bulky solution) or a more modern solution using semiconductor devices. A typical solid-state circuit used for this purpose is the AC voltage controller or AC chopper. Another use of voltage control is in the so-called 'soft-start' of the machine. This is discussed in the section on starting methods.

Rotor resistance control

Torque is dependent on the rotor resistance. The maximum value is independent of the rotor resistance. The slip at maximum torque is dependent on the rotor resistance. Therefore, we may expect that if the rotor resistance is changed, the maximum torque point shifts to higher slip values, while retaining a constant torque. Fig. 2.15 (Anon, 2018a) shows a family of torque-speed characteristic obtained by changing the rotor resistance.

While the maximum torque and synchronous speed remain constant, the slip at which maximum torque occurs increases with increase in rotor resistance, and so does the starting torque. Whether the load is of constant torque type or fan-type, it is evident that the speed control range is more with this method. Further, rotor resistance control could also be used as a means of generating high starting torque.

For all its advantages, the scheme has two serious drawbacks. Firstly, in order to vary the rotor resistance, it is necessary to connect external variable resistors (winding resistance itself cannot be changed). This therefore necessitates a slip-ring machine, since only in that case rotor terminals are available outside. For cage rotor machines, there are no rotor terminals. Secondly, the method is not very efficient since the additional resistance and operation at high slips entails dissipation.

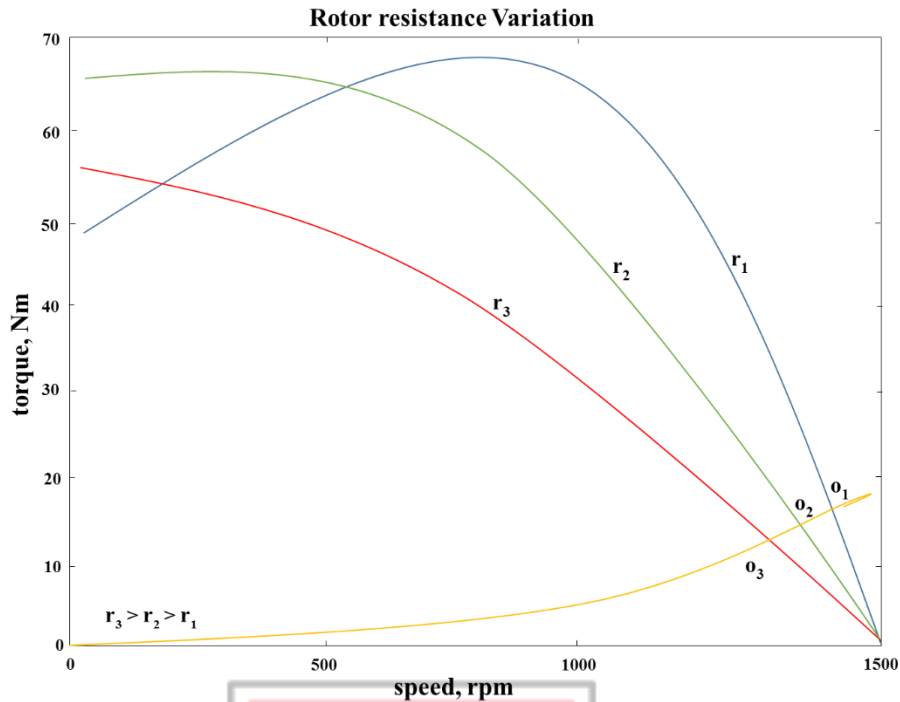


Fig. 2.15 Speed-Torque Curves: Rotor Resistance Variation

The resistors connected to the slip-ring brushes should have good power dissipation capability. Water based rheostats may be used for this. A ‘solid-state’ alternative to a rheostat is a chopper-controlled resistance where the duty ratio control of the chopper presents a variable resistance load to the rotor of the induction machine.

2.2.8 Pole Changing Schemes

Sometimes induction machines have a special stator winding capable of being externally connected to form two different number of pole numbers. Since the synchronous speed of the induction machine is given by $n_s = f_s/p$ (in rev/s) where p is the number of pole pairs, this would correspond to changing the synchronous speed. With the slip now corresponding to the new synchronous speed, the operating speed is changed. This method of speed control is a stepped variation and generally restricted to two steps.

If the changes in stator winding connections are made so that the air gap flux remains constant, then at any winding connection, the same maximum torque is achievable. Such winding arrangements are therefore referred to as constant-torque connections. If however such connection changes result in air gap flux changes that are inversely proportional to the synchronous speeds, then such connections are called constant-horsepower type. Fig. 2.16

(Anon, 2018a) serves to illustrate the basic principle. Consider a magnetic pole structure consisting of four pole faces A, B, C, D as shown in Fig. 2.16.

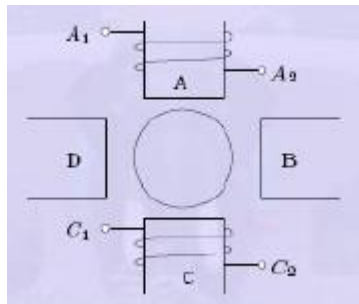


Fig. 2.16 Pole Arrangement

Coils are wound on A and C in the directions shown. The two coils on A and C may be connected in series in two different ways - A₂ may be connected to C₁ or C₂. A₁ with the other terminal at C then form the terminals of the overall combination. Thus, two connections result as shown in Fig. 2.17 (a) and (b).

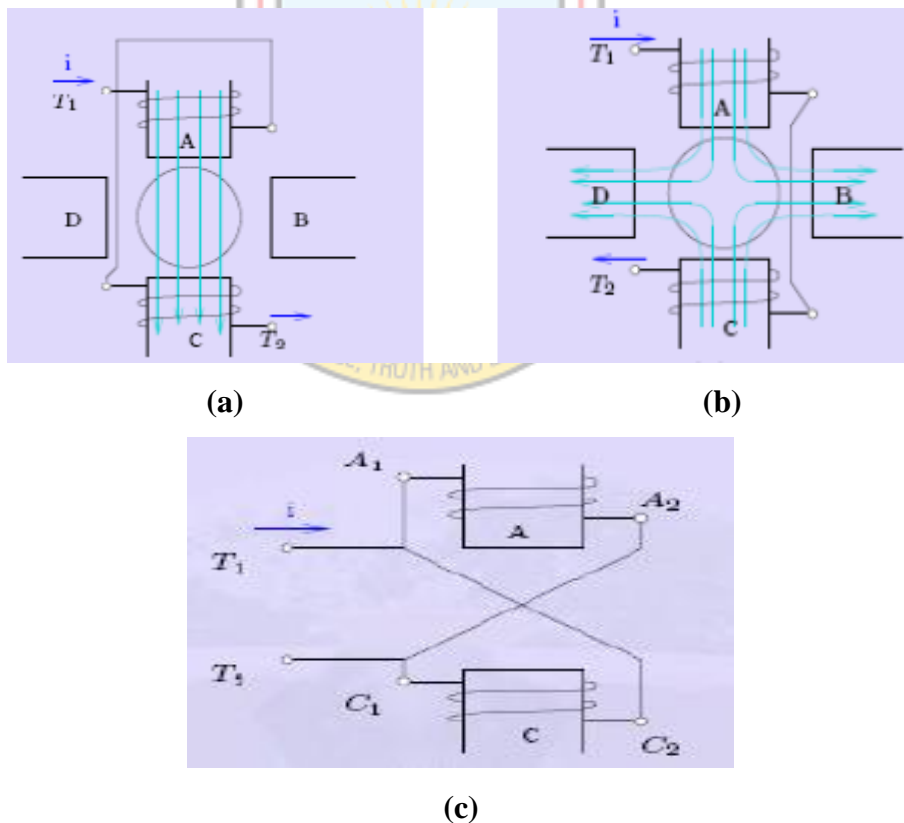


Fig. 2.17 Pole Changing: (a) Flux lines out of pole A into pole C (b) Flux lines out of poles A and C (c) One coiled induced emf to balance the applied voltage

For a given direction of current flow at terminal A₁, say into terminal A₁, the flux directions within the poles are shown in the figures. In case (a) of Fig. 2.17 (Anon, 2018a), the flux

lines are out of the pole A (seen from the rotor) for and into pole C, thus establishing a two-pole structure. In case (b) however, the flux lines are out of the poles in A and C. The flux lines will then have to complete the circuit by flowing into the pole structures on the sides. If, when seen from the rotor, the pole emanating flux lines is considered as north pole and the pole into which they enter is termed as south, then the pole configurations produced by these connections is a two-pole arrangement in Fig. 2.18(a) and a four-pole arrangement in Fig. 2.18(b). Thus, by changing the terminal connections we get either a two pole air-gap field or a four-pole field. In an induction machine this would correspond to a synchronous speed reduction in half from case (a) to case (b).

Further note that irrespective of the connection, the applied voltage is balanced by the series addition of induced electromotive forces (emfs) in two coils. Therefore, the air-gap flux in both cases is the same. Cases (a) and (b) therefore form a pair of constant torque connections.

Consider, on the other hand a connection as shown in the Fig. 2.17(c). The terminals T_1 and T_2 are where the input excitation is given. Note that current direction in the coils now resembles that of case (b), and hence this would result in a four-pole structure. However, in Fig. 2.17(c), there is only one coil induced emf to balance the applied voltage. Therefore, flux in case (c) would therefore be halved compared to that of case (b) (or case (a), for that matter). Cases (a) and (c) therefore form a pair of constant horse-power connections. It is important to note that in generating a different pole number, the current through one coil (out of two, coil C in this case) is reversed.

2.2.9 Stator Frequency Control

The expression for the synchronous speed indicates that by changing the stator frequency also it can be changed. This can be achieved by using power electronic circuits called inverters which convert DC to AC of desired frequency. Depending on the type of control scheme of the inverter, the ac generated may be variable-frequency-fixed amplitude or variable-frequency variable-amplitude type. Power electronic control achieves smooth variation of voltage and frequency of the ac output. This when fed to the machine is capable of running at a controlled speed.

However, consider the equation for the induced emf in the induction machine; $V = 4.44 N\phi mf$, where N is the number of the turns per phase, m is the peak flux in the air gap and f

is the frequency. Note that in order to reduce the speed, frequency has to be reduced. If the frequency is reduced while the voltage is kept constant, thereby requiring the amplitude of induced emf to remain the same, flux has to increase. This is not advisable since the machine likely to enter deep saturation. If this is to be avoided, then flux level must be maintained constant which implies that voltage must be reduced along with frequency. The ratio is held constant in order to maintain the flux level for maximum torque capability.

Actually, it is the voltage across the magnetizing branch of the exact equivalent circuit that must be maintained constant, for it is that which determines the induced emf. Under conditions where the stator voltage drop is negligible compared the applied voltage, the above equation is valid.

In this mode of operation, the voltage across the magnetizing inductance in the 'exact' equivalent circuit reduces in amplitude with reduction in frequency and so does the inductive reactance. This implies that the current through the inductance and the flux in the machine remains constant. The speed torque characteristics at any frequency may be estimated as before. There is one curve for every excitation frequency considered corresponding to every value of synchronous speed. The curves are shown in Fig. 2.18 (Anon, 2018a). It may be seen that the maximum torque remains constant.

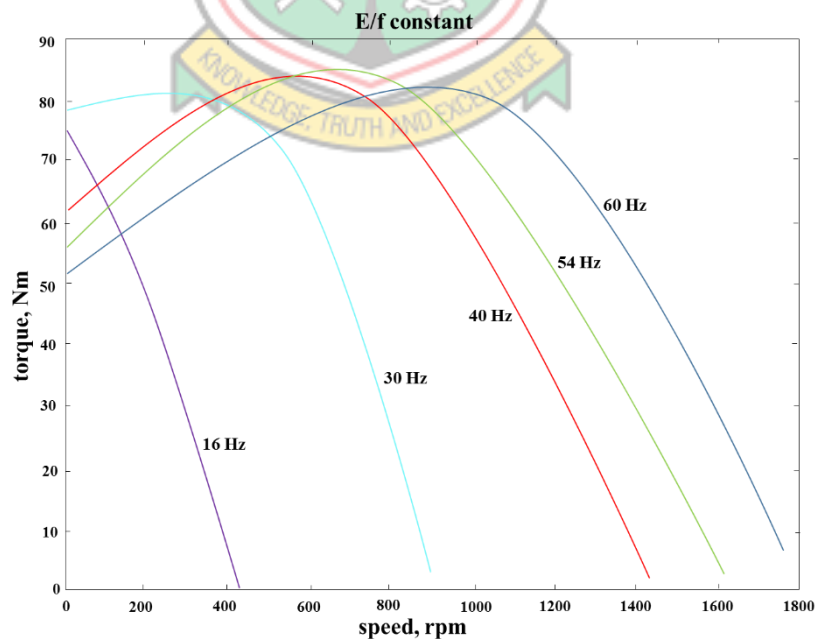


Fig. 2.18 Torque-Speed Curves with E/f Held Constant

With this kind of control, it is possible to get a good starting torque and steady state performance. However, under dynamic conditions, this control is insufficient. Advanced control techniques such as field- oriented control (vector control) or direct torque control (DTC) are necessary.

2.3 Induction Motor Failure

Induction motors are rugged, low cost, low maintenance, reasonably small sized, reasonably highly efficient and operating with an easily available power supply. They are reliable in operations but are subject to different types of undesirable faults.

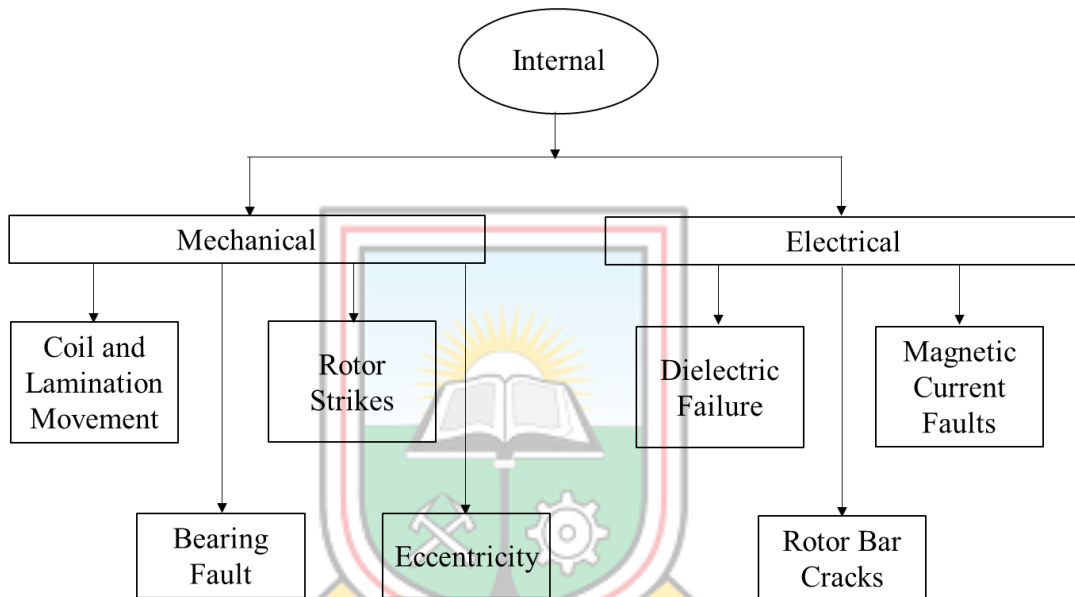


Fig. 2.19 Block Diagram Presentation of Internal Faults

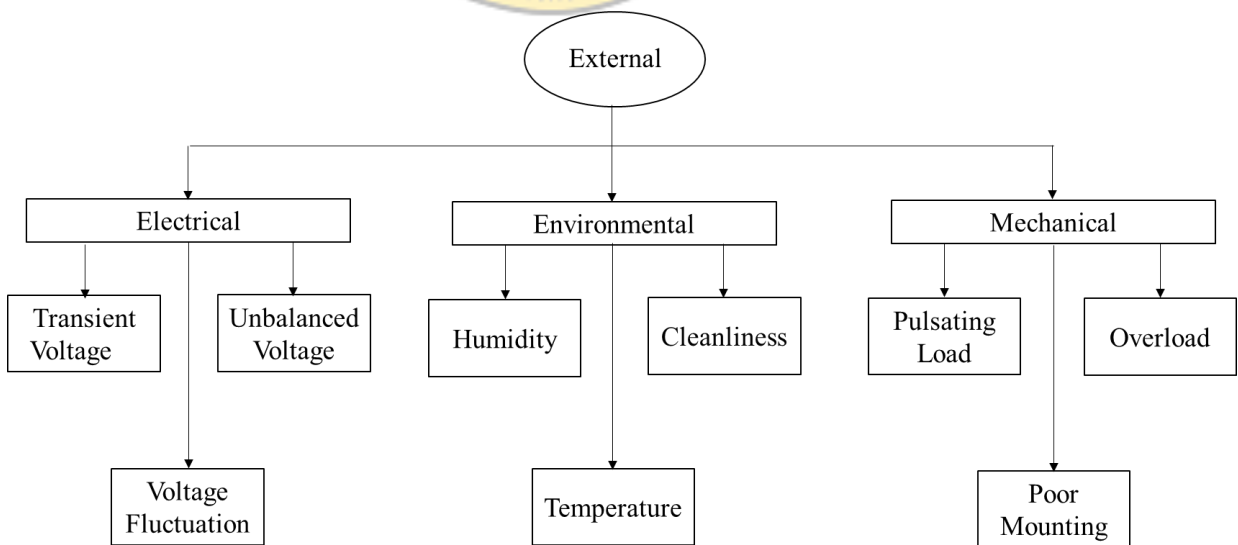


Fig. 2.20 Block Diagram Representation of External Faults

Sources of induction motor faults may be internal or external. In Fig. 2.19 and Fig. 2.20 (Bhowmik *et al.*, 2013), block diagrams of internal and external faults are depicted.

The most vulnerable parts for fault in the induction motor are bearing, stator winding, rotor bar, and shaft. Besides, due to non-uniformity of the air gap between stator-inner surface and rotor-outer surface motor, faults also occur (Karmakar *et al.*, 2016). Faults in induction motors can be categorized as:

- i. Electrical-related faults due to unbalance supply voltage or current, single phasing, under or over voltage or current, reverse phase sequence, earth fault, overload, inter-turn short-circuit fault, and crawling;
- ii. Mechanical-related faults due to broken rotor bar, mass unbalance, air gap eccentricity, bearing damage, rotor winding failure and stator winding failure; and
- iii. Environmental-related faults such as ambient temperature, external moisture as well as vibrations of machine due to reasons like installation defect and foundation defect affect the performance of induction motor.

Industrial processes make use of a large number of asynchronous motors even in sensitive applications. Consequently, a defect can induce high losses in terms of cost and can be dangerous in terms of security and safety. Motor failures are mostly directly or indirectly caused by insulation breakdown, bearing wear or extensive heating of different motor parts involved in motor operation (Anon, 2018b). Multiple faults may occur simultaneously in an induction motor which may result in unbalanced stator currents and voltages, oscillations in torque, reduction in efficiency and torque, overheating and excessive vibration. Normally electric motors do not fail suddenly. It happens over time and regular inspection will detect a problem before a serious situation develops. Three main components of electric motors that experience faults are the stator, rotor and bearings. These faults may be a growing one with only small effects on the operation, a partial non-catastrophic one with emergency operation possible or a catastrophic one with total drive breakdown (Anon, 2018b). Incipient fault detection is preferably done to find faults before complete motor failure in order to avoid service downtime and large losses.

2.3.1 Broken Rotor Bar Fault

This occurs when there is a crack or complete break in one or more of the rotor bars in a squirrel cage induction motor. Rotor asymmetry in squirrel cage induction motor occurs mainly due to manufacturing defect such as non-uniform metallurgical stresses occurring in cage assemble during the brazing process. This leads to failure during rotation of the rotor. Heavy end rings of rotor result in large centrifugal forces which may cause extra stresses on the rotor bars.

As a result, rotor bars may get damaged resulting in asymmetrical distribution of rotor currents. If any of the rotor bars gets cracked for such asymmetry or long run of the motor, overheating will occur in the cracked position which may lead to breaking of the bar. Consequently, the side bars will carry higher currents for which larger thermal and mechanical stresses may happen on these side bars. If the rotor continues to rotate in this condition, the side bars may also get cracked. Thus, damage may spread to various locations of the rotor, leading to fracture of multiple bars, in end rings or at the joints of bars and end rings. Moreover, long start-up time and frequent starts and stops of the motor may enhance possibilities of crack increase. Fig. 2.21 (Karmakar *et al.*, 2016) shows rotor and parts of broken rotor bar.

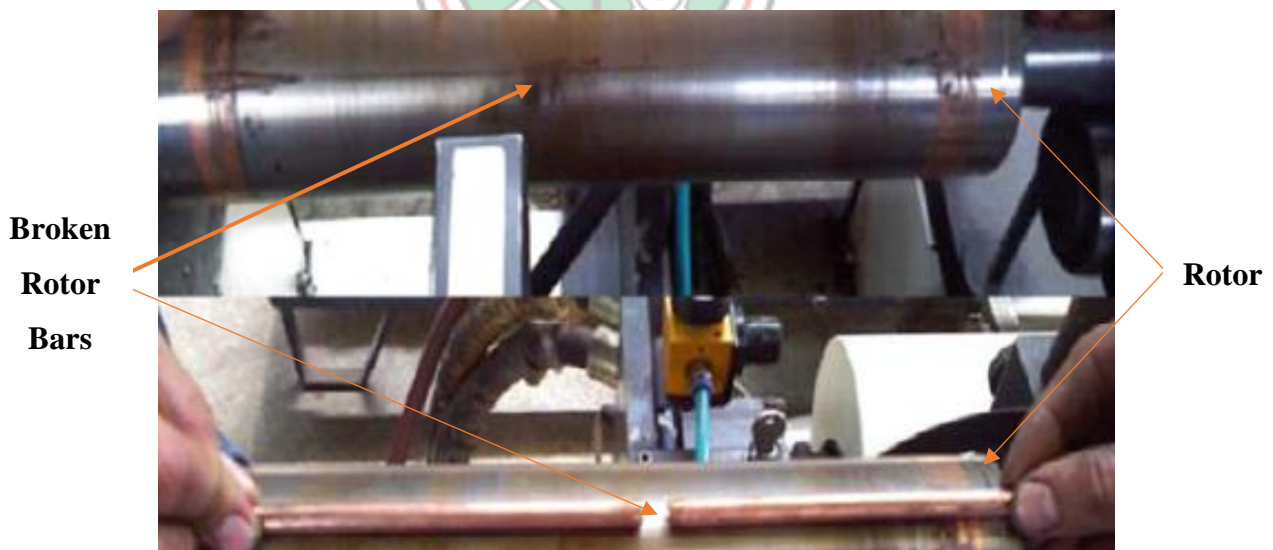


Fig. 2.21 Photograph of Rotor and Parts of Broken Rotor Bars

Conversely, the main causes of rotor broken bar of an induction motor are manufacturing defects, thermal stresses, mechanical stress caused by bearing faults, frequent starts of the

motor at rated voltage and rotor bar metal fatigue. Cracked or broken bar fault produces a series of sideband frequencies. This can cause ripples of torque and speed. Magnitude of lower sideband over the fundamental can be used as an indicator of rotor broken bar fault (Karmakar *et al.*, 2016).

2.3.2 Rotor Mass Unbalance

The rotor is placed inside the stator bore and it rotates coaxially with the stator. In a healthy motor, rotor is centrally aligned with the stator and the axis of rotation of the rotor is the same as the geometrical axis of the stator. This results in identical air gap between the outer surface of the rotor and the inner surface of the stator. However, if the rotor is not centrally aligned or its axis of rotation is not the same as the geometrical axis of the stator, then the air gap will not be identical and the situation is referred to as air-gap eccentricity. In fact, air-gap eccentricity is common to rotor fault in an induction motor. Air-gap eccentricity may occur due to any of the rotor faults like rotor mass unbalance fault and bowed rotor fault. Due to this air-gap eccentricity fault in an induction motor, electromagnetic pull will be unbalanced. The rotor side where the air gap is minimum will experience greater pull and the opposite side will experience lower pull and as a result rotor will tend to move in the greater pull direction across that gap. The chance of rotor pullover is normally greatest during the starting period when motor current is also the greatest. In severe case rotor may rub the stator which may result in damage to the rotor and/or stator. Air-gap eccentricity can also cause noise and/or vibration.

General description of rotor mass unbalance

This rotor mass unbalance occurs mainly due to manufacturing defect, if not may occur even after an extended period of operation, for non-symmetrical addition or subtraction of mass around the centre of rotation of rotor or due to internal misalignment or shaft bending due to which the centre of gravity of the rotor does not coincide with the centre of rotation. In severe case of rotor eccentricity, due to unbalanced electromagnetic pull if rotor rubs the stator then a small part of material of rotor body may wear out which is being described here as subtraction of mass, resulting in rotor mass unbalance fault. Fig. 2.22 (Karmakar *et al.*, 2016) shows rotor mass unbalance fault.

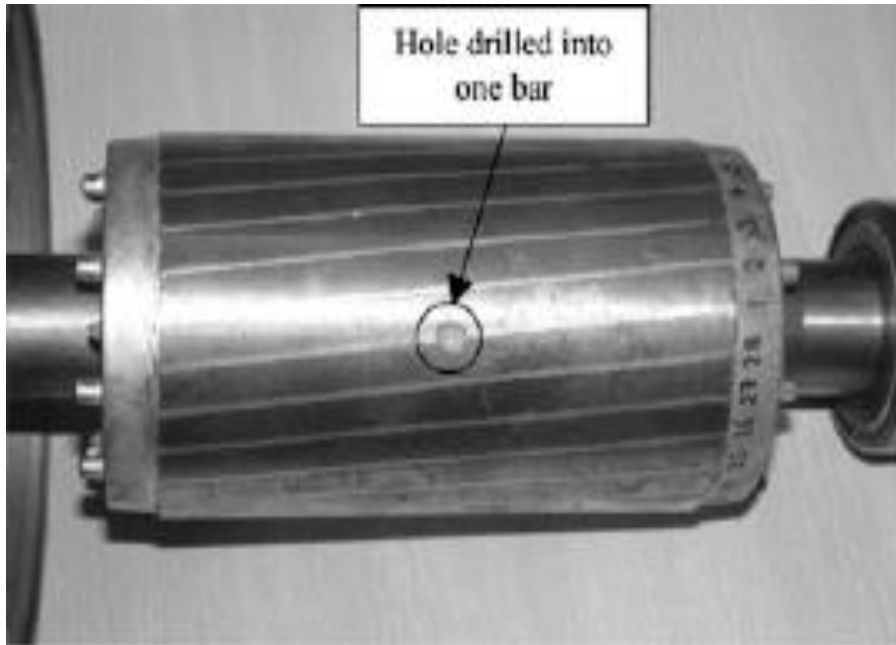


Fig. 2.22 Rotor with Mass Unbalance Fault

Classification of mass unbalance

There are three types of mass unbalanced rotor as shown in Fig. 2.21 (Karmakar *et al.*, 2016). These are:

- i. Static mass unbalanced rotor;
- ii. Couple unbalance rotor; and
- iii. Dynamic unbalance rotor.

Static mass unbalanced rotor: For this fault shaft rotational axis and weight distribution axis of rotor are parallel but offset, as shown in Fig. 2.23(a). Without special equipment this type of eccentricity is difficult to detect.

Couple unbalance rotor: It is shown in Fig. 2.23(b). If this fault occurs then the shaft rotational axis and weight distribution axis of rotor intersect at the centre of the rotor.

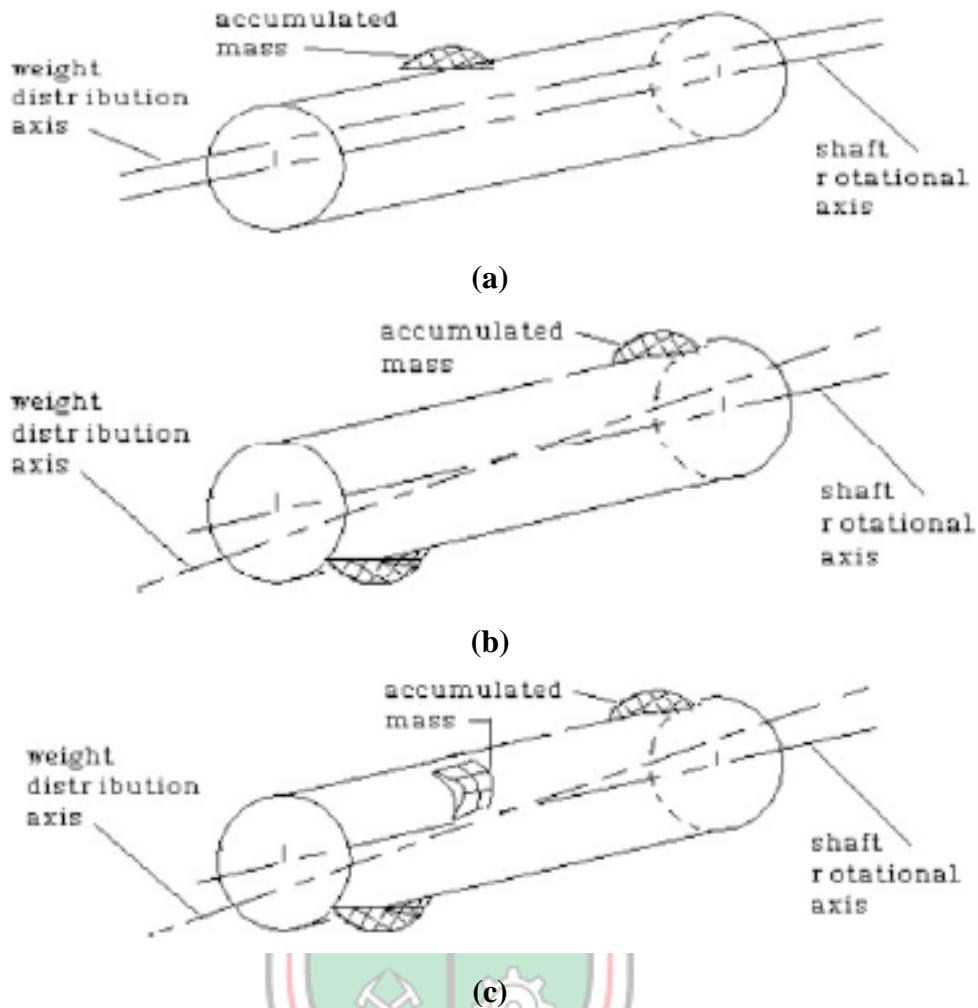


Fig. 2.23 Mass Unbalanced Rotor Fault Types: (a) Static (b) Couple and (c) Dynamic

Dynamic unbalance rotor: It is shown in Fig. 2.23(c). If this fault occurs then shaft rotational axis and weight distribution axis of rotor do not coincide. It is the combination of coupling unbalance and static unbalance. The main causes of rotor mass unbalance in an induction motor can be mentioned, pointwise, as follows:

- i. Manufacturing defect;
- ii. Internal misalignment or shaft bending; and
- iii. It may occur after an extended period of operation, for non-symmetrical addition or subtraction of mass around the centre of rotation of rotor.

Effect of rotor mass unbalance

If an induction motor rotor mass unbalance occurs, its effect will be as follows:

- i. Mass unbalance produces dynamic eccentricity which results in oscillation in the air gap length;

- ii. Oscillation in the air gap length which causes variation in air gap flux density, and hence variation in induced voltage in the winding; and
- iii. Induced voltage which causes current whose frequencies are determined by the frequency of the air gap flux density harmonics

2.3.3 Bearing Fault

Two sets of bearings are placed at both the ends of the rotor of an induction motor to support the rotating shaft. They held the rotor in place and help it to rotate freely by decreasing the frictions. Each bearing consists of an inner and an outer ring called races and a set of rolling elements called balls in between these two races. Normally, in case of motor, inner race is attached to the shaft and load is transmitted through the rotating balls—this decreases the friction. Using lubricant (oil or grease) in between the races friction is further decreased. Fig. 2.24 (a) shows a typical ball bearing and (b) shows a dissected ball bearing (Karmakar *et al.*, 2016).

Any physical damage of the inner race or in the outer race or on the surface of the balls is termed as bearing fault. In terms of induction motor failure, bearing is the weakest component of an induction motor. It is the single largest cause of fault in induction motor (Karmakar *et al.*, 2016).

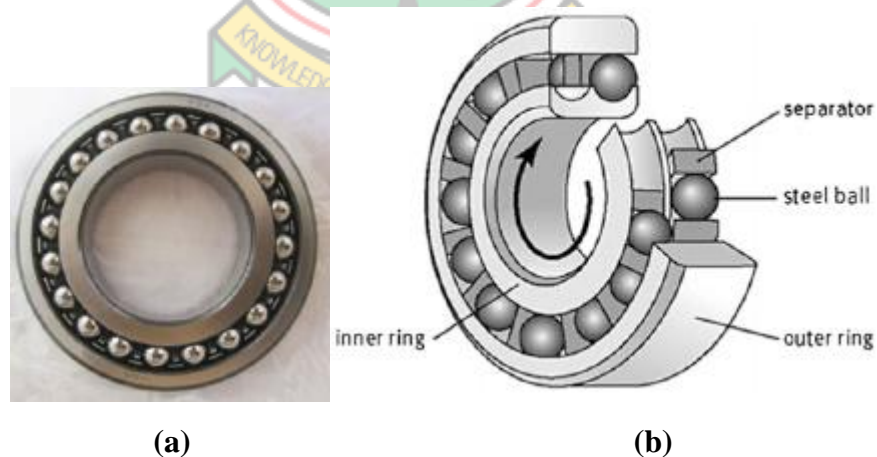


Fig. 2.24 Ball Bearing: (a) Typical and (b) Dissected

Causes and effects of bearing failure

Excessive loads, tight fits, and excessive temperature rise: All of these can anneal the two races and ball materials. They can also degrade, even destroy, the lubricant. If the load exceeds the elastic limit of the bearing material, brinelling occurs.

Fatigue failure: This is due to long run of the bearings. It causes fracture and subsequently removal of small discrete particles of materials from the surfaces of races or balls. This type of bearing failure is progressive, that is, if once initiated will spread when further operation of bearings takes place. For this bearing failure, vibration and noise level of motor will increase.

Corrosion: This results, if bearings are exposed to corrosive fluids (acids, etc.) or corrosive atmosphere. If lubricants deteriorate or the bearings are handled carelessly during installation, then also corrosion of bearings may take place. Early fatigue failure may creep in due to corrosion.

Contamination: It is one of the leading factors of bearing failure. Lubricants get contaminated by dirt and other foreign particles which are most often present in industrial environment. High vibration and wear are the effects of contamination.

Lubricant failure: For restricted flow of lubricant or excessive temperature this takes place. It degrades the property of the lubricant for which excessive wear of balls and races takes place which results in overheating. If bearing temperature gets too high, grease (the lubricant) melts and runs out of bearing. Discoloured balls and ball tracks are the symptoms of lubricant failure.

Misalignment of bearings: For this, wear in the surfaces of balls and races takes place which results in rise in temperature of the bearings.

It is observed that for any of the bearing failures, normally friction increases which causes rise in temperature of the bearings and increase in vibration of the concerned machine. For this, bearing temperature and vibration can provide useful information regarding bearing condition and hence machine health.

2.3.4 Stator Fault

Stator of an induction motor is subjected to various stresses such as mechanical, electrical, thermal, and environmental. Depending upon the severity of these stresses stator faults may occur. If for a well-designed motor operations and maintenance are done properly, then these stresses remain under control. The stator faults can be classified as:

- i. Faults in laminations and frame of stator; and

ii. Faults in stator winding.

Though most stator faults are due to a combination of above stresses, the second one is more common.

2.3.5 Stator Winding Fault

This fault is due to failure of insulation of the stator winding. It is mainly termed as inter-turn short-circuit fault. Different types of stator winding faults are:

- i. Short circuit between two turns of same phase (turn-to-turn fault);
- ii. Short circuit between two coils of same phase (coil to coil fault);
- iii. Short circuit between turns of two phases (phase to phase fault);
- iv. Short circuit between turns of all three phases;
- v. Short circuit between winding conductors and the stator core (coil to ground fault); and
- vi. Open-circuit fault when winding gets break.

Short-circuit winding fault shows up when total or a partial of the stator windings get shorted. Open-circuit fault shows up when total or a partial of the stator windings get disconnected and no current flows in that phase or line as shown in Fig. 2.25 (Karmakar *et al.*, 2016).

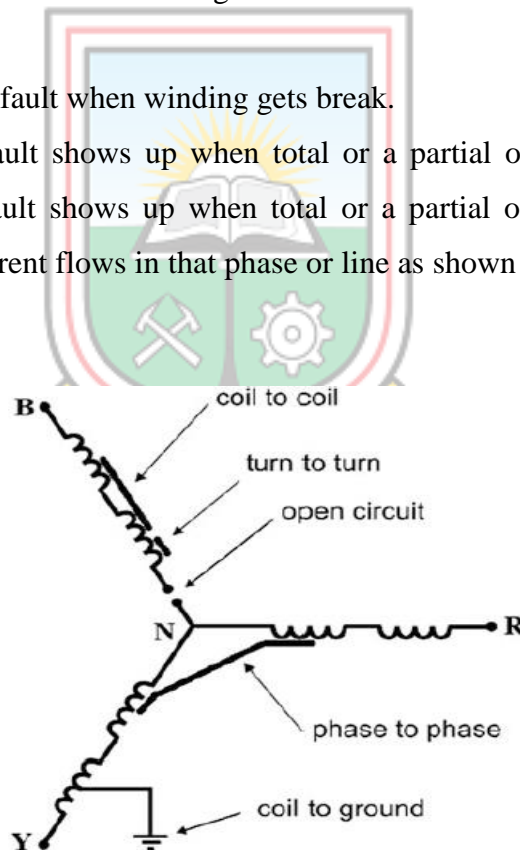


Fig. 2.25 Star-Connected Stator Showing Different Types of Stator Winding Faults



Fig. 2.26 Photograph of Damaged Stator Winding

Causes and effects of stator winding faults

Mechanical stresses: These are due to movement of stator coil and rotor striking the stator. Coil movement which is due to the stator current (as force is proportional to the square of the current) may loosen the top sticks and also may cause damage to the copper conductor and its insulation. Rotor may strike the stator due to rotor-to-stator misalignment or due to shaft deflection or due to bearing failure and if strikes then the striking force will cause the stator laminations to puncture the coil insulation resulting coil to ground fault. High mechanical vibration may disconnect the stator winding producing the open-circuit fault.

Electrical stresses: These are mainly due to the supply voltage transient. This transient arises due to different faults (like line-to-line, line-to-ground, or three-phase fault), due to lightning, opening, or closing of circuit breakers or due to variable frequency drives. This transient voltage reduces life of stator winding and in severe case may cause turn-to-turn or turn-to-ground fault.

Thermal stresses: These are mainly due to thermal overloading and are the main reason, among the other possible causes, for deterioration of the insulation of the stator winding. Thermal stress happens due to over current flowing due to sustained overload or fault, higher ambient temperature, obstructed ventilation and unbalanced supply voltage. A thumb rule is there which states that winding temperature will increase by 25% in the phase having the highest current if there is a voltage unbalance of 3.5% per phase. Winding temperature will also increase if within a short span of time a number of starts and stops are made in the

motor. What may be the reason, if winding temperature increases and the motor is operated over its temperature limit, the best insulation may also fail quickly. The thumb rule, in this regard, states that for every 10°C increase in temperature above the stator winding temperature limit, the insulation life is reduced by 50%.

Environmental stresses: These stresses may arise if the motor operates in a hostile environment with too hot or too cold or too humid. The presence of foreign material can contaminate insulation of stator winding and also may reduce the rate of heat dissipation from the motor, resulting reduction in insulation life. Air flow should be free where the motor is situated, otherwise the heat generated in the rotor and stator will increase the winding temperature which will reduce the life of insulation.

2.3.6 Single Phasing Fault

For proper working of any three-phase induction motor, it must be connected to a three-phase alternating current (ac) power supply of rated voltage and load. Once these three-phase motors are started, they will continue to run even if one of the three-phase supply lines gets disconnected. For a three-phase motor, when one of the phases gets lost, then the condition is known as single phasing.

Causes of single phasing fault

Single phasing fault in an induction motor may be due to:

- i. A downed line or a blown fuse of the utility system;
- ii. An equipment failure of the supply system; and
- iii. Short circuit in one phase of the star-connected or delta-connected motor.

Effects of single phasing fault

The effects of this type of fault are viewed as follows:

- i. Single phasing fault motor windings get over heated, primarily due to flow of negative sequence current;
- ii. If during running condition of the motor single phasing fault occurs motor continues to run due to the torque produced by the remaining two phases and this torque is produced as per the demand by the load. As a result, healthy phases

may be overloaded and hence overheated leading to critical damage to the motor itself; and

- iii. A three-phase motor will not start if a single phasing fault already persists in the supply line.

2.3.7 Crawling

It is an electromechanical fault of an induction motor. When an induction motor, though the full-load supply is provided, does not accelerate but runs at a speed nearly one-seventh of its synchronous speed, the phenomenon is known as crawling of the motor.

General description of crawling

The air-gap flux in between stator and rotor of an induction motor is not purely sinusoidal because it contains some odd harmonics. Due to these harmonics, unwanted torque is developed. The flux due to third harmonics and its multiples produced by each of the three phases differs in time phase by 120° and hence neutralize each other. For this reason, harmonics present in air-gap flux are normally 5th, 7th, or 11th among others.

The fundamental air-gap flux rotates at synchronous speed given by $N_s = 120f/P$ rpm where f is the supply frequency and P is the number of poles. However, harmonic fluxes rotate at N_s/k rpm speed (k denotes the order of the harmonics), in the same direction of the fundamental except the 5th harmonic. Flux due to 5th harmonic rotates in opposite direction to the fundamental flux. Magnitudes of 11th and higher order harmonics being very small 5th and 7th harmonics are the most important and predominant harmonics.

Like fundamental flux, these two harmonic fluxes also produce torque. Thus, total motor torque has three components, namely:

- i. Fundamental torque rotating at synchronous speed N_s ;
- ii. 5th harmonic torque rotating at speed $N_s/5$ in the opposite direction of fundamental; and
- iii. 7th harmonic torque rotating at speed $N_s/7$ in the same direction of fundamental.

Thus 5th harmonic torque produces a braking action whose magnitude is very small and hence can be neglected; consequently, the resultant torque can be taken as the sum of the fundamental torque and the 7th harmonic torque as shown in Fig. 2.27 (Karmakar *et al.*, 2016). The 7th harmonic torque has value zero at one-seventh of the synchronous speed. The resultant torque shows a dip near slip $6/7$, which is more significant because torque here

decreases with increase in speed. The motor under loaded condition will not accelerate up to its normal speed but will remain running at a speed nearly one-seventh of the synchronous speed. This phenomenon is called crawling of the induction motor. It is predominant in the squirrel-cage type induction motor. By proper selection of the number of stator and rotor slots, the crawling effect can be reduced.

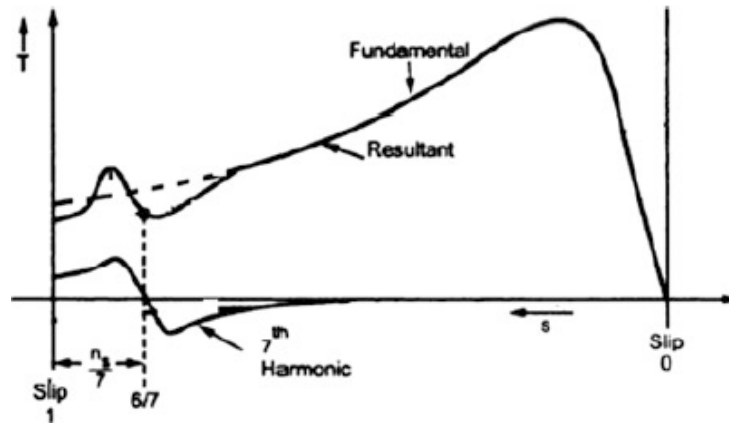


Fig. 2.27 Torque-Slip Curve Showing Resultant of Fundamental and 7th Harmonic Torque

Causes of crawling

Crawling is caused by the 7th harmonic. The 7th harmonic is introduced due to abnormal magneto motive force. Another reason is high harmonic content in the power supply to the motor.

Effects of crawling

The following are the effects of crawling:

- i. Motor under loaded condition will not accelerate up to its normal speed;
- ii. Loaded motor will remain running at a speed nearly one-seventh of the synchronous speed;
- iii. There will be much higher stator current; and
- iv. Motor vibration and noise will be high.

2.3.8 Over Voltage, Under Voltage, Overload and Blocked Rotor

Over and under voltages occur due to change of voltage level at supply end. Over voltage causes stress on insulation, whereas under voltage causes excessive line current increasing temperature of the winding. These faults are normally detected by over/under voltage relays.

Overload occurs due to increase of mechanical load above the rating of the motor. At excessive mechanical load, rotor fails to rotate and gets blocked. This situation is equivalent to short circuit. Normally, overload and blocked rotor are protected by over current relay or simply fuse.

2.4 Condition Monitoring and Its Necessity

Induction motors are the main workhorse of industrial prime movers due to their ruggedness, low cost, low maintenance, reasonably small size, reasonably high efficiency, and operating with an easily available power supply. About 50% of the total generated power of a nation is consumed by these induction motors. These statistics gives an idea regarding the use of huge number of induction motors, but they have some limitations in their operating conditions. If these conditions exceed then some premature failure may occur in stator or/and rotor. This failure, in many applications in industry, may shut down, even, the entire industrial process resulting loss of production time and money. Hence, it is an important issue to avoid any kind of failure of induction motor. Operators and technicians of induction motors are under continual pressure to prevent unscheduled downtime and also to reduce maintenance cost of motors.

Maintenance of electrical motors can be done in three forms: breakdown maintenance, fixed-time maintenance, and condition-based maintenance. In breakdown maintenance, the strategy is 'run the motor until it fails' which means maintenance action is taken only when the motor gets break down. In this case though the motor may run comparatively for a long time before the maintenance is done but when break down occurs it is necessary to replace the entire machine which is much costlier compared to replacing or repairing the faulty parts of the motor. Also, it causes loss of productivity due to downtime. In fixed-time maintenance, motor is required to stop for inspection which causes long downtime. Also trained and experienced technical persons are required to recognize each and every fault correctly. All these necessitate the condition-based maintenance of the motor. In this form of maintenance, motor is allowed to run normally and action is taken at the very first sign of an incipient fault.

In condition monitoring, when a fault has been identified, sufficient data is required for the plant operator for the best possible decision making on the correct course of action. If data is insufficient there remains the chance for wrong diagnosis of fault which leads to

inappropriate replacement of components, and if the root of the problem is not identified properly, the replacement or any other action taken already will succumb to the same fate.

In condition monitoring, signals from the concerned motor are continuously fed to the data acquisition system and the health of the motor is continuously evaluated during its operation for which it is also referred as online condition monitoring of motor, and hence it is possible to identify the faults even while they are developing. The operator/technician can take preparation for the preventive maintenance and can arrange for necessary spare parts, in advance, for repairing. Thus condition monitoring can optimize maintenance schedule and minimize motors downtime and thereby increase the reliability of the motor. Advantages of using condition monitoring can be mentioned pointwise as follows:

- i. Prediction of motor failure;
- ii. Optimization of the maintenance schedule of the motor;
- iii. Reduction of maintenance cost;
- iv. Reduction of the downtime of the machine; and
- v. Improvement of the reliability of the motor.

Condition monitoring and fault detection are usually carried out by investigating the corresponding anomalies in machine current, voltage and leakage flux. Other methods include monitoring the core temperature, bearing vibration level and pyrolysed products. Fault conditions such as insulation defects and bearing degradation may also be diagnosed (Bhowmik *et al.*, 2013).

2.5 Failure Prediction Methods or Techniques

According to Vieira *et al.* (2009), online failure prediction aims to identify situations that will evolve into a failure. Classification of failure prediction methods are usually based on the type of input data used, namely data from failure tracking, symptom monitoring, detected error reporting and undetected error auditing. System monitoring, however, is mostly used as it is effective and offers reliable data based on analysis of time series and/or type of symptoms. In order to build high availability systems based on failure prediction, methods are developed not only to capture, select, or interpret essential data and predict future system states but also to provide proactive recovery and failure avoidance schemes which build on these predictions and help to self-manage the system.

Thus, it has become necessary to diagnose motor faults for effective maintenance plans by management so as to avoid complete failure of systems or machines in the future. Using baseline characteristics of a healthy motor as a reference data, any deviation in motor operating characteristics obtained from system monitoring may be used to perform fault detection and diagnosis irrespective of unavoidable manufacturing defects in the system. Depending on the region of fault occurrence, five main categories of faults, namely stator faults, eccentricity faults, rotor faults, bearing faults and vibration faults are diagnosed based on various failure prediction methods discussed in this section (Bhowmik *et al.*, 2013).

2.5.1 Vibration Spectrum Analysis

This technique is used to detect bearing faults. High frequency components of vibration are created due to friction or forces occurring in the rolling element bearing in electrical machines under normal conditions. In case of a defect in bearings or breaks in lubrication layer between the friction surfaces, shock pulses are produced.

The method analyses the vibration spectrum of an induction machine using piezoelectric accelerometer which works on Fast Fourier Transform to extract from a time domain signal, the frequency domain representation. In diagnosing bearing fault, the harmonic vibration spectrum of the healthy motor and that with defective bearing is analysed individually. Upon comparison, it is realized that the vibration amplitude for faulty motor is larger than that of a healthy motor. Dynamic simulation of motor running with bearing fault to analyse frequency spectrum of electromagnetic torque produced by the faulty motor may provide similar result when compared with its vibration spectrum.

2.5.2 Park Vector Approach and Complex Wavelets

Park vector transformation approach is used to diagnose stator faults on the three-phase induction motor due to the impact of fault on the machine current. This technique uses Park's Transform to derive a two-dimensional Park's current vector components which are expressed as functions of the phase currents of the three-phase induction motor. Thus, the locus of instantaneous spatial vector sum of the measured three phase stator currents forms the basis for Park's vector.

This maps a circle which has its centre at the origin of the coordinates. This locus is distorted by stator winding faults and thus provides easy fault diagnosis. In other words, a graphical

representation of the Park's current vector for a faulty motor gives an elliptical shape which is a distortion of the circularly shaped Park's current vector representation of a healthy motor. The amount of distortion of the circular shape depends on the level of stator fault of the motor. Simulation and experimental results are finally analysed using complex wavelets.

2.5.3 Motor Current Signature Analysis (MCSA)

This technique can be used to detect rotor faults and eccentricity. In case of a fault, Current harmonics in the stator current, caused by a backward rotating field in the air gap, are analysed by MCSA. This requires only one current sensor whose function is based on signal processing techniques like Fast Fourier Transform (FFT).

An equipment set-up which comprises current transformer, signal conditioning unit, data collector/analyser and computer, is used for measuring the motor current. Data is acquired by performing FFT on the stator current. The data obtained, is analysed after FFT is normalized as a function of the first harmonic amplitude. Conversely, harmonic contents or percentage amplitude for harmonics increase with increase in the level of faults like number of broken rotor bars and eccentricity.

2.5.4 Intelligent Techniques

Several intelligent techniques like Fuzzy logic systems, Artificial Neural Networks and Neuro-Fuzzy Systems usually have three prime steps for induction motor condition monitoring. These are:

- i. Signature extraction;
- ii. Fault detection; and
- iii. Fault severity estimation.

Apart from the above-mentioned techniques, some other methods for incipient fault detection of induction motors are the finite element method, vibration testing and analysis, Concordia transform, external magnetic field analysis, multiple reference frames theory, power decomposition technique, KU transformation theory, zero crossing time method and modal analysis method. This work, however, makes use of the artificial neural network for failure prediction of induction motors.

2.6 Artificial Neural Network

According to Jha (2013), Artificial Neural Network (ANN) is a non-linear mapping structure inspired by observed process in natural network of neurons in the human brain. It consists of highly interconnected simple computational units called neurons. It imitates the learning process of the human brain and can process problems which involve complex, non-linear, imprecise and noisy data. It is ideally suited for modelling and predicting the outcome of new independent input data after training.

ANNs are parallel computational models consisting of densely interconnected adaptive processing units. They are used for a wide variety of applications where statistical methods are traditionally employed. ANN is therefore being recognised as a powerful tool for data analysis. By their adaptive nature, “learning by example” replaces “programming” in solving problems. This feature makes such computational models very appealing especially in application domains where a problem to be solved is not understood fully but training data is readily available. Backpropagation algorithm is the most widely used learning algorithm in an ANN. Various types of ANN include Multilayered Perceptron, Radial Basis Function and Kohonen networks. In fact majority of the networks are more closely related to traditional mathematical and/or statistical models such as non-parametric pattern classifiers, clustering algorithms, non-linear filters, and statistical regression models than they are to neurobiology models.

ANNs are constructed with layers of units. All units in a particular layer perform similar tasks. The first and last layers of a multilayer ANN consist of input units (independent variables) and output units (dependent or response variables) respectively. All other units (hidden units) make up the hidden layer. The behaviour of a unit is governed by an input function and an output or activation function. These functions are normally the same for all units within the whole ANN. Input into a node is a weighted sum of outputs from nodes connected to it. There exists a threshold term which is a baseline input to a node in the absence of any other inputs. A weight is termed inhibitory if it is negative as it decreases net input, otherwise it is called excitatory.

Each unit takes its net input and applies an activation function to it. In instances where the inputs and outputs are binary encoded, the threshold function becomes very useful. The activation function mainly maps the outlying values of the obtained neural input back to a

bounded interval. The activation function shows a great variety. However, most common choice is the sigmoid function since it maps a wide domain of values into the interval.

2.6.1 Development of an ANN Model

A neural network forecasting model is developed by the following steps:

- i. Variable selection;
- ii. Formation of training, testing and validation sets;
- iii. Neural network architecture; and
- iv. Model building.

Suitable variable selection procedures are used to select the input variables important for modelling or forecasting variable(s) under study in the first step. This is followed by the formation of three distinct data sets called training, testing and validation sets. These data sets are used by the neural network not only to learn current data patterns (training set) and evaluate the overall ability of the supposedly trained network (testing set) but also to check the performance of the trained network using the validation set. The third step defines the network structure which includes number of hidden layers and hidden nodes as well as the number of output nodes and the activation function. The next step involves model building.

The model of a very popular and frequently used multilayer feed forward neural network or multilayer perceptron (MLP) learned by back propagation algorithm is constructed based on supervised procedure or on examples of data with known output. The examples presented are assumed to implicitly contain the information necessary to establish the relation for building the model. An MLP allows prediction of an output object for a given input object. Its non-linear elements or neurons are arranged in successive layers with a unidirectional flow of information from input layer to output layer through hidden layer(s). With adequate data, only one hidden layer is always sufficient for an MLP as it can learn to approximate virtually any function to any degree of accuracy. MLPs are therefore also known as universal approximates. Generally, learning methods in neural networks are classified into three basic types, namely, supervised learning, unsupervised learning or reinforced learning. A neural network learns off-line if the learning phase and the operation phase are distinct. On-line learning occurs when it learns and operates at the same time. Supervised learning is usually performed off-line based on training data, whereas unsupervised learning is performed on-

line based on given data. In reinforced learning, data is usually not given, but generated by interactions with the environment.

2.6.2 Architecture of Neural Networks

The two most widely used ANN architecture are the feed-forward networks and the feedback or recurrent networks. Other types of ANN architecture include stochastic network, physical network, bi-directional network, Elman and Jordan network, Hopfield network, self-organising map and long short-term memory networks. Feed-forward networks have no feedback loops and are extensively used in pattern recognition. Thus, signals are allowed to travel one way only; from input to output. In feedback networks however, signals do not travel in one way only due to the presence of a feedback loop. In addition, their state changes continuously (dynamic) until an equilibrium point is reached. They remain at this point until the input changes and a new equilibrium needs to be found.

The MLP network is trained using a supervised learning algorithm like the backpropagation algorithm. The backpropagation algorithm uses data to adjust the network's weights and thresholds so as to reduce the error in its prediction on the training set. It computes how fast the error, which is the difference between the actual and the desired activity, changes due to an alteration in:

- i. The activity of an output unit;
- ii. The total input received by an output unit;
- iii. Weight on the connection into an output unit; and
- iv. The activity of a unit in the previous layer.

2.6.3 Uses and Applications of Neural Networks

According to (Anon, 2018c), Artificial neural networks can be used for;

- i. Classification: The aim is to predict the class of an input vector;
- ii. Pattern matching: The aim is to produce a pattern best associated with a given input vector;
- iii. Pattern completion: The aim is to complete the missing parts of a given input vector;

- iv. Optimisation: The aim is to find the optimal values of parameters in an optimisation problem;
- v. Control: An appropriate action is suggested based on given input vectors;
- vi. Function approximation/times series modelling: The aim is to learn the functional relationships between input and desired output vectors; and
- vii. Data mining: With the aim of discovering hidden patterns from data (knowledge discovery).

A 1988 Defense Advanced Research Project Agent (DARPA) Neural Network Study, (DARPA88) lists various neural network applications, beginning with the adaptive channel equalizer in about 1984. This device, which is an outstanding commercial success, is a single-neuron network used in long distance telephone systems to stabilize voice signals. The DARPA report goes on to list other commercial applications, including a small word recognizer, a process monitor, a sonar classifier and a risk analysis system (Hagan *et al.*, 2014).

Thousands of neural networks have been applied in hundreds of fields in the many years since the DARPA report was written. A list of some of those applications follows:

- i. Aerospace: High performance aircraft autopilots, flight path simulations, aircraft control systems, autopilot enhancements, aircraft component simulations, aircraft component fault detectors;
- ii. Automotive: Automobile automatic guidance systems, fuel injector control, automatic braking systems, misfire detection, virtual emission sensors, warranty activity analyzers;
- iii. Banking: Check and other document readers, credit application evaluators, cash forecasting, firm classification, exchange rate forecasting, predicting loan recovery rates, measuring credit risk;
- iv. Defense: Weapon steering, target tracking, object discrimination, facial recognition, new kinds of sensors, sonar, radar and image signal processing including data compression, feature extraction and noise suppression, signal/image identification;
- v. Electronics: Code sequence prediction, integrated circuit chip layout, process control, chip failure analysis, machine vision, voice synthesis, nonlinear modelling;

- vi. Entertainment: Animation, special effects, market forecasting;
- vii. Financial: Real estate appraisal, loan advisor, mortgage screening, corporate bond rating, credit line use analysis, portfolio trading program, corporate financial analysis, and currency price prediction;
- viii. Insurance: Policy application evaluation, product optimization;
- ix. Manufacturing: Manufacturing process control, product design and analysis, process and machine diagnosis, real-time particle identification, visual quality inspection systems, beer testing, welding quality analysis, paper quality prediction, computer chip quality analysis, analysis of grinding operations, chemical product design analysis, machine maintenance analysis, project bidding, planning and management, dynamic modelling of chemical process systems;
- x. Medical: Breast cancer cell analysis, EEG and ECG analysis, prosthesis design, optimization of transplant times, hospital expense reduction, hospital quality improvement, emergency room test advisement;
- xi. Oil and Gas: Exploration, smart sensors, reservoir modelling, well treatment decisions, seismic interpretation;
- xii. Robotics: Trajectory control, forklift robot, manipulator controllers, vision systems, autonomous vehicles;
- xiii. Speech: Speech recognition, speech compression, vowel classification, text to speech synthesis;
- xiv. Securities: Market analysis, automatic bond rating, stock trading advisory systems;
- xv. Telecommunications: Image and data compression, automated information services, real-time translation of spoken language, customer payment processing systems; and
- xvi. Transportation: Truck brake diagnosis systems, vehicle scheduling, routing systems; In conclusion, the number of neural network applications, the money that has been invested in neural network software and hardware, and the depth and breadth of interest in these devices is enormous (Hagan *et al.*, 2014).

2.7 Related Works

Bhowmik *et al.* (2013) reviewed methods of diagnosing and monitoring fault in induction motors. Various techniques, models and algorithms in detecting different types of motor faults were analysed briefly. This paper however suggested the enhancement of monitoring systems for diagnosis by the combination of Artificial Neural Networks and expert knowledge.

Eltabach *et al.* (2004) presented a paper that looked at failure predictions in three-phase line-operated induction machines through spectral analysis of electric and electromagnetic signals. Fault characteristics frequencies generated in the estimated and the measured signal spectrum, as a result of broken rotor bar which is a mechanical abnormality, were analysed. Thus, external and internal methods of diagnosis based respectively on spectral analysis of stator current or instantaneous electric powers and electromagnetic torque computed by stator or rotor flux estimation, were compared for broken rotor bar detection in induction motors.

Han *et al.* (2006) proposed an online fault diagnosis system for induction motors through the combination of Discrete Wavelet Transforms (DWT), feature extraction, genetic algorithm (GA), and Artificial Neural Networks (ANN) techniques. The combination of advanced techniques reduces the learning times and increases the diagnosis accuracy. ANN has gained popularity over other techniques, as it is efficient in discovering similarities among large bodies of data and can represent any nonlinear model without knowledge of its actual structure and can give results in a short time during the recall phase.

Bachir *et al.* (2006) proposed a diagnosis procedure based on parameter estimation of the stator and rotor faults occurring in a squirrel-cage induction motor. First, a study of an original model of the machine was made taking into account the effects of inter-turn faults resulting in the shorting of one or more circuits of stator-phase winding. Thus, additional parameters were introduced to explain the fault in the three stator phases. A new faulty model dedicated to broken rotor bars detection was then proposed using the estimation technique which was performed by taking into account prior information available on the safe system operating in nominal conditions. On the whole, a special three-phase induction machine was designed and constructed in order to simulate true faulty experiments.

Experimental test results showed good agreement and demonstrated the possibility of detection and localisation of previous failures.

Kadir *et al.* (2006) proposed an algorithm for the control of AC induction motors and the power inverter with embedded systems fault prediction and diagnosis. This algorithm was implemented using a dual core digital signal processor. It employed various techniques for detecting and predicting different faults of the AC drive system.

Antonino-Daviu *et al.* (2006) proposed a method for the diagnosis of rotor bar failures in induction machines, based on the analysis of the stator current during the start up using the discrete wavelet transform. The result of this approach was compared with those obtained from classical Fourier analysis of the stator current in steady state. The reliability of the proposed method for the diagnosis of bar breakages was similar to that of the classical approach in the case of loaded motors, but, in addition, the method could detect faults in an unloaded condition. The method also allowed a correct diagnosis of a healthy machine in some particular cases where Fourier analysis led to an incorrect fault diagnosis.

Ballal *et al.* (2007) combined positive features of neural networks and fuzzy logic together for the detection of stator inter-turn insulation and bearing wear faults in single-phase induction motor. Thus, adaptive neural fuzzy inference systems were developed for the detection of these two faults. Motor intakes current, speed, winding temperature, bearing temperature, and the noise of the machine were the measurable input parameters used to generate experimental data. Simulation results revealed that the five input parameter system predicted more accurate results.

Rangel-Magdaleno *et al.* (2009) presented a novel methodology for online half-broken-rotor detection on induction motors. They combined current and vibration analysis correlating the signal spectra to enhance detectability for mechanically loaded and unloaded operating conditions of the motor, which the other isolated techniques are unable to detect. The proposed methodology was implemented in a low-cost Field-Programmable Gate Array (FPGA), giving a special purpose System-On-a-Chip (SOC) solution for online operation, with the development of a complex post processing decision making unit.

Ghate and Dudul (2011) developed the radial-basis-function-multilayer-perceptron cascade connection neural-network based fault detection scheme for the small and medium sizes of three-phase induction motors. Simple statistical parameters of stator current were

considered as input features and experimental results showed ability of the proposed classifier for detecting faults such as stator winding inter-turn short and/or rotor eccentricity. The network was tested for good classification accuracy with enough robustness to noises. The classifier was then found to be suitable for real world applications.

Hu *et al.* (2011) proposed a novel transform demodulation algorithm as a means of extracting signature frequency components of faults and easily detect incipient fault of induction motors which otherwise, was a key problem in motor current signature analysis technique. With both simulated and experimental data of broken rotor bars, the ability of the proposed algorithm to extract more detailed fault signature frequency components and realize the incipient fault detection of induction motors was shown.

Suwatthikul and Sornmuang (2011) presented an application of an adaptive network based fuzzy inference system for diagnosing faults in the bearing shield of a single-phase induction motor. The experimental results showed that the vibration parameters can efficiently indicate the occurrence of the faults which can be detected by the system.

Kraleti *et al.* (2012) presented a paper on model based diagnostics and prognostics of three-phase induction motor for vapour compressor applications. Faults under consideration were incipient electrical faults: insulation degradation and broken rotor bars. Two online approximators were used to discover the system parameter degradation and facilitate fault isolation, or root-cause analysis, and a Time To Failure (TTF) prediction before the occurrence of a failure.

Yu *et al.* (2014) developed a model-based Remaining Useful Life (RUL) prediction method for induction motor with stator winding short circuit fault. The induction motor model with stator winding short circuit fault is introduced based on reference frame transformation theory. A particle filter method is used to realize unknown parameter estimation and RUL prediction. Simulation results were provided to validate the proposed method.

Morsalin *et al.* (2014) proposed an innovative idea to detect induction motor stator's inter-turn short circuit fault using non-invasive heuristic approach by Artificial Neural Network (ANN). In this fault detection research, a 0.5 hp, single phase 50 Hz induction motor at no load condition is used as an experimental prototype. Generalized Feed forward neural network is used as NN with Levenberg Marquardt gradient descend algorithm for training.

Araujo *et al.* (2015) provided an analysis about early incipient and recurring failures in three-phase induction motor bearings when driven by pulse width modulation inverters, focusing on a real industrial process. Over the investigation, it was concluded, that the presence of common-mode currents at the verified levels could cause damages to the motor bearings, which was confirmed when the machine stopped working due to another bearing failure.

Mahmoud *et al.* (2016) proposed an inverse approach for inter-turn fault detection in asynchronous machines using magnetic pendulous oscillation technique. The machine behaviour was simulated under healthy and faulty cases in both transient and steady state conditions. The proposed inverse problem was validated numerically and experimentally. Results showed the robustness of the proposed scheme against the measurement noise.

Kayri (2016) did a comparative study on the predictive ability of Bayesian regularization with levenberg-marquardt artificial neural networks. Analysis were done by Sum Squared Error (SSE), Sum Squared Weight (SSW) and correlation of regression and concluded that the Bayesian regularization training algorithm shows better performance than the levenberg-marquardt algorithm.

Lizarraga-Morales *et al.* (2017) proposed a novel FPGA-based methodology for early broken rotor bar (BRB) detection and classification through homogeneity estimation. Obtained results demonstrated the high efficiency of the proposed methodology as a deterministic technique for incipient BRB diagnosis in induction motors, which can detect and differentiate among half, one, or two BRBs with very high accuracy.

The use of ANN's in predicting failure of 5.8 MW 11kV motor on nominal load provides a new area of research. The network is a generalised feed-forward network and the input data samples are current, winding temperatures and power all in the time domain.

2.8 Summary

In this chapter, construction and working of three phase induction motors as well as various faults associated with their operation have been discussed. In addition, several research works which employ various techniques in failure prediction of induction motors have been reviewed. This work however employs the use of artificial neural networks for failure prediction of three phase induction motors in the industry. Subsequent chapters reveal how this methodology is carried out and its validation by means of simulation results.

CHAPTER 3

SAG MILL MOTOR

3.1 Introduction

The SAG Mill motor is a three phase, slipring induction motor of the type CSLGH 900/6-214, manufactured by ABB, Australia and supplied by Polysius to Goldfields, Damang mine in 1997. The motor has a vertical drive shaft and drives a SAG Mill of size 8M×5.1M which is the first stage of grinding at the milling circuit of the carbon in leach (CIL) plant. The motor has a starting torque of at least 1.3×rated load torque and a maximum of 2.0×rated load torque. The motor has an installed flanged-on tachogenerator. It has slip energy recovery system and a constant load torque over the speed range with single-quadrant operation sufficing. The winding, bearing and air circulation temperatures are monitored using PT100 transducers (three-wire system). Measuring transducers with galvanic isolation are installed in the service cabinet for remote indication of motor current and motor speed (measuring signal 4-20 MA) with feedback converter transformer. The motor is connected to the mill through coupling and mounted on foundation blocks by machine/bag bolts. It is started by liquid starters and has installed fans for cooling. The motor also has oil supply unit for motor bearing lubrication. Fig. 3.1, 3.2 and 3.3 shows the photograph of the non-drive, drive and side view of the SAG Mill Motor respectively.



Fig. 3.1 Non-drive Side of the SAG Mill Motor

3.1.1 The SAG Mill Motor Rating

Table 3.1 below highlights the SAG Mill motor rating from the manufacturer;

Table 3.1 SAG Mill Motor Rating

TYPE	CSLGH 900/6-214
MANUFACTURER	ABB
NECESSARY MOTOR RATING	P = 5 650 kW
TYPE RATING ACC. TO CATALOGUE	P = 6 350 kW
MOTOR RATING (REDUCED/INCREASED)	P = 5 800 kW
SPEED RANGE	N = 788-970 per min.
VOLTAGE /FREQUENCY	U = 11 000 V / F = 50 Hz.
RATED CURRENT	I = 353 A
TYPE OF PROTECTION	IP 56/65
TYPE OF CONSTRUCTION	IM B3
FRAME SIZE (IEC-PUBL.);	
EFFICIENCY ; COS PHI	97% / 0.89
STANDSTILL VOLTAGE OF ROTOR	$U_2 = 2\ 640\ V$
ROTOR CURRENT	$I_2 = 1\ 305\ A$
DIRECTION OF ROTATION (FACING DRIVE END)	ANTICLOCKWISE
WEIGHT	33 700 kg.

(Source: Anon, 1997)



Fig. 3.2 Drive Side of the SAG Mill Motor



Fig. 3.3 Side View of the SAG Mill Motor

3.2 Main Components of SAG Mill Motor

3.2.1 Cooling Fans

The SAG Mill Motor is fitted with cooling fans at different locations on the motor for the air circuit. One fan is located at the slipring compartment for cooling, two separate fans are located inside the motor for the internal air circuit and three fans are also mounted on top of the motor for external air circuit.

Table 3.2, 3.3 and 3.4 below shows the ratings of the motors for external air circuit, internal air circuit and slipring compartment respectively;

- i. External Air Circuit

Table 3.2 SAG Mill External Air Circuit Motor Rating

TYPE	DX 100L
MANUFACTURER	SIEMENS
NECESSARY MOTOR RATING	P = 3 kW
TYPE RATING ACCORDING TO CAT.	P = 3 kW
SPEED RANGE	N = 2 900 per min.
VOLTAGE / FREQUENCY	U = 415 V / F = 50 Hz
RATED CURRENT	I = 5.7 A
TYPE OF PROTECTION	IP 55
TYPE OF CONSTRUCTION	IM B5
EFFICIENCY / COS PHI	80% / 0.92
WEIGHT	30 kg.

(Source: Anon, 1997)

ii. Internal Air Circuit

Table 3.3 SAG Mill Internal Air Circuit Motor Rating

TYPE	D132S – 4
MANUFACTURER	SIEMENS
NECESSARY MOTOR RATING	P = 5.5 kW
TYPE RATING ACCORDING TO CAT.	P = 5.5 kW
SPEED RANGE	N = 1 450 per min.
VOLTAGE / FREQUENCY	U = 415 V / F = 50 Hz
RATED CURRENT	I = 11.1 A
TYPE OF PROTECTION	IP 55
TYPE OF CONSTRUCTION	IM VI
FRAME SIZE (IEC – PUBL)	132 S
EFFICIENCY / COS PHI	80% / 0.81
WEIGHT	60 kg

(Source: Anon, 1997)

3.2.2 Carbon Brush and Sliprings

The sliprings are the current link between the rotor winding and the stationary brushes. Asynchronous and Synchronous machines with fixed brushes are fitted with steel or bronze sliprings. The slipring contact surface is machined with a spiral type grooving. After being in operation for some time a patina will form on the slipring contacts surface.

A carbon brush is a sliding contact used to transmit electrical current from a static to a rotating part in a motor or generator, and as regards DC machines, ensures a spark-free commutation. A carbon brush can be made of one or more carbon blocks or equipped with one or more shorts/terminals (Anon, 2019b).

iii. Slipping Compartment

Table 3.4 SAG Mill Slipping Compartment Motor Rating

TYPE	D 100L – 4
MANUFACTURER	SIEMENS
NECESSARY MOTOR RATING	P = 3 kW
TYPE RATING ACCORDING TO CAT.	P = 3 kW
SPEED RANGE	N = 1 430 per min.
VOLTAGE / FREQUENCY	U = 415 V / F = 50 Hz
RATED CURRENT	I = 6.3 A
TYPE OF PROTECTION	IP 55
TYPE OF CONSTRUCTION	IM VI
FRAME SIZE (IEC – PUBL)	100 L
EFFICIENCY / COS PHI	80% / 0.83
WEIGHT	30 kg.

(Source: Anon, 1997)

Commissioning

When a wound rotor induction motor is put into service for the first time, the patina on the sliprings is usually not sufficiently developed to produce the minimum brush wear. If then, the machine is run at no-load for several hours e.g. as in cascade drive systems, a considerably higher than normal brush wear must be reckoned with. This can result in leakage paths being quickly converted by a layer of carbon dust thus creating an increased risk of flash-over.

In order to prevent damage, the following checks are to be carried out during the commissioning period.

- i. Record length of brushes: After approximately 10 hours of operation, measure and record the overall length of one brush per track on each slipping as shown in Fig. 3.4 (Anon, 1997).

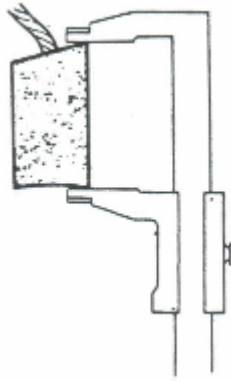


Fig. 3.4 Measurement of the Carbon brush

- ii. Determine brush wear: Measure length of brushes at intervals of 30 hours and evaluate brush wear. When a brush wear of 4-5 mm has been recorded since the first check then clean the insulating paths on the sliprings and on the brush gear. When the brush wear is less, the intervals between checks can be increased to 60 hours, whereby cleaning should be done every 4-5 mm of brush wear as shown in Fig. 3.5 (Anon, 1997).
- iii. Normal operational condition: The brushes may be considered as being run-in when the wear is less than 6 mm/1000 hours. The brush gear is then to be maintained as indicated in the maintenance plan. The responsibility for ensuring that this instruction is followed lies with the commissioning personnel.

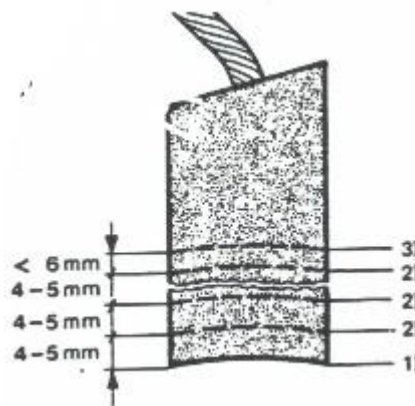


Fig. 3.5 Carbon Brush wear measurement

Inspection work during normal operation of brushes

Check the brushes at intervals indicated in the maintenance plan for wear and freedom of movement in the brush-holders. Every brush should rest on the slipring with its whole contact surface which should be smooth and free of scores and grooves.

Cleaning work on the brush

The brush-holders, carrier bolt insulation, the insulation between the sliprings, and the shaft lead bolts are all to be cleaned every time the brushes are changed.

The brush gear and the slipring compartment are to be checked for degree of dirt deposit every month and are to be cleaned every three months. It is recommended that this work be planned for inclusion in general machine maintenance or periods of shut-down.

The brush gear must never be cleaned with solvents. Brushes, brush-holders and sliprings are best cleaned of carbon dust with a vacuum cleaner, then blown down with a strong blast of compressed air and finally rubbed down with clean dry cloths. Only small cloths should be used, and they should be changed frequently. This ensures that the carbon dust will be properly removed and not distributed or rubbed into the surface being cleaned. During operation, an oxide film containing graphite forms on the sliprings. When complete (> 1000 service hours), this film (patina) should have a smooth surface with an appearance giving a reflection between mat and a silky gloss. The film hue may be light grey to black, depending on the brush grade, the current density, atmospheric humidity and temperature. The most important criterion for satisfactory service is the uniformity of the film over the width and circumference of the sliprings, i.e. it should not be streaky, stained or broken.

It is important to note that the oxide film must not be destroyed by unnecessary grinding or handstoning, not even when replacing the brushes. Only in the case of firmly adhered deposits of oil and carbon dust is wet cleaning with Sangajol (white spirit) permitted, in which case all brushes are to be removed before starting. After cleaning, blow the brush gear down with compressed air and dry down using clean oil-free cloths. The brushes may only be refitted approximately 24 hours afterwards by which time possible residual solvent will have completely evaporated. In order to ensure that the brushes are refitted into their original brush-holders, it is recommended that all be labelled with matching numbers before brush removal.

The brushes of other machines in the same room, whether stationary or running, will also be endangered by the solvent vapour. However, they can be protected by providing a

generous flow of fresh air at their locations. Preference is to be given to those solvents with the lowest possible aromatic content.

Changing the brushes

Changing the brushes while the machine is running is extremely dangerous for both personnel and machine. Therefore brushes should only be changed when the machine is switched off and at rest. One side face of each slipring is provided with a notch to indicate the limit of wear. When worn to this notch, brushes must be replaced with new ones of identical quality. To check the brushes, they must be pulled from the brush-holders when the machine is shut-down. When not more than 1/3 of the brushes per slipring are to be changed, they need not be ground in. They will run in naturally within 1-2 weeks. Subsequently to this running-in period, further brushes can be changed on the same slipring if necessary. It is only necessary to grind the brushes in when a larger number or all of the brushes are to be changed simultaneously.

Machines with brush-wear supervision

If the machine is provided with brush-wear supervision, then the following points must also be observed;

- i. One brush with a signal contact is provided for each track. When the brush wear reaches a certain limit these monitoring brushes give a signal to initiate alarm.
- ii. After alarm annunciation, the brushes must be changed within the next 200 hours of operation. All the brushes of the same track should have the same amount of wear as the monitoring brush i.e. all should be changed simultaneously.

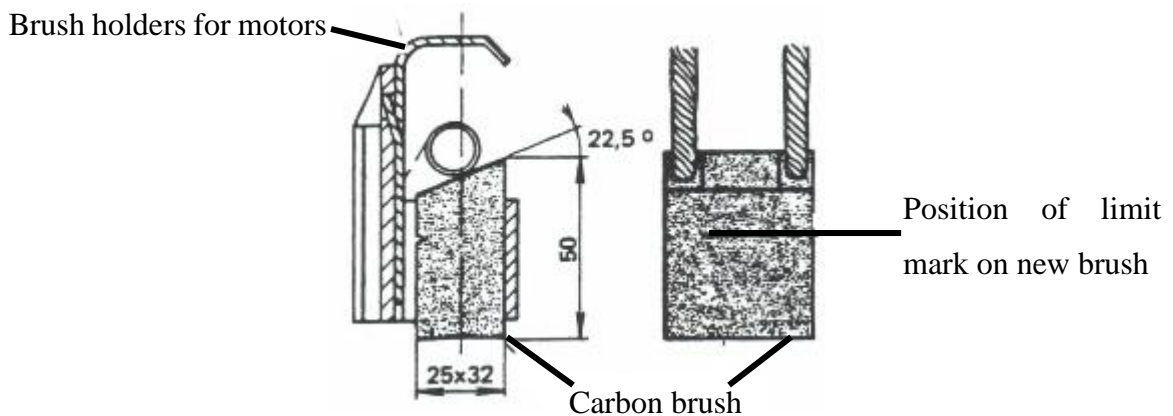


Fig. 3.6 Carbon Brush and Holders

Grinding in the brushes

For this operation, a long strip of emery cloth is inserted underneath the brushes and each brush in turn lapped (in the direction of rotation) by pulling the strip to and fro (the brush must be lifted off the emery cloth at each “return” stroke, i.e. against direction of rotation). Satisfactory lapping is indicated by a complete circular arc on the contact surface of the brushes, showing a slightly greater curvature than the contact surface of the sliprings. This difference is caused by the thickness of the emery cloth, and disappears after the first few hours of operation. The sliprings, brushes and brush-holders are thoroughly cleaned after the grinding process. Fig. 3.6 shows the carbon brush and brush-holders (Anon, 1997).

Trueing the sliprings

Sliprings which are out-of-round, heavily scored, or rough, should be carefully skimmed true on a lathe or ground with a fine oil stone. The surface roughness condition (Ra denotes ‘Center Line Average value CLA’ for England or ‘Arithmetical Average AA’ for USA) must be N7 (0.0016 mm). After reworking, chamfer the edges of the spiral grooving as shown in Fig. 3.7 (Anon, 1997).

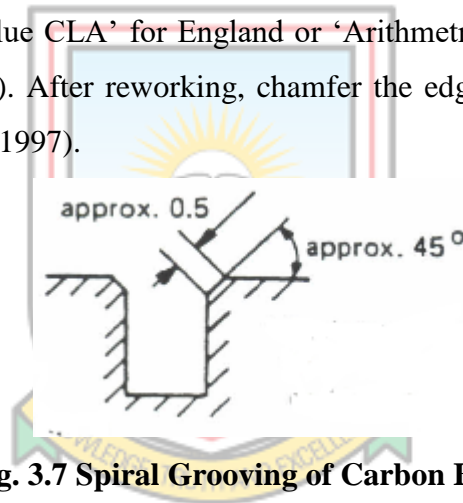


Fig. 3.7 Spiral Grooving of Carbon Brush

Brush-holders

There should be a gap of about 2 mm between the slipring and the brush-holder frames. The brush-holders should always be reset for this clearance after trueing the slings.

Number of brushes

The number of brushes per slipring is based on a nominal loading of 100 A/brush. The original brush arrangement may not be changed without first consulting the machine manufacturer.

Brush pressure

The correct average brush pressure is approximately 2 N/cm². The brush-holder spring force is 16 N. Fig. 3.8 shows the position of carbon brushes on the sliprings (Anon, 1997).

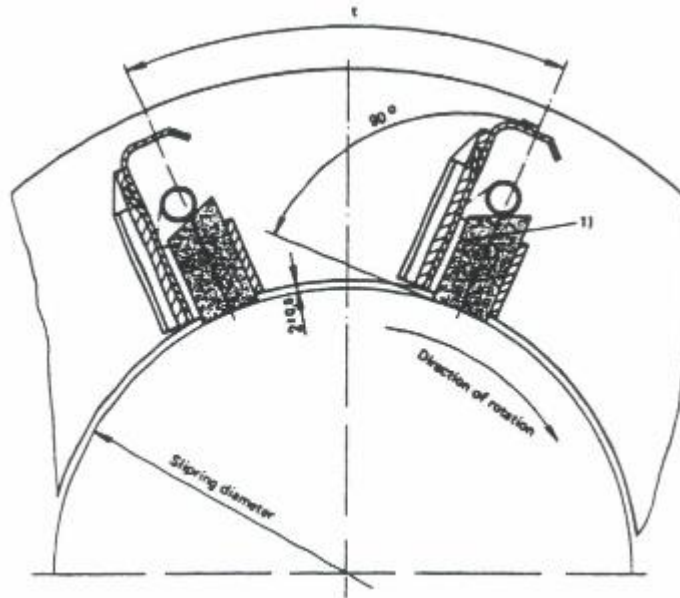


Fig. 3.8 Positioning of Carbon Brushes on Sliprings

3.2.3 Windings

The SAG Mill Motor uses Micadur-Compact (MC[®]) windings. Full impregnation of all winding components with a curable resin under vacuum is the characteristic feature of the Micadur-Compact winding insulation system used for medium-sized and large high-voltage machines. Subsequent curing of the resin results in a completely rigid winding bonded to the walls of the slots, having excellent mechanical and electrical properties. There has been no evidence so far of any of the dielectric or thermal ageing effects which indicate basically vulnerable parts of the insulation. Any repair procedure specifically drawn up for MC windings must therefore be able to meet the following essential requirements.

- i. The method of repair must primarily be suitable for the replacement of parts of windings which have suffered mechanical damage, and to a lesser extent dielectric or thermal damage. The parts of the overhang (or end-coils) prone to damage are those nearest the air-gap, or the winding head (coil ends).
- ii. The method of repair must be applicable to the facilities available at the site (ovens, vacuum tank, tools, personnel, etc.), due allowance being made for the particular needs of a curable resin.
- iii. Adequate stocks of spare materials must be kept in order that the time for delivery may be as short as possible.
- iv. Spare materials not suitable for storage must be obtainable at short notice.

The windings are fitted with resistance temperature detectors (RTD's) with alarm and trip settings of 145°C and 150°C respectively (Anon, 1997).

3.2.4 Bearings

The SAG Mill Motor is fixed with oil lubricated sleeve bearings supporting the drive and non-drive ends of the main rotor and shaft. Sleeve bearings operate with a thin film of oil between the shaft and journal, and thus theoretically with continuous non-stopping operation are non-wearing and do not have a limited life. Therefore selection criteria do not depend on a life calculation, but it rather relates to loading, which for these motors is advised as follows;

- i. Drive end bearing: Specific bearing loading (excluding UMP) = 1.11 N/mm².
- ii. Non-Drive end bearing: Specific bearing loading (excluding UMP) = 0.56 N/mm².

The life calculation referred to is only applicable to antifricition (i.e. grease lubricated ball & roller type bearings), which are not fitted to the main motor shaft.

Fig. 3.9 shows a picture of the bearing lubrication plate (Anon, 1997). The bearing is also fitted with temperature detectors (RTD's) with an alarm and trip settings of 85°C and 95°C respectively.

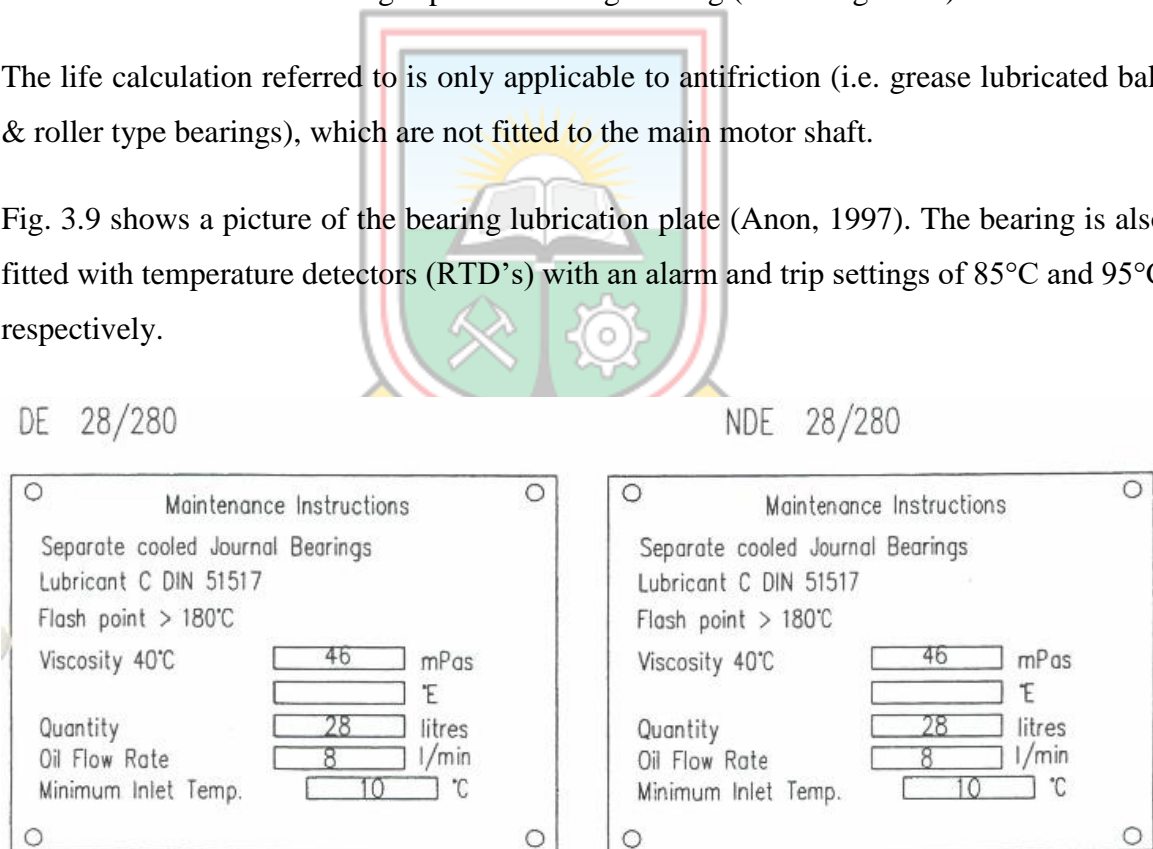


Fig. 3.9 Bearing Lubrication Plate

Oil change

Oil changing is largely dependent upon the operating time, the number of switching operations, the operating temperatures and the amount of oil contamination. An oil change

can also be necessitated by strong turbidity or by a sudden increase in temperature without any external influence.

Maintenance

Table 3.5 shows the maintenance plan for the bearings.

Table 3.5 Maintenance Plan for Bearings

Part of Machine	Maintenance or Inspection Work	Time Interval
Plain bearings and oil supply system for flood or jacking oil	Check physical, chemical and mechanical properties of the oil.	Before first commissioning After 6 months 1) After 18 months 1)
	Check condition of oil through sight window (discolouring, contamination), possibly clean and re-use.	After 6 months 1) After 18 months 1)
	Measure and record temperature at measuring points provided, by hand checks or by thermometer if fitted.	Weekly 2)
	Measure machine vibration using either the vibration sensors if provided or a transportable measuring instrument. Measuring points: middle of bearing housing, horizontal and vertical.	Monthly 2)
	Check oil rings for smooth, uniform running and oil transport. This can be done through openings in bearing housings. Only applicable for horizontal machines.	Monthly 2)
	Check bearing seals for oil leakage and clean if dirty.	Monthly 2)
Oil supply unit for flood or jacking oil	Check oil supply unit with regard to following: Proper operation Oil level, leakage incl. bolted connections, seals on bearing oil piping, Clean filters.	Monthly 2) After indication from filter monitor (optical/electrical)
Plain bearings with insulated shells (only horizontal machines)	Check bearing shell insulation.	Before first commissioning Quarterly 1)
Plain bearings	Visually inspect sliding faces of bearing components for edge pressure, scoring, pressure marks, and eliminate same if present. The bearing components must be dismantled for this inspection. In the case of strong turbidity, immediately change oil and determine and eliminate cause.	6 months after first commissioning, 18 months after first commissioning

Table 3.5 Maintenance Plan for Bearings Cont'd

Part of Machine	Maintenance or Inspection Work	Time Interval
Plain bearings and oil supply unit for flood or jacking oil	Change oil. Wash and flush off bearings	Annually 2) 3)
	Replace worn parts (If bearing parts are changed, change oil after 3 hours running time to remove metal particles rubbed off during running in).	After evaluation of above-mentioned periodical inspection.
	Check for rust	At Overhaul 4)
Oil-water cooler (If provided)	Check water piping for leakage.	Weekly 1)
	Check inner surfaces of cooler tubes for deposits and possible signs of corrosion.	Every 2 years 1)
1) Compare with earlier measurements and observations. 2) Valid when no special measures taken to extend oil change interval. 3) After 4000 hours of operation or 1 year at the latest. This also applies to machines often stationary. 4) Remove possible rust by using a fine oil stone. Where painting is not possible, coat bare surfaces with an anti-corrosion covering.		

(Source: Anon, 1997)

3.3 The Liquid Starter

The SAG Mill Motor uses EPM liquid rotor starter to control its starting and the starting current is generally limited to a maximum of 250% full load current (FLC). Optimal starting torque for each application is normally selected by the choice of the initial value of resistance. The principle of the EPM starter is that, the resistance automatically varies during the starting period. This type of starter is designed to provide the optimum starting characteristics, which results in smooth progressive acceleration to full load speed. It can also be used for speed variation and torque control. Plug braking can also be implemented with this system. The variation in the resistance is achieved by displacement of the electrodes in the electrolyte. At the end of the acceleration, the electrodes are shorted out.

3.3.1 Electrodes

The three electrodes are arranged in a line and each comprises of a fixed and a moving electrode. Polypropylene compartmentalisation ensures isolation between the phases. The electrodes, cast in GS or bronze consist of concentric cylinders which merge with each other in the minimum resistance position. The fixed electrodes, situated at the lower end of the isolated compartments, are fed from an insulated copper bar. Since this bar does not pass through the wall of the tank, it is impossible for the electrolyte to leak. Fig. 3.10 shows the

electrode arrangement (Anon, 1997). The moving electrodes travel vertically inside an isolated compartment guided by a nylon slide. The assembly is supported by two story brass rods mounted on the moving electrode system. This assembly, common to all three electrodes, constitutes the neutral point. The low current density in the order of 1A per cm², ensures an extremely long electrode life.

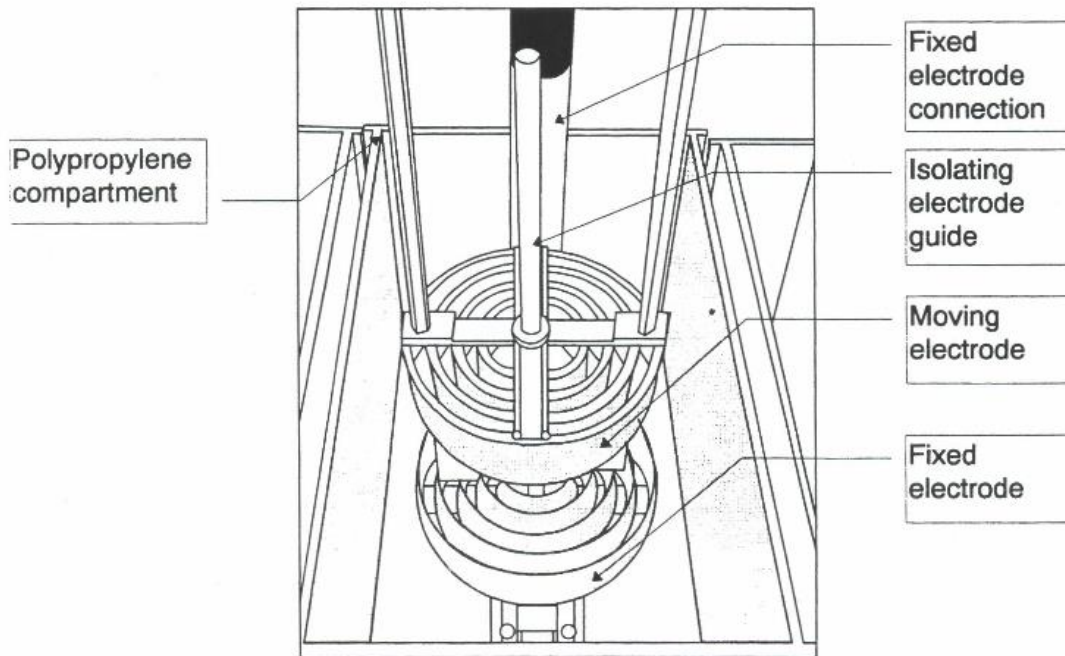


Fig. 3.10 Electrolytic Resistance (Electrodes)

3.3.2 Control

Displacement of the moving electrode assembly is controlled by a motor driven worm screw assembly (geared motor, motor together with an electronic speed controller, servo motor). A hand wheel is used for commissioning and emergency operation. The standard starting or regulation time is approximately 20 seconds. It has two auxiliary limit switches (1×Start and 1×Final position of starter) which eliminates the residual resistance at the end of starting. The overload relay will trip the electrode control motor if an accidental blockage occurs. An electrical interlock prevents a new start if the moving electrodes are not at the start position. The return to the start position is automatically effected after the shorting contactor is closed. If a power failure occurs during starting, the electrodes return automatically to the start position. When the supply is restored, a new start cycle is possible. It has a temperature

monitor and filling level limit switch. Fig. 3.11 and Fig.3.12 shows the electrode control system and EPM starter with heat exchanger respectively (Anon, 1997).

The number of consecutive starts from cold condition is $Z = 3$ and frequency of starts from warm condition of starter is $H = 0.5 \times$ Per Hour.

Table 3.6 details the rating of the starter motor;

Table 3.6 Liquid Starter Motor Rating

TYPE	EPM 3/2 – EB 600 47 C9
MANUFACTURER	AOIP
NECESSARY MOTOR RATING	$P = 0.45$ kW
TYPE RATING ACCORDING TO CAT.	$P = 0.45$ kW
SPEED RANGE	$N = 279$ per min.
VOLTAGE / FREQUENCY	$U = 415$ V / $F = 50$ Hz
RATED CURRENT	$I = 1.2$ A
TYPE OF PROTECTION	IP 54
TYPE OF CONSTRUCTION	IM
WEIGHT	4 080 kg.

(Source: Anon, 1997)

3.3.3 Electrolyte

The electrolyte generally comprises a solution of sodium carbonate or sodium borate. The cooling of the electrolyte is effected by natural convection and forced circulation (via the agitator) but in this application, heat exchanger is employed to augment the heat dissipation.

Table 3.7 below details the rating of the starter agitator motor;

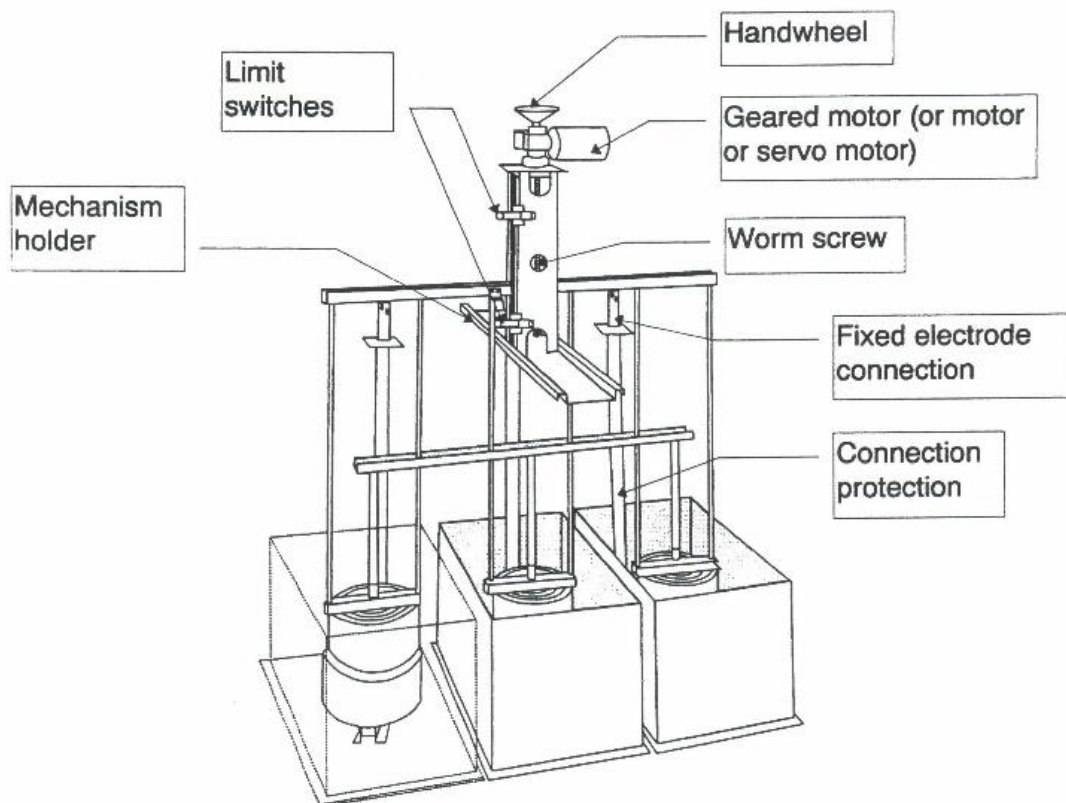


Fig. 3.11 Electrode Control System

Table 3.7 Liquid Starter Agitator Motor Rating

TYPE	MU71814 – EPM 3/2
MANUFACTURER	AOIP
NECESSARY MOTOR RATING	$P = 0.37 \text{ kW}$
TYPE RATING ACCORDING TO CAT.	$P = 0.37 \text{ kW}$
SPEED RANGE	$N = 1\ 400 \text{ per min.}$
VOLTAGE / FREQUENCY	$U = 415\text{V} / F = 50 \text{ Hz}$
RATED CURRENT	$I = 1.2 \text{ A}$
TYPE OF PROTECTION	IP 54
TYPE OF CONSTRUCTION	IM
EFFICIENCY / COS PHI	$\% / 0.60$

(Source: Anon, 1997)

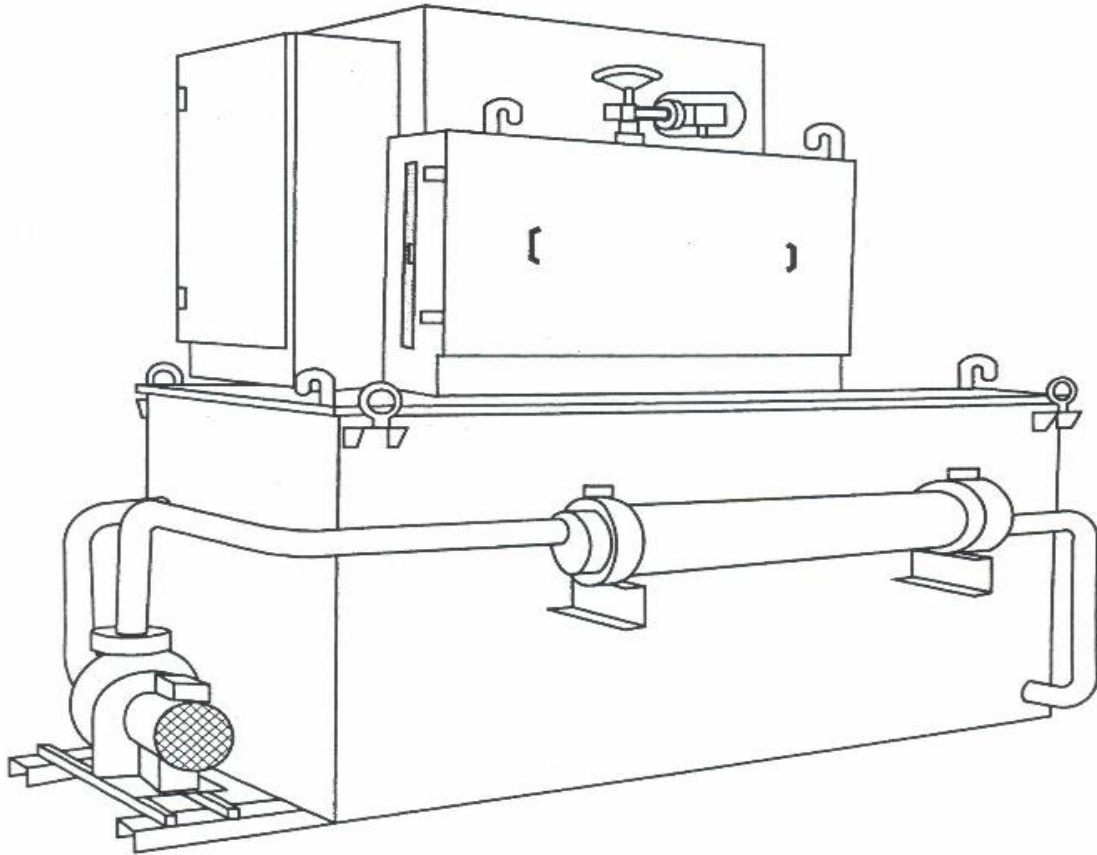


Fig. 3.12 EPM with Heat Exchanger

3.3.4 Enclosures

The starter comprises 1 medium voltage (MV) enclosure which contains the shorting contactor and 1 low voltage (LV) enclosure containing the controls. Dimensions of the MV enclosures depends on the shorting contactor rating. Power cables entry is carried out at the base. The cable guide plate of the enclosure should be drilled during installation. Cables come on the terminal outputs mounted on front of the enclosure as shown in Fig. 3.13 (Anon, 1997).

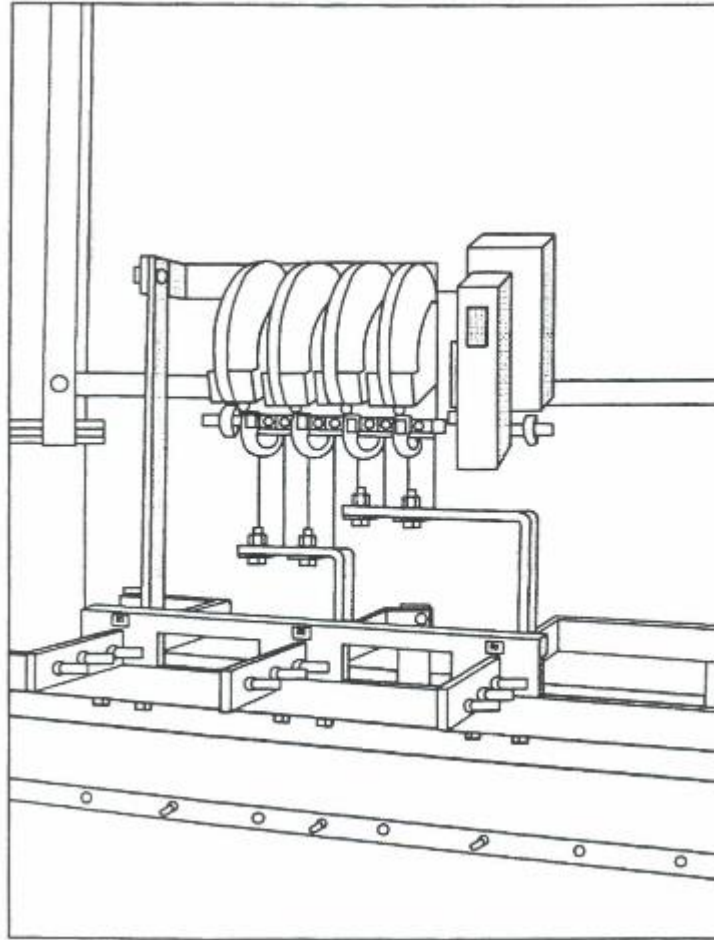


Fig. 3.13 EPM MV Enclosure

The controls are built – in the LV enclosure. This enclosure lies on the right part of the MV enclosure. Connecting the control cables is performed at the base through the back plate. Control cables come on the screw terminals as shown in Fig. 3.14 (Anon, 1997). Enclosure protection is IP 54

3.3.5 Maintenance

The electrode level must be checked and topped up with drinking water once a year. The electrode worm screw should also be greased at the same time.

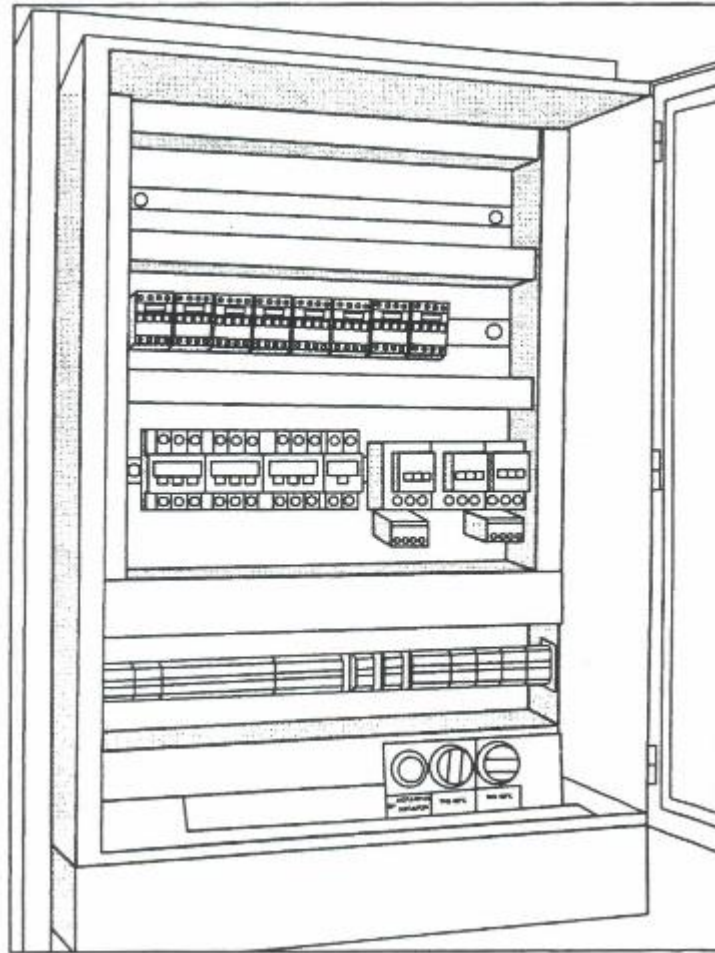


Fig. 3.14 EPM LV Enclosure

3.4 Oil Supply Unit for Motor Bearings

The oil supply system is manufactured by Rickmeier GmbH and is designed to supply the SAG Mill motor bearing with sufficient oil. The most important requirement to ensure proper functioning, high reliability and long running life is a constantly clean pumping conveying product, which does not corrode the gear pump materials and contains no wear promoting activities. The fitting position of the oil supplying system is horizontal.

3.4.1 Assembly Design of the Oil Supplying System

The system design as well as the scope of the design are discussed below;

Oil tank

All components are mounted on a common oil tank. The oil tank is steel welded. The oil level can be checked in the minimum and maximum condition by means of an oil gauge. The tank is filled with oil through the filling and air filter.

Pump unit

Two gear pump units are mounted on the oil tank for low pressure circuit. They each comprise the motor, bracket, coupling and gear pump. For the security of the pump aggregates, non – return valves has been built – in in the pressure line downstream from the pump. For the security of the system, pressure relief valves are built into the circuits. They open if the set operating pressure is exceeded and allow the oil to flow, without pressure, back into the tank. Additionally, a pressure reducing valve is built into the inlet pipe of the radial piston pumps to protect against high pressure. The maximum permissible operating pressure for pump is 300 bars.

Pressure gauge

They are filled with glycerine and used to optically check the pressure. The vibration - free glycerine pressure gauge is designed such that the mechanical works including dial face and pointer are flushed with colourless, neutral glycerine. Slight leakage of glycerine does not affect the pressure gauge operation.

Filter

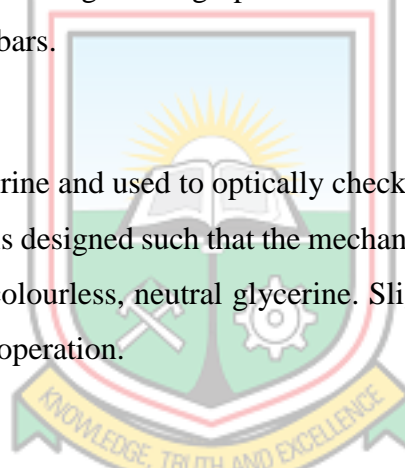
Contaminated oil is prevented from reaching the motor bearing by means of a built – in filter in the pressure line. When the filter element becomes dirty, this is then shown both optically with the contamination display and electrically.

Oil-water-heat exchanger

An oil-water-heat exchanger is built into the pressure line to draw off excess heat.

Electrical monitoring

Temperature: The adjustment from oil temperature is achieved by a resistance thermometer built in the oil tank. This one switch on the magnetic valve of the heater exchanger if required. For the security of the maximum temperature contact-thermometer has been built in the pressure line after the heat exchanger. Additional maximum oil temperature can be checked optically by a thermometer, built-in the oil tank.



Pressure switches: The pressure is controlled at the unit ends with the pressure switches.

Flow-meter: The flow-meter indicates optical and electrically the oil flow of the low pressure circuit.

Level switch: The level switch controls the minimum oil level to protect against running the pump and the consumer without oil.

3.4.2 Maintenance and Repairs

Oil change

A new system requires that the oil must be drained off and renewed after approximately 200 operating hours. Further oil changes are necessary depending upon the operating conditions, generally every 1500 operating hours, but never less than once a year. It is sensible to change the oil when it is at operating at heated environment. If for organisational reasons, the oil must be changed in a cold environment, then it should be slowly warmed up to 50°C to reduce its viscosity.

Cleaning the filter

The filter should be cleaned as often as the operating conditions require, generally shown by means of the filter's built-in contamination display optically and /or electrically. Otherwise it should be cleaned at least every 2000 operating hours (=approximately 1 year with single-shift working) and every time the oil is changed. The cleaning method can be found in the respective technical data sheet of the filter.

Checking the oil level

The oil level should also be checked, provided no leaks have been found, at least once a month. The oil level should be checked daily for a while in a newly installed system. If you discover an oil loss, top up with the same type of oil.

Choosing the oil

Only by using carefully selected oils can the performance, operating reliability and life expectancy of the pumps be guaranteed. Some recommended lubricating oil by motor manufacturers (ABB) are;

- i. Shell Tellus OI C 22, 32, 46, 58 & 100.
- ii. Aral Alur E 22, Aral Motanol GM 32, Aral Motanol HK 32, 68 & 100 and

- iii. Mobil Velocite Oil No. 10, Mobil Vactra Oil Heavy, Mobil DTE Oil Light, Medium & Heavy Medium.

Bearing oil examination is only of practical value if it is intended to extend the oil change interval or if carried out prior to changing a relatively large volume of oil. The properties of the bearing oil to be checked and recorded are kinetic viscosity at 20°C & 40°C (mm²/s), Neutralisation numbers (mg/g), Air release capability at 50°C (min.), Foaming tendency (foaming per unit volume), Inhibitor content (mass %), IR – Aging bands at 1710 cm⁻¹ and impurities in oil (particle count test) (number of particles per 100ml oil).

3.4.3 Operating Faults

Table 3.8 can be used for solving faults that may occur during operation. It must be noted that the list is not conclusive.

Table 3.8 Troubleshooting Operating Faults of Oil Supply Unit

Obstruction	Responsible	Check
No, or too little oil	System	Oil Level Bleeding Pump
	Electric Motor	Supply Rotational direction
	Gear Pump	Gear teeth (wear)
	Pressure Relief Valve	Piston function (movability)
	Filter	Dirt (Filter element)
Noise	System	Oil Level Suction line (clogged, leaking)
	Electric Motor	Bearing (wear) Fan
	Coupling	Gear ring
	Gear Pump	Gear teeth (wear)
	Pressure Relief Valve	Piston Function (movability)

(Source: Anon., 1997)

3.5 Start – Up, Operation, Shutdown

3.5.1 Start-Up Frequency

The SAG Mill Motor is subjected to increased thermal and mechanical stresses during the start-up phase. Therefore, the start-up frequency agreed at the order stage should be observed in order to avoid damage. Table 3.9 is a step-by-step procedure in start-up, operation and shutdown of the SAG Mill Motor.

Table 3.9 Start-Up, Operation and Shutdown of SAG Mill Motor

Type of Machine	Start-Up/Operation	Shutdown
SAG Mill Motor (Slipring/Wound rotor)	Switch standstill heating off.	Switch standstill heating on.
	Switch plain bearing cooling system on.	Switch plain bearing cooling system off.
	Admit air-water heat exchanger water supply.	Stop air-water heat exchanger water supply.
	Switch fan motor on.	Switch fan motor off.
	Close stator switch to start motor.	Open stator switch.
	Switch rotor stator gradually from starting to operating setting, then the short-circuit and brush-lifting system likewise.	Switch short-circuit and brush-lifting system, then rotor starter from operating to starting setting.
	Important note: Re-switching a running motor causes current and torque fluctuations. Re-closure at an instant when the system is in phase-opposition to the residual stator voltage will subject the motor and the driven machine and gear to high forces. Therefore the whole shaft train must be dimensioned to accept these forces or suitable protective equipment provided to avoid them.	

(Source: Anon, 1997)

3.6 Maintenance of SAG Mill Motor

Conscientious and thorough maintenance of a machine and plant is the best protection against faults and operation failures. The more critical operational interruptions are for the process, then the greater is the worth of the maintenance investment. As a basic rule for all maintenance work performed on site, the applicable safety regulations must be obeyed and the necessary protective measures taken for heavy-current installations.

It is recommended that a time schedule be set up for each individual machine and that maintenance cards be employed. These maintenance cards can either be kept in a card-register or hung in plastic envelopes at a vantage point on the machine, so that the state of maintenance can be checked at any time.

Maintenance includes daily patrols by the operating personnel through the whole plant to inspect the operating conditions and to observe and note down important operating quantities. During these daily patrols, special attention is to be paid to possible deviations from the usual state of operation, especially with regard to instruments (limit values, lines or marks), short-circuit monitoring, liquid levels, temperatures, vibration or odours.

If daily patrols are not feasible due to the location of the plant (e.g. inaccessible, too remote etc.), the machines must be fitted with suitable monitoring equipment. Ideally, the periodic inspections should not be carried out simply by a suitably trained engineer, but always the same man. This is the only way to ensure that deviations from the normal operational behaviour are noticed.

Any special observations are to be entered in the log book. Should a fault condition arise, carefully kept log books help to determine the cause of the fault and give information to aid remedying and eliminating the same. The actual maintenance work, most of which is performed during planned periods of shut-down, can be distinguished as follows:

- i. Continuous repetitive inspections and exchanging components subject to wear, and remedying any faults or defects recognised.
- ii. Making-up or replacing consumables.
- iii. Cleaning

Table 3.10 contains recommendations based on many years of experience. The time intervals are based on an eight hour operating day under normal conditions. The actual circumstances under which the machines operate are often quite different so that for each particular case certain time intervals may need to be adapted to the prevailing site conditions such as dirt deposits, loading and switching frequency.

The recommended maintenance intervals also assume fault-free operation. After each serious fault (shut-down) an extra non-scheduled inspection of the machine or plant component in question is necessary. The cause of each shut-down is to be clarified prior to restarting. When any changes in appearance or operational behaviour are noticed it must be carefully considered whether and when intervention is necessary or whether initially a thorough inspection would be sufficient. Similarly, in the case of extraordinary operating conditions (short-circuit, overload etc.) which represent either electrical or mechanical

overloading of the machine, the maintenance or inspection work is to be immediately carried out (Anon, 1997).

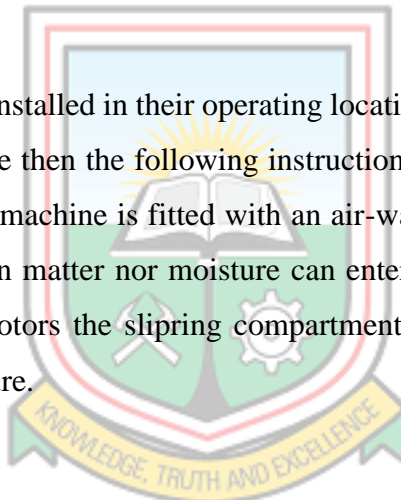
The SAG Mill Motor shut-down is planned together with relining of the SAG Mill. This happens once every month ending and is tied to the planned maintenance of majority of the CIL plant machinery.

Table 3.10 shows the maintenance plan for the SAG Mill motor.

Early identification of abnormal operation symptoms and rapid remedial action are essential as a means of preventing a minor fault from developing into really serious trouble later on. Table 3.11 may help you to trace and remedy possible faults. Always disconnect the motor from the mains before you attempt to trace a fault or attend to the stator switch.

3.7 Storage

If the machines are to be installed in their operating locations but will not be commissioned for a longer period of time then the following instructions for protection and maintenance are to be observed. If the machine is fitted with an air-water heat exchanger i.e. enclosure IP 44, then neither foreign matter nor moisture can enter into the machine. However, for wound rotor induction motors the slipping compartments are to be protected against the ingress of dust and moisture.



3.7.1 Plain Bearings

Apply a coating of TECTYL502 C (supplier: VALVOLINE) to the bearing journals, bearing shells, oil rings, and other bare surfaces inside the bearing housings.

TECTYL502 C is soluble in oil at approximately 50°C and therefore need to be removed when preparing the machine for operation. Abnormal heavy foaming of the bearing lube oil during the test runs indicates that it has been highly contaminated by the TECTYL502 C. In such cases the oil must be changed before final commissioning.

The shaft must not be turned during the conservation period because the actual bearing surfaces will be dry i.e. the weight of the rotor will have pressed the oil film out from between the journal and the shell. Pour oil through the opening in the top bearing cover unto the bearing journal before putting the machine back into service.

Table 3.10 Maintenance Plan for SAG Mill Motor

Part of Machine	Maintenance or Inspection Work	Time Interval
Stator winding Cooling air Rotor winding	Measure temperature at provided measuring points (e.g. built-in RTD's).	Weekly 1)
Stator winding Rotor winding	Measure insulation resistance	Quarterly 1)
Bearing insulation (bearing endshield or pedestal) when provided	Measure insulation resistance between the insulated parts of bearing endshields or bearing pedestals and the steel foundation, using a megger rated at 500 V or maximum 625 V.	Quarterly 1)
Rotor, inside and outside of machine	Visually inspect all accessible places for rust.	Every 3 years 4)
Whole machine	Measure vibration using fitted vibration sensors when provided or portable measuring equipment. Measuring points: middle of bearing housing, horizontal and vertical.	Monthly 1) 3)
	Listen for unusual machine noise or change in noise (e.g. rubbing or knocking sounds etc.)	Weekly 1)
	Visually inspect interior of machine for degree of dirt deposit	Quarterly
Power Supply, instrumentation and control connections	Check condition and fastening of all cables and connections.	Monthly
	Check for degree of dirt deposit	Quarterly
Earthing brushes (when provided)	Visually inspect for wear and free movement in holders. Clean contact surfaces of brushes and shaft with a fine polishing cloth.	Monthly 1) 2)
	Ensure there is brush pressure	Quarterly
Rotor	Check degree of dirt deposit on sliprings and lead bolts, and clean when necessary.	Monthly 1)
Slipring compartment	Check dirt deposit on the insulating parts of the brush gear. Clean when dirty.	Monthly 1)
1) Compare with earlier measurements and observations. 2) Determine rate of wear in mm per 1000 hours of operation and compare with earlier figures to obtain information on the functioning of the earth brushes. 3) For set values and evaluation of vibration measurement.		

(Source: Anon, 1997)

Table 3.11 Troubleshooting Fault of SAG Mill Motor

Fault	Possible Cause	Remedy
Motor will not start, is completely dead.	At least two supply leads open-circuited.	Check fuses, supply leads and terminals.
	No voltage.	Check mains supply leads.
Motor hums but will not start.	One stator or rotor phase open-circuited.	Check supply leads and repair break.
Motor will not start under load but emits normal magnetic noise.	Excessive torque resistance.	Remedy drive faults. Uncouple motor and check no-load operation. (Be careful because of run-up time and axial guidance)
	Mains voltage too low.	Measure mains voltage.
	Open-circuited rotor circuit (starter and supply leads).	Check rotor circuit.
Motor idles but will not take on load.	One mains supply lead open-circuited after starting.	Check mains supply lead(s).
	Open-circuited rotor circuit, fault in rotor supply (brushes not seated properly, faulty short-circuited contacts).	Check rotor circuit for breaks, brushes for jamming and wear, short-circuited contacts for burning.
Motor overheats when idling.	Wrong stator winding connection (e.g. delta instead of star).	Restore correct connections as per diagram.
	Mains voltage too high.	Check mains voltage and no-load current.
Motor overheats when idling.	Loss of cooling due to blocked air passages.	Clean air passages.
	Wrong direction of fan rotation (motors with inclined fan blades designed for a single direction of rotation).	Check fan and direction of rotation.
Motor overheats under load.	Motor overloaded.	Check current flow.
	Voltage too high or too low.	Check voltage.
	Motor single-phasing.	Trace break in supply lead.

(Source: Anon, 1997)

3.7.2 Rolling Contact Bearings

No special measures are necessary for or during the conservation period, however fresh grease must be injected into both bearings before putting the machine back into service. Remove grease chamber cover and inject fresh grease until the old grease has been expelled. Should a bearing need changing consult the equipment manual for instructions.

3.7.3 Bare Surfaces

Apply a protective covering of TECTYL 502 (Supplier: VALVOINE) to all bare parts of the shaft outside of the enclosure e.g. coupling, shaft surfaces, etc.

Surfaces on the bedplate not covered by the motor feet or shims, and the edges of the shims themselves, are to be protected with paint as called for in project specifications.

3.7.4 Coolers, Piping

The coolers and the associated piping within the scope of the motor supply were cleaned, and dried by blowing through with warm air before packing. It must be ensured that they are still clean and dry before the machines are conserved.

3.7.5 Space Heaters

Space heaters can remain switched on in order to avoid condensation within the machine. Periodically check that they are operating.

3.7.6 Filters

Temporarily seal up cooling air inlet and outlet filter frames on the slipping compartment.

3.7.7 Brushes

Raise the brushes from the surface of the sliprings and jam at an angle in top of brush-holders by means of spring pressure.

3.7.8 Openings

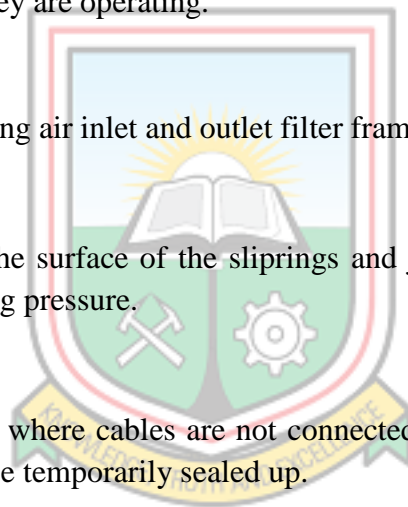
If there are any openings where cables are not connected up to terminal boxes, or piping flanges, etc. these are to be temporarily sealed up.

3.7.9 Inspections, Records

The conservation measures are to be given a final check and recorded together with the date of the beginning of the conservation period. Thereafter carry out regular inspections, the first after six months and record results. Renew conservation measures when and where necessary (Anon, 1997).

3.8 Summary

In this chapter, main components and working of three phase CSLGH 900/6-214 induction motor (SAG Mill Motor) have been discussed. In addition, some auxiliary equipment of the SAG Mill motor have been reviewed. The operation, maintenance and storage of the SAG Mill Motor was looked at.



CHAPTER 4

METHODS USED

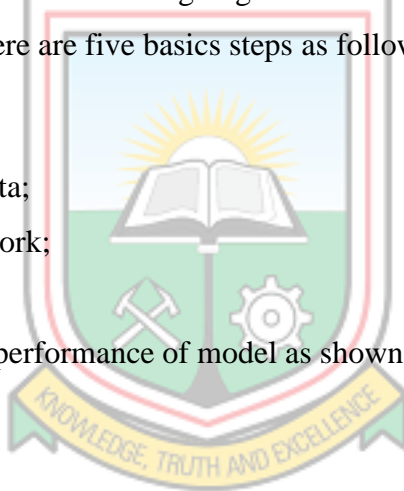
4.1 Introduction

In designing a model for failure prediction of three phase 5.8 MW, 11 kV slip ring SAG Mill induction motor at Goldfields Ghana Limited, Damang mine, Artificial Neural Networks was employed in modelling and simulations on data collected (Power, Current and Winding Temperatures) from the company.

4.2 Designing and Programming of ANN Models

Fig. 4.1 (Ghate and Dudul, 2011) shows a generalized flow chart of ANN – based fault classification of induction motors. Designing ANN models follows a number of systemic procedures. In general, there are five basic steps as follows:

- i. Collecting data;
- ii. Pre-processing data;
- iii. Building the network;
- iv. Train; and
- v. Validate and test performance of model as shown in Fig. 4.2.



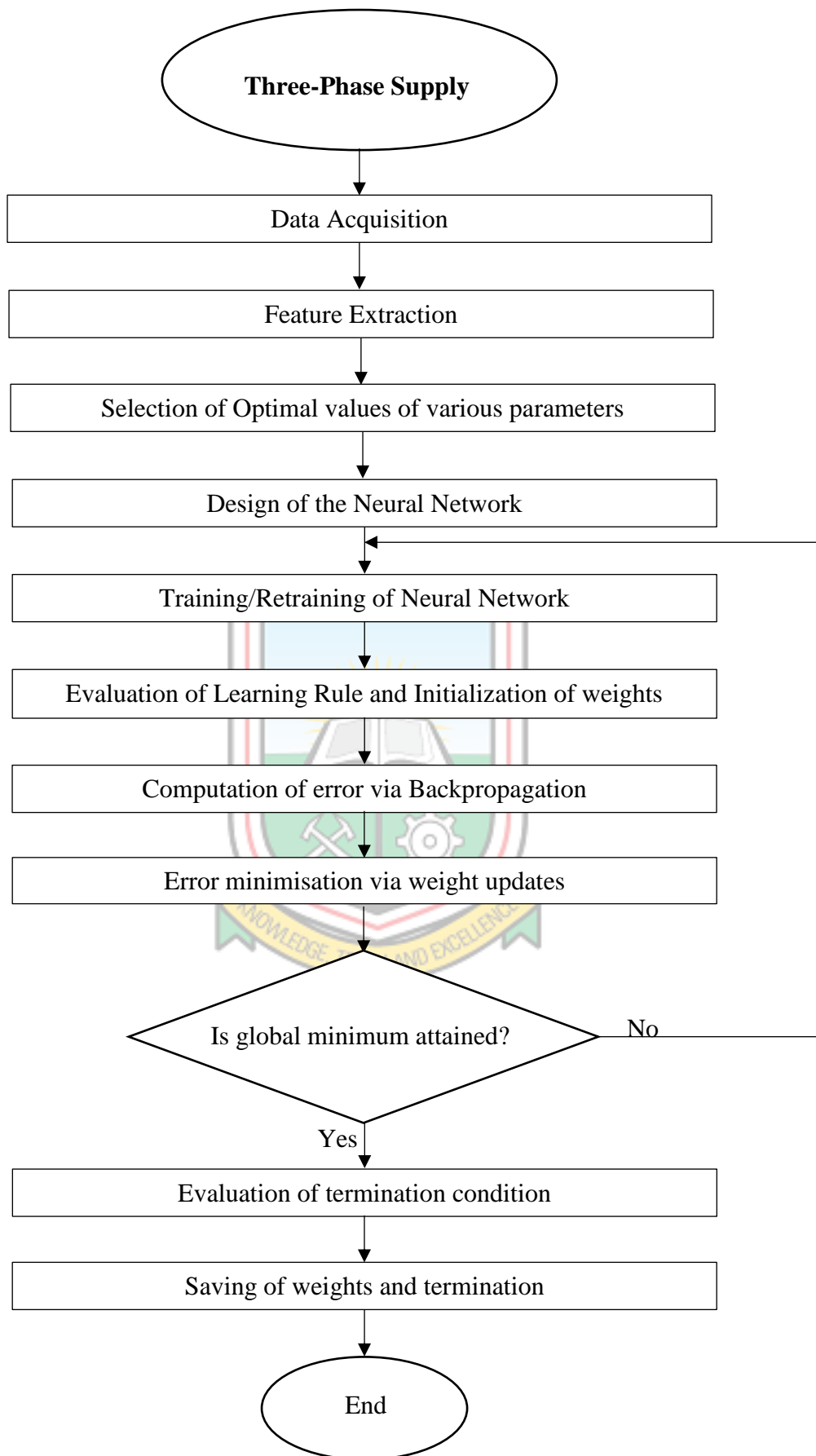


Fig. 4.1 General Flow of ANN – Based Fault Classification of Induction Motors

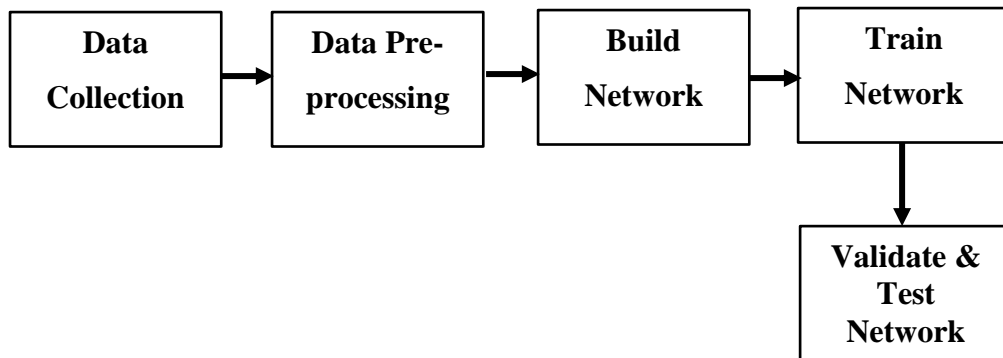


Fig. 4.2 Basic Block Diagram for Designing Artificial Neural Network Model

4.3 Data Collection

Collecting and preparing sample data is the first step in designing ANN models. As it is outlined in Fig. 4.2, measurement data of SAG Mill motor winding temperatures ($^{\circ}\text{C}$), motor current (A) and motor power (MW) and corresponding motor condition i.e. Motor healthy or Motor faulty (MH/MF) for Damang mine for 93-day period from 6th January, 2019 to 8th April, 2019 was collected through the Citect as shown in Fig. 4.3. Fig. 4.4 and Fig. 4.5 shows graphical representation of SAG Mill motor winding temperatures, current and power before normalisation. A total of 5×879 data samples were collected.

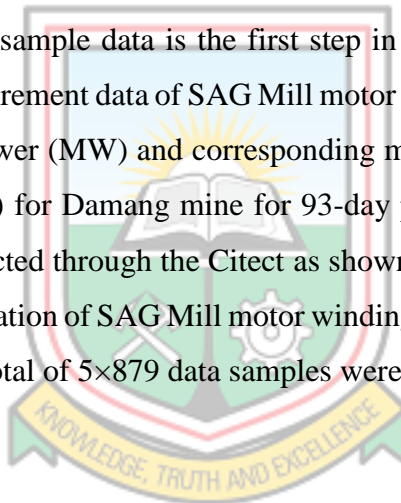




Fig. 4.3 Trends of SAG Mill Motor Current, Power and Winding Temperatures

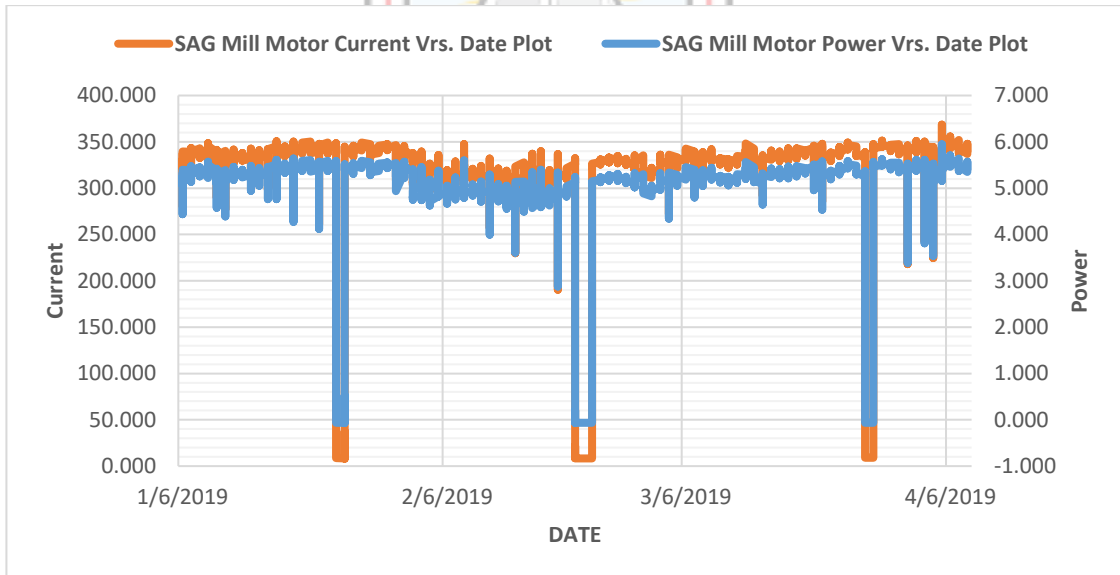


Fig. 4.4 Graph Showing Trends of SAG Mill Motor Current and Power

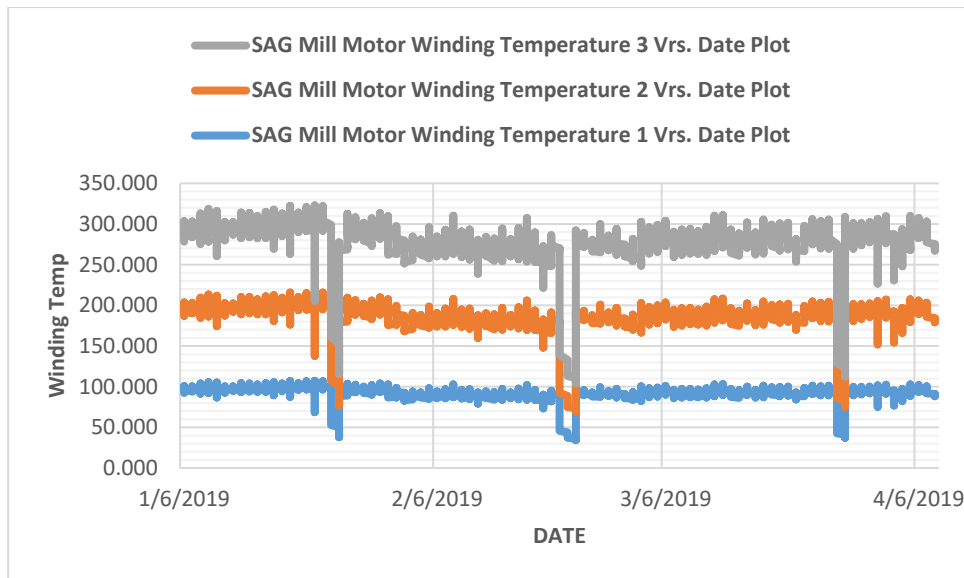


Fig. 4.5 Graph Showing Trends of SAG Mill Motor Winding Temperatures

4.4 Data Pre-Processing

After data collection, data pre-processing procedures are conducted to train the ANNs more efficiently. The procedure is normalization of data. Normalization procedure before presenting the input data to the network is generally a good practice, since mixing variables with large magnitudes and small magnitudes will confuse the learning algorithm on the importance of each variable and may force it to finally reject the variable with the smaller magnitude (Tymvios *et al.*, 2008). Fig. 4.6 and Fig. 4.7 are graphs showing SAG Mill motor current, power and temperatures after normalisation. A total of 5×837 data samples were considered healthy after normalisation.

Data samples that were out of range after normalisation were taken to be faulty data samples. These faulty data samples totalling 5×42 are shown in Fig. 4.8.

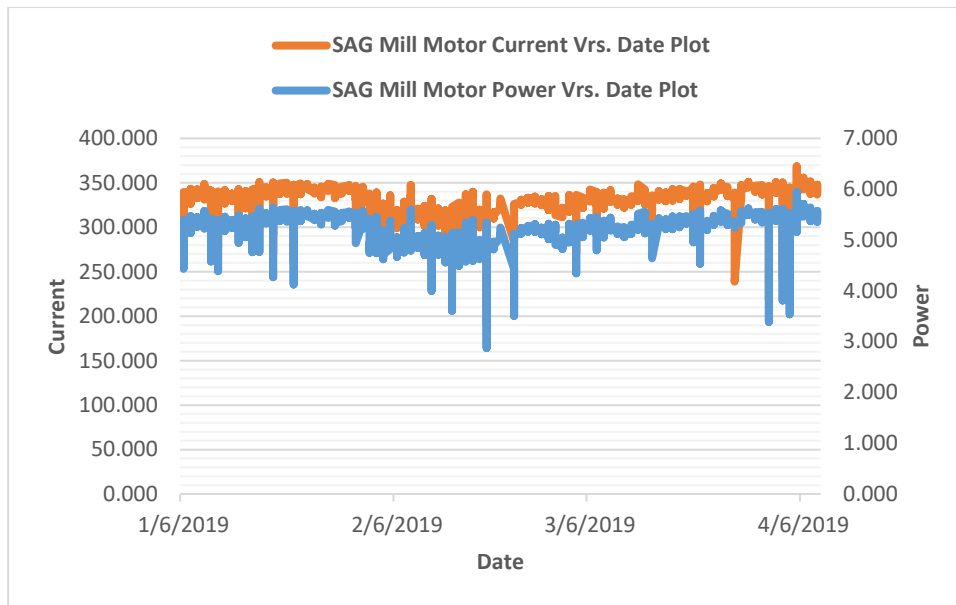


Fig. 4.6 Graph Showing Trends of SAG Mill Motor Current and Power after

Normalisation

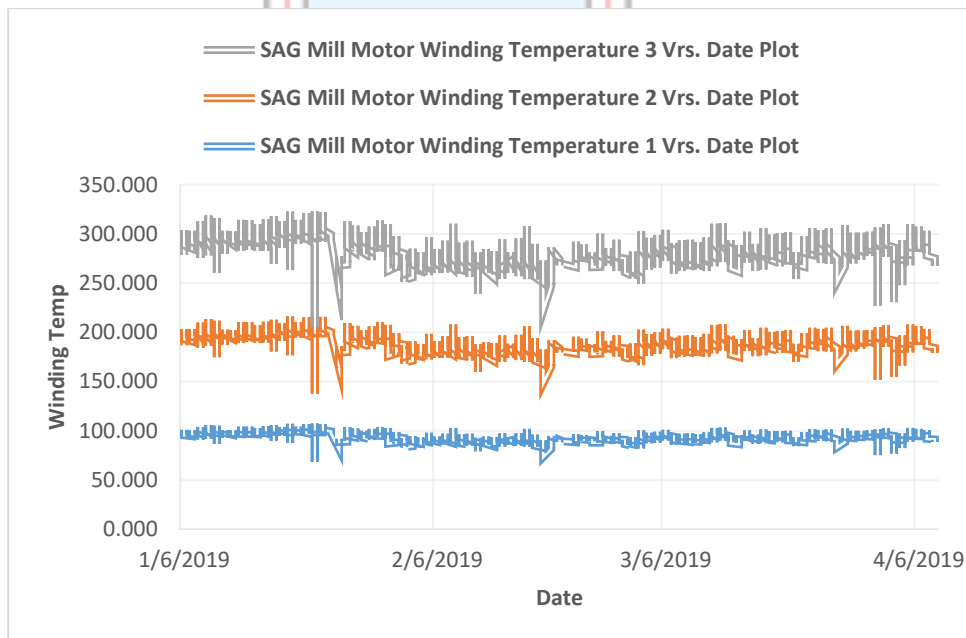


Fig. 4.7 Graph Showing Trends of SAG Mill Motor Winding Temperatures after Normalisation

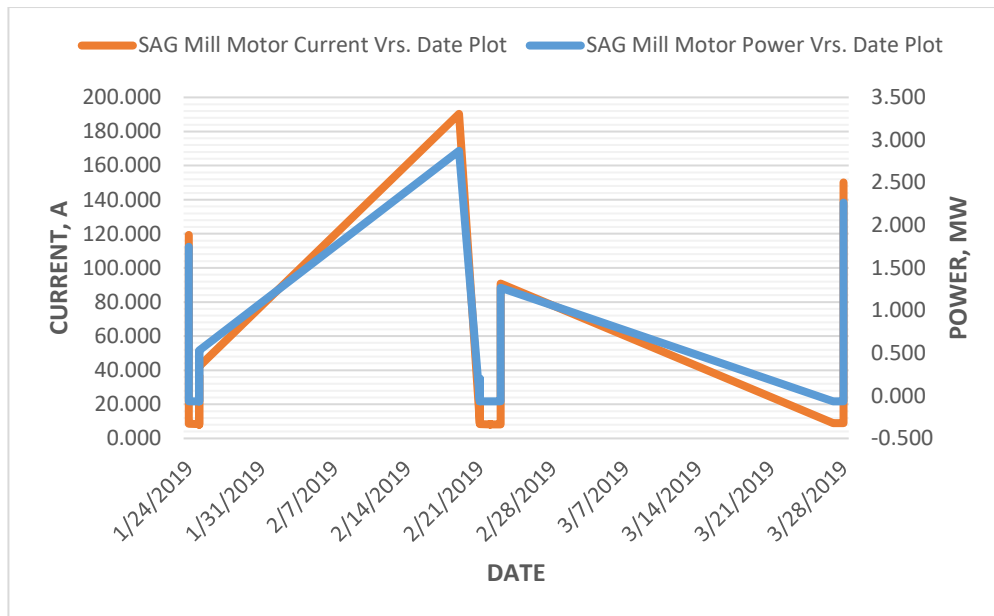


Fig. 4.8 Graph Showing Trends of Faulty SAG Mill Motor Current and Power

4.5 Building the Network

At this stage, the number of hidden layers, neurons in each layer, transfer function in each layer, training function, weight/bias learning function, and performance function are specified. In this work, generalized feed-forward neural networks was used.

4.5.1 Feed-Forward Neural Network with Backpropagation Algorithm

In feed-forward neural networks, otherwise known as multilayer perceptrons, the input vector of independent variables P_i is related to the target t_i (SAG Mill motor condition) using the architecture depicted in Fig. 4.9. This figure shows one of the commonly used networks, namely, the layered feed-forward neural network with one hidden layer. Here each single neuron is connected to those of a previous layer through adaptable synaptic weights. Knowledge is usually stored as a set of connection weights, and then, the weights are adjusted so that the network attempts to produce the desired output. The weights after training contain meaningful information, whereas before training they are random and have no meaning.

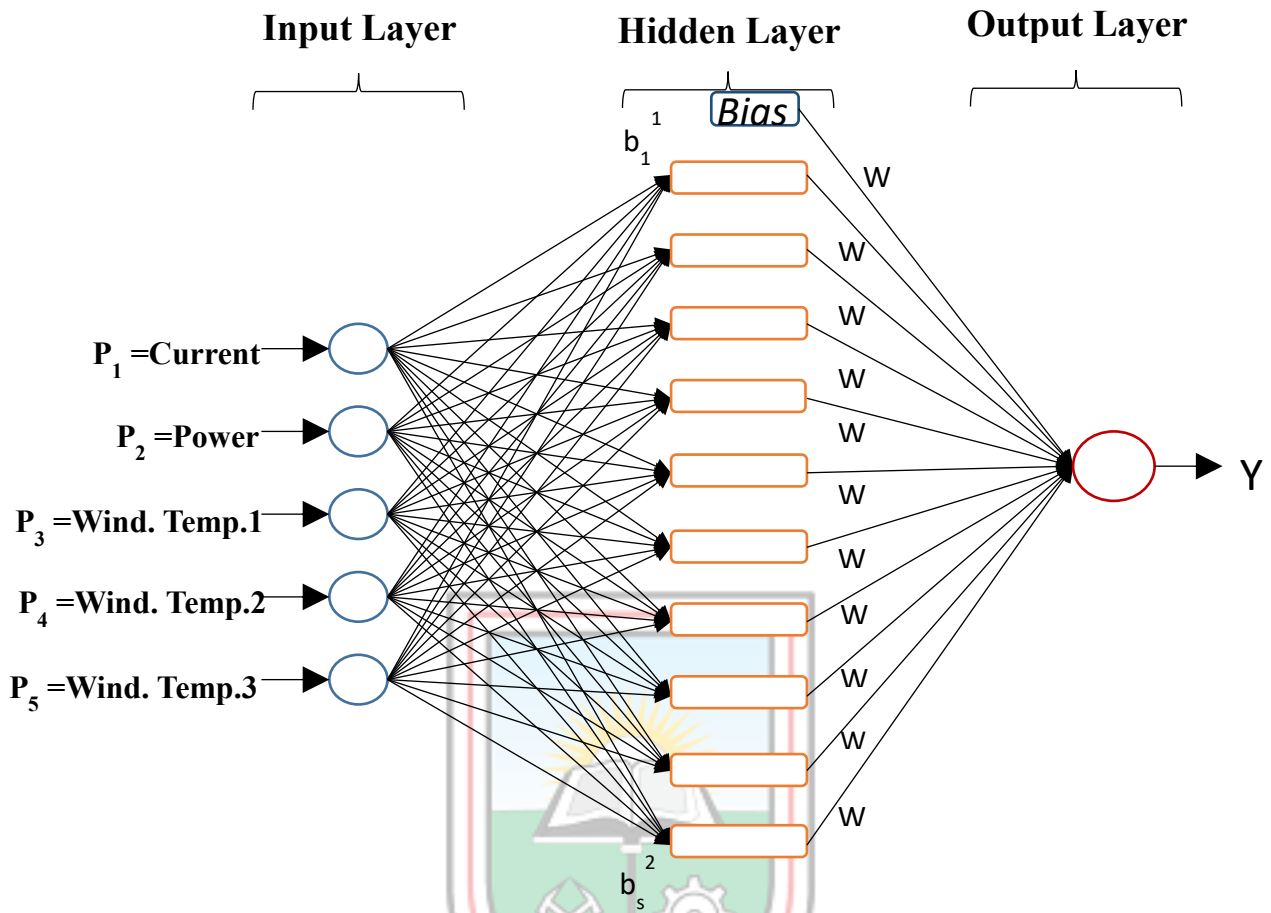


Fig. 4.9 Architecture of Feed-Forward Network

The architecture of the network examined in the study was such that $p'_i = (p_{i1}, p_{i2}, \dots, p_{i5})$ contained values for 5 input (independent) variables from individual i . The input variables are associated with each of N neurons in a hidden layer by using weights (w_{kj} , $k = 1, 2, \dots, N$) which are specific to each independent variable (j) to neuron (k) connection. Following Kayri (2016), the mapping has two forms for the relationship between output t and independent variables:

$$\text{Hidden Layer } n_k^{(1)} = \sum_{j=1}^R p_j + b_k^{(1)} ; a_k^1 = f_{\text{level-one}}(n_k^{(1)}) \quad (4.1)$$

$$\text{Output Layer } n_k^{(2)} = \sum_{j=1} w_k^{(2,1)} a_j^1 + b_k^{(2)} ; \hat{t} = a_k^{(2)} = f_{\text{level-two}}(n_k^{(2)}) \quad (4.2)$$

In the case of N neurons in the neural network, the biases are $b_1^{(1)}, b_2^{(1)}, \dots, b_N^{(1)}$.

Prior to activation, the input value for neuron k is;

$$b_k^{(1)} + \sum_{j=1}^5 w_{kj} p_j. \quad (4.3)$$

Then an activation function $f(\cdot)$ (Linear or nonlinear) is applied to the input in each neuron and v is transformed as;

$$f_k \left(b_k^{(1)} + \sum_{j=1}^5 w_{kj} p_j \right) = f_k(n_k^{(1)}), k=1, 2, \dots, N. \quad (4.4)$$

After applying activation, the activated quantity is then transferred to the output layer and gathered as;

$$\sum_{k=1}^N w_k^1 f_k \left(b_k^{(1)} + \sum_{j=1}^5 w_{kj} p_j \right) + b^{(2)}, \quad (4.5)$$

where w_k ($k=1, 2, \dots, N$) are $b^{(1)}$ and $b^{(2)}$

Bias parameters in the hidden and output layers. At the end of the process, this activated quantity is carried out again with function $g(\cdot)$ as;

$$g \left[\sum_{k=1}^N w_k^1 f_k(\cdot) + b^{(2)} \right] = f_k(n_k^{(2)}), \quad (4.6)$$

Which then becomes the estimated target variable (motor condition) value of t_1 in the training data set:

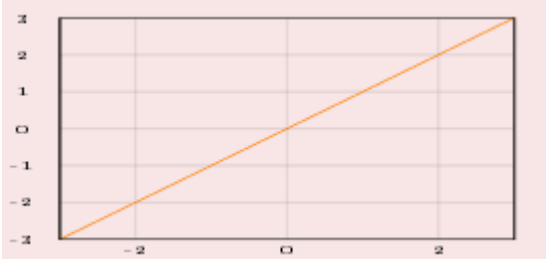
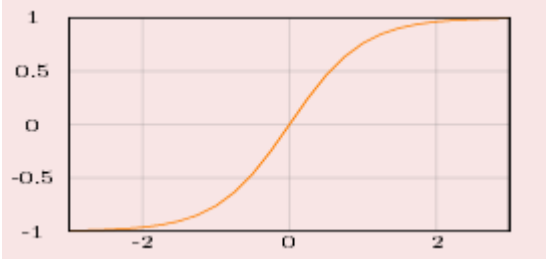
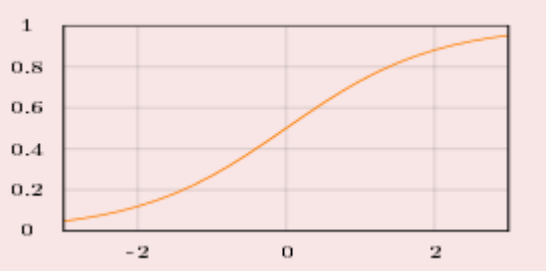
$$\hat{t}_1 = \sum_{k=1}^N w_k^1 f_k \left(\sum_{j=1}^R w_{kj} p_j + b_k^{(1)} \right) + b^{(2)}; j = 1, 2, \dots, R, k=1, 2, \dots, N \quad (4.7)$$

4.6 Training the Network

Training is the process of modifying the network using a learning mode in which an input is presented to the network along with the desired output. During the training process, the weights are adjusted in order to make the actual outputs (predicated) close to the target (measured) outputs of the network. In this study, 70% of the data was used for training. Two different types of training algorithms were investigated for developing the feed-forward network. These are Levenberg-Marquardt algorithm and Bayesian Regularisation algorithm.

MATLAB provides built-in transfer functions which are used in this study; linear (purelin), Hyperbolic Tangent Sigmoid (tansig) and Logistic Sigmoid (logsig). The graphical illustration and mathematical form of such functions are shown in Table 4.1.

Table 4.1 MATLAB Built-in Transfer Function

Functional Name	Graphical Illustration	Mathematical Form
Linear		$f(x) = x$
Hyperbolic Tangent Sigmoid		$f(x) = \frac{e^x - e^{-x}}{e^x + e^{-x}}$
Logistic Sigmoid		$f(x) = \frac{1}{1 + e^{-x}}$

(Source: Shamisi *et al.*, 2011)

4.7 Validating and Testing the Network

The next step is to validate and test the performance of the developed model. At this stage unseen data are fed to the model. For this case study, 15% of SAG Mill motor data was used for validating and another 15% used for testing the ANN models. Validation data generalize the network validation and stops training before overfitting which occurs when a network memorizes the training data but not learn to generalize new inputs.

In order to evaluate the performance of the developed ANN models quantitatively and verify whether there is any underlying trend in performance of ANN models, statistical analysis involving mean squared error were conducted. MSE provides information on the short-term

performance which is a measure of the variation of predicated values around the measured data. The lower the MSE, the more accurate is the estimation. The expressions for the aforementioned statistical parameter is:

$$MSE = \frac{1}{n} \sum_{i=1}^n (I_p - I_i)^2 \quad (4.8)$$

where I_p denotes the predicted power of SAG Mill motor in MW,
 I_i denotes the measured power of SAG Mill motor in MW, and
 n denotes the number of observations.

On the other hand, regression is a statistical analysis assessing the correlation between two variables. The regression line equation can be written as

$$y = a + bx \quad (4.9)$$

Slope:

$$b = \frac{N \sum XY - (\sum X)(\sum Y)}{(N \sum X^2 - \sum X)^2} \quad (4.10)$$

Intercept:

$$a = \frac{\sum Y - b(\sum X)}{N} \quad (4.11)$$

where N = Number of data samples
 X = first group
 Y = second group and regression coefficient,

$$R = \frac{\sum XY \frac{\sum X \sum Y}{N}}{\sqrt{\left(\sum X \frac{(\sum X)^2}{N} \right) \left(\sum Y \frac{(\sum Y)^2}{N} \right)}} \quad (4.12)$$

$R=1$ represents close relationship and $R=0$ represents random relationship

4.8 Programming the Neural Network Model

MATLAB is a numerical computing environment and also a programming language. It allows easy matrix manipulation, plotting of functions and data, implementation of algorithms, creating user interfaces and interfacing with programs in other languages. The Deep Learning Toolbox (formerly Neural Network Toolbox) provides a framework for designing and implementing deep neural networks with algorithms, pretrained models, and apps. Apps and plots help you visualize activations, edit network architectures, and monitor training progress (The MathWorks, 2019).

In this work MATLAB software (R2017a) is used to write script files for developing feed-forward ANN models and performance functions for calculating the model performance error statistics such as MSE. Fig. 4.11 shows the procedural steps to develop the ANN models. The FFNN program starts by reading data from an Excel file (Training1.xlsx). “xlsread” function is used to read the data specified in the Excel file.

```
Data_Inputs = xlsread('Training1.xlsx');
```

MATLAB helps devise the FFNN model by using the built-in function “newff” which creates a feed-forward back-propagation network. The designer can specify the number of hidden layers, the neurons in each layer, the transfer function in each layer, the training function, the weights/bias learning function, and the performance function. Moreover, this command will automatically initialize the weights and biases, it also divides the input data into 70% for training, 15% for validation and 15% for testing. The function is called as follows:

```
net = newff(P,T,S);
```

where P is $R \times Q1$ matrix of $Q1$ representative R -element input vectors,

T is $SN \times Q2$ matrix of $Q2$ representative SN -element target vectors, and

S is sizes of $N-1$ hidden layers, $S1$ to $S(N-1)$, default =0.

The network is next configured as follows:

```
net.trainparam.min_grad = 0.00000001;  
net.trainParam.epochs = 1000;  
net.trainParam.lr = 0.6;  
net.trainParam.max_fail =50;  
net.trainFcn='trainlm';
```

```
net.performFcn = 'mse'
```

where “trainParam.min_grad”: denotes the minimum performance gradient

“trainParam.lr”: denotes the learning rate

“trainParam.epoch”: denotes the maximum number of epochs to train

“trainParam.max_fail”: denotes the maximum validation failures

“trainFcn”: denotes the function used to train the network. It can be set to the name of any training function (LM='trainlm'; Levenberg-Marquardt back-propagation)

“performFcn”: denotes network performance function. It can be set to the name of any performance function (Mean Square Error (MSE). MSE is the average squared error between network outputs, O and target outputs).

The FFNN network is trained using the “trainFcn” and “trainParam” train functions. The trained network is then saved in MATLAB by calling the function

```
net1 = train(net,P,T)
```

“net1” is a variable name which can be changed according to the network train function and configuration in order to yield a meaningful name.

When the training is complete, the network performance should be checked. Therefore, unseen data (testing1) will be exposed to the network. The testing simulation process is called with the statement:

```
a = sim(net1, P); % simulate network
```

Fig. 4.10 shows screen captions of the FFNN ANN training window obtained using the “nntraintool” GUI toolbox in MATLAB.

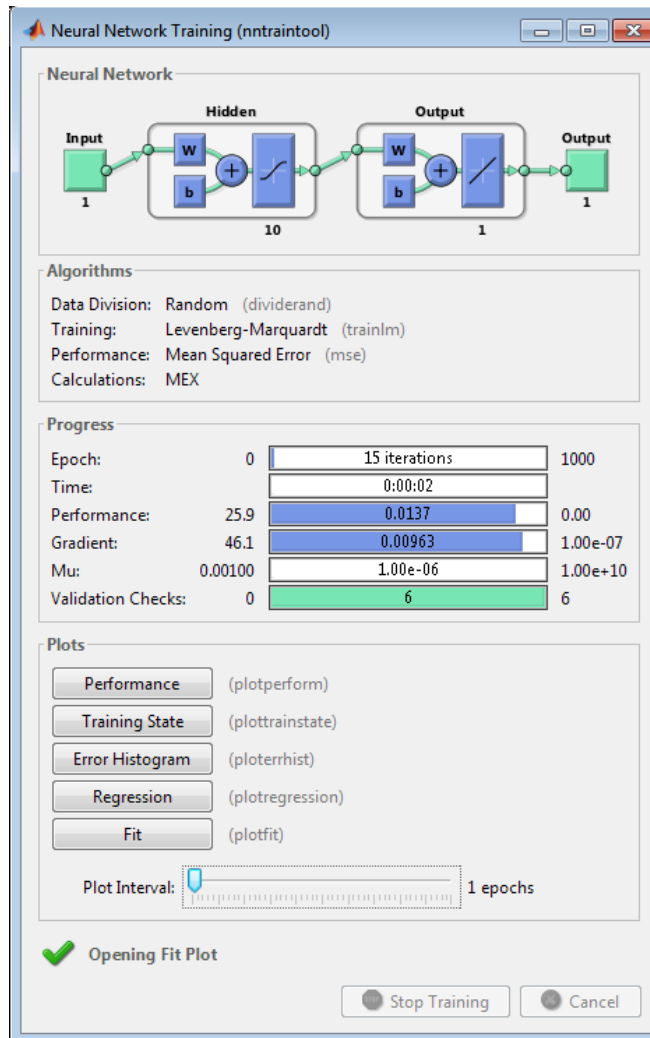


Fig. 4.10 FFNN Network Training Window

Fig. 4.11 shows flowchart for developing Feed – Forward networks using MATLAB.

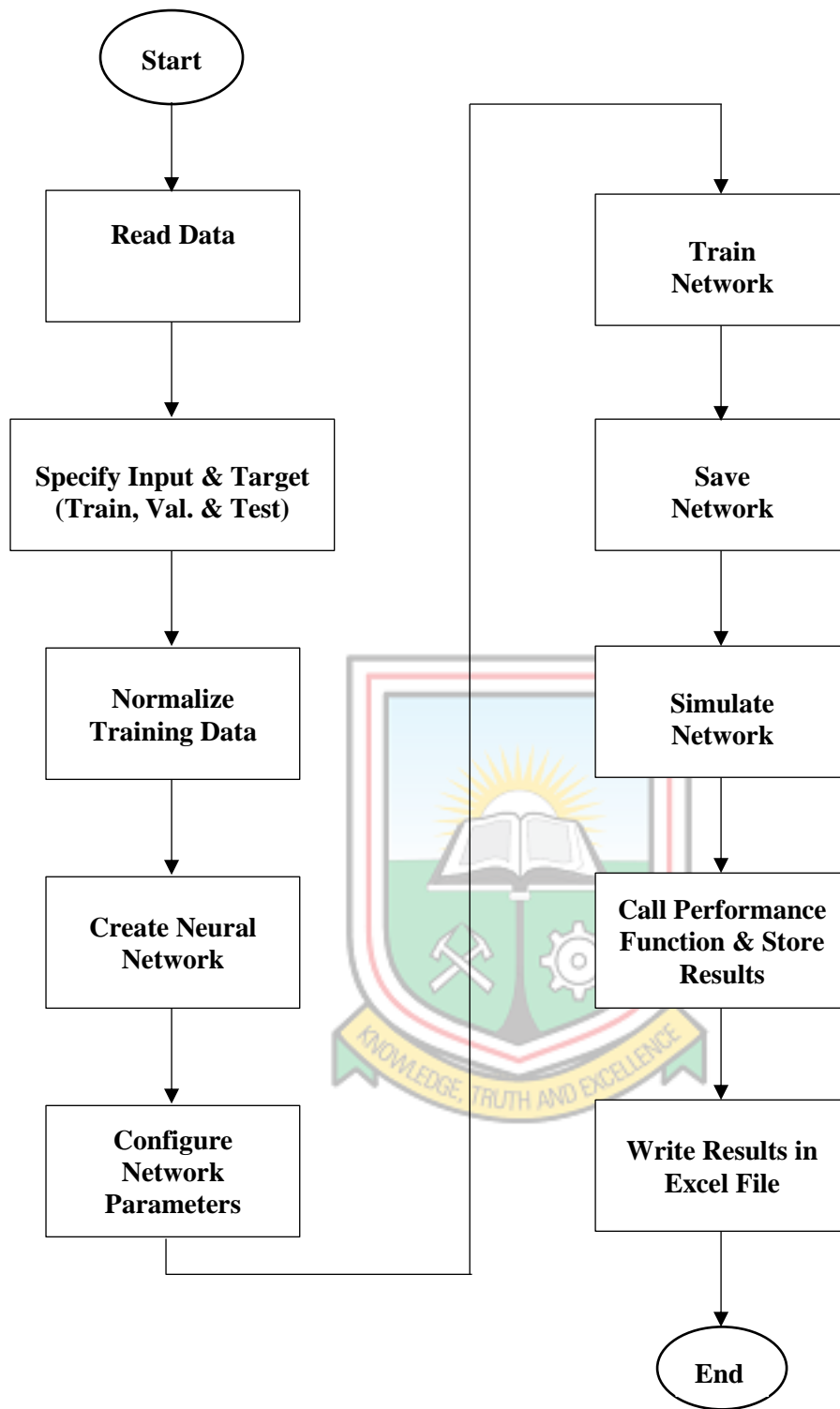


Fig. 4.11 Flowchart for Developing Feed – Forward Networks Using MATLAB

4.9 Implementation of Proposed Methodology

The proposed methodology is implemented using a microprocessor to achieve online failure detection. In addition to the cost – effectiveness of microprocessor implementation, it is flexible and its re-configurability allows changes and refinements while in operation.

Fig. 4.12 shows the block diagram of the proposed methodology implementation. The data acquisition system receives current, power and three winding temperature signals from the sensors connected to the power supply to the stator windings of the motor. Signal processing is performed by the microprocessor and the result further analyzed by a postprocessor decision-making block that simply states the motor condition in two possible values, i.e., MH (a healthy motor) and MF (a faulty motor), making the process online with no expert technician required for the diagnosis.

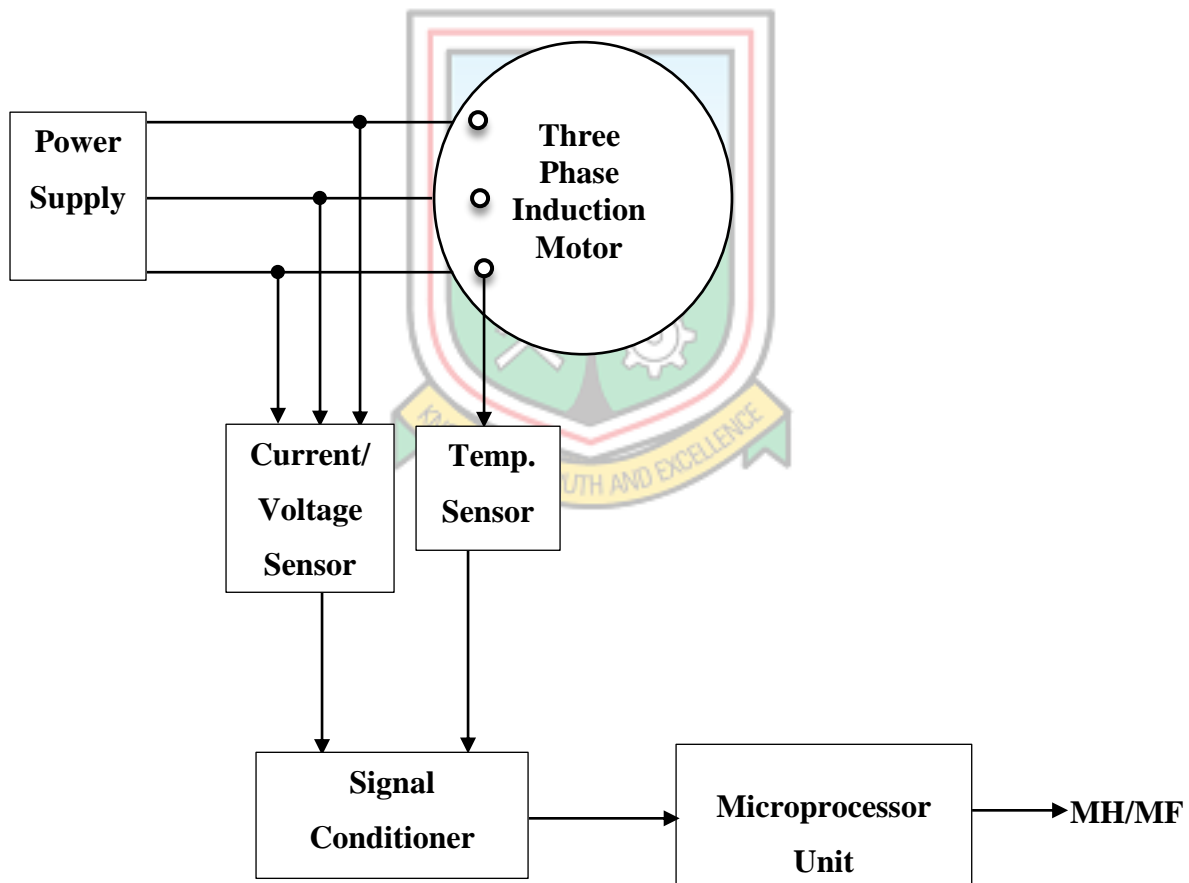


Fig. 4.12 Overall Block Diagram of Implementation of Proposed Methodology

CHAPTER 5

RESULTS AND DISCUSSION

5.1 Introduction

The results of MATLAB simulations using Artificial Neural Network tool box of SAG Mill motor current, temperature and power data from Goldfields Damang Mine are presented here.

5.2 Simulation Results using Feed-Forward Network

In this section, results of using current and winding temperature readings representing three sides of the SAG Mill motor is used as the input to the network with Mill motor power as the target of the network. Two training algorithms i.e. Levenberg-Marquardt (LM) and Bayesian Regularization (BR) were used in training the network. Simulation results of Correlation coefficient for network performance (R), mean squared error (MSE) against epochs, Error Histograms and training state plot for model Validation are presented here.

5.2.1 Simulation Results of FFNN Using Levenberg-Marquardt Training Algorithm

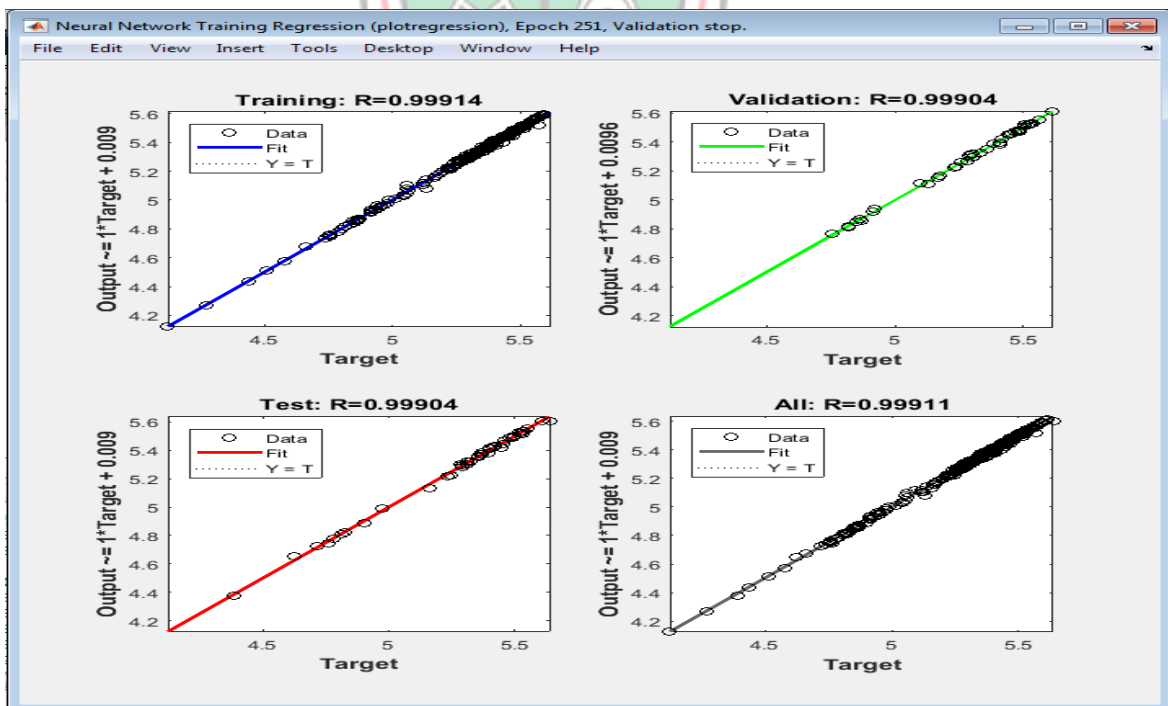


Fig. 5.1 Correlation Coefficient for Network Performance, R (LM)

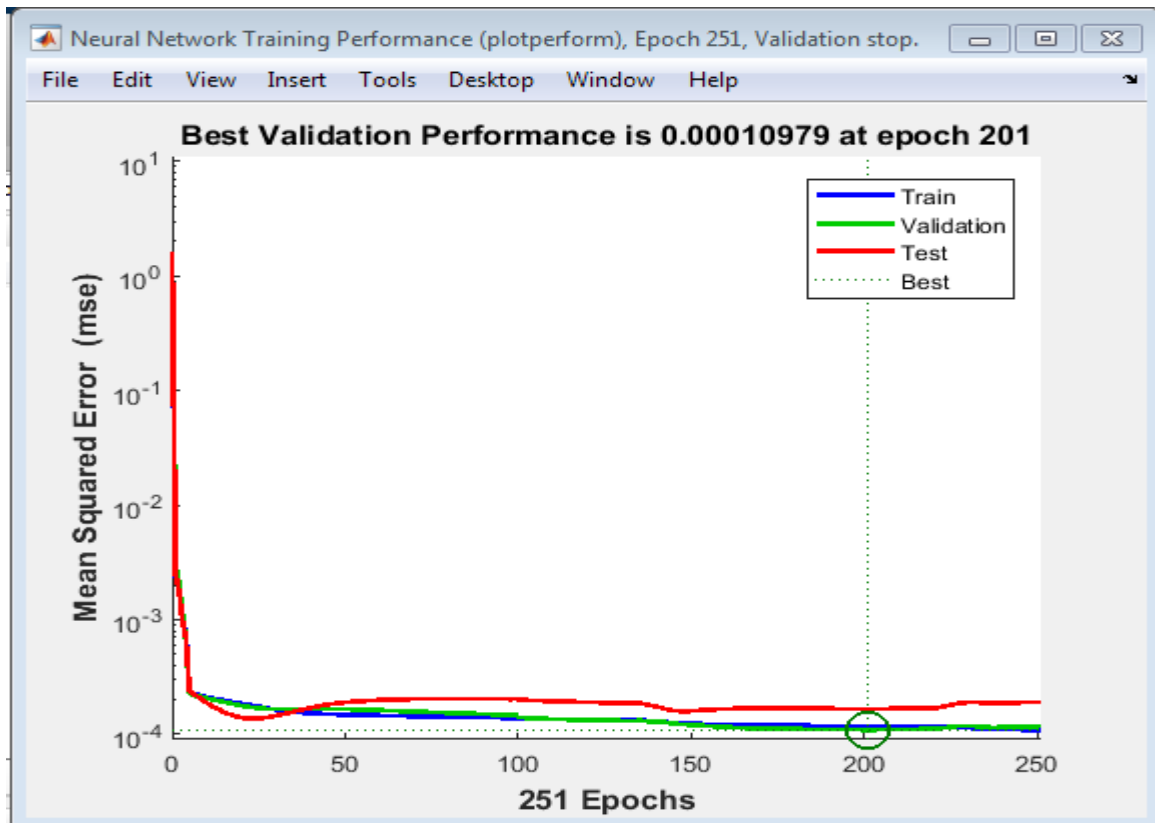


Fig. 5.2 Mean Squared Error (MSE) against Epochs (LM)

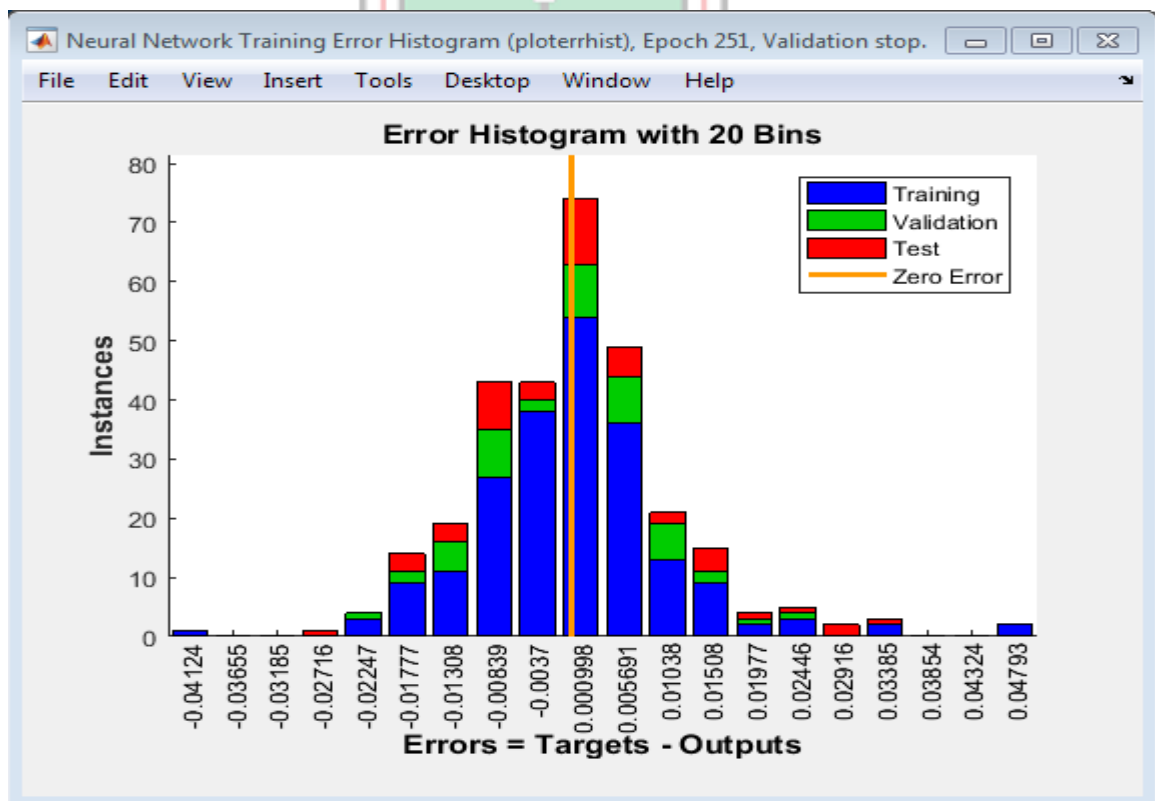


Fig. 5.3 Error Histogram (LM)

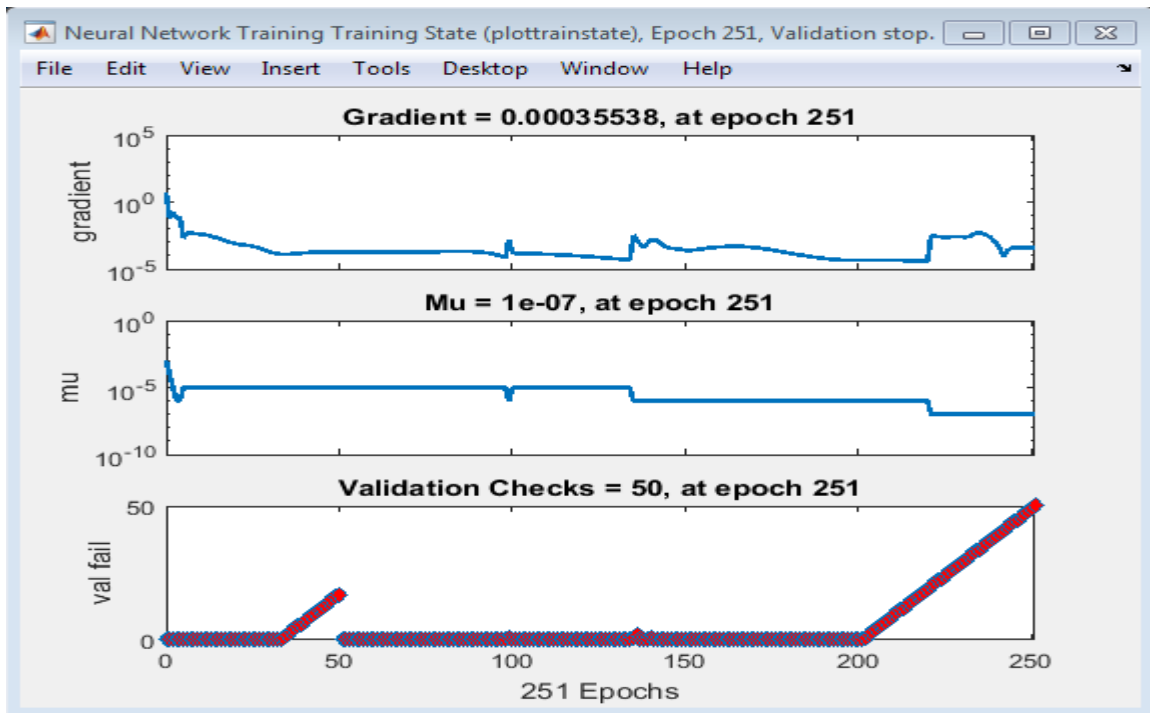


Fig. 5.4 Training State Plot for Model Validation (LM)

5.2.2 Simulation Results of FFNN Using Bayesian Regularization Training Algorithm

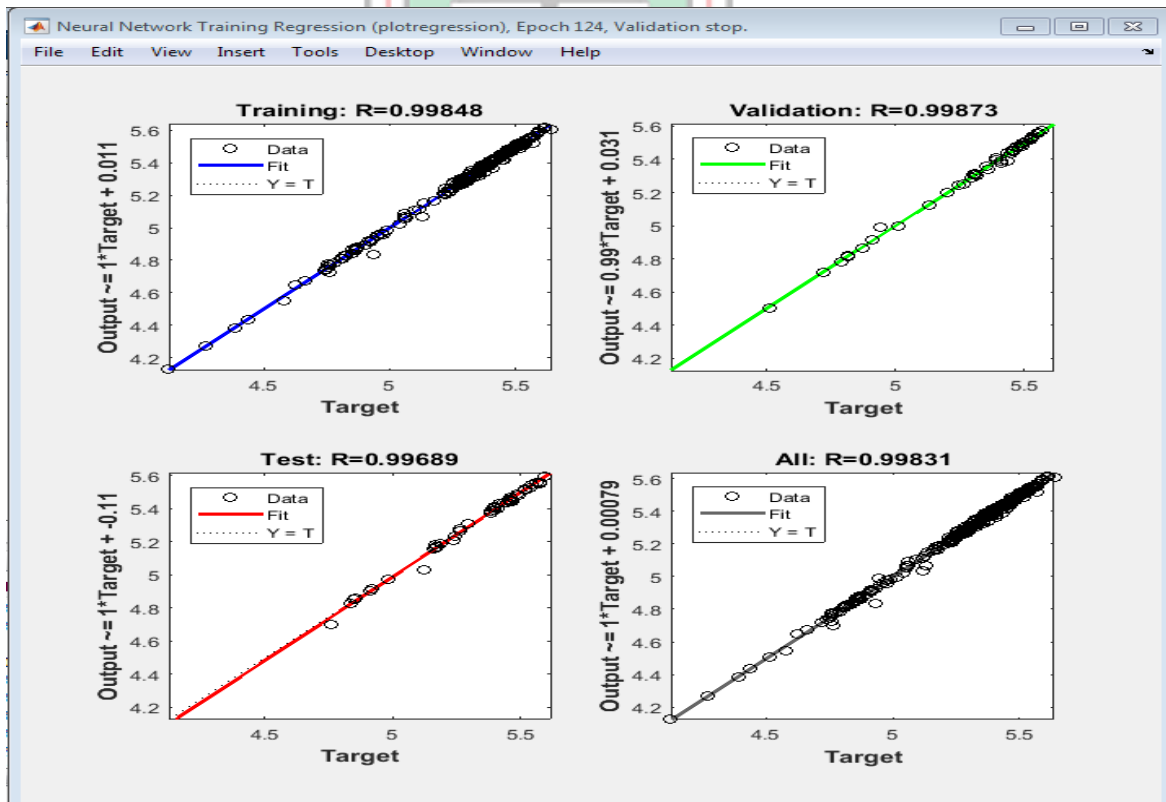


Fig. 5.5 Correlation Coefficient for Network Performance, R (BR)

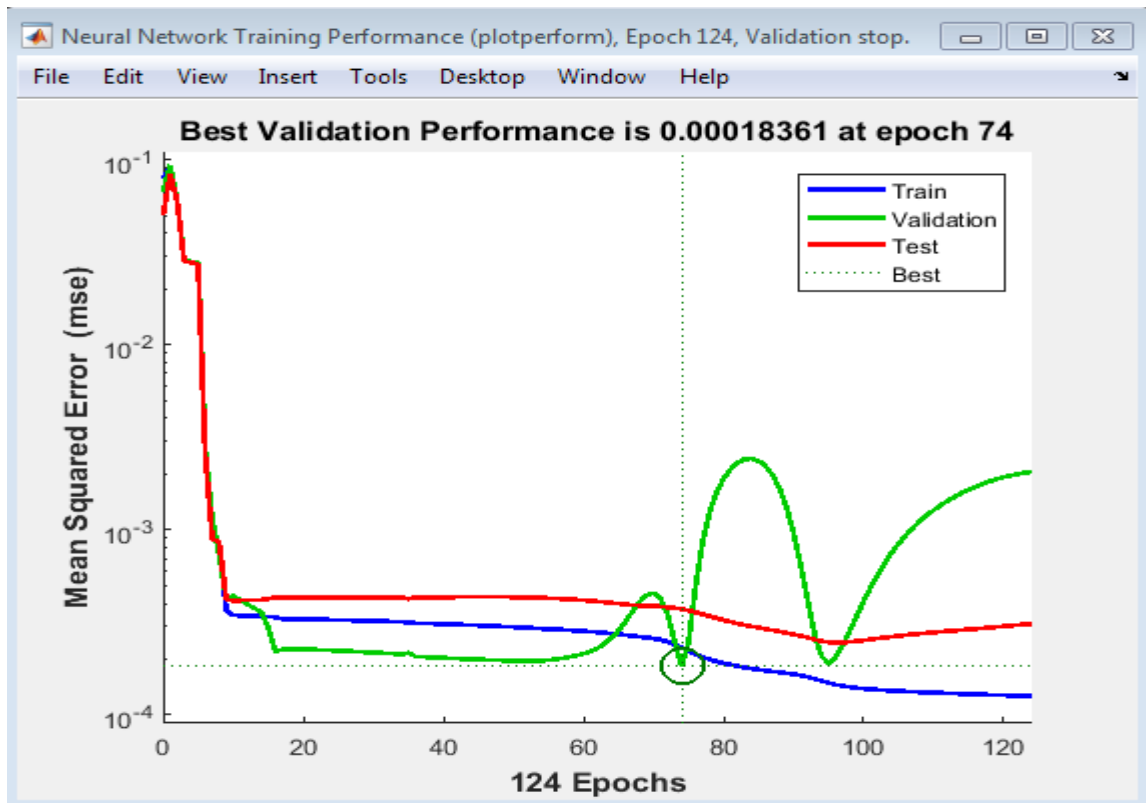


Fig. 5.6 Mean Squared Error (MSE) against Epochs (BR)

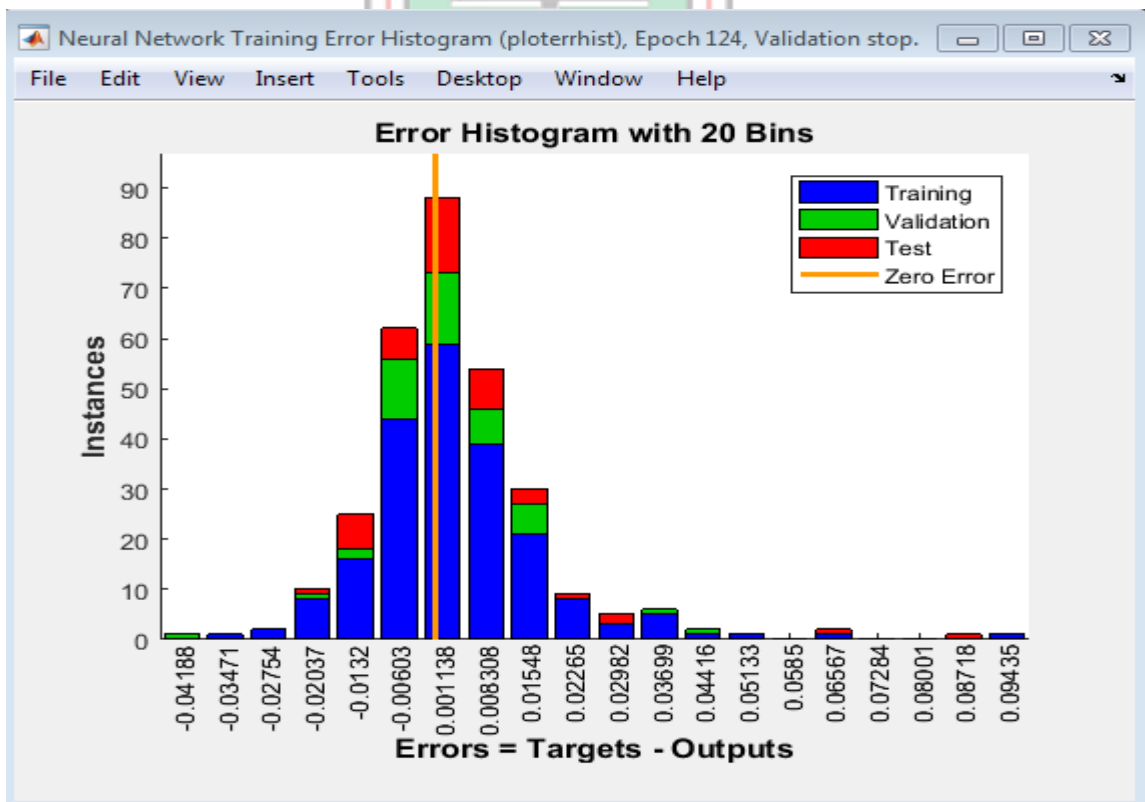


Fig. 5.7 Error Histogram (BR)

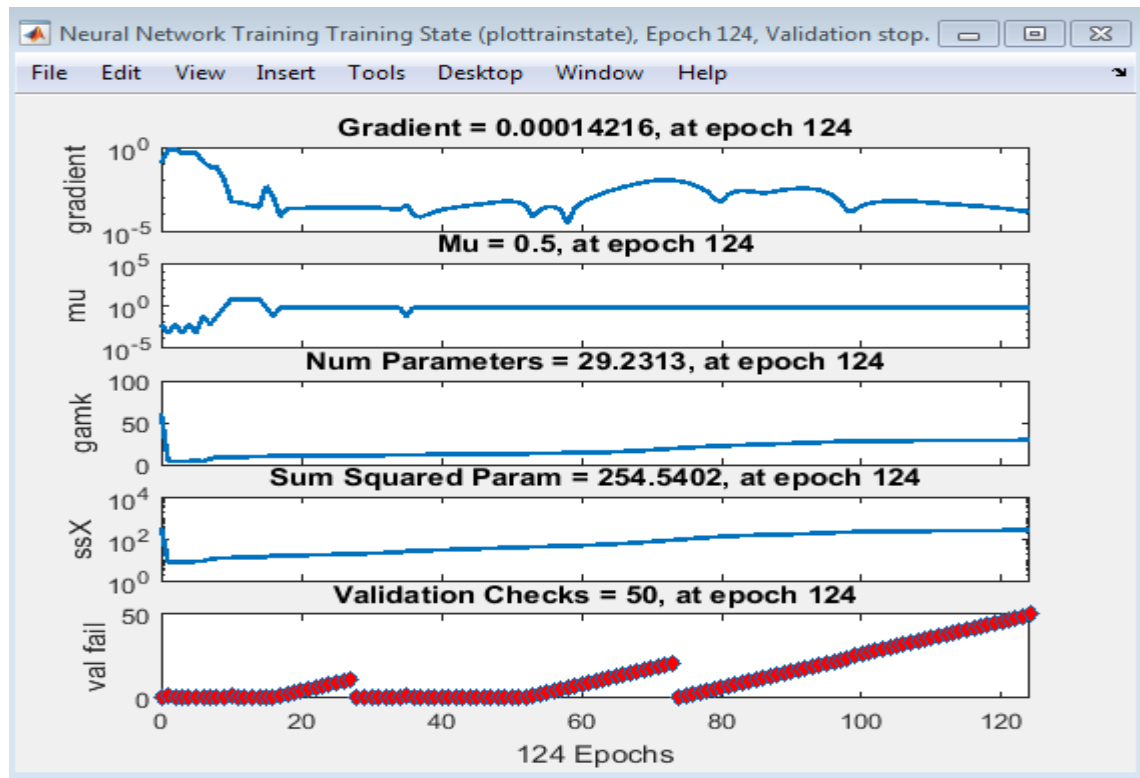


Fig. 5.8 Training State Plot for Model Validation

5.3 Discussion of Simulation Results

This section presents discussions of the MATLAB simulated results using FFNN presented in Section 5.2. Table 5.1 shows the computed values of mean squared error (mse) and correlation coefficient of network performance, R. It shows values of mse and R values for different number of data samples for training, validation and testing of the generated FFNN. The data samples range from 100, 200, 300, 400 and 500.

Table 5.1 Statistical Error Parameters of Developed FFNN Models for Different Data Sample Size

Number of Data Samples	Levenberg - Marquardt Algorithm				Bayesian Regularisation Algorithm			
	A/F – LOGSIG		A/F – TANSIG		A/F - LOGSIG		A/F - TANSIG	
	MSE	R	MSE	R	MSE	R	MSE	R
100	1.48E-04	0.99724	2.48E-04	0.99842	2.55E-04	0.99702	2.32E-04	0.99668
200	1.03E-04	0.99894	2.76E-04	0.99751	1.87E-04	0.99812	1.67E-04	0.99843
300	1.33E-04	0.99904	1.74E-04	0.99911	3.70E-04	0.99831	3.03E-04	0.99701
400	8.93E-04	0.99565	4.46E-04	0.99685	5.50E-03	0.9755	5.41E-04	0.99738
500	0.0064	0.96889	6.40E-03	0.96977	6.50E-03	0.96807	6.40E-03	0.96863

In this study, the network was decided to consist of one hidden layer with 10 neurons. The criterion R and MSE were selected to evaluate the networks to find the optimum solution. The complexity and size of the network was also an important consideration and therefore smaller ANN's had to be selected. A regression analysis between the network response and the corresponding targets was performed to investigate the network response in more detail. Thus Levenberg – Marquardt (LM) and Bayesian Regularisation (BR) were selected. The R-values in Table 5.1 represent the correlation coefficient between the outputs and targets. The R-values did not increase beyond 10 neurons in the hidden layer. Consequently, the network with 10 neurons in the hidden layer would be considered satisfactory. From all the networks trained, few ones could provide the low error condition, from which the simplest network was chosen. The results showed that the training algorithm of Levenberg-Marquardt was sufficient for predicting SAG Mill motor failures. There is a high correlation between the predicted values by the ANN model and the measured values collected from normal real time running of 5.8 MW, 11 kV SAG Mill motor, which imply that the model succeeded in prediction of SAG Mill motor failures.

It is also observed in Fig. 5.1 and Fig. 5.5 that the ANN provided the best accuracy in modelling induction motor failures with correlation coefficients of 0.999 and 0.998 for Levenberg-Marquardt and Bayesian Regularisation respectively. Generally, the artificial neural network offers the advantage of being fast, accurate and reliable in the prediction or approximation affairs, especially when numerical and mathematical methods fail. There is also a significant simplicity in using ANN due to its power to deal with multivariate and complicated problems.

The measured values collected from the real time, on load running of the 5.8 MW, 11 kV SAG Mill motor showed some linearity between the current, temperatures and the power. The power of the SAG Mill motor at nominal load ranges from 4 MW – 5.6 MW with the current and temperatures reading 300 A – 349 A and 80°C - 109°C respectively.

From Table 5.1, it can be seen that the artificial neural network showed good R and MSE values when data samples of 300 was used. This was the same for Levenberg-Marquardt and Bayesian Regularisation, while using Log-sigmoid and tan-sigmoid as transfer functions for the hidden layer. The results for R-values for data samples of 300 were 0.99904, 0.99911, 0.99831 and 0.99701 respectively, while MSE values were 1.33E-04, 1.74E-04, 3.70E-04 and 3.03E-04 respectively. This simulation was repeated for data

samples of 100, 200, 400 and 500. It was observed that increasing the number of data samples resulted in bad R-values. Data samples of 100 gave better results than 200, 200 gave better results than 400 and 400 than 500 in that order.

Training stops after 251 iterations. At this position, performance of network, 150×10^{-4} , gradient decrease into 3.55×10^{-4} and also value of $\mu 10^{-7}$ is shown in Fig.5.4. Validation performance reach minimum at epoch 201. Training continues for more 51 iterations and stops at epoch 251. Gradient and μ increases gradually as shown in Fig. 5.4

From error histogram shown in Fig. 5.3, most error occurs between -0.04 to +0.05. Errors also occur at 0.065, 0.087 and 0.094 of training data on histogram also represents the point for which output 4.5 and target value 4.6, output 4.8 – target 4.9 and output 5.1- target 5.2 on training correlation coefficient for network performance plot shown in Fig. 5.1

5.4 Discussions on Using the Network for Prediction

Two matrices of 5×669 and 5×31 constructed by power, current and three winding temperature values normalized sample data of SAG Mill motor at healthy and faulty on load condition respectively as input are used to analyze network performance. Among them, 70%, 15% and rest data are used as training, cross validation and testing data. The target of the network is 1 or 0, with 1 indicating healthy motor condition and 0 indicating faulty motor condition. For any output value between 1 and 0 represents the probability of fault condition, in training the network, there was 1 hidden layer with 10 neurons and tansigmoid as the transfer function. The output layer had 1 neuron and the transfer function was logsigmoid.

Fresh data samples consisting of 5×169 and 5×10 healthy and faulty on load power, current and three winding temperatures of the SAG Mill motor were fed into the network to detect health. Table 5.2, Fig. 5.9 and Fig. 5.10 show detection efficiency and confusion plot of network using Levenberg-Marquardt and Bayesian Regularization algorithm respectively. Out of the 169 healthy data samples, using Levenberg-Marquardt training algorithm could rightly predict them as true detection (TD) and false detection (FD) of 0. The network could also predict a TD of 10 out of 10 faulty data fed into it. This shows the network with Levenberg-Marquardt training algorithm can detect healthy and faulty conditions of the SAG Mill motor with 100% accuracy. Bayesian Regularization training algorithm could detect 169 healthy samples as TD and 9 out of 10 faulty data samples as TD and 1 FD,

therefore network with Bayesian Regularization could detect healthy and faulty conditions of the SAG Mill motor with 99.4% efficiency.

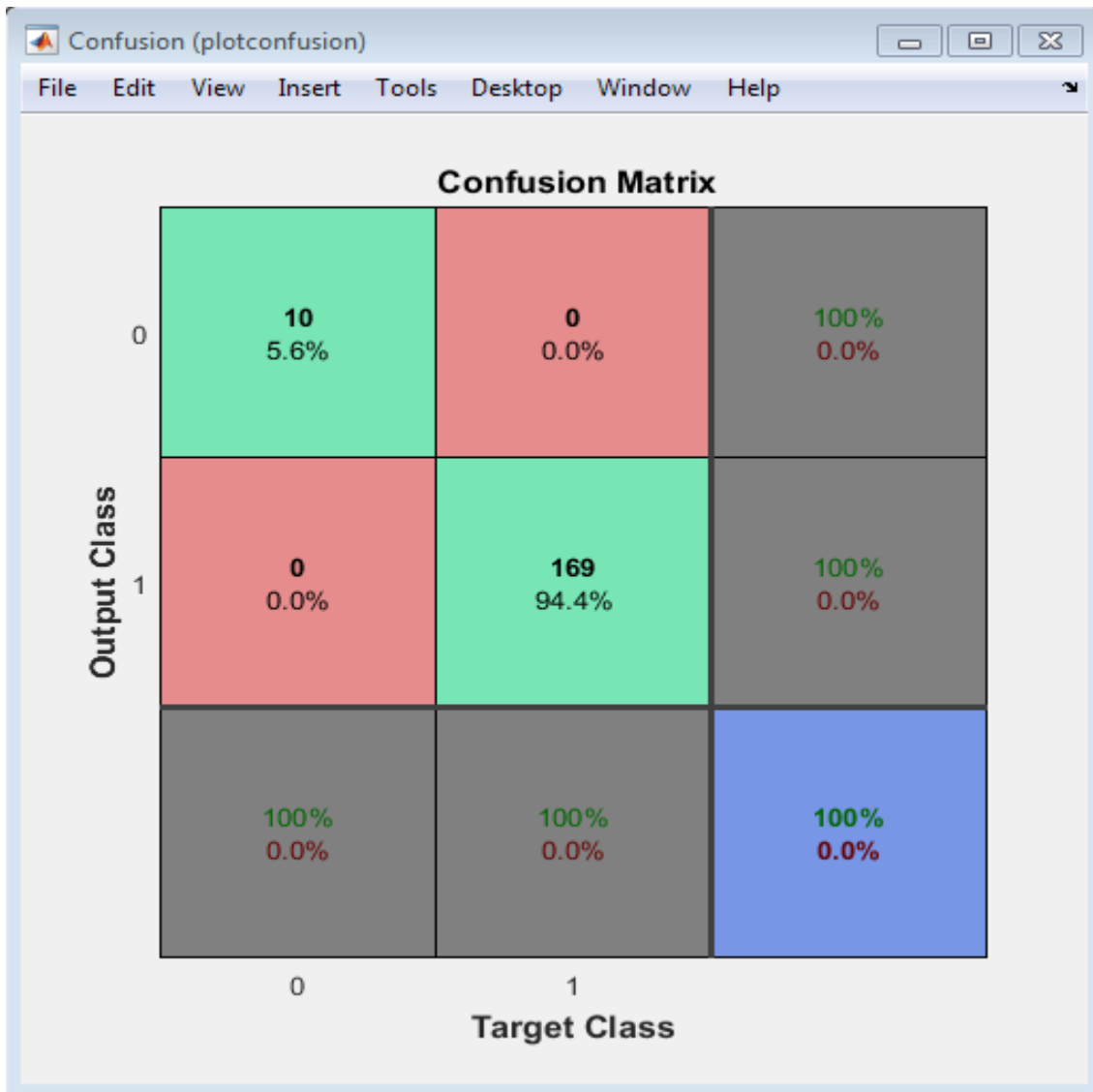


Fig. 5.9 Plot of Confusion Matrix Using Levenberg-marquardt Algorithm

Table 5.2 Detection Accuracy

Total Number Data Samples	Healthy		Faulty		Accuracy
	TD	FD	TD	FD	
Levenberg-Marquardt	169/169	0/169	10/10	0/10	100%
Bayesian Regularization	169/169	0/169	9/10	1/10	99.4%

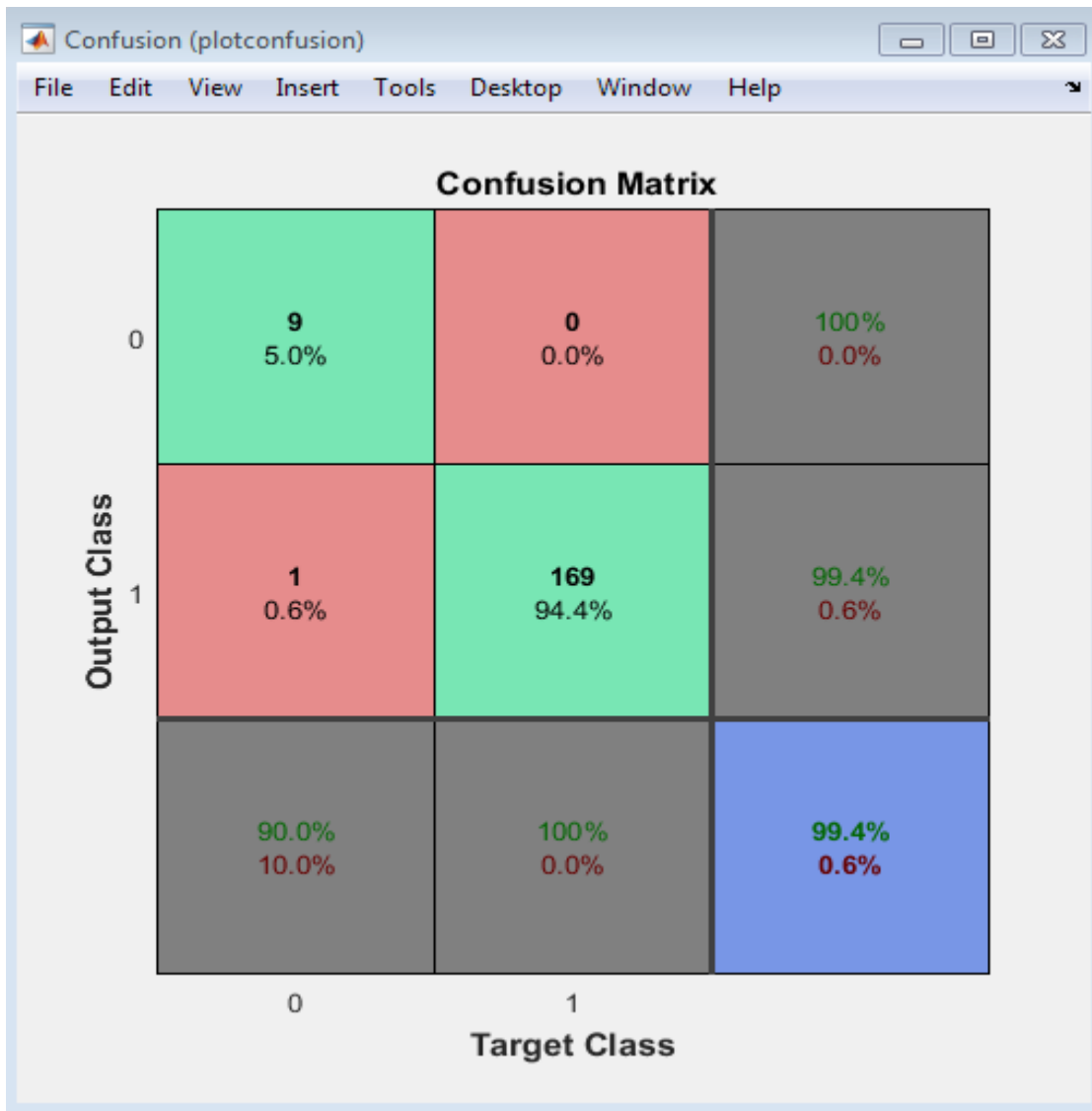


Fig. 5.10 Plot of Confusion Matrix Using Bayesian Regularization Algorithm

5.5 Summary of Findings

The findings as regards simulations of data samples measured on 5.8 MW, 11 kV SAG Mill motor at the Goldfields Ghana Ltd, Damang Mine from 6th January, 2019 to 8th April, 2019 are be summarised as follows:

- i. A smaller Feed-Forward neural network size of 4-10-1 provides optimum performance for prediction of SAG Mill motor failures;
- ii. Though Bayesian Regularisation training algorithm has not been extensively used in failure prediction of three phase slip ring induction motor as compared to Levenberg-Marquardt, yet it gives acceptable results in terms of accuracy but at a relatively low efficiency;

- iii. Data samples of 100, 200, 300, 400 and 500 were used in this work. Data samples of 300 with Levenberg-Marquardt training algorithm and tansigmoid activation function of the hidden layer provided the best results for R-Values and MSE;
- iv. Morsalin *et al* (2014), used similar network (2-10-1) on 0.5 hp, 220 – 240 V, 50 Hz single phase induction motor on no load to predict inter-turn failure and achieved R-value of 0.9994 but this work used a network (4-10-1) and achieved R-value of 0.99911;
- v. The network stopped training at 251 iteration, network performance of 150×10^{-4} at this position. Gradient decreases into 3.55×10^{-4} and $\mu 10^{-7}$. Validation performance reaches minimum at epoch 201; and
- vi. The network with Levenberg-Marquardt training algorithm can detect healthy and faulty conditions of the SAG Mill motor with 100% accuracy and 99.4% using Bayesian Regularization as the training algorithm.



CHAPTER 6

CONCLUSIONS AND RECOMMENDATIONS

6.1 Conclusions

From the results and discussions, the following conclusions can be drawn:

- i. The proposed Feed – Forward Neural Network with Levenberg-Marquardt training algorithm is capable of predicting imminent faults of on load 5.8 MW, 11 kV SAG Mill three phase slip ring induction motor at Goldfields Ghana Ltd., Damang mine with 100% accuracy;
- ii. Correlation coefficient of network performance, R and Mean squared error, MSE proved to be very good statistical tools for artificial neural network model analysis; and
- iii. Bayesian Regularisation training algorithm proved to be a good alternative to Levenberg-Marquardt algorithm in failure prediction networks.

6.2 Recommendations

It is recommended that:

- i. With relevant data on speed and vibration of SAG Mill Motor, fault detection range and accuracy of detection of network can be increased.
- ii. Calculated increase in hidden layer size beyond the applied size of 10 will increase the power of the network but care must be taken to prevent overfitting ;
- iii. MATLAB/SIMULINK and Finite Element Method Magnetics (FEMM) could be considered in generating signals for this research since it will be very difficult to set up a prototype of three phase 5.8 MW, 11 kV slip ring induction motor taking into consideration size and cost,; and
- iv. Wavelet techniques and Fuzzy logic could be used to find exact location of fault, and identification and evaluation of fault severity.

6.3 Research Contributions

- i. Bayesian Regularisation training algorithm showed to be a good alternative to Levenberg-Marquardt algorithm in failure prediction networks.

REFERENCES

- Anon (1997), “Electrical Documentation on Slipring Induction Motors for SAG Mill and Ball Mill” Goldfields Damang Mine, pp. 1 - 140.
- Anon (2018a), “Induction Motors”, <http://chettinadtech.ac.in/storage/12-07-12/12-07-12-10-43-28-1527-Thenmozhi.pdf>. Accessed: May 9, 2018.
- Anon (2018b), “Chapter 3: Causes and Effects of Electrical Faults”, https://shodhganga.inflibnet.ac.in/bitstream/10603/42008/8/08_chapter%203.pdf. Accessed: May 9, 2018.
- Anon (2018c), “Artificial Neural Network (ANN)”, www.cs.kumamoto-u.ac.jp/eps/epslab/ICinPS/Lecture-2.pdf. Accessed: May 9, 2018.
- Anon (2019a), “Gold Prices – Historical Annual Data”, www.macrotrends.net/gold/1333/historical_prices-100-year-chart. Accessed: July 2, 2019.
- Anon (2019b), “Carbon Brushes for Motors and Generators”, www.mersen.com. Accessed: May 28, 2019.
- Al Shamisi, M. H., Assi, A. H. and Hejase, H. A. N. (2011), “Using MATLAB to Develop Artificial Neural Network Models for Predicting Global Solar Radiation in AI Ain City - UAE”, *Engineering Education and Research Using MATLAB*, Dr. Assi, A.(Ed.), InTech, pp. 220 – 238.
- Antonino-Daviu, J. A., Riera-Guasp, M., Folch, J. R. and Palomares, M. P. M. (2006), “Validation of a New Method for the Diagnosis of Rotor Bar Failures via Wavelet Transform in Industrial Induction Machines” *IEEE Transactions on Industry Applications*, Vol. 42, No. 4, pp. 990 - 996.
- Araujo, R. S., Rodrigues, R. A., Paula, H., Filho, B. J. C., Baccarini, L. M. R. and Rocha, A. V. (2015), “Premature Wear and Recurring Bearing Failures in an Inverter-Driven Induction Motor – Part II: The Proposed Solution” *IEEE Transactions on Industry Applications*, Vol. 51, No. 1, pp. 92 - 100.

- Baccarini, L. M. R., Silva, V. V. R., Menezes, B. R. and Caminhas, W. M. (2011), "SVM Practical Industrial Application for Mechanical Faults Diagnostic" *Expert Systems with Applications*, Vol. 38, No. 1, pp. 6980 - 6984.
- Bachir, S., Tnani, S., Trigeassou, J. and Champenois, G. (2006), "Diagnosis by Parameter Estimation of Stator and Rotor Faults Occurring in Induction Machines", *IEEE Transactions on Industrial Electronics*, Vol. 53, No. 3, pp. 963 - 973.
- Ballal, M. S., Khan, Z. J., Suryawanshi, H. M. and Sonolikar, R. L. (2007), "Adaptive Neural Fuzzy Inference System for the Detection of Inter-Turn Insulation and Bearing Wear Faults in Induction Motor", *IEEE Transactions on Industrial Electronics*, Vol. 54, No. 1, pp. 250 - 258.
- Bhowmik, P. A., Pradhan, S. and Prakash, M. (2013), "Fault Diagnostic and Monitoring Methods of Induction Motor: A Review", *International Journal of Applied Control, Electrical and Electronics Engineering*, Vol. 1, No. 1, 18 pp.
- Eltabach, M., Charara, A. and Zein, I. (2004), "A Comparison of External and Internal Methods of Signal Spectral Analysis for Broken Rotor Bars Detection in Induction Motors", *IEEE Transactions on Industrial Electronics*, Vol. 51, No. 1, pp. 107-121.
- Ghate, V. N. and Sanjay V. Dudul, S. V. (2011), "Cascade Neural-Network-Based Fault Classifier for Three-Phase Induction Motor", *IEEE Transactions on Industrial Electronics*, Vol. 58, No. 5, pp. 1555 - 1563.
- Hagan, M. T., Demuth, H. B., Beale, M. H. and Jesus, O., *Neural Network Design, 2nd Edition*, Martin Hagan Publishers, Oklahoma, 2014, pp. 1-5 – 1-9.
- Han, T., Yang, B., Choi, W., and Kim, J. (2006), "Fault Diagnosis System of Induction Motors Based on Neural Network and Genetic Algorithm Using Stator Current Signals" *International Journal of Rotating Machinery* Vol. 2006, Article ID 61690, 13pp.
- Hu, N. Q., Xia, L. R., Gu, F. S. and Qin, G. J. (2011), "A Novel Transform Demodulation Algorithm for Motor Incipient Fault Detection", *IEEE Transactions on Instrumentation and Measurement*, Vol. 60, No. 2, pp. 480-487.

- Jha, G. K. (2013), “Artificial Neural Networks”, *Indian Agricultural Research Institute*, New Delhi, India, 10 pp.
- Kadir, A., Alukaidey, T., Al-Ayasrah, O. and Salman, R. (2006), “Embedded Control with Predictive Diagnostics Algorithm of the Induction Machine Drive System”, *Proceedings of the 2006 American Control Conference*, Minneapolis, Minnesota, USA, pp. 1080-1085.
- Karmakar, S., Chattopadhyay, S., Mitra, M. and Sengupta, S. (2016), “Induction Motor Fault Diagnosis”, *Springer Science and Business Media*, Singapore, 23 pp.
- Kayri, M. (2016), “Predictive Abilities of Bayesian Regularization and Levenberg-Marquardt Algorithms in Artificial Neural Networks: A Comparative Empirical Study on Social Data”, *Mathematical and Computational Applications*, Vol.21, No. 2, 11pp.
- Kraleti, R. S., Zawodniok, M. and Jagannathan, S. (2012), “Model Based Diagnostics and Prognostics of Three-Phase Induction Motor for Vapor Compressor Applications”, *Proceedings of IEEE Conference on Prognostics and Health Management*, pp. 1-7.
- Lizarraga-Morales, R. A., Rodriguez-Donate, C., Cabal-Yepez, E., Lopez-Ramirez, L. M., and Ferrucho-Alvarez, E. R. (2017), “Novel FPGA-based Methodology for Early Broken Rotor Bar Detection and Classification Through Homogeneity Estimation”, *IEEE Transactions on Instrumentation and Measurement*, Vol. 66, No. 7, 10 pp.
- Mahmoud, H., Abdallah, A. A., Bianchi, N., El-Hakim, S. M., Shaltout, A. and Dupré, L. (2016), “An Inverse Approach for Interturn Fault Detection in Asynchronous Machines Using Magnetic Pendulous Oscillation Technique”, *IEEE Transactions on Industry Applications*, Vol. 52, No. 1, pp. 226-233.
- Morsalin, S., Mahmud, K., Mohiuddin, H., Halim, R. and Saha, P. (2014), “Induction Motor Inter-turn Fault Detection Using Heuristic Noninvasive Approach by Artificial Neural Network with Levenberg Marquardt Algorithm”, *IEEE International Conference on Informatics, Electronics & Vision*, Dhaka, Bangladesh, 6 pp.
- Rangel-Magdaleno, J. J., Romero-Troncoso, R. J., Osomio-Rios, R. A., Cabal-Yepez, E. and Contreras-Medina, L. M. (2009), “Novel Methodology for Online Half-Broken-

Bar Detection on Induction Motors” *IEEE Transactions on Instrumentation and Measurement*, Vol. 58, No. 5, pp. 1690 – 1698.

Suwatthikul, J. and Sornmuang, S. (2011), “Fault Detection and Diagnosis of a Motor Bearing Shield” *The 6th IEEE International Conference on Intelligent Data Acquisition and Advanced Computing Systems: Technology and Applications*, Prague, Czech Republic, pp. 332 - 335.

The MathWorks, (2019), “MATLAB”, <https://www.mathworks.com/products/deep-learning.html>. Accessed: July 4, 2019.

Tymvios, F., Michaelides, S. and Skouteli, C. (2008), “Estimation of Surface Solar Radiation with Artificial Neural Networks”, *Modelling Solar Radiation at the Earth Surface*, Viorel Badescu, Germany, pp. 221 – 256.

Vieira, M., Madeira, H. and Irrera, I. (2009), “Fault Injection for Failure Prediction Methods Validation”, *40th International Conference on Dependable Systems and Networks*, Chicago, USA, 6 pp.

Yu, M., Wang, D., Ukil, A., Vaiyapuri, V., Sivakumar, N., Jayampathi, C., Gupta, A. K. and Nguyen, V. (2014), “Model-based Failure Prediction for Electric Machines using Particle Filter”, *13th International Conference on Control, Automation, Robotics and Vision*, Marina Bay Sands, Singapore, pp. 1811 - 1816.

APPENDICES

APPENDIX A

RAW DATA OF SAG MILL MOTOR

Table A1. Raw Data of SAG Mill Motor from 6th January, 2019 to 8th April, 2019

DATE	TIME	SAG MOTOR POWER	SAG MOTOR CURRENT	SAG MILL MOTOR WINDING TEMP. 1	SAG MILL MOTOR WINDING TEMP. 2	SAG MILL MOTOR WINDING TEMP. 3
6/1/2019	10:26:29 AM	5.324	337.125	92.355	94.208	91.888
6/1/2019	12:57:22 PM	4.436	280.121	93.648	95.184	92.999
6/1/2019	3:28:15 PM	5.246	331.270	95.820	97.483	95.320
6/1/2019	5:59:08 PM	5.058	321.761	100.747	102.679	100.297
6/1/2019	8:30:01 PM	5.272	332.942	97.556	99.639	97.172
6/1/2019	11:00:54 PM	5.395	339.629	95.430	97.512	95.064
7/1/2019	1:31:47 AM	5.386	339.323	94.343	96.431	94.003
7/1/2019	4:02:40 AM	5.454	342.538	95.026	97.065	94.640
7/1/2019	6:33:33 AM	5.472	343.427	95.728	97.772	95.362
7/1/2019	9:04:26 AM	5.246	331.535	94.016	96.081	93.758
7/1/2019	11:35:19 AM	5.331	336.167	97.145	99.088	96.728
7/1/2019	2:06:12 PM	5.135	326.394	97.921	99.836	97.554
7/1/2019	4:37:05 PM	5.381	339.135	100.630	102.554	100.072
7/1/2019	7:07:58 PM	5.288	334.742	98.671	100.715	98.217
7/1/2019	9:38:51 PM	5.398	340.527	96.553	98.580	96.145
8/1/2019	12:09:44 AM	5.445	342.527	95.485	97.540	95.109
8/1/2019	2:40:37 AM	5.255	332.831	92.630	94.704	92.383
8/1/2019	5:11:30 AM	5.415	340.715	92.727	94.763	92.419
8/1/2019	7:42:23 AM	5.365	338.574	91.274	93.301	91.005
7/1/2019	9:04:26 AM	5.612	353.611	94.436	96.670	94.224
9/1/2019	11:22:06 AM	5.495	344.908	97.572	99.534	97.108
9/1/2019	1:52:59 PM	5.470	343.515	102.447	104.367	101.882
9/1/2019	4:23:52 PM	5.354	337.338	104.434	106.312	103.858
9/1/2019	6:54:45 PM	5.573	348.572	105.745	107.680	105.146
9/1/2019	9:25:38 PM	5.563	348.210	102.703	104.819	102.211

Table A1. Raw Data of SAG Mill Motor from 6th January, 2019 to 8th April, 2019

Cont'd

DATE	TIME	SAG MOTOR POWER	SAG MOTOR CURRENT	SAG MILL MOTOR WINDING TEMP. 1	SAG MILL MOTOR WINDING TEMP. 2	SAG MILL MOTOR WINDING TEMP. 3
9/1/2019	11:56:31 PM	5.504	345.392	98.818	100.958	98.395
10/1/2019	2:27:24 AM	5.382	339.273	95.519	97.588	95.205
10/1/2019	4:58:17 AM	4.577	289.705	86.487	88.096	85.938
10/1/2019	7:29:10 AM	5.324	335.837	89.512	91.432	89.202
10/1/2019	10:00:03 AM	5.168	327.747	91.957	93.835	91.665
10/1/2019	12:30:56 PM	5.094	324.025	96.367	98.235	96.007
10/1/2019	3:01:49 PM	5.412	341.031	102.322	104.082	101.724
10/1/2019	5:32:42 PM	5.396	340.403	104.988	106.861	104.373
10/1/2019	8:03:35 PM	5.421	341.390	102.711	104.725	102.191
10/1/2019	10:34:28 PM	5.295	335.216	97.654	99.688	97.283
11/1/2019	1:05:21 AM	5.395	340.210	95.816	97.834	95.473
11/1/2019	3:36:14 AM	5.390	340.247	95.261	97.351	94.916
11/1/2019	6:07:07 AM	5.291	334.604	93.591	95.623	93.342
11/1/2019	8:38:00 AM	5.255	332.731	92.659	94.645	92.464
11/1/2019	11:08:53 AM	5.302	333.652	95.351	97.206	95.001
11/1/2019	1:39:46 PM	4.388	277.199	93.437	94.967	92.984
11/1/2019	4:10:39 PM	5.160	325.423	100.456	102.329	100.186
11/1/2019	6:41:32 PM	5.128	323.820	100.167	102.194	99.892
11/1/2019	9:12:25 PM	5.252	330.693	98.484	100.536	98.294
11/1/2019	11:43:18 PM	5.311	333.773	97.616	99.622	97.430
12/1/2019	2:14:11 AM	5.292	332.758	95.651	97.685	95.472
12/1/2019	4:45:04 AM	5.383	337.912	96.465	98.531	96.219
12/1/2019	7:15:57 AM	5.458	341.772	96.351	98.342	96.110
12/1/2019	9:46:50 AM	5.174	326.857	95.030	97.094	94.901
12/1/2019	12:17:43 PM	5.276	332.244	96.230	98.173	95.994
12/1/2019	2:48:36 PM	5.200	328.273	98.631	100.602	98.424
12/1/2019	5:19:29 PM	5.314	333.787	100.244	102.185	99.935
12/1/2019	7:50:22 PM	5.337	335.122	99.272	101.323	99.043
12/1/2019	10:21:15 PM	5.294	332.527	96.855	98.895	96.705
13/1/2019	12:52:08 AM	5.301	332.832	95.618	97.670	95.475
13/1/2019	3:23:01 AM	5.239	329.831	93.518	95.608	93.433
13/1/2019	5:53:54 AM	5.326	334.356	93.604	95.683	93.473
13/1/2019	8:24:47 AM	5.393	337.734	93.624	95.688	93.475
13/1/2019	10:55:40 AM	5.358	336.123	97.014	98.958	96.766
13/1/2019	1:26:33 PM	5.293	333.057	100.740	102.653	100.408
13/1/2019	3:57:26 PM	5.309	333.537	103.840	105.700	103.433
13/1/2019	6:28:19 PM	5.314	333.635	104.212	106.152	103.842
13/1/2019	8:59:12 PM	5.397	337.998	100.826	102.918	100.558

Table A1. Raw Data of SAG Mill Motor from 6th January, 2019 to 8th April, 2019

Cont'd

DATE	TIME	SAG MOTOR POWER	SAG MOTOR CURRENT	SAG MILL MOTOR WINDING TEMP. 1	SAG MILL MOTOR WINDING TEMP. 2	SAG MILL MOTOR WINDING TEMP. 3
13/1/2019	11:30:05 PM	5.235	329.565	96.776	98.866	96.616
14/1/2019	2:00:58 AM	5.290	332.406	95.724	97.778	95.547
14/1/2019	4:31:51 AM	5.231	329.331	94.153	96.224	94.050
14/1/2019	7:02:44 AM	5.293	332.787	94.041	96.117	93.909
14/1/2019	9:33:37 AM	5.263	331.366	94.779	96.813	94.651
14/1/2019	12:04:30 PM	5.484	342.780	99.019	100.945	98.692
14/1/2019	2:35:23 PM	5.229	329.737	100.777	102.712	100.441
14/1/2019	5:06:16 PM	5.287	332.514	104.131	105.959	103.691
14/1/2019	7:37:09 PM	4.944	314.751	98.999	101.066	98.870
14/1/2019	10:08:02 PM	5.306	334.430	96.665	98.693	96.471
15/1/2019	12:38:55 AM	5.384	338.315	96.357	98.374	96.146
15/1/2019	3:09:48 AM	5.430	340.831	96.589	98.607	96.347
15/1/2019	5:40:41 AM	5.056	321.311	93.571	95.617	93.511
15/1/2019	8:11:34 AM	5.370	337.653	94.787	96.790	94.582
15/1/2019	10:42:27 AM	5.335	335.170	97.039	99.003	96.818
15/1/2019	1:13:20 PM	5.396	338.847	101.113	103.023	100.743
15/1/2019	3:44:13 PM	5.263	332.005	102.679	104.558	102.340
15/1/2019	6:15:06 PM	5.314	334.699	102.681	104.639	102.378
15/1/2019	8:45:59 PM	5.264	332.091	98.957	101.046	98.728
15/1/2019	11:16:52 PM	5.289	333.384	96.907	98.937	96.720
16/1/2019	1:47:45 AM	5.303	334.246	95.399	97.423	95.239
16/1/2019	4:18:38 AM	5.329	335.534	95.076	97.117	94.904
16/1/2019	6:49:31 AM	5.460	342.470	96.823	98.869	96.562
16/1/2019	9:20:24 AM	4.760	298.247	96.113	97.846	95.680
16/1/2019	11:51:17 AM	5.121	319.788	93.732	95.440	93.355
16/1/2019	2:22:10 PM	5.347	336.404	101.815	103.691	101.398
16/1/2019	4:53:03 PM	5.280	333.112	104.479	106.382	104.047
16/1/2019	7:23:56 PM	5.408	340.045	101.916	103.901	101.539
16/1/2019	9:54:49 PM	5.450	341.934	97.708	99.845	97.492
17/1/2019	12:25:42 AM	5.522	345.572	95.041	97.166	94.791
17/1/2019	2:56:35 AM	4.763	299.713	89.432	91.193	88.989
17/1/2019	5:27:28 AM	5.439	341.179	90.533	92.476	90.314
17/1/2019	7:58:21 AM	5.485	343.572	92.917	94.902	92.698
17/1/2019	10:29:14 AM	5.559	347.468	96.808	98.718	96.434
17/1/2019	1:00:07 PM	5.614	350.690	102.866	104.743	102.397
17/1/2019	3:31:00 PM	5.395	339.057	104.792	106.708	104.394

Table A1. Raw Data of SAG Mill Motor from 6th January, 2019 to 8th April, 2019

Cont'd

DATE	TIME	SAG MOTOR POWER	SAG MOTOR CURRENT	SAG MILL MOTOR WINDING TEMP. 1	SAG MILL MOTOR WINDING TEMP. 2	SAG MILL MOTOR WINDING TEMP. 3
17/1/2019	6:01:53 PM	5.504	344.635	105.423	107.390	105.037
17/1/2019	8:32:46 PM	5.485	343.151	101.330	103.420	101.017
17/1/2019	11:03:39 PM	5.494	343.270	99.048	101.122	98.785
18/1/2019	1:34:32 AM	5.460	341.449	97.424	99.528	97.191
18/1/2019	4:05:25 AM	5.481	342.719	95.999	98.056	95.767
18/1/2019	6:36:18 AM	5.484	342.864	95.564	97.585	95.351
18/1/2019	9:07:11 AM	5.344	335.599	94.565	96.640	94.371
18/1/2019	11:38:04 AM	5.449	340.944	97.338	99.289	97.040
18/1/2019	2:08:57 PM	5.528	345.020	102.001	103.901	101.565
18/1/2019	4:39:50 PM	5.326	334.506	103.796	105.738	103.366
18/1/2019	7:10:43 PM	5.453	341.541	101.456	103.551	101.127
18/1/2019	9:41:36 PM	5.398	338.798	99.620	101.708	99.332
19/1/2019	12:12:29 AM	5.517	345.083	97.993	100.066	97.696
19/1/2019	2:43:22 AM	5.391	338.277	95.740	97.837	95.531
19/1/2019	5:14:15 AM	5.120	324.146	93.320	95.413	93.227
19/1/2019	7:45:08 AM	5.300	333.522	92.928	94.974	92.779
19/1/2019	10:16:01 AM	4.270	270.893	87.487	89.009	86.965
19/1/2019	12:46:54 PM	5.638	350.346	97.372	99.052	96.923
19/1/2019	3:17:47 PM	5.518	344.053	105.452	107.232	104.932
19/1/2019	5:48:40 PM	5.532	345.849	107.034	108.935	106.548
19/1/2019	8:19:33 PM	5.520	345.108	102.926	104.939	102.614
19/1/2019	10:50:26 PM	5.449	341.133	98.154	100.203	97.903
20/1/2019	1:21:19 AM	5.491	343.635	97.764	99.799	97.507
20/1/2019	3:52:12 AM	5.439	340.736	96.143	98.141	95.911
20/1/2019	6:23:05 AM	5.519	344.969	97.338	99.360	97.077
20/1/2019	8:53:58 AM	5.440	340.924	97.589	99.598	97.352
20/1/2019	11:24:51 AM	5.374	337.667	98.885	100.839	98.591
20/1/2019	1:55:44 PM	5.451	342.079	102.074	103.924	101.654
20/1/2019	4:26:37 PM	5.388	338.774	104.114	105.982	103.697
20/1/2019	6:57:30 PM	5.480	343.624	104.240	106.126	103.773
20/1/2019	9:28:23 PM	5.459	342.632	100.782	102.828	100.473
20/1/2019	11:59:16 PM	5.590	349.375	98.954	100.955	98.648
21/1/2019	2:30:09 AM	5.607	350.249	98.317	100.353	98.055
21/1/2019	5:01:02 AM	5.522	345.502	96.521	98.534	96.281
21/1/2019	7:31:55 AM	5.570	348.152	96.577	98.574	96.315
21/1/2019	10:02:48 AM	5.437	341.189	96.536	98.524	96.277
21/1/2019	12:33:41 PM	5.555	347.419	100.411	102.267	99.983
21/1/2019	3:04:34 PM	5.495	343.977	104.626	106.432	104.131
21/1/2019	5:35:27 PM	5.455	342.203	106.627	108.359	106.078
21/1/2019	8:06:20 PM	5.445	341.816	103.983	105.996	103.603

Table A1. Raw Data of SAG Mill Motor from 6th January, 2019 to 8th April, 2019

Cont'd

DATE	TIME	SAG MOTOR POWER	SAG MOTOR CURRENT	SAG MILL MOTOR WINDING TEMP. 1	SAG MILL MOTOR WINDING TEMP. 2	SAG MILL MOTOR WINDING TEMP. 3
21/1/2019	10:37:13 PM	5.360	337.603	97.735	99.810	97.486
22/1/2019	1:08:06 AM	5.401	339.662	95.933	97.978	95.749
22/1/2019	3:38:59 AM	4.123	261.343	92.424	94.095	91.764
22/1/2019	6:09:52 AM	4.511	281.711	68.380	69.368	67.941
22/1/2019	8:40:45 AM	5.381	337.332	91.038	92.862	90.830
22/1/2019	11:11:38 AM	5.458	341.905	97.197	99.064	96.864
22/1/2019	1:42:31 PM	5.535	346.048	102.307	104.152	101.837
22/1/2019	4:13:24 PM	5.573	348.065	107.261	109.028	106.677
22/1/2019	6:44:17 PM	5.350	336.271	105.609	107.584	105.206
22/1/2019	9:15:10 PM	5.343	336.075	99.488	101.547	99.256
22/1/2019	11:46:03 PM	5.533	346.261	98.394	100.444	98.112
23/1/2019	2:16:56 AM	5.594	349.453	98.367	100.434	98.080
23/1/2019	4:47:49 AM	5.592	349.258	98.653	100.724	98.301
23/1/2019	7:18:42 AM	5.380	338.352	96.659	98.731	96.508
23/1/2019	9:49:35 AM	5.436	341.318	96.971	98.960	96.722
23/1/2019	12:20:28 PM	5.518	345.013	100.992	102.920	100.613
23/1/2019	2:51:21 PM	5.371	337.257	103.742	105.587	103.339
23/1/2019	5:22:14 PM	5.482	343.570	106.883	108.732	106.354
23/1/2019	7:53:07 PM	5.508	344.968	104.726	106.710	104.336
23/1/2019	10:24:00 PM	5.479	343.293	100.909	102.990	100.598
24/1/2019	12:54:53 AM	5.551	346.933	99.118	101.228	98.862
24/1/2019	3:25:46 AM	5.582	348.691	98.960	101.036	98.657
24/1/2019	5:56:39 AM	5.507	345.169	98.221	100.278	97.959
24/1/2019	8:27:32 AM	5.464	342.995	97.290	99.350	97.019
24/1/2019	10:58:25 AM	1.747	119.284	90.106	91.183	89.420
24/1/2019	1:29:18 PM	-0.065	8.884	75.351	76.529	75.462
24/1/2019	4:00:11 PM	-0.065	8.962	67.131	68.522	68.141
24/1/2019	6:31:04 PM	-0.065	8.902	61.383	62.842	62.803
24/1/2019	9:01:57 PM	-0.065	8.981	56.445	57.736	57.677
24/1/2019	11:32:50 PM	-0.065	8.592	52.889	54.045	53.992
25/1/2019	2:03:43 AM	-0.065	8.464	49.909	51.051	50.884
25/1/2019	4:34:36 AM	-0.065	8.751	47.195	48.416	48.091
25/1/2019	7:05:29 AM	0.517	37.170	44.843	46.103	45.628
25/1/2019	9:36:22 AM	-0.065	8.016	42.762	44.036	43.487
25/1/2019	12:07:15 PM	-0.065	8.225	40.544	41.751	41.261
25/1/2019	2:38:08 PM	0.530	42.103	37.779	38.787	38.810
25/1/2019	5:09:01 PM	5.409	338.865	81.157	82.532	80.939
25/1/2019	7:39:54 PM	5.516	344.753	91.810	94.063	91.710
25/1/2019	10:10:47 PM	5.390	337.968	88.536	90.699	88.493
26/1/2019	12:41:40 AM	5.426	339.917	88.854	90.965	88.793

Table A1. Raw Data of SAG Mill Motor from 6th January, 2019 to 8th April, 2019

Cont'd

DATE	TIME	SAG MOTOR POWER	SAG MOTOR CURRENT	SAG MILL MOTOR WINDING TEMP. 1	SAG MILL MOTOR WINDING TEMP. 2	SAG MILL MOTOR WINDING TEMP. 3
26/1/2019	3:12:33 AM	5.538	345.806	90.156	92.280	90.028
26/1/2019	5:43:26 AM	5.494	343.474	89.801	91.915	89.698
26/1/2019	8:14:19 AM	5.467	342.098	90.309	92.395	90.239
26/1/2019	10:45:12 AM	5.408	338.806	92.777	94.889	92.653
26/1/2019	1:16:05 PM	5.310	334.061	95.470	97.501	95.265
26/1/2019	3:46:58 PM	5.464	342.334	100.755	102.678	100.353
26/1/2019	6:17:51 PM	5.484	343.378	103.716	105.725	103.301
26/1/2019	8:48:44 PM	5.411	339.824	96.960	99.176	96.792
26/1/2019	11:19:37 PM	5.490	343.874	94.870	97.097	94.744
27/1/2019	1:50:30 AM	5.433	340.808	92.962	95.183	92.938
27/1/2019	4:21:23 AM	5.513	344.965	93.405	95.672	93.300
27/1/2019	6:52:16 AM	5.576	348.248	93.816	96.071	93.709
27/1/2019	9:23:09 AM	5.531	345.620	93.365	95.533	93.252
27/1/2019	11:54:02 AM	5.465	342.374	95.368	97.482	95.189
27/1/2019	2:24:55 PM	5.519	345.330	100.171	102.171	99.810
27/1/2019	4:55:48 PM	5.493	343.839	102.271	104.223	101.872
27/1/2019	7:26:41 PM	5.559	346.992	100.666	102.806	100.339
27/1/2019	9:57:34 PM	5.589	349.173	96.881	99.079	96.712
28/1/2019	12:28:27 AM	5.558	347.694	94.334	96.614	94.225
28/1/2019	2:59:20 AM	5.466	342.884	92.703	94.867	92.623
28/1/2019	5:30:13 AM	5.532	346.171	92.428	94.641	92.306
28/1/2019	8:01:06 AM	5.483	343.028	92.724	94.911	92.671
28/1/2019	10:31:59 AM	5.522	345.064	93.108	95.263	93.009
28/1/2019	1:02:52 PM	5.536	346.022	97.293	99.362	97.039
28/1/2019	3:33:45 PM	5.282	332.883	99.314	101.401	99.131
28/1/2019	6:04:38 PM	5.516	345.552	100.003	102.056	99.680
28/1/2019	8:35:31 PM	5.350	336.950	96.435	98.648	96.337
28/1/2019	11:06:24 PM	5.341	336.150	92.746	94.975	92.703
29/1/2019	1:37:17 AM	5.371	337.839	91.048	93.241	91.034
29/1/2019	4:08:10 AM	5.396	339.341	90.376	92.583	90.356
29/1/2019	6:39:03 AM	5.471	342.813	90.406	92.572	90.414
29/1/2019	9:09:56 AM	5.434	340.548	90.682	92.866	90.682
29/1/2019	11:40:49 AM	5.523	345.485	93.367	95.478	93.231
29/1/2019	2:11:42 PM	5.467	342.400	98.090	100.132	97.830
29/1/2019	4:42:35 PM	5.515	344.945	101.895	103.883	101.498
29/1/2019	7:13:28 PM	5.486	343.688	101.096	103.229	100.784
29/1/2019	9:44:21 PM	5.532	345.928	95.405	97.567	95.238
30/1/2019	12:15:14 AM	5.548	347.136	94.052	96.220	93.899
30/1/2019	2:46:07 AM	5.558	347.684	93.494	95.712	93.376
30/1/2019	5:17:00 AM	5.556	347.351	93.270	95.424	93.142
30/1/2019	7:47:53 AM	5.528	345.861	93.290	95.548	93.203

Table A1. Raw Data of SAG Mill Motor from 6th January, 2019 to 8th April, 2019

Cont'd

DATE	TIME	SAG MOTOR POWER	SAG MOTOR CURRENT	SAG MILL MOTOR WINDING TEMP. 1	SAG MILL MOTOR WINDING TEMP. 2	SAG MILL MOTOR WINDING TEMP. 3
30/1/2019	10:18:46 AM	5.431	340.974	93.960	96.132	93.880
30/1/2019	12:49:39 PM	5.538	346.271	98.024	100.040	97.761
30/1/2019	3:20:32 PM	5.519	345.138	102.191	104.174	101.801
30/1/2019	5:51:25 PM	5.548	347.121	103.978	106.045	103.571
30/1/2019	8:22:18 PM	5.442	341.618	97.625	99.886	97.489
30/1/2019	10:53:11 PM	5.468	343.168	94.748	96.950	94.668
31/1/2019	1:24:04 AM	5.541	346.649	94.257	96.496	94.163
31/1/2019	3:54:57 AM	5.533	346.410	93.341	95.588	93.283
31/1/2019	6:25:50 AM	5.496	344.605	92.625	94.893	92.528
31/1/2019	8:56:43 AM	5.501	344.850	91.666	93.852	91.618
31/1/2019	11:27:36 AM	5.240	330.611	93.187	95.335	93.178
31/1/2019	1:58:29 PM	5.513	345.318	98.016	100.042	97.736
31/1/2019	4:29:22 PM	5.477	343.519	102.711	104.686	102.324
31/1/2019	7:00:15 PM	5.132	320.134	100.460	102.415	100.092
31/1/2019	9:31:08 PM	4.934	308.113	86.770	88.832	86.656
1/2/2019	12:02:01 AM	5.330	333.116	87.955	90.184	87.992
1/2/2019	2:32:54 AM	5.409	337.062	88.442	90.666	88.422
1/2/2019	5:03:47 AM	5.359	334.579	87.729	89.971	87.785
1/2/2019	7:34:40 AM	5.217	327.456	86.827	89.096	86.926
1/2/2019	10:05:33 AM	5.308	331.909	88.085	90.210	88.104
1/2/2019	12:36:26 PM	5.571	345.385	95.443	97.567	95.251
1/2/2019	3:07:19 PM	5.410	337.165	98.509	100.613	98.333
1/2/2019	5:38:12 PM	5.435	338.412	98.092	100.359	97.980
1/2/2019	8:09:05 PM	5.449	339.490	95.016	97.330	95.009
1/2/2019	10:39:58 PM	5.469	340.793	93.380	95.690	93.402
2/2/2019	1:10:51 AM	5.355	335.381	92.543	94.855	92.589
2/2/2019	3:41:44 AM	5.223	328.245	90.113	92.399	90.260
2/2/2019	6:12:37 AM	5.375	336.341	90.770	93.028	90.856
2/2/2019	8:43:30 AM	5.408	337.806	91.028	93.242	91.080
2/2/2019	11:14:23 AM	5.041	318.952	92.065	94.304	92.187
2/2/2019	1:45:16 PM	4.812	307.185	91.258	93.403	91.376
2/2/2019	4:16:09 PM	4.787	305.757	88.799	91.104	89.061
2/2/2019	6:47:02 PM	4.810	306.815	83.368	85.689	83.678
2/2/2019	9:17:55 PM	4.750	303.413	82.919	85.246	83.276
2/2/2019	11:48:48 PM	4.951	314.020	83.461	85.812	83.792
3/2/2019	2:19:41 AM	5.062	319.612	84.334	86.684	84.597
3/2/2019	4:50:34 AM	5.214	327.139	85.773	88.007	85.938
3/2/2019	7:21:27 AM	5.457	339.449	88.514	90.790	88.606
3/2/2019	9:52:20 AM	5.280	330.949	89.711	91.940	89.756

Table A1. Raw Data of SAG Mill Motor from 6th January, 2019 to 8th April, 2019

Cont'd

DATE	TIME	SAG MOTOR POWER	SAG MOTOR CURRENT	SAG MILL MOTOR WINDING TEMP. 1	SAG MILL MOTOR WINDING TEMP. 2	SAG MILL MOTOR WINDING TEMP. 3
3/2/2019	12:23:13 PM	4.740	303.034	88.013	90.150	88.234
3/2/2019	2:54:06 PM	4.758	304.409	90.871	92.909	90.985
3/2/2019	5:24:59 PM	4.868	310.103	94.242	96.341	94.272
3/2/2019	7:55:52 PM	4.856	309.542	92.250	94.478	92.390
3/2/2019	10:26:45 PM	4.849	309.255	88.715	90.954	88.939
4/2/2019	12:57:38 AM	4.987	316.042	87.314	89.537	87.511
4/2/2019	3:28:31 AM	5.167	325.535	87.779	90.047	87.901
4/2/2019	5:59:24 AM	5.171	325.746	88.140	90.433	88.341
4/2/2019	8:30:17 AM	5.186	326.652	88.462	90.649	88.595
4/2/2019	11:01:10 AM	4.954	314.622	88.420	90.626	88.637
4/2/2019	1:32:03 PM	4.805	306.785	90.898	92.998	91.043
4/2/2019	4:02:56 PM	4.757	304.219	93.020	95.112	93.098
4/2/2019	6:33:49 PM	4.624	297.343	90.559	92.752	90.765
4/2/2019	9:04:42 PM	4.778	305.633	88.304	90.489	88.548
4/2/2019	11:35:35 PM	4.716	302.106	86.528	88.849	86.868
5/2/2019	2:06:28 AM	4.822	307.879	85.537	87.762	85.853
5/2/2019	4:37:21 AM	4.820	307.764	85.095	87.337	85.442
5/2/2019	7:08:14 AM	4.865	309.799	85.961	88.222	86.255
5/2/2019	9:39:07 AM	4.915	312.640	86.235	88.427	86.468
5/2/2019	12:10:00 PM	4.915	312.177	88.205	90.441	88.443
5/2/2019	2:40:53 PM	5.359	334.805	94.137	96.260	94.071
5/2/2019	5:11:46 PM	5.375	335.951	98.082	100.214	97.900
5/2/2019	7:42:39 PM	4.922	312.839	94.011	96.309	94.092
5/2/2019	10:13:32 PM	4.871	310.021	88.685	90.933	88.913
6/2/2019	12:44:25 AM	4.850	308.892	86.710	88.991	86.995
6/2/2019	3:15:18 AM	4.919	312.523	85.821	88.131	86.141
6/2/2019	5:46:11 AM	4.979	315.443	86.212	88.479	86.500
6/2/2019	8:17:04 AM	5.056	319.424	86.328	88.598	86.602
6/2/2019	10:47:57 AM	4.836	307.858	86.655	88.868	86.908
6/2/2019	1:18:50 PM	4.664	299.147	87.948	90.053	88.181
6/2/2019	3:49:43 PM	5.013	317.202	93.856	95.914	93.868
6/2/2019	6:20:36 PM	4.974	315.411	94.136	96.396	94.195
6/2/2019	8:51:29 PM	5.041	318.733	92.230	94.511	92.381
6/2/2019	11:22:22 PM	4.866	310.028	88.711	91.052	89.016
7/2/2019	1:53:15 AM	4.866	309.988	87.056	89.342	87.356
7/2/2019	4:24:08 AM	4.867	310.360	86.639	88.848	86.965
7/2/2019	6:55:01 AM	4.932	313.055	86.927	89.200	87.205
7/2/2019	9:25:54 AM	4.816	307.546	85.941	88.176	86.243
7/2/2019	11:56:47 AM	4.755	304.017	88.000	90.168	88.250
7/2/2019	2:27:40 PM	4.900	311.441	92.599	94.705	92.714
7/2/2019	4:58:33 PM	5.234	328.814	96.990	99.071	96.886

Table A1. Raw Data of SAG Mill Motor from 6th January, 2019 to 8th April, 2019

Cont'd

DATE	TIME	SAG MOTOR POWER	SAG MOTOR CURRENT	SAG MILL MOTOR WINDING TEMP. 1	SAG MILL MOTOR WINDING TEMP. 2	SAG MILL MOTOR WINDING TEMP. 3
7/2/2019	7:29:26 PM	4.854	309.431	94.951	97.198	95.047
7/2/2019	10:00:19 PM	4.966	315.355	89.713	91.975	89.950
8/2/2019	12:31:12 AM	4.911	312.650	87.286	89.588	87.577
8/2/2019	3:02:05 AM	5.157	324.970	89.062	91.297	89.225
8/2/2019	5:32:58 AM	4.936	313.635	86.923	89.225	87.227
8/2/2019	8:03:51 AM	5.174	325.787	88.087	90.329	88.279
8/2/2019	10:34:44 AM	5.061	319.778	90.291	92.484	90.414
8/2/2019	1:05:37 PM	5.368	335.575	96.083	98.150	95.972
8/2/2019	3:36:30 PM	5.061	319.716	97.929	100.038	97.920
8/2/2019	6:07:23 PM	5.596	347.469	102.844	104.943	102.540
8/2/2019	8:38:16 PM	4.791	306.168	94.453	96.757	94.617
8/2/2019	11:09:09 PM	4.923	312.958	90.546	92.837	90.796
9/2/2019	1:40:02 AM	4.901	311.819	87.683	89.941	87.947
9/2/2019	4:10:55 AM	4.839	308.720	86.273	88.539	86.566
9/2/2019	6:41:48 AM	4.867	310.103	85.602	87.879	85.916
9/2/2019	9:12:41 AM	4.971	314.739	86.752	88.946	86.972
9/2/2019	11:43:34 AM	4.993	316.799	91.241	93.326	91.327
9/2/2019	2:14:27 PM	4.996	316.390	95.589	97.647	95.573
9/2/2019	4:45:20 PM	5.082	320.881	96.303	98.460	96.298
9/2/2019	7:16:13 PM	5.035	318.383	89.321	91.675	89.541
9/2/2019	9:47:06 PM	5.060	319.636	86.905	89.125	87.073
10/2/2019	12:17:59 AM	4.881	310.553	86.052	88.351	86.337
10/2/2019	2:48:52 AM	4.853	309.448	84.557	86.866	84.895
10/2/2019	5:19:45 AM	4.980	315.649	84.993	87.292	85.295
10/2/2019	7:50:38 AM	5.140	324.051	87.431	89.701	87.632
10/2/2019	10:21:31 AM	4.919	312.753	87.610	89.810	87.854
10/2/2019	12:52:24 PM	4.813	307.548	90.633	92.707	90.779
10/2/2019	3:23:17 PM	4.705	301.496	93.833	95.913	93.926
10/2/2019	5:54:10 PM	4.963	314.779	97.044	99.109	97.001
10/2/2019	8:25:03 PM	4.799	306.698	92.565	94.825	92.710
10/2/2019	10:55:56 PM	4.911	312.400	90.036	92.273	90.245
11/2/2019	1:26:49 AM	4.927	313.307	87.897	90.113	88.111
11/2/2019	3:57:42 AM	4.931	313.634	86.949	89.197	87.194
11/2/2019	6:28:35 AM	4.968	315.297	86.918	89.183	87.187
11/2/2019	8:59:28 AM	4.910	312.399	87.080	89.371	87.359
11/2/2019	11:30:21 AM	5.296	332.167	91.647	93.767	91.674
11/2/2019	2:01:14 PM	4.693	301.278	92.889	95.028	93.006
11/2/2019	4:32:07 PM	3.996	257.018	79.211	80.629	79.190
11/2/2019	7:03:00 PM	4.758	304.559	91.260	93.331	91.417
11/2/2019	9:33:53 PM	4.802	306.521	88.849	91.119	89.093
12/2/2019	12:04:46 AM	4.940	314.111	86.678	88.830	86.905
12/2/2019	2:35:39 AM	4.973	315.632	86.246	88.533	86.525

Table A1. Raw Data of SAG Mill Motor from 6th January, 2019 to 8th April, 2019

Cont'd

DATE	TIME	SAG MOTOR POWER	SAG MOTOR CURRENT	SAG MILL MOTOR WINDING TEMP. 1	SAG MILL MOTOR WINDING TEMP. 2	SAG MILL MOTOR WINDING TEMP. 3
12/2/2019	5:06:32 AM	5.087	321.369	85.972	88.299	86.242
12/2/2019	7:37:25 AM	5.051	319.135	86.024	88.434	86.345
12/2/2019	10:08:18 AM	4.953	314.304	86.210	88.422	86.452
12/2/2019	12:39:11 PM	4.907	311.902	89.710	91.778	89.830
12/2/2019	3:10:04 PM	4.769	304.984	91.885	93.926	92.021
12/2/2019	5:40:57 PM	4.712	302.035	93.988	96.071	94.052
12/2/2019	8:11:50 PM	4.909	312.459	91.970	94.184	92.084
12/2/2019	10:42:43 PM	4.766	305.234	86.487	88.761	86.759
13/2/2019	1:13:36 AM	4.890	311.181	84.069	86.351	84.396
13/2/2019	3:44:29 AM	4.871	310.502	84.315	86.596	84.633
13/2/2019	6:15:22 AM	5.040	318.609	84.523	86.795	84.821
13/2/2019	8:46:15 AM	5.054	318.986	85.976	88.179	86.195
13/2/2019	11:17:08 AM	4.876	309.821	88.670	90.767	88.865
13/2/2019	1:48:01 PM	4.558	293.612	89.611	91.710	89.858
13/2/2019	4:18:54 PM	4.737	303.025	92.640	94.737	92.765
13/2/2019	6:49:47 PM	4.796	306.308	93.363	95.537	93.504
13/2/2019	9:20:40 PM	4.603	295.718	89.352	91.623	89.676
13/2/2019	11:51:33 PM	4.719	302.360	86.812	89.019	87.126
14/2/2019	2:22:26 AM	4.648	298.509	85.332	87.621	85.732
14/2/2019	4:53:19 AM	4.767	304.924	84.515	86.748	84.882
14/2/2019	7:24:12 AM	4.746	303.707	84.528	86.806	84.889
14/2/2019	9:55:05 AM	4.611	296.028	83.900	86.194	84.324
14/2/2019	12:25:58 PM	4.983	314.496	90.292	92.475	90.510
14/2/2019	2:56:51 PM	4.946	310.330	93.921	96.134	94.114
14/2/2019	5:27:44 PM	4.911	309.188	97.350	99.611	97.466
14/2/2019	7:58:37 PM	3.606	229.620	86.479	88.002	86.124
14/2/2019	10:29:30 PM	5.136	323.234	88.055	90.120	88.141
15/2/2019	1:00:23 AM	5.145	327.949	90.080	92.136	89.978
15/2/2019	3:31:16 AM	4.684	302.732	86.437	88.562	86.598
15/2/2019	6:02:09 AM	4.790	308.236	85.994	88.111	86.134
15/2/2019	8:33:02 AM	5.139	326.452	87.434	89.536	87.459
15/2/2019	11:03:55 AM	4.692	303.080	87.990	90.114	88.139
15/2/2019	1:34:48 PM	4.763	306.528	91.329	93.261	91.287
15/2/2019	4:05:41 PM	4.491	292.084	92.050	94.005	92.103
15/2/2019	6:36:34 PM	4.686	302.811	93.124	95.139	93.134
15/2/2019	9:07:27 PM	4.877	312.645	92.327	94.391	92.329
15/2/2019	11:38:20 PM	4.852	311.621	90.117	92.249	90.197
16/2/2019	2:09:13 AM	4.702	303.894	86.268	88.379	86.489
16/2/2019	4:40:06 AM	4.654	301.090	84.840	86.969	85.048
16/2/2019	7:10:59 AM	4.821	309.460	84.926	87.046	85.129
16/2/2019	9:41:52 AM	5.342	337.171	90.541	92.585	90.424

Table A1. Raw Data of SAG Mill Motor from 6th January, 2019 to 8th April, 2019

Cont'd

DATE	TIME	SAG MOTOR POWER	SAG MOTOR CURRENT	SAG MILL MOTOR WINDING TEMP. 1	SAG MILL MOTOR WINDING TEMP. 2	SAG MILL MOTOR WINDING TEMP. 3
16/2/2019	12:12:45 PM	4.726	304.862	92.632	94.695	92.613
16/2/2019	2:43:38 PM	4.756	306.651	93.403	95.311	93.332
16/2/2019	5:14:31 PM	4.837	311.139	97.098	99.049	96.969
16/2/2019	7:45:24 PM	5.073	323.753	97.750	99.809	97.612
16/2/2019	10:16:17 PM	4.572	297.199	90.373	92.589	90.577
17/2/2019	12:47:10 AM	4.741	306.343	87.078	89.199	87.252
17/2/2019	3:18:03 AM	4.681	302.815	85.288	87.480	85.526
17/2/2019	5:48:56 AM	4.663	301.834	84.978	87.146	85.199
17/2/2019	8:19:49 AM	4.641	300.719	83.853	86.064	84.129
17/2/2019	10:50:42 AM	4.587	297.919	86.130	88.174	86.352
17/2/2019	1:21:35 PM	4.624	299.666	90.126	92.123	90.214
17/2/2019	3:52:28 PM	5.386	339.616	98.904	100.845	98.552
17/2/2019	6:23:21 PM	5.398	340.013	101.994	104.010	101.656
17/2/2019	8:54:14 PM	5.139	326.836	97.604	99.828	97.496
17/2/2019	11:25:07 PM	4.797	309.177	90.081	92.269	90.180
18/2/2019	1:56:00 AM	4.623	299.608	85.827	88.018	86.050
18/2/2019	4:26:53 AM	4.658	301.642	84.307	86.479	84.566
18/2/2019	6:57:46 AM	4.669	302.070	83.777	85.945	84.042
18/2/2019	9:28:39 AM	4.997	319.715	87.085	89.191	87.182
18/2/2019	11:59:32 AM	4.903	314.673	90.582	92.581	90.587
18/2/2019	2:30:25 PM	4.778	308.002	93.670	95.742	93.652
18/2/2019	5:01:18 PM	4.953	317.166	95.947	97.978	95.810
18/2/2019	7:32:11 PM	4.779	308.256	90.735	92.938	90.814
18/2/2019	10:03:04 PM	4.730	304.983	84.483	86.709	84.690
19/2/2019	12:33:57 AM	4.888	313.648	82.661	84.796	82.813
19/2/2019	3:04:50 AM	5.069	322.755	84.505	86.646	84.601
19/2/2019	5:35:43 AM	5.338	336.865	87.029	89.168	87.021
19/2/2019	8:06:36 AM	5.139	326.624	86.962	89.125	86.995
19/2/2019	10:37:29 AM	4.946	316.674	86.438	88.511	86.483
19/2/2019	1:08:22 PM	4.831	310.753	89.103	91.098	89.126
19/2/2019	3:39:15 PM	4.729	304.889	90.236	92.295	90.248
19/2/2019	6:10:08 PM	2.873	190.348	78.882	80.310	78.341
19/2/2019	8:41:01 PM	4.840	310.505	73.199	74.965	73.335
19/2/2019	11:11:54 PM	4.885	313.129	81.457	83.568	81.634
20/2/2019	1:42:47 AM	4.894	313.870	82.727	84.940	82.920
20/2/2019	4:13:40 AM	4.877	313.009	82.616	84.785	82.783
20/2/2019	6:44:33 AM	4.855	311.989	82.054	84.257	82.277
20/2/2019	9:15:26 AM	4.820	310.505	82.522	84.640	82.699
20/2/2019	11:46:19 AM	4.816	309.819	86.554	88.564	86.627
20/2/2019	2:17:12 PM	4.965	317.082	92.042	93.982	91.911

Table A1. Raw Data of SAG Mill Motor from 6th January, 2019 to 8th April, 2019

Cont'd

DATE	TIME	SAG MOTOR POWER	SAG MOTOR CURRENT	SAG MILL MOTOR WINDING TEMP. 1	SAG MILL MOTOR WINDING TEMP. 2	SAG MILL MOTOR WINDING TEMP. 3
20/2/2019	4:48:05 PM	4.897	314.250	94.754	96.727	94.656
20/2/2019	7:18:58 PM	4.882	313.863	94.195	96.290	94.107
20/2/2019	9:49:51 PM	5.041	321.684	90.693	92.827	90.674
21/2/2019	12:20:44 AM	5.130	326.404	89.328	91.461	89.341
21/2/2019	2:51:37 AM	5.121	325.888	89.001	91.118	89.048
21/2/2019	5:22:30 AM	5.177	328.820	88.606	90.735	88.651
21/2/2019	7:53:23 AM	5.243	332.422	89.387	91.537	89.375
21/2/2019	10:24:16 AM	4.428	283.619	88.172	90.041	87.957
21/2/2019	12:55:09 PM	-0.065	8.810	59.574	60.208	59.189
21/2/2019	3:26:02 PM	-0.065	8.717	53.722	54.426	53.986
21/2/2019	5:56:55 PM	-0.065	8.774	50.639	51.196	51.099
21/2/2019	8:27:48 PM	0.202	21.698	48.066	48.809	48.661
21/2/2019	10:58:41 PM	-0.065	8.329	45.833	46.731	46.409
22/2/2019	1:29:34 AM	-0.065	8.237	43.928	44.836	44.433
22/2/2019	4:00:27 AM	-0.065	8.353	42.261	43.103	42.664
22/2/2019	6:31:20 AM	-0.065	8.297	40.769	41.548	41.061
22/2/2019	9:02:13 AM	-0.065	8.215	39.463	40.264	39.738
22/2/2019	11:33:06 AM	-0.065	8.238	38.575	39.409	38.921
22/2/2019	2:03:59 PM	-0.065	8.445	38.007	39.000	38.526
22/2/2019	4:34:52 PM	-0.065	8.261	37.888	39.000	38.997
22/2/2019	7:05:45 PM	-0.065	8.201	37.500	38.727	38.828
22/2/2019	9:36:38 PM	-0.065	8.255	36.951	38.068	37.998
23/2/2019	12:07:31 AM	-0.065	8.182	36.219	37.348	37.114
23/2/2019	2:38:24 AM	-0.065	8.299	35.515	36.680	36.240
23/2/2019	5:09:17 AM	-0.065	8.313	34.744	35.884	35.412
23/2/2019	7:40:10 AM	-0.065	8.356	34.148	35.240	34.704
23/2/2019	10:11:03 AM	1.269	90.723	37.643	38.698	38.072
23/2/2019	12:41:56 PM	3.503	226.964	66.914	68.095	66.783
23/2/2019	3:12:49 PM	5.118	324.472	92.413	94.310	92.308
23/2/2019	5:43:42 PM	5.092	322.924	96.727	98.844	96.597
23/2/2019	8:14:35 PM	5.084	322.706	93.031	95.183	93.000
23/2/2019	10:45:28 PM	5.148	326.521	90.960	93.048	90.967
24/2/2019	1:16:21 AM	5.176	328.066	90.241	92.431	90.282
24/2/2019	3:47:14 AM	5.191	328.762	89.813	92.002	89.868
24/2/2019	6:18:07 AM	5.189	328.819	90.219	92.316	90.217
24/2/2019	8:49:00 AM	5.169	327.783	90.068	92.168	90.061
24/2/2019	11:19:53 AM	5.192	328.914	91.984	94.042	91.917
24/2/2019	1:50:46 PM	5.138	326.380	95.716	97.744	95.539
24/2/2019	4:21:39 PM	5.128	325.288	94.895	97.102	94.777
24/2/2019	6:52:32 PM	5.236	331.106	92.937	95.112	92.833
24/2/2019	9:23:25 PM	5.212	329.949	92.212	94.391	92.169

Table A1. Raw Data of SAG Mill Motor from 6th January, 2019 to 8th April, 2019

Cont'd

DATE	TIME	SAG MOTOR POWER	SAG MOTOR CURRENT	SAG MILL MOTOR WINDING TEMP. 1	SAG MILL MOTOR WINDING TEMP. 2	SAG MILL MOTOR WINDING TEMP. 3
24/2/2019	11:54:18 PM	5.230	330.987	91.175	93.334	91.184
25/2/2019	2:25:11 AM	5.193	329.173	90.232	92.447	90.218
25/2/2019	4:56:04 AM	5.162	327.705	89.535	91.693	89.583
25/2/2019	7:26:57 AM	5.268	333.081	90.276	92.445	90.235
25/2/2019	9:57:50 AM	5.230	330.887	91.170	93.262	91.135
25/2/2019	12:28:43 PM	5.166	327.690	92.562	94.707	92.481
25/2/2019	2:59:36 PM	5.227	330.642	92.964	95.049	92.851
25/2/2019	5:30:29 PM	5.266	332.832	92.509	94.726	92.464
25/2/2019	8:01:22 PM	5.279	333.162	88.379	90.520	88.398
25/2/2019	10:32:15 PM	5.271	332.758	87.956	90.064	87.980
26/2/2019	1:03:08 AM	5.239	331.113	87.993	90.196	88.050
26/2/2019	3:34:01 AM	5.312	334.727	88.378	90.486	88.439
26/2/2019	6:04:54 AM	5.273	333.031	88.024	90.260	88.030
26/2/2019	8:35:47 AM	5.233	330.663	87.694	89.881	87.722
26/2/2019	11:06:40 AM	5.157	326.792	90.368	92.408	90.324
26/2/2019	1:37:33 PM	5.184	328.238	94.470	96.525	94.304
26/2/2019	4:08:26 PM	5.272	333.015	98.623	100.659	98.326
26/2/2019	6:39:19 PM	5.282	333.545	99.444	101.558	99.153
26/2/2019	9:10:12 PM	5.252	331.812	95.260	97.463	95.138
26/2/2019	11:41:05 PM	5.213	329.869	91.786	93.975	91.766
27/2/2019	2:11:58 AM	5.208	329.810	90.326	92.525	90.340
27/2/2019	4:42:51 AM	5.189	328.992	89.656	91.848	89.695
27/2/2019	7:13:44 AM	5.133	326.067	88.450	90.647	88.524
27/2/2019	9:44:37 AM	5.111	324.990	88.609	90.724	88.676
27/2/2019	12:15:30 PM	5.203	329.691	91.472	93.540	91.393
27/2/2019	2:46:23 PM	5.244	331.701	94.583	96.680	94.413
27/2/2019	5:17:16 PM	5.199	329.017	94.355	96.515	94.232
27/2/2019	7:48:09 PM	5.230	331.056	92.835	94.987	92.729
27/2/2019	10:19:02 PM	5.149	327.119	90.797	92.981	90.817
28/2/2019	12:49:55 AM	5.121	325.886	89.568	91.762	89.629
28/2/2019	3:20:48 AM	5.125	326.146	89.067	91.268	89.144
28/2/2019	5:51:41 AM	5.060	322.780	87.250	89.484	87.380
28/2/2019	8:22:34 AM	5.158	327.341	86.589	88.814	86.725
28/2/2019	10:53:27 AM	5.319	335.457	91.369	93.455	91.278
28/2/2019	1:24:20 PM	5.151	326.448	94.750	96.818	94.619
28/2/2019	3:55:13 PM	5.019	319.607	96.457	98.494	96.328
28/2/2019	6:26:06 PM	5.117	324.810	97.371	99.412	97.224
28/2/2019	8:56:59 PM	5.017	319.675	94.210	96.419	94.193
28/2/2019	11:27:52 PM	5.176	328.106	91.296	93.431	91.315
1/3/2019	1:58:45 AM	5.301	335.305	90.852	93.012	90.799

Table A1. Raw Data of SAG Mill Motor from 6th January, 2019 to 8th April, 2019

Cont'd

DATE	TIME	SAG MOTOR POWER	SAG MOTOR CURRENT	SAG MILL MOTOR WINDING TEMP. 1	SAG MILL MOTOR WINDING TEMP. 2	SAG MILL MOTOR WINDING TEMP. 3
1/3/2019	4:29:38 AM	5.154	327.850	89.471	91.625	89.487
1/3/2019	7:00:31 AM	5.080	324.200	88.037	90.184	88.140
1/3/2019	9:31:24 AM	5.082	323.656	87.967	90.174	88.064
1/3/2019	12:02:17 PM	4.992	319.129	86.009	88.234	86.180
1/3/2019	2:33:10 PM	4.977	318.276	87.939	90.039	88.040
1/3/2019	5:04:03 PM	5.004	319.524	90.667	92.745	90.677
1/3/2019	7:34:56 PM	4.902	314.492	88.848	91.027	88.936
1/3/2019	10:05:49 PM	4.885	313.802	86.140	88.377	86.349
2/3/2019	12:36:42 AM	4.823	311.078	84.737	87.006	84.994
2/3/2019	3:07:35 AM	4.862	312.452	83.998	86.253	84.270
2/3/2019	5:38:28 AM	4.950	316.747	84.183	86.435	84.402
2/3/2019	8:09:21 AM	4.936	316.174	84.184	86.488	84.450
2/3/2019	10:40:14 AM	4.918	315.408	85.863	88.024	86.043
2/3/2019	1:11:07 PM	5.050	322.037	91.507	93.537	91.440
2/3/2019	3:42:00 PM	4.965	317.608	93.343	95.415	93.258
2/3/2019	6:12:53 PM	4.989	318.646	92.526	94.628	92.456
2/3/2019	8:43:46 PM	4.957	317.122	90.349	92.518	90.407
2/3/2019	11:14:39 PM	4.946	316.757	86.200	88.454	86.382
3/3/2019	1:45:32 AM	5.010	320.152	84.425	86.700	84.641
3/3/2019	4:16:25 AM	5.017	320.119	83.936	86.238	84.152
3/3/2019	6:47:18 AM	4.963	317.205	82.156	84.412	82.421
3/3/2019	9:18:11 AM	5.099	324.116	83.595	85.873	83.795
3/3/2019	11:49:04 AM	5.148	326.925	87.919	89.969	87.924
3/3/2019	2:19:57 PM	5.323	336.297	96.078	98.052	95.831
3/3/2019	4:50:50 PM	5.292	334.800	100.361	102.415	100.034
3/3/2019	7:21:43 PM	5.173	328.329	99.480	101.654	99.299
3/3/2019	9:52:36 PM	5.148	327.087	93.794	96.016	93.773
4/3/2019	12:23:29 AM	5.173	328.808	90.543	92.775	90.586
4/3/2019	2:54:22 AM	5.159	327.809	89.140	91.353	89.183
4/3/2019	5:25:15 AM	5.095	324.217	87.433	89.686	87.535
4/3/2019	7:56:08 AM	5.140	326.659	87.104	89.328	87.212
4/3/2019	10:27:01 AM	5.038	321.058	88.720	90.811	88.770
4/3/2019	12:57:54 PM	5.144	327.068	92.920	94.955	92.819
4/3/2019	3:28:47 PM	5.221	331.149	98.063	100.109	97.826
4/3/2019	5:59:40 PM	4.341	271.937	93.631	95.185	93.137
4/3/2019	8:30:33 PM	5.302	334.147	93.865	96.136	93.742
4/3/2019	11:01:26 PM	5.338	336.256	92.689	94.915	92.563
5/3/2019	1:32:19 AM	5.287	333.383	90.797	92.986	90.757
5/3/2019	4:03:12 AM	5.230	330.598	89.833	92.065	89.853
5/3/2019	6:34:05 AM	5.157	326.931	87.986	90.224	88.050

Table A1. Raw Data of SAG Mill Motor from 6th January, 2019 to 8th April, 2019

Cont'd

DATE	TIME	SAG MOTOR POWER	SAG MOTOR CURRENT	SAG MILL MOTOR WINDING TEMP. 1	SAG MILL MOTOR WINDING TEMP. 2	SAG MILL MOTOR WINDING TEMP. 3
5/3/2019	9:04:58 AM	5.149	326.376	87.834	90.030	87.901
5/3/2019	11:35:51 AM	5.151	326.862	91.427	93.506	91.378
5/3/2019	2:06:44 PM	5.053	321.595	94.844	96.900	94.701
5/3/2019	4:37:37 PM	5.108	324.510	97.550	99.564	97.327
5/3/2019	7:08:30 PM	5.261	332.696	98.980	101.121	98.735
5/3/2019	9:39:23 PM	5.263	332.694	94.703	96.952	94.584
6/3/2019	12:10:16 AM	5.185	328.767	91.201	93.431	91.201
6/3/2019	2:41:09 AM	5.247	332.069	90.805	93.000	90.826
6/3/2019	5:12:02 AM	5.208	330.145	90.314	92.557	90.356
6/3/2019	7:42:55 AM	5.226	330.693	90.204	92.489	90.235
6/3/2019	10:13:48 AM	5.433	341.530	92.748	94.881	92.645
6/3/2019	12:44:41 PM	5.427	341.096	97.133	99.228	96.900
6/3/2019	3:15:34 PM	5.328	335.899	100.142	102.211	99.865
6/3/2019	5:46:27 PM	5.289	333.754	100.741	102.877	100.452
6/3/2019	8:17:20 PM	5.391	338.742	98.730	100.978	98.561
6/3/2019	10:48:13 PM	5.454	342.661	95.567	97.842	95.459
7/3/2019	1:19:06 AM	5.397	339.749	93.906	96.151	93.858
7/3/2019	3:49:59 AM	5.095	323.835	90.305	92.640	90.425
7/3/2019	6:20:52 AM	5.100	323.869	85.703	87.983	85.877
7/3/2019	8:51:45 AM	5.391	339.234	88.611	90.774	88.618
7/3/2019	11:22:38 AM	5.220	330.096	90.474	92.559	90.440
7/3/2019	1:53:31 PM	4.799	303.979	91.071	92.898	90.851
7/3/2019	4:24:24 PM	5.126	324.979	94.973	97.083	94.864
7/3/2019	6:55:17 PM	5.174	327.819	96.191	98.378	96.100
7/3/2019	9:26:10 PM	5.165	327.380	93.211	95.436	93.221
7/3/2019	11:57:03 PM	5.118	325.093	90.470	92.689	90.537
8/3/2019	2:27:56 AM	5.088	323.533	88.263	90.482	88.375
8/3/2019	4:58:49 AM	5.046	320.940	86.944	89.266	87.121
8/3/2019	7:29:42 AM	5.053	321.376	86.526	88.802	86.753
8/3/2019	10:00:35 AM	5.122	325.111	88.187	90.326	88.271
8/3/2019	12:31:28 PM	5.180	327.827	93.605	95.695	93.503
8/3/2019	3:02:21 PM	5.109	324.339	97.138	99.184	96.974
8/3/2019	5:33:14 PM	5.266	332.592	96.177	98.482	96.093
8/3/2019	8:04:07 PM	5.386	338.946	90.617	92.862	90.575
8/3/2019	10:35:00 PM	5.307	334.849	89.422	91.687	89.419
9/3/2019	1:05:53 AM	5.276	333.057	88.611	90.859	88.674
9/3/2019	3:36:46 AM	5.285	333.394	87.975	90.249	88.013
9/3/2019	6:07:39 AM	5.263	332.566	87.221	89.465	87.279
9/3/2019	8:38:32 AM	5.442	341.991	88.772	90.992	88.731
9/3/2019	11:09:25 AM	5.412	340.627	92.577	94.690	92.419
9/3/2019	1:40:18 PM	5.327	335.868	95.905	97.986	95.663

Table A1. Raw Data of SAG Mill Motor from 6th January, 2019 to 8th April, 2019

Cont'd

DATE	TIME	SAG MOTOR POWER	SAG MOTOR CURRENT	SAG MILL MOTOR WINDING TEMP. 1	SAG MILL MOTOR WINDING TEMP. 2	SAG MILL MOTOR WINDING TEMP. 3
9/3/2019	4:11:11 PM	5.310	334.944	97.399	99.421	97.159
9/3/2019	6:42:04 PM	5.238	331.307	95.807	98.022	95.655
9/3/2019	9:12:57 PM	5.183	328.437	89.799	91.989	89.807
9/3/2019	11:43:50 PM	5.230	330.754	88.626	90.843	88.670
10/3/2019	2:14:43 AM	5.238	330.897	87.713	89.984	87.765
10/3/2019	4:45:36 AM	5.247	331.566	87.243	89.423	87.285
10/3/2019	7:16:29 AM	5.266	332.380	87.090	89.353	87.166
10/3/2019	9:47:22 AM	5.241	331.174	88.630	90.746	88.622
10/3/2019	12:18:15 PM	5.208	329.609	93.076	95.128	92.923
10/3/2019	2:49:08 PM	5.131	325.645	96.496	98.506	96.285
10/3/2019	5:20:01 PM	5.121	325.294	96.312	98.421	96.202
10/3/2019	7:50:54 PM	5.240	331.417	91.581	93.831	91.543
10/3/2019	10:21:47 PM	5.251	332.041	88.977	91.174	89.002
11/3/2019	12:52:40 AM	5.228	330.953	88.062	90.268	88.087
11/3/2019	3:23:33 AM	5.222	330.746	87.744	89.971	87.803
11/3/2019	5:54:26 AM	5.190	329.018	87.197	89.477	87.280
11/3/2019	8:25:19 AM	5.245	331.489	86.597	88.808	86.702
11/3/2019	10:56:12 AM	5.155	327.240	89.274	91.368	89.248
11/3/2019	1:27:05 PM	5.058	322.044	93.795	95.819	93.654
11/3/2019	3:57:58 PM	5.102	324.471	98.199	100.199	97.943
11/3/2019	6:28:51 PM	5.075	322.769	98.157	100.275	98.000
11/3/2019	8:59:44 PM	5.069	322.462	93.723	95.939	93.706
11/3/2019	11:30:37 PM	5.197	329.473	90.788	93.004	90.790
12/3/2019	2:01:30 AM	5.222	330.846	89.230	91.387	89.265
12/3/2019	4:32:23 AM	5.183	328.748	88.359	90.597	88.441
12/3/2019	7:03:16 AM	5.192	329.252	88.186	90.457	88.244
12/3/2019	9:34:09 AM	5.140	326.329	88.835	90.925	88.847
12/3/2019	12:05:02 PM	5.116	325.334	92.420	94.484	92.313
12/3/2019	2:35:55 PM	5.131	325.635	97.293	99.275	97.051
12/3/2019	5:06:48 PM	5.251	331.638	102.860	104.815	102.472
12/3/2019	7:37:41 PM	5.300	334.653	102.263	104.413	101.974
12/3/2019	10:08:34 PM	5.300	334.859	95.707	97.969	95.582
13/3/2019	12:39:27 AM	5.286	334.196	92.469	94.672	92.410
13/3/2019	3:10:20 AM	5.256	332.632	90.970	93.131	90.963
13/3/2019	5:41:13 AM	5.199	329.707	89.743	91.901	89.751
13/3/2019	8:12:06 AM	5.214	330.168	89.990	92.130	89.978
13/3/2019	10:42:59 AM	5.315	335.056	92.242	94.360	92.144
13/3/2019	1:13:52 PM	5.441	341.452	97.803	99.834	97.528
13/3/2019	3:44:45 PM	5.293	333.974	101.737	103.761	101.404
13/3/2019	6:15:38 PM	5.354	336.836	103.091	105.108	102.742

Table A1. Raw Data of SAG Mill Motor from 6th January, 2019 to 8th April, 2019

Cont'd

DATE	TIME	SAG MOTOR POWER	SAG MOTOR CURRENT	SAG MILL MOTOR WINDING TEMP. 1	SAG MILL MOTOR WINDING TEMP. 2	SAG MILL MOTOR WINDING TEMP. 3
13/3/2019	8:46:31 PM	5.514	345.506	99.764	101.952	99.486
13/3/2019	11:17:24 PM	5.562	348.234	96.397	98.561	96.138
14/3/2019	1:48:17 AM	5.453	342.651	94.351	96.566	94.197
14/3/2019	4:19:10 AM	5.129	325.800	89.942	92.153	89.956
14/3/2019	6:50:03 AM	5.161	327.507	88.785	90.919	88.830
14/3/2019	9:20:56 AM	5.198	329.267	89.412	91.488	89.389
14/3/2019	11:51:49 AM	5.238	331.539	93.691	95.704	93.502
14/3/2019	2:22:42 PM	5.166	327.585	97.147	99.178	96.886
14/3/2019	4:53:35 PM	5.299	334.468	95.644	97.902	95.516
14/3/2019	7:24:28 PM	5.197	329.012	88.600	90.841	88.648
14/3/2019	9:55:21 PM	5.162	327.642	87.401	89.630	87.513
15/3/2019	12:26:14 AM	5.089	323.864	86.251	88.438	86.378
15/3/2019	2:57:07 AM	5.288	334.210	87.410	89.602	87.451
15/3/2019	5:28:00 AM	5.313	335.621	88.146	90.372	88.144
15/3/2019	7:58:53 AM	5.266	332.992	87.853	89.979	87.877
15/3/2019	10:29:46 AM	5.186	328.878	88.561	90.629	88.552
15/3/2019	1:00:39 PM	5.266	332.993	91.953	93.992	91.793
15/3/2019	3:31:32 PM	5.281	333.660	94.928	96.948	94.772
15/3/2019	6:02:25 PM	5.249	332.307	95.548	97.635	95.349
15/3/2019	8:33:18 PM	4.642	291.939	88.220	89.837	87.921
15/3/2019	11:04:11 PM	5.287	333.139	91.040	93.136	90.951
16/3/2019	1:35:04 AM	5.239	330.598	90.602	92.737	90.574
16/3/2019	4:05:57 AM	5.288	333.256	90.042	92.204	89.979
16/3/2019	6:36:50 AM	5.319	334.862	89.708	91.932	89.665
16/3/2019	9:07:43 AM	5.315	334.517	89.614	91.710	89.542
16/3/2019	11:38:36 AM	5.425	340.576	95.008	97.038	94.774
16/3/2019	2:09:29 PM	5.357	336.654	99.178	101.215	98.854
16/3/2019	4:40:22 PM	5.266	331.703	100.103	102.185	99.861
16/3/2019	7:11:15 PM	5.323	335.231	98.059	100.189	97.848
16/3/2019	9:42:08 PM	5.280	332.866	93.677	95.891	93.570
17/3/2019	12:13:01 AM	5.311	334.624	90.894	93.020	90.823
17/3/2019	2:43:54 AM	5.300	334.064	89.803	91.922	89.756
17/3/2019	5:14:47 AM	5.269	332.615	88.588	90.742	88.604
17/3/2019	7:45:40 AM	5.212	329.308	87.718	89.871	87.773
17/3/2019	10:16:33 AM	5.282	332.885	86.798	88.928	86.834
17/3/2019	12:47:26 PM	5.411	339.445	91.712	93.785	91.557
17/3/2019	3:18:19 PM	5.390	338.817	94.283	96.360	94.018
17/3/2019	5:49:12 PM	5.348	336.699	96.016	98.044	95.718
17/3/2019	8:20:05 PM	5.337	336.236	94.671	96.811	94.458
17/3/2019	10:50:58 PM	5.283	333.582	92.067	94.238	91.962

Table A1. Raw Data of SAG Mill Motor from 6th January, 2019 to 8th April, 2019

Cont'd

DATE	TIME	SAG MOTOR POWER	SAG MOTOR CURRENT	SAG MILL MOTOR WINDING TEMP. 1	SAG MILL MOTOR WINDING TEMP. 2	SAG MILL MOTOR WINDING TEMP. 3
18/3/2019	1:21:51 AM	5.258	332.457	89.496	91.635	89.471
18/3/2019	3:52:44 AM	5.226	330.448	87.854	90.024	87.855
18/3/2019	6:23:37 AM	5.213	329.811	87.131	89.454	87.132
18/3/2019	8:54:30 AM	5.332	336.219	88.376	90.514	88.339
18/3/2019	11:25:23 AM	5.395	339.436	92.819	94.831	92.619
18/3/2019	1:56:16 PM	5.465	342.902	98.837	100.847	98.493
18/3/2019	4:27:09 PM	5.369	337.732	101.335	103.378	100.995
18/3/2019	6:58:02 PM	5.334	336.123	99.644	101.768	99.347
18/3/2019	9:28:55 PM	5.375	338.368	95.800	97.981	95.631
18/3/2019	11:59:48 PM	5.320	335.334	92.607	94.755	92.472
19/3/2019	2:30:41 AM	5.377	338.404	91.948	94.055	91.857
19/3/2019	5:01:34 AM	5.427	341.024	92.007	94.138	91.902
19/3/2019	7:32:27 AM	5.428	341.078	91.665	93.877	91.506
19/3/2019	10:03:20 AM	5.410	340.320	93.059	95.143	92.872
19/3/2019	12:34:13 PM	5.466	342.757	96.937	99.001	96.664
19/3/2019	3:05:06 PM	5.254	331.645	99.178	101.208	98.903
19/3/2019	5:35:59 PM	5.312	334.899	98.955	101.079	98.659
19/3/2019	8:06:52 PM	5.407	339.916	95.958	98.199	95.774
19/3/2019	10:37:45 PM	5.472	343.024	90.211	92.481	90.132
20/3/2019	1:08:38 AM	5.432	340.805	89.232	91.410	89.105
20/3/2019	3:39:31 AM	5.426	340.636	88.876	90.991	88.820
20/3/2019	6:10:24 AM	5.400	339.271	88.321	90.556	88.296
20/3/2019	8:41:17 AM	5.393	338.783	89.000	91.139	88.941
20/3/2019	11:12:10 AM	5.343	336.403	92.596	94.659	92.439
20/3/2019	1:43:03 PM	5.365	337.595	96.755	98.780	96.472
20/3/2019	4:13:56 PM	5.334	336.027	99.682	101.681	99.318
20/3/2019	6:44:49 PM	5.317	335.260	97.667	99.808	97.407
20/3/2019	9:15:42 PM	5.385	339.105	95.356	97.462	95.152
20/3/2019	11:46:35 PM	5.405	340.169	93.880	96.047	93.696
21/3/2019	2:17:28 AM	5.476	343.791	93.267	95.472	93.075
21/3/2019	4:48:21 AM	5.413	340.539	92.690	94.811	92.511
21/3/2019	7:19:14 AM	4.955	312.871	89.064	91.025	88.802
21/3/2019	9:50:07 AM	5.352	337.049	92.122	94.199	91.970
21/3/2019	12:21:00 PM	5.509	345.724	96.503	98.534	96.154
21/3/2019	2:51:53 PM	5.443	341.868	99.951	102.003	99.539
21/3/2019	5:22:46 PM	5.337	336.050	99.318	101.478	98.996
21/3/2019	7:53:39 PM	5.362	337.364	94.324	96.585	94.160
21/3/2019	10:24:32 PM	5.471	342.849	90.281	92.481	90.178
22/3/2019	12:55:25 AM	5.550	346.511	89.809	92.006	89.669
22/3/2019	3:26:18 AM	5.581	348.050	90.177	92.349	90.008
22/3/2019	5:57:11 AM	5.512	344.866	89.445	91.537	89.362

Table A1. Raw Data of SAG Mill Motor from 6th January, 2019 to 8th April, 2019

Cont'd

DATE	TIME	SAG MOTOR POWER	SAG MOTOR CURRENT	SAG MILL MOTOR WINDING TEMP. 1	SAG MILL MOTOR WINDING TEMP. 2	SAG MILL MOTOR WINDING TEMP. 3
22/3/2019	8:28:04 AM	5.404	339.259	88.434	90.661	88.368
22/3/2019	10:58:57 AM	5.413	339.729	89.685	91.889	89.569
22/3/2019	1:29:50 PM	4.531	285.651	84.236	85.971	83.872
22/3/2019	4:00:43 PM	5.517	345.419	89.966	91.931	89.764
22/3/2019	6:31:36 PM	5.280	333.058	93.155	95.212	93.004
22/3/2019	9:02:29 PM	5.262	332.108	91.444	93.619	91.367
22/3/2019	11:33:22 PM	5.282	333.387	88.754	90.954	88.695
23/3/2019	2:04:15 AM	5.321	335.312	88.114	90.209	88.105
23/3/2019	4:35:08 AM	5.349	336.722	88.099	90.301	88.044
23/3/2019	7:06:01 AM	5.309	334.754	88.136	90.259	88.096
23/3/2019	9:36:54 AM	5.375	338.491	90.123	92.207	90.026
23/3/2019	12:07:47 PM	5.306	334.744	93.531	95.618	93.355
23/3/2019	2:38:40 PM	5.193	329.077	95.127	97.142	94.900
23/3/2019	5:09:33 PM	5.273	332.749	98.618	100.613	98.313
23/3/2019	7:40:26 PM	5.307	334.835	96.475	98.653	96.291
23/3/2019	10:11:19 PM	5.343	337.310	92.921	95.044	92.802
24/3/2019	12:42:12 AM	5.368	338.144	92.055	94.255	91.936
24/3/2019	3:13:05 AM	5.347	337.208	91.283	93.471	91.236
24/3/2019	5:43:58 AM	5.367	338.149	91.113	93.297	91.005
24/3/2019	8:14:51 AM	5.296	334.666	91.197	93.303	91.120
24/3/2019	10:45:44 AM	5.361	338.039	92.820	94.844	92.672
24/3/2019	1:16:37 PM	5.472	343.967	97.924	99.949	97.606
24/3/2019	3:47:30 PM	5.460	343.074	101.385	103.363	100.985
24/3/2019	6:18:23 PM	5.455	342.307	99.629	101.825	99.359
24/3/2019	8:49:16 PM	5.478	344.343	94.680	96.874	94.493
24/3/2019	11:20:09 PM	5.349	337.513	92.100	94.159	92.053
25/3/2019	1:51:02 AM	5.476	344.378	91.599	93.796	91.490
25/3/2019	4:21:55 AM	5.427	341.752	89.364	91.495	89.327
25/3/2019	6:52:48 AM	5.511	346.048	89.890	92.074	89.834
25/3/2019	9:23:41 AM	5.528	346.569	91.399	93.524	91.283
25/3/2019	11:54:34 AM	5.579	348.775	94.901	96.976	94.677
25/3/2019	2:25:27 PM	5.585	349.425	99.237	101.299	98.865
25/3/2019	4:56:20 PM	5.554	347.961	100.626	102.753	100.270
25/3/2019	7:27:13 PM	5.563	348.653	99.408	101.530	99.036
25/3/2019	9:58:06 PM	5.518	346.620	96.169	98.281	95.878
26/3/2019	12:28:59 AM	5.490	345.245	94.143	96.232	93.907
26/3/2019	2:59:52 AM	5.451	343.290	92.282	94.363	92.117
26/3/2019	5:30:45 AM	5.404	340.816	90.624	92.715	90.492
26/3/2019	8:01:38 AM	5.307	335.487	89.226	91.308	89.124
26/3/2019	10:32:31 AM	5.303	335.232	91.662	93.589	91.451
26/3/2019	1:03:24 PM	5.328	336.526	97.587	99.481	97.243

Table A1. Raw Data of SAG Mill Motor from 6th January, 2019 to 8th April, 2019

Cont'd

DATE	TIME	SAG MOTOR POWER	SAG MOTOR CURRENT	SAG MILL MOTOR WINDING TEMP. 1	SAG MILL MOTOR WINDING TEMP. 2	SAG MILL MOTOR WINDING TEMP. 3
26/3/2019	3:34:17 PM	5.293	334.857	100.832	102.746	100.433
26/3/2019	6:05:10 PM	5.303	335.192	101.235	103.260	100.860
26/3/2019	8:36:03 PM	5.353	337.961	96.414	98.511	96.179
26/3/2019	11:06:56 PM	5.342	337.548	93.783	95.922	93.586
27/3/2019	1:37:49 AM	5.244	332.257	91.032	93.119	90.903
27/3/2019	4:08:42 AM	5.313	336.054	89.524	91.534	89.388
27/3/2019	6:39:35 AM	5.367	338.796	89.826	91.864	89.670
27/3/2019	9:10:28 AM	3.700	238.687	83.098	84.827	82.745
27/3/2019	11:41:21 AM	-0.065	9.014	49.743	50.394	49.185
27/3/2019	2:12:14 PM	-0.065	8.977	47.234	48.137	46.998
27/3/2019	4:43:07 PM	-0.065	8.895	45.586	46.773	46.051
27/3/2019	7:14:00 PM	-0.065	8.972	44.118	45.281	44.807
27/3/2019	9:44:53 PM	-0.065	9.027	42.424	43.327	42.873
28/3/2019	12:15:46 AM	-0.065	8.995	40.827	41.727	41.137
28/3/2019	2:46:39 AM	-0.065	8.960	39.430	40.486	39.767
28/3/2019	5:17:32 AM	-0.065	8.909	38.131	39.314	38.547
28/3/2019	7:48:25 AM	-0.065	8.940	36.981	38.198	37.445
28/3/2019	10:19:18 AM	2.266	150.140	46.695	47.807	46.988
28/3/2019	12:50:11 PM	5.333	335.061	88.240	90.015	88.080
28/3/2019	3:21:04 PM	5.442	341.443	98.813	100.819	98.465
28/3/2019	5:51:57 PM	5.565	347.463	102.252	104.383	101.859
28/3/2019	8:22:50 PM	5.436	340.962	95.467	97.775	95.272
28/3/2019	10:53:43 PM	5.476	343.114	93.764	95.993	93.562
29/3/2019	1:24:36 AM	5.497	344.709	90.402	92.579	90.257
29/3/2019	3:55:29 AM	5.489	344.609	89.302	91.392	89.171
29/3/2019	6:26:22 AM	5.514	345.647	89.682	91.895	89.509
29/3/2019	8:57:15 AM	5.562	348.127	90.962	93.072	90.745
29/3/2019	11:28:08 AM	5.569	348.479	96.292	98.319	95.937
29/3/2019	1:59:01 PM	5.562	347.747	99.842	101.916	99.429
29/3/2019	4:29:54 PM	5.620	351.104	98.806	101.082	98.484
29/3/2019	7:00:47 PM	5.624	351.217	92.819	94.957	92.550
29/3/2019	9:31:40 PM	5.527	346.199	92.352	94.526	92.120
30/3/2019	12:02:33 AM	5.503	345.251	91.645	93.761	91.405
30/3/2019	2:33:26 AM	5.441	341.943	91.277	93.430	91.052
30/3/2019	5:04:19 AM	5.403	339.960	90.655	92.798	90.472
30/3/2019	7:35:12 AM	5.489	344.567	91.829	93.934	91.634
30/3/2019	10:06:05 AM	5.494	344.739	93.609	95.722	93.338
30/3/2019	12:36:58 PM	5.482	343.851	96.842	98.894	96.483
30/3/2019	3:07:51 PM	5.451	342.297	99.771	101.834	99.421
30/3/2019	5:38:44 PM	5.533	346.389	95.684	97.976	95.456
30/3/2019	8:09:37 PM	5.525	346.070	93.883	96.142	93.662

Table A1. Raw Data of SAG Mill Motor from 6th January, 2019 to 8th April, 2019

Cont'd

DATE	TIME	SAG MOTOR POWER	SAG MOTOR CURRENT	SAG MILL MOTOR WINDING TEMP. 1	SAG MILL MOTOR WINDING TEMP. 2	SAG MILL MOTOR WINDING TEMP. 3
30/3/2019	10:40:30 PM	5.547	347.009	93.453	95.729	93.260
31/3/2019	1:11:23 AM	5.552	347.456	93.222	95.429	92.995
31/3/2019	3:42:16 AM	5.479	343.792	92.330	94.498	92.078
31/3/2019	6:13:09 AM	5.437	341.719	91.835	93.934	91.708
31/3/2019	8:44:02 AM	5.443	341.394	92.301	94.476	92.120
31/3/2019	11:14:55 AM	5.470	343.225	94.413	96.509	94.140
31/3/2019	1:45:48 PM	5.346	336.667	96.991	99.026	96.714
31/3/2019	4:16:41 PM	5.443	342.024	100.205	102.250	99.800
31/3/2019	6:47:34 PM	5.443	342.302	98.293	100.461	97.985
31/3/2019	9:18:27 PM	5.418	340.557	95.804	97.973	95.557
31/3/2019	11:49:20 PM	5.432	341.533	94.019	96.175	93.803
1/4/2019	2:20:13 AM	5.429	341.508	93.466	95.672	93.312
1/4/2019	4:51:06 AM	5.411	340.349	91.976	94.135	91.814
1/4/2019	7:21:59 AM	3.385	217.987	75.310	76.619	74.887
1/4/2019	9:52:52 AM	5.372	337.435	87.407	89.322	87.299
1/4/2019	12:23:45 PM	5.527	346.026	96.994	98.995	96.697
1/4/2019	2:54:38 PM	5.439	341.924	100.987	103.012	100.611
1/4/2019	5:25:31 PM	5.373	338.311	101.555	103.643	101.222
1/4/2019	7:56:24 PM	5.336	336.425	98.406	100.568	98.244
1/4/2019	10:27:17 PM	5.489	344.662	96.304	98.450	96.121
2/4/2019	12:58:10 AM	5.425	341.013	93.800	95.995	93.662
2/4/2019	3:29:03 AM	5.379	338.768	92.115	94.285	92.007
2/4/2019	5:59:56 AM	5.439	342.111	92.151	94.365	91.988
2/4/2019	8:30:49 AM	5.378	338.778	91.445	93.592	91.324
2/4/2019	11:01:42 AM	5.406	339.666	94.270	96.294	94.064
2/4/2019	1:32:35 PM	5.515	345.579	99.978	101.974	99.605
2/4/2019	4:03:28 PM	5.520	346.203	102.460	104.455	102.069
2/4/2019	6:34:21 PM	5.612	350.853	102.582	104.715	102.227
2/4/2019	9:05:14 PM	5.494	345.029	98.882	101.077	98.654
2/4/2019	11:36:07 PM	5.518	346.196	95.618	97.782	95.436
3/4/2019	2:07:00 AM	5.549	347.761	94.724	96.989	94.516
3/4/2019	4:37:53 AM	5.558	348.163	94.242	96.396	94.066
3/4/2019	7:08:46 AM	5.544	347.742	93.373	95.608	93.175
3/4/2019	9:39:39 AM	5.611	350.342	95.203	97.295	94.965
3/4/2019	12:10:32 PM	4.727	299.753	95.232	97.156	94.831
3/4/2019	2:41:25 PM	3.811	242.440	76.701	77.792	76.059
3/4/2019	5:12:18 PM	5.557	347.365	92.946	95.141	92.829
3/4/2019	7:43:11 PM	5.562	347.829	91.167	93.305	91.008
3/4/2019	10:14:04 PM	5.523	346.081	90.889	93.035	90.713
4/4/2019	12:44:57 AM	5.475	343.302	90.314	92.429	90.204
4/4/2019	3:15:50 AM	5.108	324.073	87.929	90.085	87.944

Table A1. Raw Data of SAG Mill Motor from 6th January, 2019 to 8th April, 2019

Cont'd

DATE	TIME	SAG MOTOR POWER	SAG MOTOR CURRENT	SAG MILL MOTOR WINDING TEMP. 1	SAG MILL MOTOR WINDING TEMP. 2	SAG MILL MOTOR WINDING TEMP. 3
4/4/2019	5:46:43 AM	5.392	338.922	88.845	90.949	88.766
4/4/2019	8:17:36 AM	5.442	341.443	90.489	92.548	90.352
4/4/2019	10:48:29 AM	5.003	311.846	92.040	93.797	91.530
4/4/2019	1:19:22 PM	3.537	224.623	82.419	83.702	81.759
4/4/2019	3:50:15 PM	5.350	335.271	94.019	95.811	93.762
4/4/2019	6:21:08 PM	5.530	344.616	97.195	99.499	97.063
4/4/2019	8:52:01 PM	5.299	333.000	92.205	94.437	92.167
4/4/2019	11:22:54 PM	5.416	339.708	90.458	92.596	90.407
5/4/2019	1:53:47 AM	5.300	333.899	90.299	92.457	90.286
5/4/2019	4:24:40 AM	5.257	331.640	89.167	91.316	89.141
5/4/2019	6:55:33 AM	5.253	331.429	88.629	90.789	88.638
5/4/2019	9:26:26 AM	5.157	322.006	91.072	92.989	90.688
5/4/2019	11:57:19 AM	5.671	352.859	93.186	95.165	92.850
5/4/2019	2:28:12 PM	5.816	361.110	98.499	100.611	98.053
5/4/2019	4:59:05 PM	5.946	368.598	102.785	104.909	102.226
5/4/2019	7:29:58 PM	5.611	350.514	100.224	102.526	99.901
5/4/2019	10:00:51 PM	5.374	337.846	94.671	96.989	94.509
6/4/2019	12:31:44 AM	5.630	350.873	94.516	96.687	94.249
6/4/2019	3:02:37 AM	5.711	355.756	95.075	97.358	94.842
6/4/2019	5:33:30 AM	5.638	351.729	94.601	96.856	94.380
6/4/2019	8:04:23 AM	5.561	347.815	93.556	95.725	93.334
6/4/2019	10:35:16 AM	5.648	352.025	96.802	98.926	96.470
6/4/2019	1:06:09 PM	5.568	347.703	98.365	100.430	97.986
6/4/2019	3:37:02 PM	5.635	351.458	101.901	103.982	101.428
6/4/2019	6:07:55 PM	5.625	351.098	101.170	103.308	100.762
6/4/2019	8:38:48 PM	5.542	346.759	97.371	99.641	97.127
6/4/2019	11:09:41 PM	5.462	342.623	94.649	96.922	94.476
7/4/2019	1:40:34 AM	5.642	351.970	94.728	96.928	94.470
7/4/2019	4:11:27 AM	5.555	347.376	94.091	96.319	93.896
7/4/2019	6:42:20 AM	5.450	342.046	92.674	94.875	92.523
7/4/2019	9:13:13 AM	5.504	344.710	93.693	95.881	93.490
7/4/2019	11:44:06 AM	5.447	341.685	95.997	98.120	95.762
7/4/2019	2:14:59 PM	5.425	340.582	98.863	100.946	98.536
7/4/2019	4:45:52 PM	5.409	339.810	100.420	102.585	100.087
7/4/2019	7:16:45 PM	5.370	337.683	95.129	97.500	95.017
7/4/2019	9:47:38 PM	5.472	343.027	91.923	94.051	91.785
8/4/2019	12:18:31 AM	5.351	336.772	90.998	93.196	90.920
8/4/2019	2:49:24 AM	5.423	340.515	88.394	90.603	88.319
8/4/2019	5:20:17 AM	5.491	343.942	88.908	91.076	88.764
8/4/2019	7:51:10 AM	5.572	347.975	89.798	91.983	89.609
8/4/2019	10:22:03 AM	5.407	339.508	90.921	93.050	90.768

APPENDIX B

RAW DATA OF MOTOR CHANGE - OUT

Table B1. Raw Data of Motor Change - Out at Damang Mine from January, 2012 to June, 2017

Material	Amount in USD	Document Date	Material Description	Reason for Changeout	Functional Location
20008701	744.88	9/21/2012	MOTOR,ENG STARTER,ELEC,CUMMINS 3636821		
20008866	917	9/26/2012	MOTOR,HYD,MILL LINER HANDLER TRACK WHEEL	REPLACE FAULTY HYDRAULIC MOTOR ON CR007	1000SR Terex Pegson Mobile Crusher
20008887	71,910.32	2/27/2017	MOTOR-G/B,TEST RUN 1ST OIL FILL CRATED,F	CHANGE FE01 G/BOX DUE TO DAMAGED COUPLIN	PRIMARY CRUSHER APRON FE001 GEARBOX
20008887	71,910.32	2/4/2013	MOTOR-G/B,TEST RUN 1ST OIL FILL CRATED,F	change gearbox on agitator 11	Eduction Water Tank Agitator
20010078	5,164.04	4/19/2016	MOTOR,AC,TYPE KEE-60-6B,VIBR,3.7KW,415V	REPLACE SN027 BURNT MOTOR	Gravity Concentrated Feed Screen to GC03
20010078	5,164.04	6/25/2015	MOTOR,AC,TYPE KEE-60-6B,VIBR,3.7KW,415V	SN027-REPLACE SCREEN FAULTY MOTOR	Gravity Concentrated Feed Screen to GC03
20010227	913.97	8/7/2014	MOTOR,HYD,13.1,LINER HANDLER, WHITE,RE188	Change Defective motor	SAG Mill Liner Handler
20010227	913.97	3/17/2012	MOTOR,HYD,13.1,LINER HANDLER, WHITE,RE188		
20010438	1,379.78	4/8/2014	MOTOR,STEPPING,AIR COMPR,39823950		
20010678	951.61	4/24/2017	MOTOR,UNIVERSAL,230V,ACID DR,M14,C/W PP-		
20010678	951.61	4/8/2017	MOTOR,UNIVERSAL,230V,ACID DR,M14,C/W PP-	PROVIDE PUMP FOR TRANSFORMER OIL FILL	Electrical Workshop
20010678	951.61	4/6/2017	MOTOR,UNIVERSAL,230V,ACID DR,M14,C/W PP-		
20010678	951.61	3/12/2017	MOTOR,UNIVERSAL,230V,ACID DR,M14,C/W PP-		
20010678	951.61	1/8/2017	MOTOR,UNIVERSAL,230V,ACID DR,M14,C/W PP-	SUPPLY ACID TRANSFER PUMP	Plant Site Mills
20010678	951.61	9/28/2016	MOTOR,UNIVERSAL,230V,ACID DR,M14,C/W PP-		
20010678	951.61	8/17/2016	MOTOR,UNIVERSAL,230V,ACID DR,M14,C/W PP-		
20010678	951.61	5/13/2016	MOTOR,UNIVERSAL,230V,ACID DR,M14,C/W PP-		
20010678	951.61	4/25/2016	MOTOR,UNIVERSAL,230V,ACID DR,M14,C/W PP-		
20010678	951.61	3/17/2016	MOTOR,UNIVERSAL,230V,ACID DR,M14,C/W PP-		
20010678	951.61	2/10/2016	MOTOR,UNIVERSAL,230V,ACID DR,M14,C/W PP-		
20010678	951.61	1/17/2016	MOTOR,UNIVERSAL,230V,ACID DR,M14,C/W PP-		
20010678	951.61	12/30/2015	MOTOR,UNIVERSAL,230V,ACID DR,M14,C/W PP-		
20010678	951.61	11/28/2015	MOTOR,UNIVERSAL,230V,ACID DR,M14,C/W PP-		
20010678	951.61	10/5/2015	MOTOR,UNIVERSAL,230V,ACID DR,M14,C/W PP-		

Table B1. Raw Data of Motor Change - Out at Damang Mine from January, 2012 to June, 2017 Cont'd

Material	Amount in USD	Document Date	Material Description	Reason for Changeout	Functional Location
20010678	951.61	9/23/2015	MOTOR, UNIVERSAL, 230V, ACID DR, M14, C/W PP-		
20010678	951.61	8/10/2015	MOTOR, UNIVERSAL, 230V, ACID DR, M14, C/W PP-		
20010678	951.61	8/3/2015	MOTOR, UNIVERSAL, 230V, ACID DR, M14, C/W PP-		
20010678	951.61	7/23/2015	MOTOR, UNIVERSAL, 230V, ACID DR, M14, C/W PP-		
20010678	951.61	7/23/2015	MOTOR, UNIVERSAL, 230V, ACID DR, M14, C/W PP-		
20010678	951.61	5/8/2015	MOTOR, UNIVERSAL, 230V, ACID DR, M14, C/W PP-		
20010678	951.61	5/1/2015	MOTOR, UNIVERSAL, 230V, ACID DR, M14, C/W PP-		
20010678	951.61	4/7/2015	MOTOR, UNIVERSAL, 230V, ACID DR, M14, C/W PP-		
20010678	951.61	3/24/2015	MOTOR, UNIVERSAL, 230V, ACID DR, M14, C/W PP-		
20010678	951.61	3/24/2015	MOTOR, UNIVERSAL, 230V, ACID DR, M14, C/W PP-		
20010678	951.61	12/17/2014	MOTOR, UNIVERSAL, 230V, ACID DR, M14, C/W PP-		
20010678	951.61	12/8/2014	MOTOR, UNIVERSAL, 230V, ACID DR, M14, C/W PP-		
20010678	951.61	10/16/2014	MOTOR, UNIVERSAL, 230V, ACID DR, M14, C/W PP-		
20010678	951.61	9/29/2014	MOTOR, UNIVERSAL, 230V, ACID DR, M14, C/W PP-		
20010678	951.61	9/5/2014	MOTOR, UNIVERSAL, 230V, ACID DR, M14, C/W PP-		
20010678	951.61	9/4/2014	MOTOR, UNIVERSAL, 230V, ACID DR, M14, C/W PP-		
20010678	951.61	8/25/2014	MOTOR, UNIVERSAL, 230V, ACID DR, M14, C/W PP-		
20010678	951.61	8/7/2014	MOTOR, UNIVERSAL, 230V, ACID DR, M14, C/W PP-		
20010678	951.61	7/26/2014	MOTOR, UNIVERSAL, 230V, ACID DR, M14, C/W PP-		
20010678	951.61	6/13/2014	MOTOR, UNIVERSAL, 230V, ACID DR, M14, C/W PP-	PROVIDE PUMP FOR POWER STATION	Main Power Station
20010678	951.61	4/10/2014	MOTOR, UNIVERSAL, 230V, ACID DR, M14, C/W PP-		
20010678	951.61	4/1/2014	MOTOR, UNIVERSAL, 230V, ACID DR, M14, C/W PP-		
20010678	951.61	1/9/2014	MOTOR, UNIVERSAL, 230V, ACID DR, M14, C/W PP-		
20010678	951.61	1/7/2014	MOTOR, UNIVERSAL, 230V, ACID DR, M14, C/W PP-		
20010678	951.61	12/10/2013	MOTOR, UNIVERSAL, 230V, ACID DR, M14, C/W PP-		
20010678	951.61	12/2/2013	MOTOR, UNIVERSAL, 230V, ACID DR, M14, C/W PP-		
20010678	951.61	11/29/2013	MOTOR, UNIVERSAL, 230V, ACID DR, M14, C/W PP-		
20010678	951.61	10/21/2013	MOTOR, UNIVERSAL, 230V, ACID DR, M14, C/W PP-		

Table B1. Raw Data of Motor Change - Out at Damang Mine from January, 2012 to June, 2017 Cont'd

Material	Amount in USD	Document Date	Material Description	Reason for Changeout	Functional Location
20010678	951.61	10/3/2013	MOTOR,UNIVERSAL,230V,ACID DR,M14,C/W PP-		
20010678	951.61	9/5/2013	MOTOR,UNIVERSAL,230V,ACID DR,M14,C/W PP-		
20010678	951.61	7/18/2013	MOTOR,UNIVERSAL,230V,ACID DR,M14,C/W PP-		
20010678	951.61	6/21/2013	MOTOR,UNIVERSAL,230V,ACID DR,M14,C/W PP-		
20010678	951.61	11/20/2012	MOTOR,UNIVERSAL,230V,ACID DR,M14,C/W PP-		
20010678	951.61	10/21/2012	MOTOR,UNIVERSAL,230V,ACID DR,M14,C/W PP-		
20010678	951.61	10/19/2012	MOTOR,UNIVERSAL,230V,ACID DR,M14,C/W PP-		
20010678	951.61	7/27/2012	MOTOR,UNIVERSAL,230V,ACID DR,M14,C/W PP-		
20010678	951.61	6/14/2012	MOTOR,UNIVERSAL,230V,ACID DR,M14,C/W PP-		
20010678	951.61	6/11/2012	MOTOR,UNIVERSAL,230V,ACID DR,M14,C/W PP-	Top up TX' 09 oil at the HV yard	33Kv Transformer To 11Kv
20010678	951.61	5/15/2012	MOTOR,UNIVERSAL,230V,ACID DR,M14,C/W PP-		
20010678	951.61	4/12/2012	MOTOR,UNIVERSAL,230V,ACID DR,M14,C/W PP-		
20010678	951.61	4/2/2012	MOTOR,UNIVERSAL,230V,ACID DR,M14,C/W PP-		
20010678	951.61	3/20/2012	MOTOR,UNIVERSAL,230V,ACID DR,M14,C/W PP-		
20010678	951.61	2/7/2012	MOTOR,UNIVERSAL,230V,ACID DR,M14,C/W PP-		
20012688	308.34	10/27/2014	MOTOR,AC,4KW,1420RPM,FT MTG,IP56,TOSHIBA	CHECK AND FIX CYANIDE PUMP AT SGS	Laboratory
20012689	1,830.97	9/21/2012	MOTOR-G/B,12:1 R,1PH,230/250V,1400RPM I/		
20012690	249.12	1/6/2014	MOTOR,AC,2.2KW,1405RPM,FT MTG,IP56,TOSHI	ME188-CHANGE GOLD ROOM RECIRCULATION MOTOR.	Pp086-Goldroom Recirculation Pump Motor
20012690	249.12	1/7/2013	MOTOR,AC,2.2KW,1405RPM,FT MTG,IP56,TOSHI	CHANGE PP#001 MOTOR BEARING	Pp001-Wet Scrubber Discharge Pump Motor
20012692	461.44	5/11/2017	MOTOR,AC,INDUCT,3PH,5.5KW,4P,D132B FRM,H	CHANGE BALL MILL MOTOR COOLER	ML002-Ball Mill Motor
20012692	461.44	3/3/2015	MOTOR,AC,INDUCT,3PH,5.5KW,4P,D132B FRM,H	CHNAGE SAG MILL INTERNAL/EXTERNAL COOLING FAN MOTOR	ML001-SAG Mill Motor
20012692	461.44	7/23/2014	MOTOR,AC,INDUCT,3PH,5.5KW,4P,D132B FRM,H	ME261 - REPLACE KILN DRIVE MOTOR	Kn001-Kiln Drive Motor
20012692	461.44	7/25/2013	MOTOR,AC,INDUCT,3PH,5.5KW,4P,D132B FRM,H	ME002 - INSPECT BALL MILL MOTOR BRUSHES	Ml002-Ball Mill Motor
20012692	461.44	3/5/2012	MOTOR,AC,INDUCT,3PH,5.5KW,4P,D132B FRM,H	Change Kiln burnt motor	Custom Furnaces Carbon Regeneration Kiln
20012693	858.06	11/15/2016	MOTOR,AC,11KW,4P,415V,D160MD FRM,FLG MTG	INSTALL 11KW MOTOR FOR INTER-TANK SCREEN REBUILD	Sn014-Cil Tank 06 Intertank Screen Motor
20012693	858.06	9/21/2016	MOTOR,AC,11KW,4P,415V,D160MD FRM,FLG MTG	Check & Change PP130 motor	Primary Crusher Lube Oil Cooler Pump
20012693	858.06	6/21/2016	MOTOR,AC,11KW,4P,415V,D160MD FRM,FLG MTG	CHANGE INTERTANK SCREEN MOTOR	Intertank Screen Cil Tank 01
20012693	858.06	11/10/2015	MOTOR,AC,11KW,4P,415V,D160MD FRM,FLG MTG	REPLACE MOTOR ON INTER TANK SCREEN NO.1	Lightnin Agitator - CIL Tank No. 8

Table B1. Raw Data of Motor Change - Out at Damang Mine from January, 2012 to June, 2017 Cont'd

Material	Amount in USD	Document Date	Material Description	Reason for Changeout	Functional Location
20012693	858.06	6/15/2015	MOTOR,AC,11KW,4P,415V,D160MD FRM,FLG MTG	ME017- CHANGE DEFECTIVE PUMP MOTOR	Pp128-Prim Crusher Lube System Oil Pump
20012693	858.06	2/27/2013	MOTOR,AC,11KW,4P,415V,D160MD FRM,FLG MTG	Replace motor with low winding resistanc	Intertank Screen Cil Tank 02
20012693	858.06	8/9/2012	MOTOR,AC,11KW,4P,415V,D160MD FRM,FLG MTG	PROVIDE MOTOR FOR INTERTANK SCREEN 5	Intertank Screen Cil Tank 01
20012695	500.00	9/16/2016	MOTOR,AC,INDUCT,3PH,7.5KW,4P,D132M FRM,H	DAME-CHANGE PP130 MOTOR	Primary Crusher Lube Oil Cooler Pump
20012695	500.00	4/24/2012	MOTOR,AC,INDUCT,3PH,7.5KW,4P,D132M FRM,H	Change out noisy motor on AG010	AG010-Electrolyte Tank Agitator Motor
20012697	158.02	2/23/2015	MOTOR,AC,INDUCT,3PH,0.55KW,4P,D80D FRM,F	CHANGE BURNT MAGNETIC MOTOR AT GOLDROOM	Gt001-Gemini Table Motor
20012697	158.02	10/22/2014	MOTOR,AC,INDUCT,3PH,0.55KW,4P,D80D FRM,F	DAMG004 - REPLACE A DAMP MOTOR	Drum Magnet Gemeni Table
20012697	158.02	9/10/2012	MOTOR,AC,INDUCT,3PH,0.55KW,4P,D80D FRM,F	REPLACE THE FAULTY GOLD ROOM FAN MOTOR	Gold Room
20012700	140.08	4/14/2016	MOTOR,AC,INDUCT,1.1KW,2P,415V,D80 FRM	REPLACE BURNT MOTOR	Light Vehicle & Ancillary Equip Workshop
20012700	140.08	4/27/2012	MOTOR,AC,INDUCT,1.1KW,2P,415V,D80 FRM	Change PP126 burnt motor	Pp126-Ball Mill Motor Hp Oil Pump No 01
20012706	945.20	2/7/2014	MOTOR,AC,INDUCT,3PH,15KW,2P,415V,D160M F	INSTALL MOTOR ON SUMP PUM FOR L.NITRATE	Krupp 54X75- Primary Crusher
20012706	945.20	6/4/2012	MOTOR,AC,INDUCT,3PH,15KW,2P,415V,D160M F	CHANGE RAW WATER PUMP MOTOR	PP048-Eduction Water Pump Motor
20012706	945.20	1/20/2012	MOTOR,AC,INDUCT,3PH,15KW,2P,415V,D160M F	PP083 burnt motor change-out	Plant Potable Water Booster Pump
20012707	1,007.49	6/11/2015	MOTOR,AC,INDUCT,3PH,15KW,4P,415V,D160L F	REPLACE MOTOR FOR PP044A	Pp044-Pretreatment Pump Motor
20012707	1,007.49	5/7/2015	MOTOR,AC,INDUCT,3PH,15KW,4P,415V,D160L F	ME174-INSTALL PP045B MOTOR	Pp045-Elution Water Pump Motor
20012707	1,007.49	2/6/2015	MOTOR,AC,INDUCT,3PH,15KW,4P,415V,D160L F	ME137- CHANGE DEFECTIVE MOTOR	Pp044-Pretreatment Pump Motor
20012707	1,007.49	2/6/2015	MOTOR,AC,INDUCT,3PH,15KW,4P,415V,D160L F	Provide PP052 standby motor to be installed	Pp052-Elution Recirculation Pump Motor
20012707	1,007.49	1/29/2013	MOTOR,AC,INDUCT,3PH,15KW,4P,415V,D160L F	15KW MOTOR FOR NEW THICKNER	Ag007-Cyanide Mixing Agitator Motor
20012707	1,007.49	1/17/2013	MOTOR,AC,INDUCT,3PH,15KW,4P,415V,D160L F	REPLACE COMPRESSOR MOTOR	Portable Air Compressor
20012709	164.13	12/24/2013	MOTOR,AC,INDUCT,3PH,3KW,2P,D100L FRM,HF/	DAME085:REPLACE THE FAULTY FAN MOTOR	ME002-Ball Mill Motor Exterior AirFan N2
20012710	279.73	5/1/2017	MOTOR,AC,INDUCT,3PH,2.2KW,4P,D100L FRM,W	UPGRADE PP025 MOTOR	Caustic Dosing Pump
20012710	279.73	4/7/2015	MOTOR,AC,INDUCT,3PH,2.2KW,4P,D100L FRM,W	REPLACE PP018 BURNT MOTOR	Pp018-Cyanide Transfer Pump Motor
20012710	279.73	7/11/2014	MOTOR,AC,INDUCT,3PH,2.2KW,4P,D100L FRM,W	ME188-REPLACE BURNT RECIRCULATION MOTOR	4277291
20012710	279.73	5/4/2012	MOTOR,AC,INDUCT,3PH,2.2KW,4P,D100L FRM,W	Change Chop Shop Grinding Machine	A.G.L. Site Mess
20012710	279.73	4/30/2012	MOTOR,AC,INDUCT,3PH,2.2KW,4P,D100L FRM,W	change AC,INDUCT,3PH,2.2KW,4P,D100L FRM,W	Ball Mill
20012711	162.86	2/13/2016	MOTOR,AC,INDUCT,3PH,1.1KW,4P,415V,D90S F	Change burnt elution column recirculation pump motor	PP052-Elution Recirculation Pump Motor
20012711	162.86	11/16/2015	MOTOR,AC,INDUCT,3PH,1.1KW,4P,415V,D90S F	DAME175 - CHANGE PP046 MOTOR	Pp046-Electrolyte Pump Motor
20012711	162.86	7/9/2012	MOTOR,AC,INDUCT,3PH,1.1KW,4P,415V,D90S F	REPLACE TANK 6 RECIRCULATION NOISY MOTOR	PP168-Tank6 Agit GB Oil Cool Pump Motor

Table B1. Raw Data of Motor Change - Out at Damang Mine from January, 2012 to June, 2017 Cont'd

Material	Amount in USD	Document Date	Material Description	Reason for Changeout	Functional Location
20012711	162.86	4/27/2012	MOTOR,AC,INDUCT,3PH,1.1KW,4P,415V,D90S F	Change PP126 burnt motor	Pp126-Ball Mill Motor Hp Oil Pump No 01
20012713	680.00	9/25/2013	MOTOR,AC,INDUCT,5.5KW,6P,240/420V,ABB,QY	REPLACE BALL MILL RECIRC. BURNT MOTOR	Ball Mill Motor Lube System
20012715	2,815.00	10/17/2015	MOTOR-G/B,HOIST CROSS TRAVEL,ABUS,GE1218	CHANGE PEBBLE CRUSHER TRAV. MOTOR	Ht011-10 Tonne Hoist Motor
20012715	2,815.00	4/9/2015	MOTOR-G/B,HOIST CROSS TRAVEL,ABUS,GE1218	REPLACE CIL CRANE HOIST TRAVELLING MOTOR	10t CIL Overhead Crane
20012715	2,815.00	12/20/2013	MOTOR-G/B,HOIST CROSS TRAVEL,ABUS,GE1218	REPLACE PEBBLE CRUSHER MOTOR	Cr002-Pebble Crusher Motor
20012715	2,815.00	2/26/2013	MOTOR-G/B,HOIST CROSS TRAVEL,ABUS,GE1218	Replace worn out motor shaft gear on pebble crusher crane.	Pebble Crusher Maint Hoist
20012715	2,815.00	1/13/2012	MOTOR-G/B,HOIST CROSS TRAVEL,ABUS,GE1218		
20012720	18,142.08	9/30/2015	MOTOR,AC,AGITATOR,110KW,6P,315S/M FRM,FT	REPLACE TK003 AGITATOR MOTOR	CIL Tank 03 Agitator Motor
20012720	18,142.08	1/26/2015	MOTOR,AC,AGITATOR,110KW,6P,315S/M FRM,FT	ME111 - CHANGE TK03 AGITATOR MOTOR	CIL Tank 03 Agitator Motor
20012722	401.05	10/8/2015	MOTOR,AC,AGITATOR,1.5KW,6P,D100L FRM,FLG	CHANGE AGITATOR 009 MOTOR FOR PRE-TREATMENT TANK	AG009-Pretreatment Tank Agitator Motor
20012722	401.05	4/29/2014	MOTOR,AC,AGITATOR,1.5KW,6P,D100L FRM,FLG	DAME159-CHANGE FAULTY MOTOR	AG008-Caustic Mixing Agitator Motor
20012724	1,338.44	12/24/2013	MOTOR,AC,TYPE SDFT90L8/2/BN6/Z,TRAVEL,0.	DACN002:REPLACE THE BURNT CIL CRANE MOTOR.	CN002-Cross Travel Drive Motor No1(East)
20012724	1,338.44	2/6/2012	MOTOR,AC,TYPE SDFT90L8/2/BN6/Z,TRAVEL,0.	change burnt pump motor	PP039-Tailings Pump No 03 Motor
20012725	1,848.68	1/30/2015	MOTOR,AC,HOIST TRAVEL,12KW,415V,GE,1001/	HT009-REPLACE LINER HANDLER HOIST MOTOR	Mill Liner Handler Hoist No 01
20012725	1,848.68	1/31/2012	MOTOR,AC,HOIST TRAVEL,12KW,415V,GE,1001/	Check and repair Kiln O/H crane	Custom Furnaces Carbon Regeneration Kiln
20012727	1,978.94	7/14/2016	MOTOR,AC,30KW,4P,415V,D200LC FRM,FT/FLG	INSTALL 30KW MOTOR AT TRASH SCREEN	SN003-Trash Screen Motor
20012727	1,978.94	7/2/2016	MOTOR,AC,30KW,4P,415V,D200LC FRM,FT/FLG	REPLACE BURNT PP011 MOTOR	PP011-Carbon Transfer Pump Motor
20012727	1,978.94	5/4/2016	MOTOR,AC,30KW,4P,415V,D200LC FRM,FT/FLG	UPGRADE SAG MILL LUBE MOTOR	Sag Mill Motor Lube System
20012727	1,978.94	4/13/2016	MOTOR,AC,30KW,4P,415V,D200LC FRM,FT/FLG	UPGRADE BALLMILL MOTOR LUBE MOTOR	Ball Mill Motor Lube System
20012727	1,978.94	7/6/2015	MOTOR,AC,30KW,4P,415V,D200LC FRM,FT/FLG	DAME203 - REPLACE BURNT MOTOR	PP008-Ball Mill Discharge Sump PumpMotor
20012727	1,978.94	10/8/2014	MOTOR,AC,30KW,4P,415V,D200LC FRM,FT/FLG	ME268-CHANGE FAULTY MOTOR AND PLUG	LH001-Liner Handler Hydraulic Pump Motor
20012728	1,064.34	3/14/2016	MOTOR,AC,7.5KW,6P,D160M FRM,FLG MTG,PEBB	ME103-REPLACE BURNT MOTOR @ PEBBLE LUBE	LU008-Pebble Crusher Lube Pump No1 Motor
20012728	1,064.34	1/22/2015	MOTOR,AC,7.5KW,6P,D160M FRM,FLG MTG,PEBB	ME214-CHANGE DEFECTIVE THICKENER MOTOR	PP057-Tails Thickener Overflow PumpMotor
30000057	9,273.15	10/27/2016	MOTOR,HYD,APRON FEEDER,CALZONI,MR300N4	FE002-CHANGE DEFECTIVE HYDRUALIC PUMP	Stockpile Reclaim Apron Feeder
30000057	9,273.15	11/5/2014	MOTOR,HYD,APRON FEEDER,CALZONI,MR300N4	CHANGE HYDRAULIC MOTOR.	Stockpile Reclaim Apron Feeder
30000057	9,273.15	12/24/2013	MOTOR,HYD,APRON FEEDER,CALZONI,MR300N4	FE002 - REPLACE APRON FEEDER HYD. MOTOR	Stockpile Reclaim Apron Feeder
30000286	7,710.60	12/22/2015	MOTOR,AC,150KW,1500RPM,W-DF315HN FRM,FT	REPLACE BURNT MOTOR @ BOOSTER STATION	Krebs 12/10Tails Booster Pump No.2 Motor

Table B1. Raw Data of Motor Change - Out at Damang Mine from January, 2012 to June, 2017 Cont'd

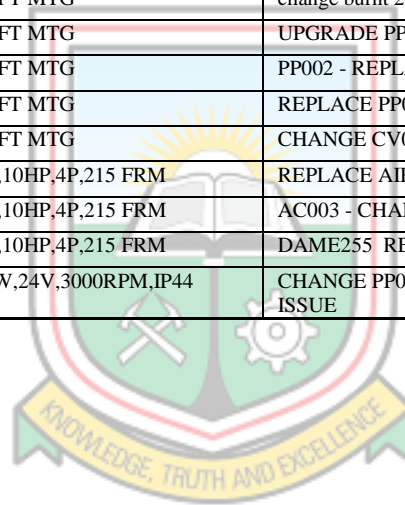
Material	Amount in USD	Document Date	Material Description	Reason for Changeout	Functional Location
30000286	7,710.60	11/5/2015	MOTOR,AC,150KW,1500RPM,W-DF315HN FRM,FT	Replace New Motor On PP224	Krebs 12/10Tails Booster Pump No.1 Motor
30000287	15,455.78	5/7/2016	MOTOR,AC,265KW,1500RPM,7-DS355SP FRM,CL	Upgraded Motor From 260kw To 265kw	Warman MCR 250 SAG Discharge Pump No. 1
30000287	15,455.78	12/24/2013	MOTOR,AC,265KW,1500RPM,7-DS355SP FRM,CL	Me149-Replace Filblast Motor	PP068-Filblast Pump Motor
30000287	15,455.78	6/7/2013	MOTOR,AC,265KW,1500RPM,7-DS355SP FRM,CL	Change Out Filblast Burnt Motor	PP068-Filblast Pump Motor
30000288	1,413.32	8/5/2015	MOTOR,AC,SPRG CHARGE,BRKR,240V	Gs018-Replace Gen-Set Breaker Motor	Gen Set No. 018 Power Station
30000288	1,413.32	8/5/2015	MOTOR,AC,SPRG CHARGE,BRKR,240V	Replace Faulty Genset 013 Battery	Gen Set No. 013 Power Station
30000290	263.42	9/16/2015	MOTOR,AC,TYPE QU90L4AT,INDUCT,3PH,1.5KW	Me080-Replace Damped Electric Motor_Motor Got Damped Because Of Oil Ingress	PP127-Ball Mill Motor HP Oil Pump No2
30000290	263.42	9/9/2015	MOTOR,AC,TYPE QU90L4AT,INDUCT,3PH,1.5KW	Install Motor At Tk003 Radiator Fan	CIL Tank 03 Agitator Motor
30000290	263.42	7/16/2015	MOTOR,AC,TYPE QU90L4AT,INDUCT,3PH,1.5KW	Replace Ball Mill Motor Hp Pump No.1 Motor	PP126-Ball Mill Motor HP Oil Pump No1
30000290	263.42	6/18/2015	MOTOR,AC,TYPE QU90L4AT,INDUCT,3PH,1.5KW	Install 1.5kw Motor At Sag Mill Hp Pump	PP123-SAG Mill Motor HP Oil Pump No2
30000290	263.42	11/26/2014	MOTOR,AC,TYPE QU90L4AT,INDUCT,3PH,1.5KW	Me079-Replace High Pump Motor	PP126-Ball Mill Motor HP Oil Pump No1
30000290	263.42	2/6/2014	MOTOR,AC,TYPE QU90L4AT,INDUCT,3PH,1.5KW	Me052 - Replace Sag Mill Motor Lube Hp Pump No.1 Motor Due To Siezed Bearing	PP123-SAG Mill Motor HP Oil Pump No2
30000290	263.42	11/25/2013	MOTOR,AC,TYPE QU90L4AT,INDUCT,3PH,1.5KW	Dame175 - Change Pump Motor	PP046-Electrolyte Pump Motor
30000290	263.42	6/5/2012	MOTOR,AC,TYPE QU90L4AT,INDUCT,3PH,1.5KW	Change PP122 Motor And Service The Dump	PP122-SAG Mill Motor HP Oil Pump No1
30000291	7,074.65	4/13/2015	MOTOR,AC,INDUCT,3PH,150KW,4P,415V,50HZ,3	Replace Burnt Pp224 Motor	Krebs 12/10Tails Booster Pump No.1 Motor
30000291	7,074.65	11/12/2014	MOTOR,AC,INDUCT,3PH,150KW,4P,415V,50HZ,3	Upgrade Motor On Booster Station Pump 001	Krebs 12/10Tails Booster Pump No.1 Motor
30000291	7,074.65	1/6/2014	MOTOR,AC,INDUCT,3PH,150KW,4P,415V,50HZ,3	Me085-Provide Motor For B/Mill Lube Fan	ME002-Ball Mill Motor Exterior AirFan N2
30000293	164.95	4/6/2016	MOTOR,AC,TYPE AEVB-UCB,AGITATOR,0.55KW,2	Replace Burnt Motor For Tyre Fixing Machine	Light Vehicle Office & Ablution Block
30000294	48,035.45	2/5/2014	MOTOR,AC,INDUCT,600KW,660V,1485RPM,50HZ	Dame093 - Replace Faulty Pp006 Motor	PP006-Cyclone Feed Pump Motor
30000294	48,035.45	10/16/2012	MOTOR,AC,INDUCT,600KW,660V,1485RPM,50HZ	Pp#06 Motor Change Out	Warman MCR350 - Cyclone Feed Pump No. 2
30000295	4,384.93	9/17/2014	MOTOR,AC,PEBBLE CRUSHER FEEDER,YASKAWA,K	Change Motor At Fuel Farm	PP212 BRV to VT electric motor-Fuel Farm
30000297	508.48	5/6/2013	MOTOR,AC,INDUCT,3PH,7.5KW,4P,415V,D132M	Me049 - Install New Mill Lube Pump Motor	PP120-SAG Mill Motor LP Oil Pump No1
30000299	1,608.82	9/3/2013	MOTOR,AC,INDUCT,3PH,22KW,6P,D200L FRM,HF	Me049-Replace Sag Mill Lp Lube Pump Motor	PP120-SAG Mill Motor LP Oil Pump No1
30000302	586.29	5/6/2016	MOTOR,AC,4KW,6P,415V,D132MD FRM,FLG MTG	Lu002-Change Recirculation Pump	SAG Mill Disch End Lube System (Fixed)

Table B1. Raw Data of Motor Change - Out at Damang Mine from January, 2012 to June, 2017 Cont'd

Material	Amount in USD	Document Date	Material Description	Reason for Changeout	Functional Location
30000302	586.29	10/11/2013	MOTOR,AC,4KW,6P,415V,D132MD FRM,FLG MTG	Me048-Change S/G Mill Flt Recir. Motor	PP104-S/Mill Float/B Rec Oil Pump Mot
30000303	172.50	10/14/2013	MOTOR,AC,INDUCT,3PH,3KW,2P,415V,D100L FR	Change Out Burnt Compressor Motor @ Hv Lube Bay-Hme Fuel Farm	HME Technician Workshop
30000306	248.60	11/23/2016	MOTOR,AC,INDUCT,3PH,0.55KW,2P,D71D FRM,F	Replace Burnt Motor For Pp006b Cooling Fan	PP006B Drive Gearbox Heat Exchanger Moto
30000306	248.60	1/16/2012	MOTOR,AC,INDUCT,3PH,0.55KW,2P,D71D FRM,F	0.55 KW Electrical Motor Change Out	Stockpile Reclaim Apron Feeder
30000307	5,836.85	2/3/2017	MOTOR,AC,110KW,4P,415V,D280M FRM,C/W RTD	Upgrade Pp027 Motor (From 90kw To 110kw)	Tamang R Raw Water Sup Pump To Plant
30000307	5,836.85	11/5/2014	MOTOR,AC,110KW,4P,415V,D280M FRM,C/W RTD	Change Noisy Motor(Bearing Failure)	Krebs 12/10Tails Booster Pump No.2 Motor
30000307	5,836.85	7/30/2014	MOTOR,AC,110KW,4P,415V,D280M FRM,C/W RTD	Change Tk08 Agitator Drive Motor	CIL Tank 07 Agitator Motor
30000308	1,087.00	10/1/2015	MOTOR,AC,7.5KW (10HP),400/440V,50HZ,HEAT	Me282-Replace Burnt Motor	PP023-Acid Metering Pump Motor
30000309	18,114.52	5/18/2017	MOTOR,AC,260KW,4P,415V,355M/L FRM,B3 MTG	Change Cv002 Drive Motor	CV002-Drive Motor
30000309	18,114.52	5/18/2017	MOTOR,AC,260KW,4P,415V,355M/L FRM,B3 MTG	Change Cv002 Drive Motor	CV002-Drive Motor
30000309	18,114.52	6/4/2015	MOTOR,AC,260KW,4P,415V,355M/L FRM,B3 MTG	Replace Pp260 Noisy Motor	Pre_Leach Thickener U/F Pump Motor No. 1
30000309	18,114.52	11/11/2012	MOTOR,AC,260KW,4P,415V,355M/L FRM,B3 MTG	Change PP68 Motor For Filblast	Pp068-Filblast Pump Motor
30000310	179.12	2/28/2016	MOTOR,AC,TYPE QY80M4B,INDUCT,0.75KW,4P,2	Me043-Change Sag Mill Recirculation Motor	SAG Mill Fixed Bearing Rec Oil PumpMotor
30000310	179.12	7/17/2015	MOTOR,AC,TYPE QY80M4B,INDUCT,0.75KW,4P,2	Install 1.5kw Motor At Sag Mill Hp Pump	PP123-SAG Mill Motor HP Oil Pump No2
30000311	969.83	3/8/2017	MOTOR,AC,15KW,415V,1455RPM,D160 FRM,TECO	Replace Burnt Scats Return Conv Motor	CV008-Drive Motor
30000311	969.83	5/31/2016	MOTOR,AC,15KW,415V,1455RPM,D160 FRM,TECO	Change Tailings Agitator Motor	AG013 - Tailing Tank No.1 Agitator Motor
30000311	969.83	2/13/2016	MOTOR,AC,15KW,415V,1455RPM,D160 FRM,TECO	15kw Motor For Tailings Agitator	AG013 - Tailing Tank No.1 Agitator Motor
30000311	969.83	8/15/2013	MOTOR,AC,15KW,415V,1455RPM,D160 FRM,TECO	Me107-Replace Cv007 Motor(Night Issue)	CV007-Drive Motor
30000311	969.83	5/20/2013	MOTOR,AC,15KW,415V,1455RPM,D160 FRM,TECO	Replace A Motor With Noisy Bearings	PP047-Barren Electrolyte Pump Motor
30000311	969.83	2/5/2013	MOTOR,AC,15KW,415V,1455RPM,D160 FRM,TECO	Change Out Burnt Pp041b Motor	PP041-Tailings Area Sump Pump Motor
30000312	1,428.90	5/1/2017	MOTOR,AC,22KW,D180 FRM,FT MTG	Change Pp#41a Burnt Motor	PP041-Tailings Area Sump Pump Motor

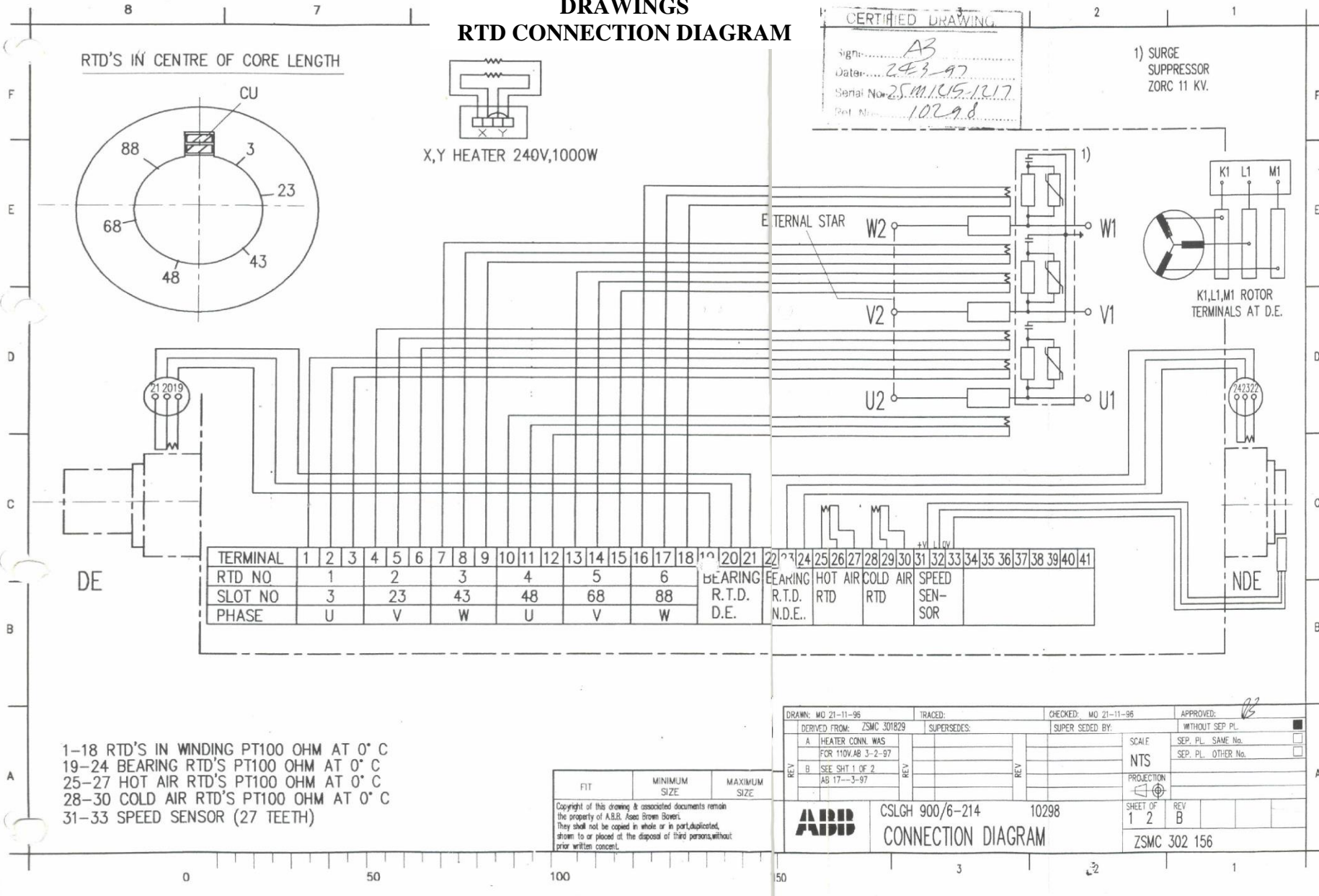
Table B1. Raw Data of Motor Change - Out at Damang Mine from January, 2012 to June, 2017 Cont'd

Material	Amount in USD	Document Date	Material Description	Reason for Changeout	Functional Location
30000312	1,428.90	1/9/2017	MOTOR,AC,22KW,D180 FRM,FT MTG	REPLACE MALFUNCTIONING DRIVE MOTOR	CIL Area Sump Pump - Between TK06/TK07
30000312	1,428.90	11/21/2016	MOTOR,AC,22KW,D180 FRM,FT MTG	REPLACE PP010 MOTOR	PP010-Carbon Transfer Pump Motor
30000312	1,428.90	9/11/2016	MOTOR,AC,22KW,D180 FRM,FT MTG	INSTALL 22KW MOTOR FOR SOS 2ND PROJECT	SOS VIBRATING SCREEN
30000312	1,428.90	8/17/2016	MOTOR,AC,22KW,D180 FRM,FT MTG	CHANGE PP007 MOTOR - 30KW	PP007-SAG Mill Discharge Sump Pump Motor
30000312	1,428.90	11/30/2015	MOTOR,AC,22KW,D180 FRM,FT MTG	UPGRADE PP023 MOTOR TO 22KW	PP023-Acid Metering Pump Motor
30000312	1,428.90	10/2/2015	MOTOR,AC,22KW,D180 FRM,FT MTG	REPLACE FAULTY MOTOR ON PP016	PP016-CIL Area Sump Pump Motor
30000312	1,428.90	7/10/2015	MOTOR,AC,22KW,D180 FRM,FT MTG	change burnt 22kw motor for PP182	PP182-Carbon Transfer Pump Motor
30000312	1,428.90	6/30/2015	MOTOR,AC,22KW,D180 FRM,FT MTG	UPGRADE PP026 MOTOR	Reagents Area Sump Pump
30000312	1,428.90	3/21/2015	MOTOR,AC,22KW,D180 FRM,FT MTG	PP002 - REPLACE BURNT MOTOR	Mill Feed Sump Pump
30000312	1,428.90	7/8/2014	MOTOR,AC,22KW,D180 FRM,FT MTG	REPLACE PP010 ELECTRICAL MOTOR.	CIL Carbon Transfer Pump - TK005
30000312	1,428.90	6/23/2014	MOTOR,AC,22KW,D180 FRM,FT MTG	CHANGE CV006 DRIVE MOTOR	CV006-Drive Motor
30000313	379.46	5/21/2014	MOTOR,AC,FAN,AIR COMPR,10HP,4P,215 FRM	REPLACE AIR COMPRESSOR THREE 3 MOTOR	AC003-Air Compressor No 03 Motor
30000313	379.46	4/9/2014	MOTOR,AC,FAN,AIR COMPR,10HP,4P,215 FRM	AC003 - CHANGE BURNT 7.5KW MOTOR	AC003-Air Compressor No 03 Motor
30000313	379.46	8/13/2013	MOTOR,AC,FAN,AIR COMPR,10HP,4P,215 FRM	DAME255 REPLACE THE BURNT MOTOR	AC003-Air Compressor No 03 Motor
30000316	669.20	2/28/2017	MOTOR,DC,PERM MAG,1.5KW,24V,3000RPM,IP44	CHANGE PP025 CAUSTIC PUMP MOTOR - NIGHT ISSUE	PP025-Caustic Dosing Pump Motor

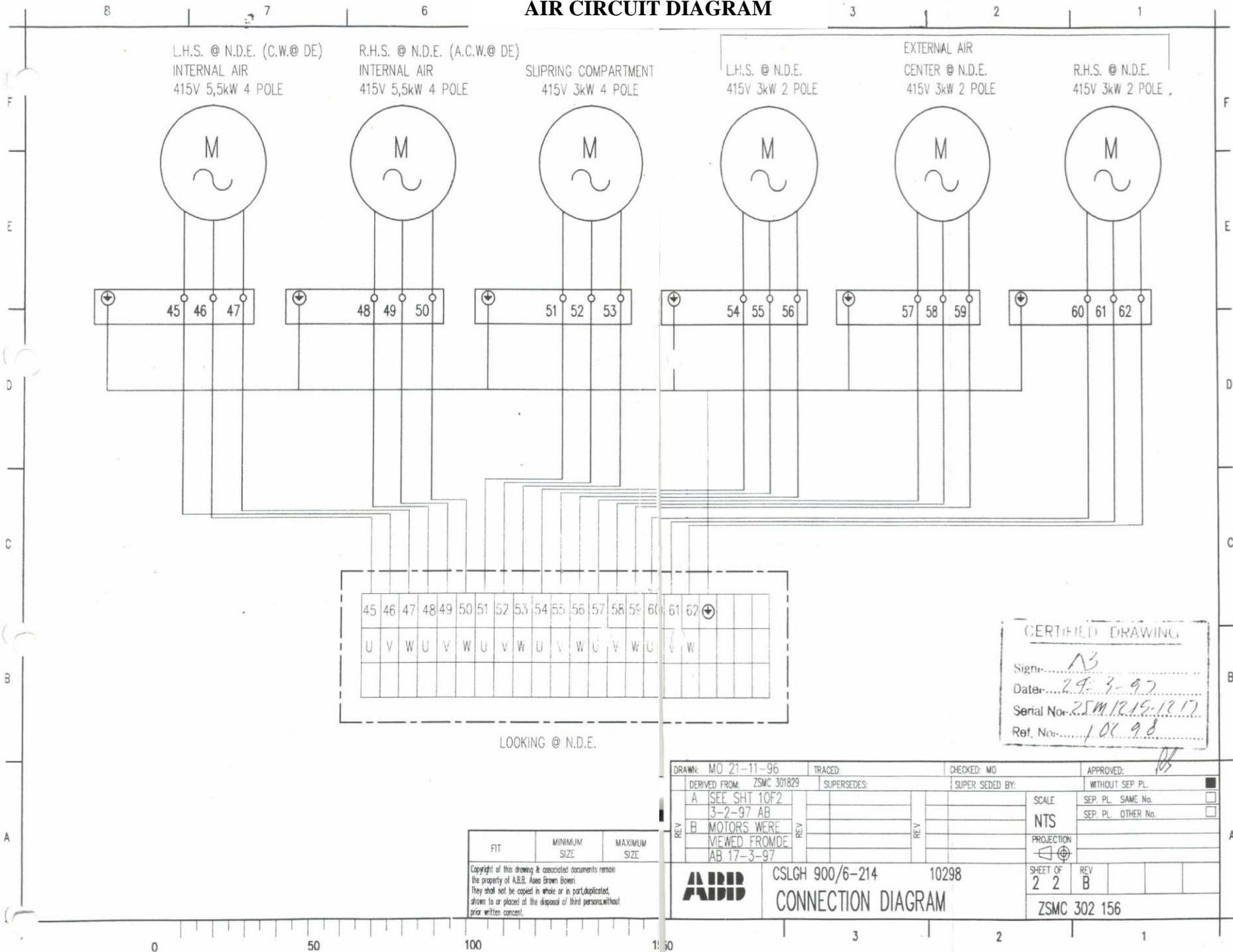


APPENDIX C

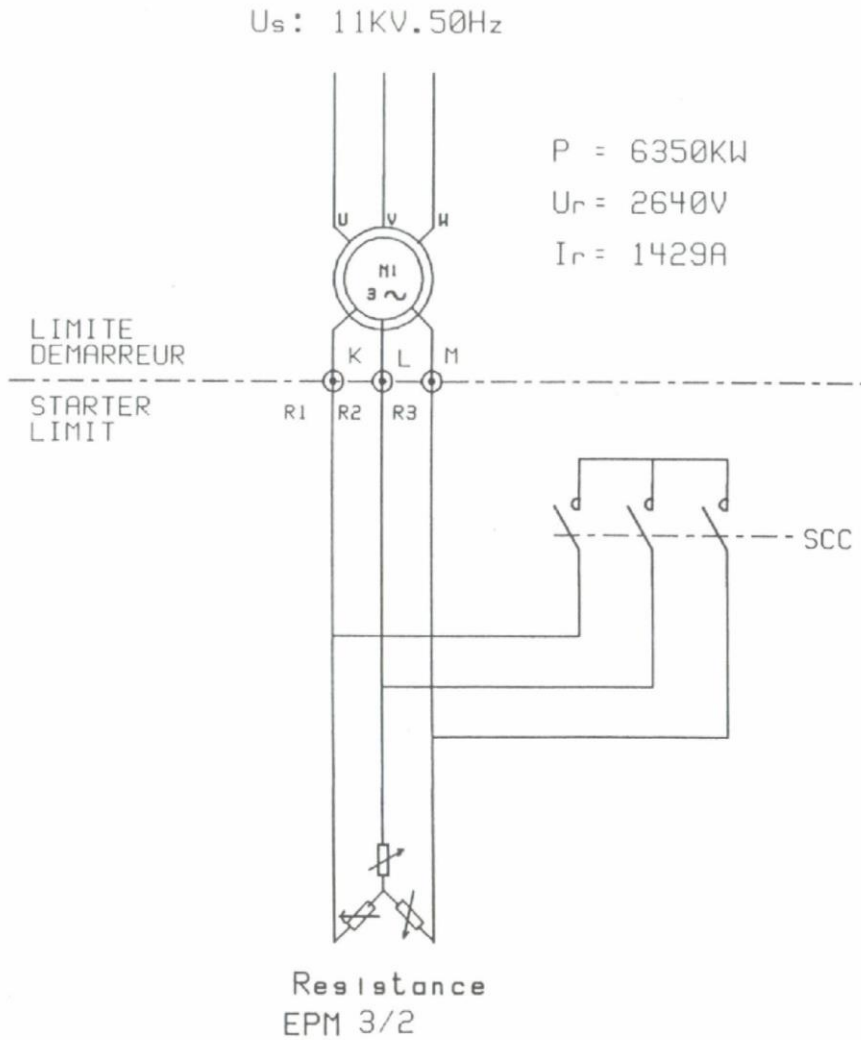
DRAWINGS RTD CONNECTION DIAGRAM



AIR CIRCUIT DIAGRAM



POWER SUPPLY DIAGRAM (1)



A	04.11.96	C	03.12.96	E	
B	19.11.96	D		F	
Design:	HP	Le:	10/12/96	54267	
Drawn:					

CIRCUIT PUISSANCE (1)
 POWER SUPPLY (1)

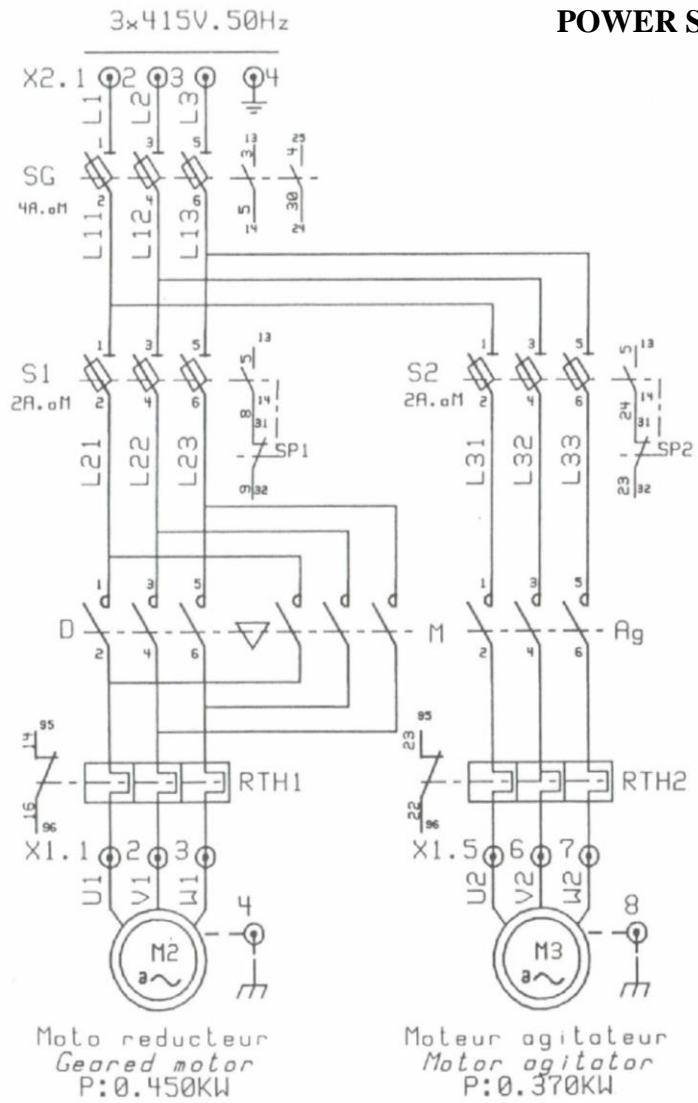


Z.I de St GUENAUT
 rue Maryse Bastie

91006 EVRY Tel:69.36.50.50
 Telex 681 301 Telecopie 60 77 02 97

9612P054
 SAG MILL
 PAGE/SHEET
 04 /18

POWER SUPPLY DIAGRAM (2)



A	04.11.96	C	03.12.96	E
B	19.11.96	D		F
Drawn:	HP	Lw:	10/12/96	54267

CIRCUIT PUISSANCE (2)
POWER SUPPLY (2)



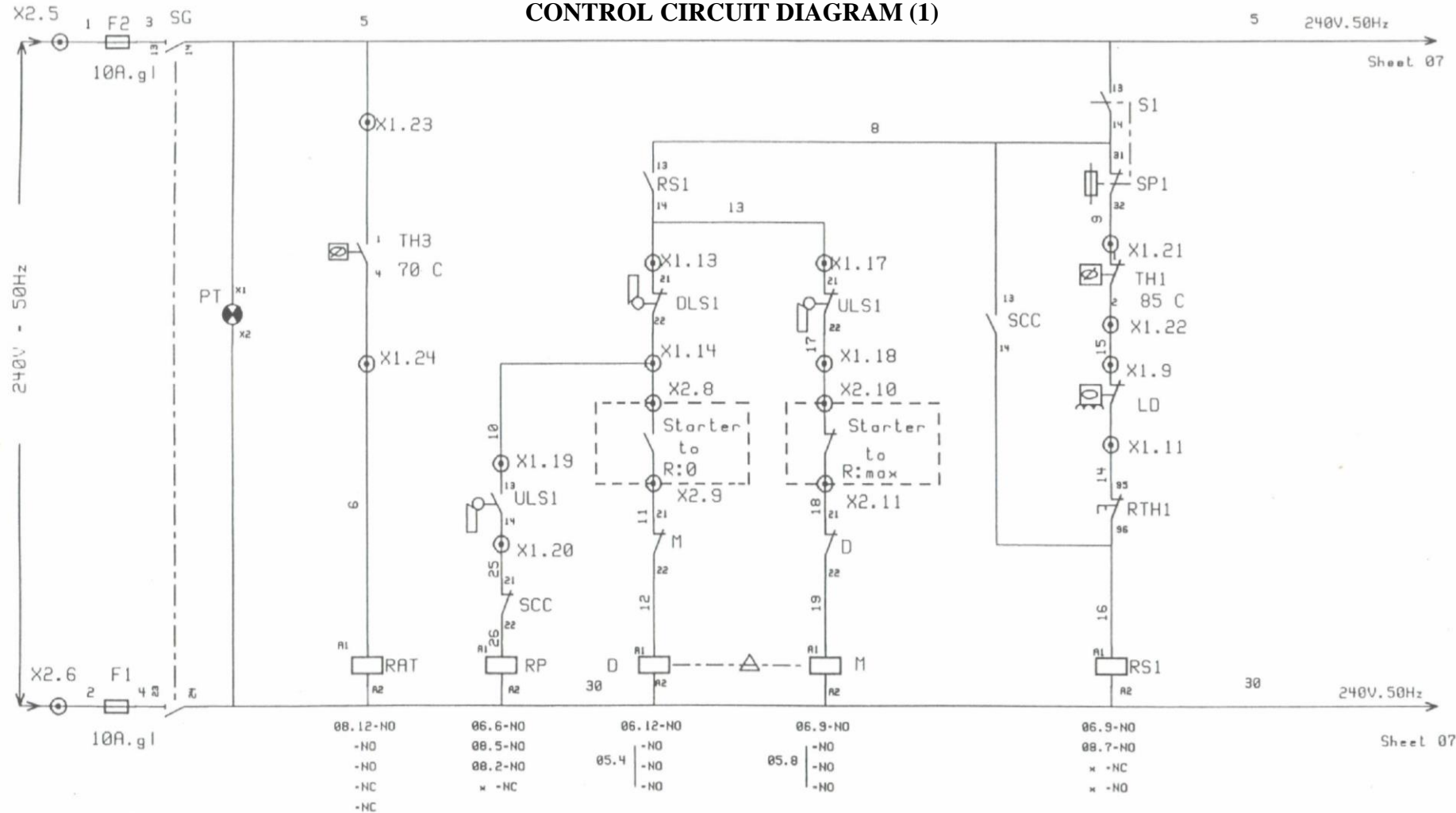
Z.I de St GUENAUT
rue Maryse Bastie

91006 EVRY Tel: 69.36.50.50
Telex 681 381 Telecopie 60 77 82 97

9612P054
SAG MILL
PAGE/SHEET
05 /18

1	2	3	4	5	6	7	8	9	10	11	12	13	14	15	16	17	18	19	20
MARCHE	PRES.TENSION	ALARME TEMPERATURE TEMPERATURE ALARM		PRET A DEMARRER	DESCENTE	MONTEE				DEFAULT									
CONTROL CIRCUIT	VOLTAGE ON	TEMPERATURE ALARM		READY TO START	ELECTRODE LOWER	ELECTRODE RAISE				STARTER FAULT									

CONTROL CIRCUIT DIAGRAM (1)



A	04.11.96	C	03.12.96	E	
B	19.11.96	D		F	
dessiné:	HP	Lé:	10/12/96	54267	

CIRCUIT CONTROLE (1)
CONTROL CIRCUIT (1)

AOP
INSTRUMENTATION

Z.I de St GUENAUT
rue Maryse Bastie

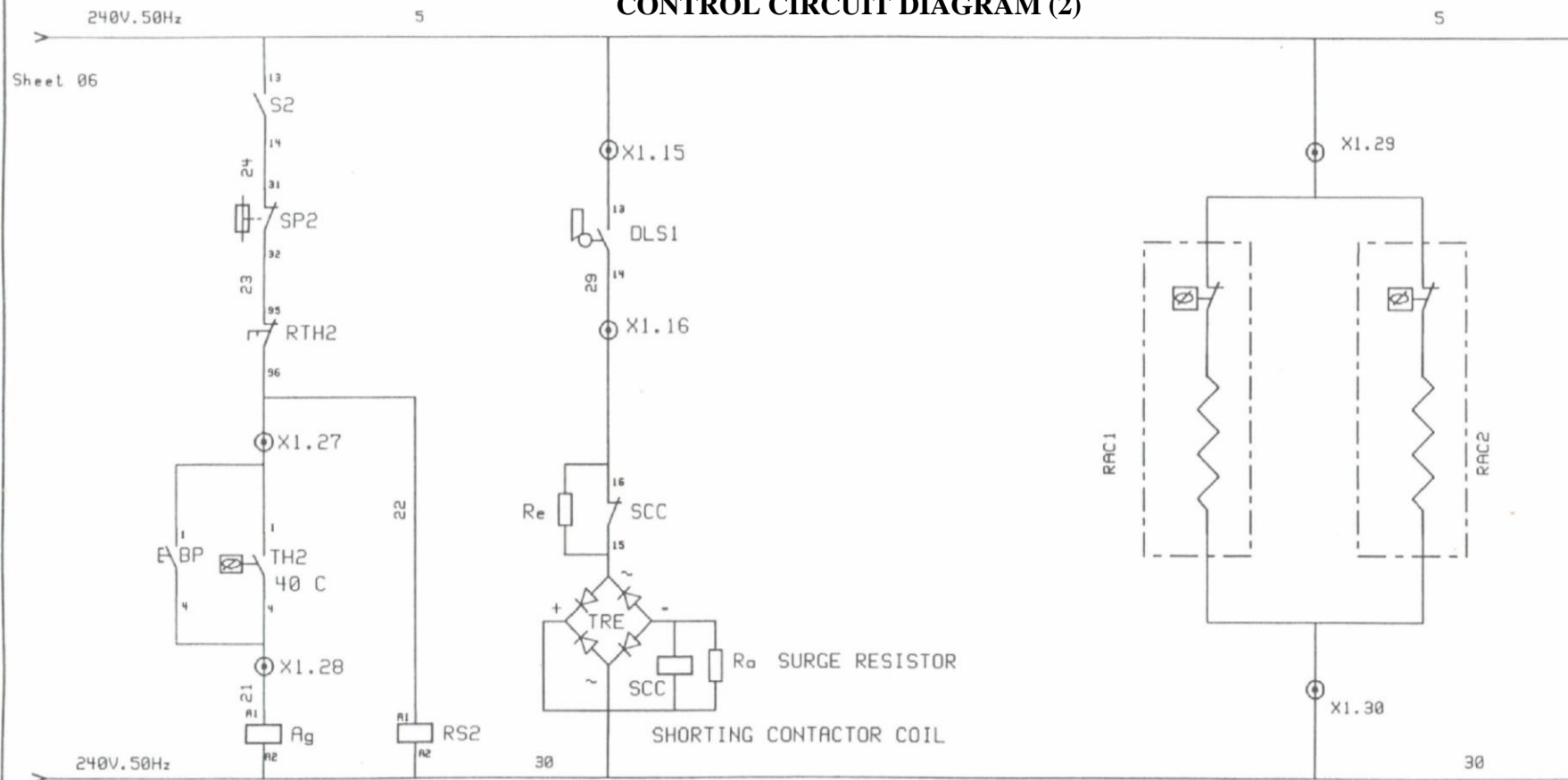
91006 EVRY Tel:69.36.50.50
Télex 681 301 Telecopie 60 77 02 97

9612P054
SAG MILL

PAGE/SHEET
06 /18

1	2	3	4	5	6	7	8	9	10	11	12	13	14	15	16	17	18	19	20
	AGITATEUR	ALARME AGITATEUR	COURT CIRCUITEUR											RESISTANCE ANTICONDENSATION					
	AGITATOR	AGITATOR ALARM	SHORTING CONTACTOR											ANTI FROST HEATER					

CONTROL CIRCUIT DIAGRAM (2)



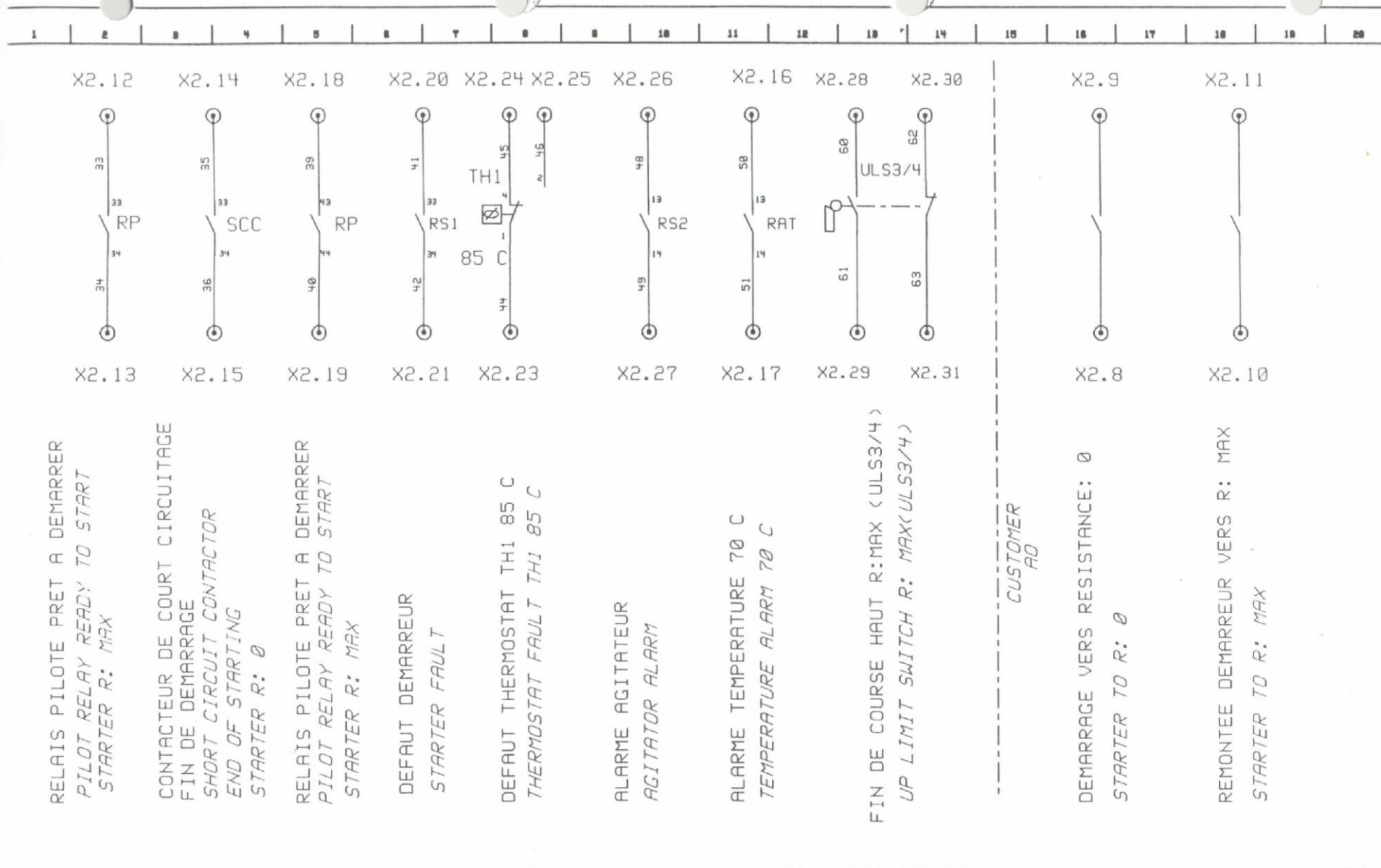
Sheet 06	x -NO	00.10-NO	06.14-NO
	-NO	x -NO	06.7-NC
05.8	-NO	x -NO	07.7-NC
	-NO	x -NC	08.3-NO
			08.13-NO

A	04.11.96	C	03.12.96	E	
B	19.11.96	D		F	
Dessine:	HP	Le:	10/12/96	54267	
Drawn:					

CIRCUIT CONTROLE (2)
CONTROL CIRCUIT (2)

	Z.I de St GUENAUT rue Maryse Bastie	9612P054 SAG MILL
	91006 EVRY Tel:69.36.50.50 Telex 681 301 Telecopie 60 77 82 97	PAGE/SHEET 07 /18

INTERFACE INDICATION DIAGRAM



RELAIS PILOTE PRET A DEMARRER
PILOT RELAY READY TO START
STARTER R: MAX

CONTACTEUR DE COURT CIRCUITAGE
FIN DE DEMARRAGE
SHORT CIRCUIT CONTACTOR
END OF STARTING
STARTER R: 0

RELAIS PILOTE PRET A DEMARRER
PILOT RELAY READY TO START
STARTER R: MAX

DEFAULT DEMARREUR
STARTER FAULT

DEFAULT THERMOSTAT TH1 85 C
THERMOSTAT FAULT TH1 85 C

ALARME AGITATEUR
AGITATOR ALARM

ALARME TEMPERATURE 70 C
TEMPERATURE ALARM 70 C

FIN DE COURSE HAUT R: MAX (ULS3/4)
UP LIMIT SWITCH R: MAX(ULS3/4)

CUSTOMER
AD

DEMARRAGE VERS RESISTANCE: 0
STARTER TO R: 0

REMONTÉE DEMARREUR VERS R: MAX
STARTER TO R: MAX

A	04.11.96	C	03.12.96	E	
B	19.11.96	D		F	
Version:	HP	Le:	10/12/96	54267	

INTERFACE



Z.I de St GUENAUT
rue Maryse Bastie

91006 EVRY Tel:69.36.50.50
Télex 681 301 Telecopie 60 77 82 97

9612P054
SAG MILL

PAGE/SHEET
08 /18

APPENDIX D

TEST REPORTS

TEMPERATURE TEST REPORT

ZSMQ 400 117

TYPE OF LOAD RUN: Bi-FREQUENCY

TEMPERATURE RISE

SERIAL NO.: ZSM 1216; W.O. NO.: 10298-02; TYPE: CSLGH 900/6-214; DATA: U 11000 V; I 383 A; P 6350 kW; n 996 rpm; Rotation: CCW;

TIME h	Cw In Leads			Amb 115	DE 203	NDE 204	Oil 205	WINDINGS				kV	I	4-φ ₂ At
	102	103	φ ₂					206	207	208	φ ₁			
0.00	29.6	29.6	20.6	20.5	48.8	40.9	24.4	41.6	42.0	42.1	41.9	11.03	383	21.4
0.30	20.4	29.4	20.4	20.4	63.2	51.2	27.9	75.1	75.7	74.5	75.1	11.03	383	54.7
1.00	19.9	20.5	20.2	25.3	67.6	53.6	29.2	88.9	90.4	87.9	89.06	11.07	383	68.87
1.30	21.4	21.9	21.45	25.6	71.0	55.0	30.0	89.5	91.4	88.5	89.80	11.08	383	68.15
2.00	20.8	21.4	21.10	26.0	74.0	56.1	30.7	88.8	91.1	88.0	89.30	11.07	383	68.20
2.30	22.1	21.3	21.70	25.9	75.7	56.8	31.0	88.5	91.2	87.9	89.20	11.05	383	67.50
3.00	21.7	21.5	21.60	26.5	77.1	57.4	31.5	88.4	90.9	87.9	89.07	11.07	383	67.47

* Found NDE bearing Rtd to be fitted badly and DE bearing had high spot. Both items rectified

$$\Delta\theta = \frac{R_h - R_c}{R_c} (235 + t_c) + t_c - t_h = \frac{113.46 - 89.70}{89.70} (235 + 21.03) + 21.03 - 21.60 = 67.24 \text{ K STATOR}$$

$$\frac{7.282 - 7.274}{7.274} (235 + 21.03) + 21.03 - 21.60 = 7.21 \text{ K ROTOR}$$

PT 100 $\Delta\theta = ^\circ\text{C max} - \text{AIR IN } \phi = 89.07 - 21.6 = 67.47 \text{ K STATOR}$

STATOR R (Ω)	h (min)	R (Ω) ROTOR
	1.00	
	1.30	
113.46	2.00	
112.98	2.30	7.282
	2.30	7.282
	3.00	7.279
	3.00	7.280
	3.30	
	4.00	

Date: 24/3/1997 Tested by: J.C. NIEKERK Approved by: J.M. Riebel Witnessed by: _____

NOISE TEST REPORT

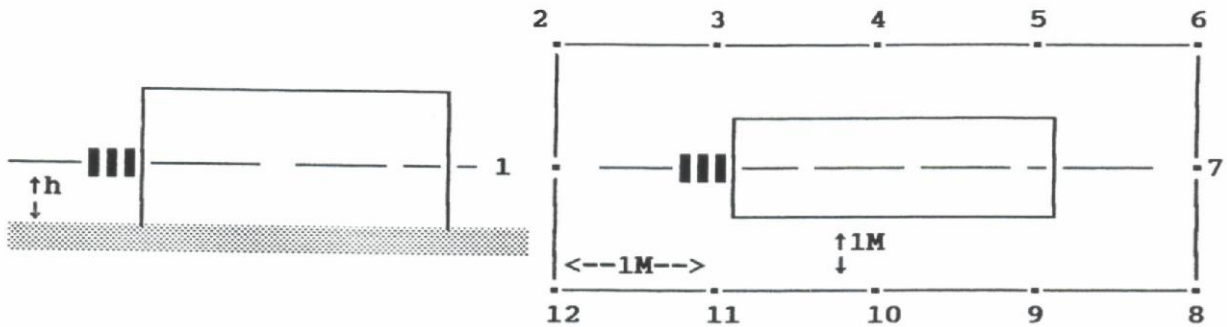


TEST REPORT

ZSMQ 400218

NOISE TEST

TYPE CSLGH 900/6-214 PLANT BALL & SAG MILL
 SERIAL No. ZSM 1216 : CLIENT ABB SWITZERLAND
 WORKS ORDER NO. 10298-02



TEST PROCEDURE HTAY 620562

BEFORE RUN dB(A)

DURING RUN dB (A)

1) 59.1	1) 82.4
2) 58.9	2) 83.6
3) 58.4	3) 84.3
4) 57.6	4) 84.2
5) 57.5	5) 83.5
6) 57.6	6) 85.7
7) 57.3	7) 86.5
8) 58.4	8) 83.3
9) 59.1	9) 83.5
10) 58.1	10) 83.2
11) 58.5	11) 82.8
12) 59.2	12) 83.2

Tested by:

J. NEL

Approved by: I.M. REHBOCK

Date 24/3/97



BEARING RUN TEST REPORT



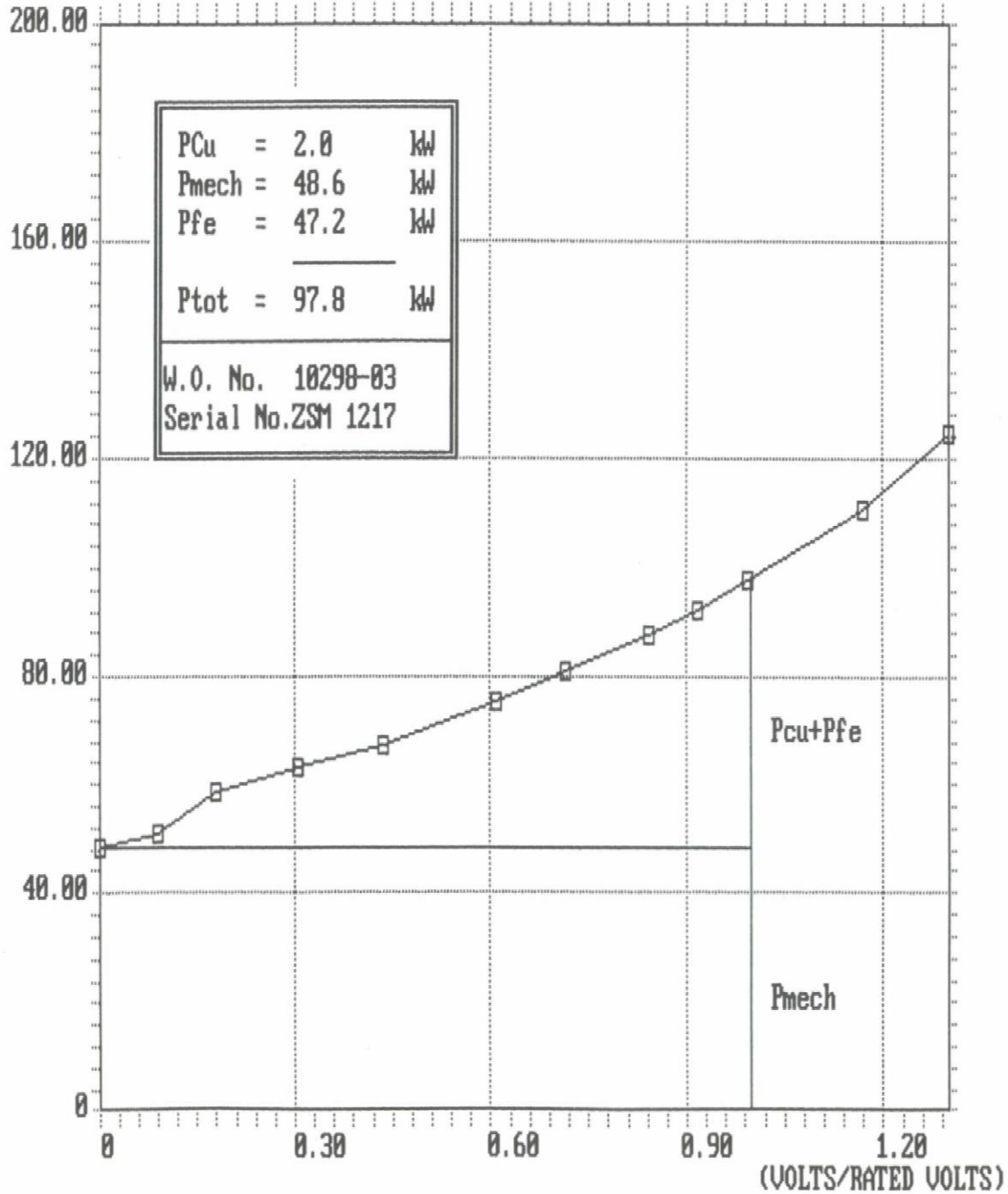
TEST REPORT		ZSMQ 400081		
BEARING RUN				
Type:	CSLGH 900/6-214	Plant:	BALL & SAG MILL	
Serial No.:	ZSM 1217	Client:	ABB SWITZERLAND	
Works Order No.:	10298-03	Subcontractor:		
Bearings:	Type DE SLEEVE	NDE SLEEVE		
Dimension	DE ϕ 280	NDE ϕ 280		
Cooling	OIL			
OIL FLOW RATE 8L/MIN PER BEARING.				
Remarks				
TIME	BEARING TEMPERATURE		COOLING IN TEMPERATURE	AMBIENT TEMPERATURE
	DE	NDE		
0.00	30.60	30.90	21.90	18.90
0.25	44.70	45.20	22.30	19.30
0.50	49.40	49.90	23.30	19.50
0.75	52.20	53.10	24.80	19.80
1.00	54.00	55.70	26.00	20.00
1.25	55.50	57.80	26.90	20.40
1.50	54.90	59.00	27.50	24.60
1.75	55.40	60.20	28.30	25.00
2.00	56.10	61.40	28.90	24.90
2.25	56.60	62.40	29.20	24.80
2.50	57.00	63.40	29.50	24.70
2.75	57.40	64.40	29.70	24.70
3.00	57.60	65.00	30.00	24.70
3.25	57.90	65.50	30.10	24.50
3.50	58.10	66.00	29.90	24.60
3.75	58.30	66.30	30.10	24.70
Tested by: J.NEL		Approved by: I.M.REHBOCK.		
Date 27/3/97				

POWER TEST REPORT

NO LOAD SEPARATION OF LOSSES

NO LOAD POWER (Kw)

NoLoad rsults



ABB

ASYNCHRONOUS MOTOR TEST REPORT



TEST REPORT FOR ASYNCHRONOUS MOTOR			ZSMQ 400318																								
WORKS ORDER NUMBER: 10298-03		ASYNCHRONOUS MOTOR																									
		SERIAL NUMBER: ZSM 1217																									
Rated Power: 5800 kW;SF	Year: 1997	Type: CSLGH 900/6-214	Mass: 33700 kg																								
Speed: 996 rpm	Duty: S1	Cosφ: 0.89	IC: 656																								
U1: 11000 V	I1: 353 A	Freq: 50 Hz	IM: 1001																								
U2: 2640 V	I2: 1305 A	3-: STAR	IP: 56																								
Mec: ES21	Rotation from DE CCW	3-: DELTA	CI: F																								
Plant: BALL & SAG MILL	Client: ABB SWITZERLAND																										
GENERAL DATA																											
Terminals: Left/Right from DE: LHS																											
Slip rings of: SS ; Brushes per slip ring: 18 ; Type: EG389P ; Dimension: 25*32*64																											
Brush lifting mechanism: NO ; Continous contact: YES ; Brush pressure: 343.8 gr/cm ²																											
DE BEARING Type: SLEEVE , Dimension: 280 mm; NDE BEARING Type: SLEEVE , Dimension: 280 mm																											
SHAFT ENDS. DEφ: 280 mm; NDEφ: ----- mm																											
After 4.5 h running no OIL loss.																											
Pt100. Winding: 6 x 107.55 Ω ≈ 19.52 °C; Bearing: 2 x 108.45 Ω																											
SPACE HEATER. Resistance: 50.9 Ω; Insulation resistance: 10 MΩ with 500 V; High voltage test: 1.5kV for 1 min																											
BEARING INSULATION. DE: +20 MΩ; NDE: +20 MΩ with 100V																											
RESISTANCE Stator winding U-V: 0.08891 Ω; V-W: 0.08904 Ω; U-W: 0.08894 Ω Winding Temp: 19.52 °C																											
Rotor winding K-L 0.00728 Ω; L-M 0.00723 Ω; K-M 0.00724 Ω																											
NO LOAD TEST			LOCKED ROTOR TEST																								
Overvolt 12650 V for 1.0 min			VIBRATION LEVELS mm/sec (rms) <table border="1" style="width: 100%; border-collapse: collapse;"> <tr> <td style="width: 33%;">H</td> <td style="width: 33%;">V</td> <td style="width: 33%;">A</td> <td></td> </tr> <tr> <td>0.43</td> <td>0.29</td> <td>0.61</td> <td>DE</td> </tr> <tr> <td>0.39</td> <td>0.31</td> <td>0.51</td> <td>NDE</td> </tr> </table> μm (double amplitude) <table border="1" style="width: 100%; border-collapse: collapse;"> <tr> <td style="width: 33%;">H</td> <td style="width: 33%;">V</td> <td style="width: 33%;">A</td> <td></td> </tr> <tr> <td>8.6</td> <td>7.1</td> <td>10.9</td> <td>DE</td> </tr> <tr> <td>8.2</td> <td>7.7</td> <td>8.3</td> <td>NDE</td> </tr> </table>	H	V	A		0.43	0.29	0.61	DE	0.39	0.31	0.51	NDE	H	V	A		8.6	7.1	10.9	DE	8.2	7.7	8.3	NDE
H	V	A																									
0.43	0.29	0.61		DE																							
0.39	0.31	0.51		NDE																							
H	V	A																									
8.6	7.1	10.9		DE																							
8.2	7.7	8.3		NDE																							
V	A	KW		V																							
12540	159.5	124.4																									
10964	107.0	97.8																									
10098	91.3	87.8																									
9301	84.6	81.0																									
8574	72.7	75.6																									
7257	62.3	67.3																									
6079	49.7	63.0																									
4642	38.1	58.4																									
3291	27.7	50.8																									
Inl. U: 107.0 ; V: 107.1 ; W: 107.0 Amps Isc.U: -----; V: -----; W: ----- Amps																											
Losses at 11000. V; Pcu: 2.0 kW; Pfe: 47.2 kW; Pmech: 48.6 kW; Ptotal: 97.8 kW																											
Bearing temp: DE 58.3 °C; NDE: 66.3 °C; Cool In: 30.1 °C; Ambient: 24.7 °C																											
Overspeed test: ----- rpm for ----- min.																											
VOLTAGE RATIO		MAGNETIC CENTRE (mm)																									
Stator : 11000 / 2200 Volts		35-40.5-45																									
Rotor : 2697 / 546.6 Volts																											
TEMPERATURE RISE		AIR GAP																									
Stator : ----- K above cooling medium.		Stator:1180.08; Rotor:1173.02; 2δ:7.06 ; δ:3.53 mm																									
Rotor : ----- K above cooling medium.																											
REMARKS SLIPRING CONCENTRICITY K=0.02mm L=0.01mm M=0.01mm																											
INSULATION RESISTANCE																											
STATOR. Prior the tests:690 MΩ with 5.0 kV at 19.52 °C; After voltage test: 2000 MΩ with 5.0 kV at 21.50 °C																											
ROTOR. Prior the tests:440 MΩ with 1.0 kV at 19.52 °C; After voltage test: +4000 MΩ with 1.0 kV at 21.50 °C																											
HIGH VOLTAGE TEST. Stator(ph/ph-earth) 24.1 kV; Rotor(winding-earth) 6.5 kV for 1 min. Winding temp. 21.50 °C																											
Date: 27/3/97 Tested by: J.NEL Approved by: I.M.REHBOCK Inspected by:																											



BALANCE AND OVERLOAD TEST REPORT

ABB <small>ASEA BROWN BOVERI</small>	TEST REPORT	Page 1 of 1			
		ZSMQ 400005			
Balance and Overspeed Test					
Type: <i>C.S.L.G.H 900/6-2/4</i>	Plant: <i>BALL & SAG MILL</i>				
Serial No: <i>Z.S.M 1216.</i>	Client: <i>A.B.B. INDUSTRY</i>				
Works Order No: <i>10298-03</i>	Subcontractor:				
Specified size: <i>5800 K.W</i>	Remarks:				
Operating speed: n_n <i>994</i>	r.p.m.				
Overspeed: n_n <i>-</i>	r.p.m.				
Rotor mass: <i>11460</i>	kg				
Number of Balancing Levels: <i>2</i>	n_e				
Max. permissible bearing vibration - S.A. (Base HTAG 20023)					
S ₁ <i>131</i>	μm at n_{w1}	<i>1000</i> r.p.m.			
S ₂ <i>131</i>	μm at n_{w2}	<i>1000</i> r.p.m.			
S ₃	μm at n_o	r.p.m.			
Actual size:					
Speed r.p.m.	Bearing arrangement	Dr. s		N. Dr. s	
		\angle	gr	\angle	gr
n_{w1}	Open	<i>120</i>	<i>3</i>	<i>295</i>	<i>8.</i>
	Closed				
n_{w2}	Open				
	Closed				
n_o	Open				
	Closed				
Overspeed Test Yes <input type="checkbox"/> No <input type="checkbox"/>	Balancing level	Dr. s		N. Dr. s	
		Outside	Inside	Outside	Inside
	Mass				
		\angle			
Approved: <i>[Signature]</i> Signature: Date: <i>24-3-97.</i>					
Actual size (Machine assembled) Vibrations in double amplitude (μm)					
Line up	On rubber pads		Fixed		
Vib. direction	horizontal	vertical	horizontal	vertical	
Bearing Dr. s					
Bearing N. Dr. s					
Shaft Dr. s					
Shaft N. Dr. s					
Rebalancing: Yes <input type="checkbox"/> No <input type="checkbox"/>	Mass	(gr): Level:			
Approved: Signature: Date:					

APPENDIX E

MATLAB SCRIPTS

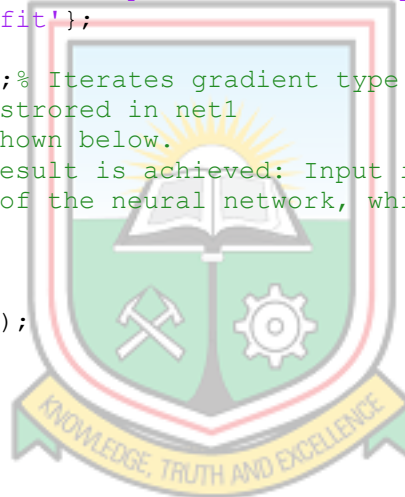
MATLAB Scripts for Levenberg-Marquardt Using Logsig

```
Data_Inputs = xlsread('Training1.xlsx');
Training_Set = Data_Inputs(1:4,1:300);%specify training set
Target_Set = Data_Inputs(5,1:300);%specify target set
P = Training_Set;
T = Target_Set;
net = newff(P,T,10,{'logsig'});
net.trainFcn = 'trainlm';
net.trainparam.min_grad = 0.00000001;
net.trainParam.epochs = 1000;
net.trainParam.lr = 0.6;
net.trainParam.max_fail =50;
net.performFcn = 'mse'; % Mean Squared Error
% Setup Division of Data for Training, Validation, Testing
% For a list of all data division functions type: help nndivide
net.divideFcn = 'dividerand'; % Divide data randomly
net.divideMode = 'sample'; % Divide up every sample
net.divideParam.trainRatio = 70/100;
net.divideParam.valRatio = 15/100;
net.divideParam.testRatio = 15/100;
net.plotFcns = {'plotperform', 'plottrainstate', 'ploterrhist', ...
'plotregression', 'plotfit'};
%Train network
net1 = train(net, P, T);% Iterates gradient type of loop
% Resulting network is stored in net1
%Convergence curve is shown below.
% Simulate how good a result is achieved: Input is the same input vector P.
% Output is the output of the neural network, which should be compared with
output data
a= sim(net1,P);
e= T-a;
perf = perform(net1,T,a);
```



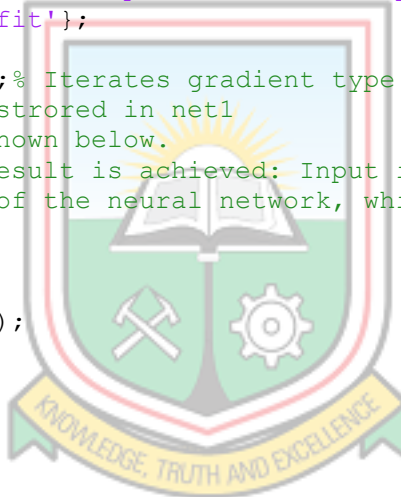
MATLAB Scripts for Levenberg-Marquardt Using Tansig

```
Data_Inputs = xlsread('Training1.xlsx');
Training_Set = Data_Inputs(1:4,1:300);%specify training set
Target_Set = Data_Inputs(5,1:300);%specify target set
P = Training_Set;
T = Target_Set;
net = newff(P,T,10,{'tansig'});
net.trainFcn = 'trainlm';
net.trainparam.min_grad = 0.00000001;
net.trainParam.epochs = 1000;
net.trainParam.lr = 0.6;
net.trainParam.max_fail =50;
net.performFcn = 'mse'; % Mean Squared Error
% Setup Division of Data for Training, Validation, Testing
% For a list of all data division functions type: help nndivide
net.divideFcn = 'dividerand'; % Divide data randomly
net.divideMode = 'sample'; % Divide up every sample
net.divideParam.trainRatio = 70/100;
net.divideParam.valRatio = 15/100;
net.divideParam.testRatio = 15/100;
net.plotFcns = {'plotperform', 'plottrainstate', 'ploterrhist', ...
'plotregression', 'plotfit'};
%Train network
net1 = train(net, P, T);% Iterates gradient type of loop
% Resulting network is stored in net1
%Convergence curve is shown below.
% Simulate how good a result is achieved: Input is the same input vector P.
% Output is the output of the neural network, which should be compared with
output data
a= sim(net1,P);
e= T-a;
perf = perform(net1,T,a);
```



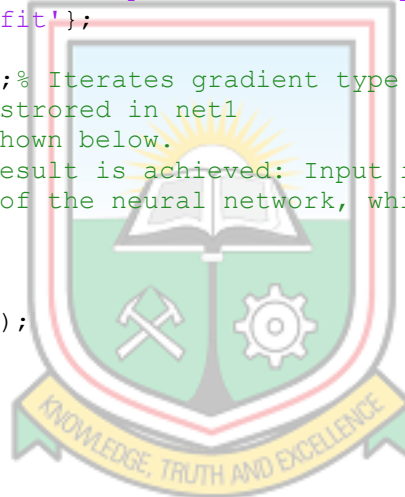
MATLAB Scripts for Bayesian Regularisation Using Logsig

```
Data_Inputs = xlsread('Training1.xlsx');
Training_Set = Data_Inputs(1:4,1:300);%specify training set
Target_Set = Data_Inputs(5,1:300);%specify target set
P = Training_Set;
T = Target_Set;
net = newff(P,T,10,{'logsig'});
net.trainFcn = 'trainbr';
net.trainparam.min_grad = 0.00000001;
net.trainParam.epochs = 1000;
net.trainParam.lr = 0.6;
net.trainParam.max_fail =50;
net.performFcn = 'mse'; % Mean Squared Error
% Setup Division of Data for Training, Validation, Testing
% For a list of all data division functions type: help nndivide
net.divideFcn = 'dividerand'; % Divide data randomly
net.divideMode = 'sample'; % Divide up every sample
net.divideParam.trainRatio = 70/100;
net.divideParam.valRatio = 15/100;
net.divideParam.testRatio = 15/100;
net.plotFcns = {'plotperform', 'plottrainstate', 'ploterrhist', ...
'plotregression', 'plotfit'};
%Train network
net1 = train(net, P, T);% Iterates gradient type of loop
% Resulting network is stored in net1
%Convergence curve is shown below.
% Simulate how good a result is achieved: Input is the same input vector P.
% Output is the output of the neural network, which should be compared with
output data
a= sim(net1,P);
e= T-a;
perf = perform(net1,T,a);
```



MATLAB Scripts for Bayesian Regularisation Using Tansig

```
Data_Inputs = xlsread('Training1.xlsx');
Training_Set = Data_Inputs(1:4,1:300);%specify training set
Target_Set = Data_Inputs(5,1:300);%specify target set
P = Training_Set;
T = Target_Set;
net = newff(P,T,10,{'Tansig'});
net.trainFcn = 'trainbr';
net.trainparam.min_grad = 0.00000001;
net.trainParam.epochs = 1000;
net.trainParam.lr = 0.6;
net.trainParam.max_fail =50;
net.performFcn = 'mse'; % Mean Squared Error
% Setup Division of Data for Training, Validation, Testing
% For a list of all data division functions type: help nndivide
net.divideFcn = 'dividerand'; % Divide data randomly
net.divideMode = 'sample'; % Divide up every sample
net.divideParam.trainRatio = 70/100;
net.divideParam.valRatio = 15/100;
net.divideParam.testRatio = 15/100;
net.plotFcns = {'plotperform', 'plottrainstate', 'ploterrhist', ...
'plotregression', 'plotfit'};
%Train network
net1 = train(net, P, T);% Iterates gradient type of loop
% Resulting network is stored in net1
%Convergence curve is shown below.
% Simulate how good a result is achieved: Input is the same input vector P.
% Output is the output of the neural network, which should be compared with
output data
a= sim(net1,P);
e= T-a;
perf = perform(net1,T,a);
```



MATLAB Scripts for Prediction Using Levenberg-Marquardt Training Algorithm

```
Data_Inputs = xlsread('Training2.xlsx');
Training_Set = Data_Inputs(1:5,1:700);%specify training set
Target_Set = Data_Inputs(6,1:700);%specify target set
P = Training_Set;
T = Target_Set;
net = newff(P,T,10,{'tansig'});
net.layers{1}.transferFcn='hardlim';
net.trainFcn = 'trainlm';
net.trainparam.min_grad = 0.00000001;
net.trainParam.epochs = 1000;
net.trainParam.lr = 0.6;
net.trainParam.max_fail =50;
net.performFcn = 'mse'; % Mean Squared Error
% Setup Division of Data for Training, Validation, Testing
% For a list of all data division functions type: help nndivide
net.divideFcn = 'dividerand'; % Divide data randomly
net.divideMode = 'sample'; % Divide up every sample
net.divideParam.trainRatio = 70/100;
net.divideParam.valRatio = 15/100;
net.divideParam.testRatio = 15/100;
net.plotFcns = {'plotperform','plottrainstate','ploterrhist', ...
'plotregression','plotfit','plotconfusion'};
%Train network
net1 = train(net, P, T);% Iterates gradient type of loop
% Resulting network is stored in net1
%Convergence curve is shown below.
% Simulate how good a result is achieved: Input is the same input vector P.
% Output is the output of the neural network, which should be compared with
output data
a= sim(net1,P);
e= T-a;
perf = perform(net1,T,a)
xlswrite('Try.xlsx', perf)
Training_Set = Data_Inputs(1:5,701:879);%specify training set
Target_Set = Data_Inputs(6,701:879);%specify target set
P1 = Training_Set;
T1 = Target_Set;
a1= sim(net1,P1)
plotconfusion(T1,a1)
```

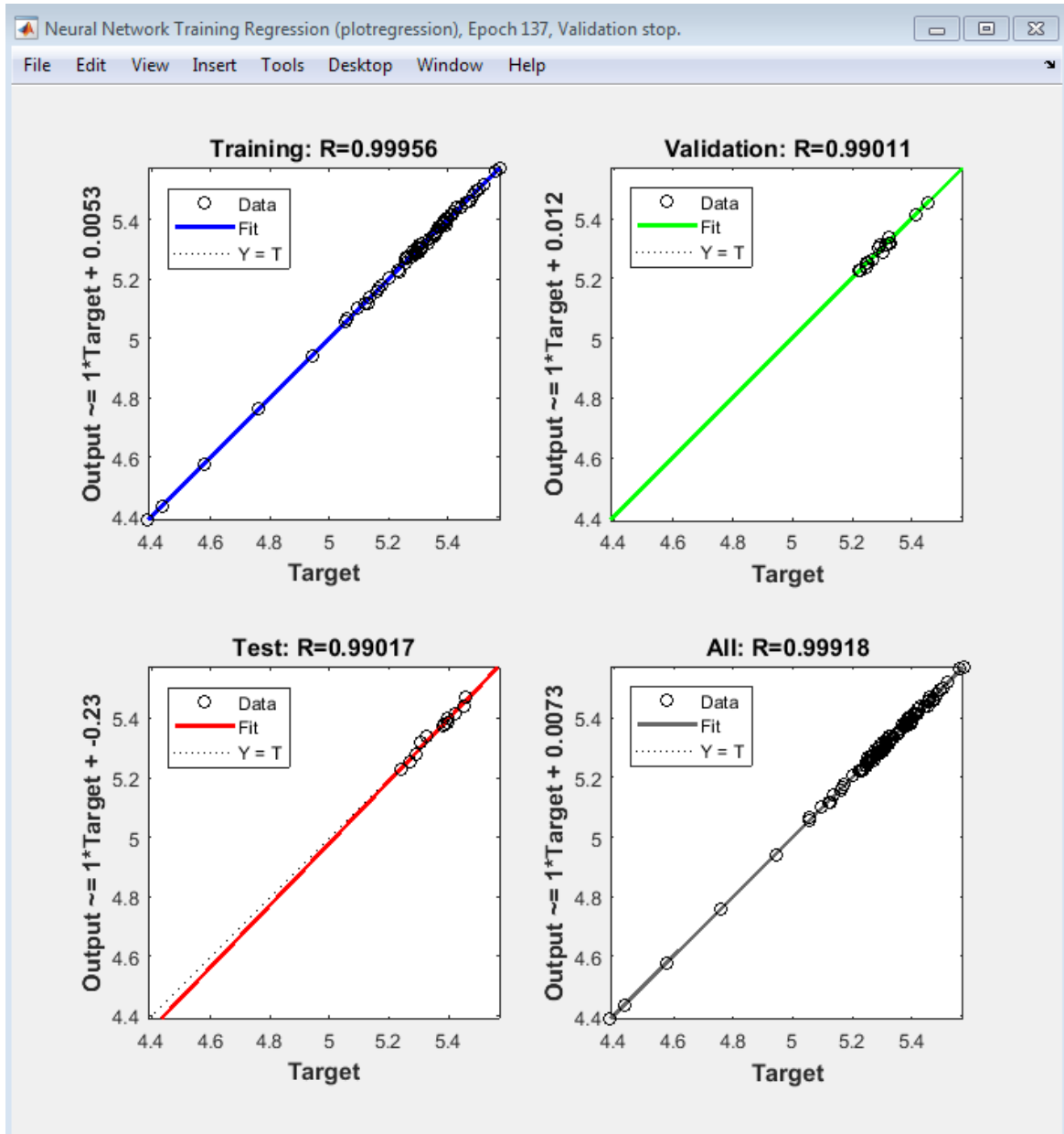
MATLAB Scripts for Prediction Using Bayesian Regularization Training Algorithm

```
Data_Inputs = xlsread('Training2.xlsx');
Training_Set = Data_Inputs(1:5,1:700);%specify training set
Target_Set = Data_Inputs(6,1:700);%specify target set
P = Training_Set;
T = Target_Set;
net = newff(P,T,10,{'tansig'});
net.layers{1}.transferFcn='hardlim';
net.trainFcn = 'trainbr';
net.trainparam.min_grad = 0.00000001;
net.trainParam.epochs = 1000;
net.trainParam.lr = 0.6;
net.trainParam.max_fail =50;
net.performFcn = 'mse'; % Mean Squared Error
% Setup Division of Data for Training, Validation, Testing
% For a list of all data division functions type: help nndivide
net.divideFcn = 'dividerand'; % Divide data randomly
net.divideMode = 'sample'; % Divide up every sample
net.divideParam.trainRatio = 70/100;
net.divideParam.valRatio = 15/100;
net.divideParam.testRatio = 15/100;
net.plotFcns = {'plotperform','plottrainstate','ploterrhist', ...
'plotregression','plotfit','plotconfusion'};
%Train network
net1 = train(net, P, T);% Iterates gradient type of loop
% Resulting network is stored in net1
%Convergence curve is shown below.
% Simulate how good a result is achieved: Input is the same input vector P.
% Output is the output of the neural network, which should be compared with
output data
a= sim(net1,P);
e= T-a;
perf = perform(net1,T,a)
xlswrite('Try.xlsx', perf)
Training_Set = Data_Inputs(1:5,701:879);%specify training set
Target_Set = Data_Inputs(6,701:879);%specify target set
P1 = Training_Set;
T1 = Target_Set;
a1= sim(net1,P1)
plotconfusion(T1,a1)
```

APPENDIX F

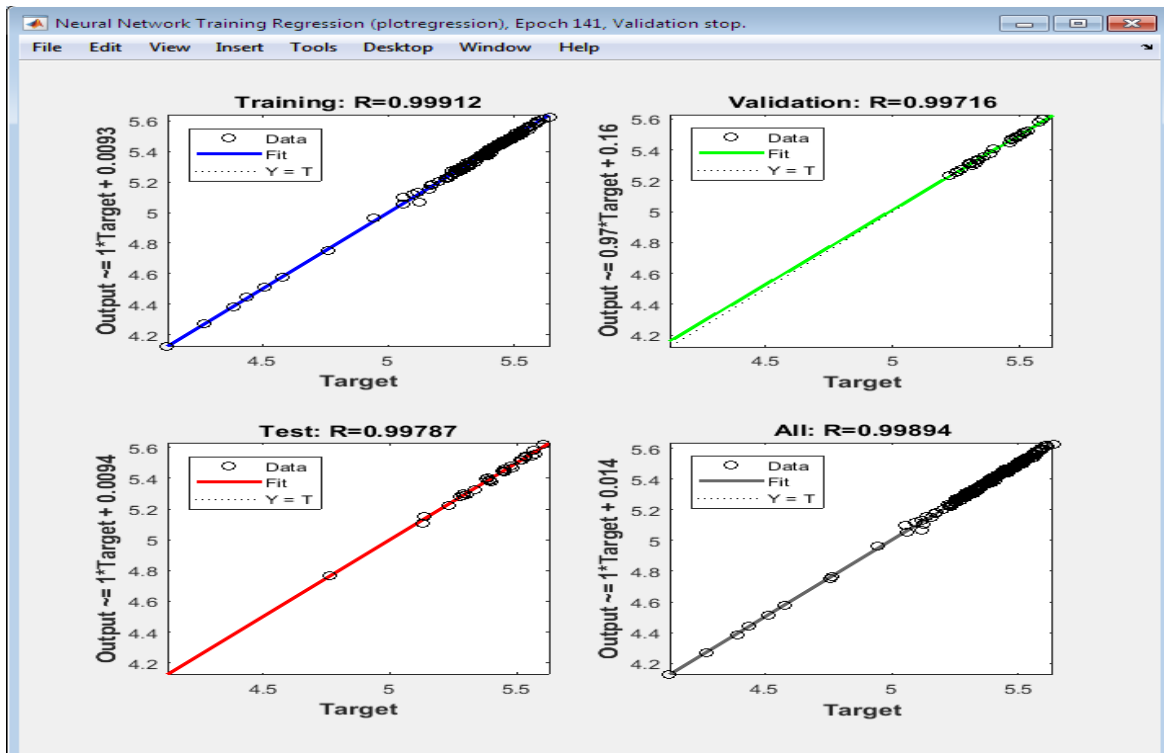
MATLAB RESULTS

MATLAB Results Using Levenberg-Marquardt/Logsigmoid

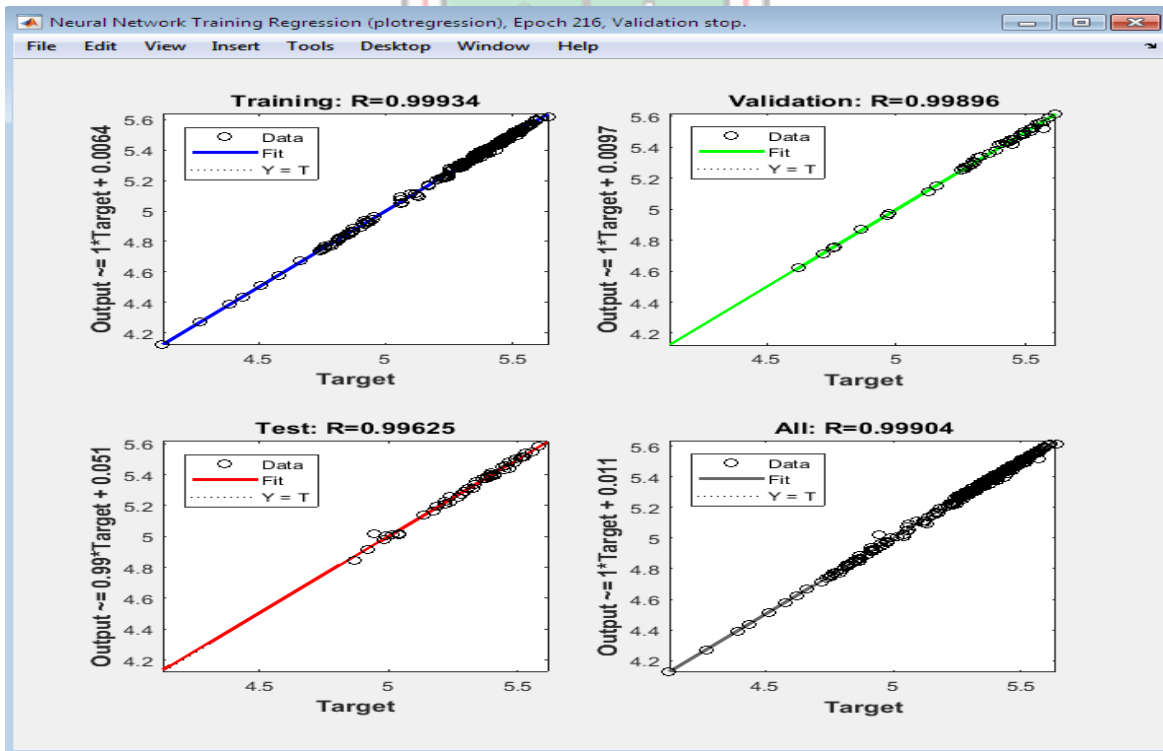


Correlation Coefficient for Network Performance, R (100 Data Samples)

MATLAB Results Using Levenberg-Marquardt/Logsigmoid Cont'd

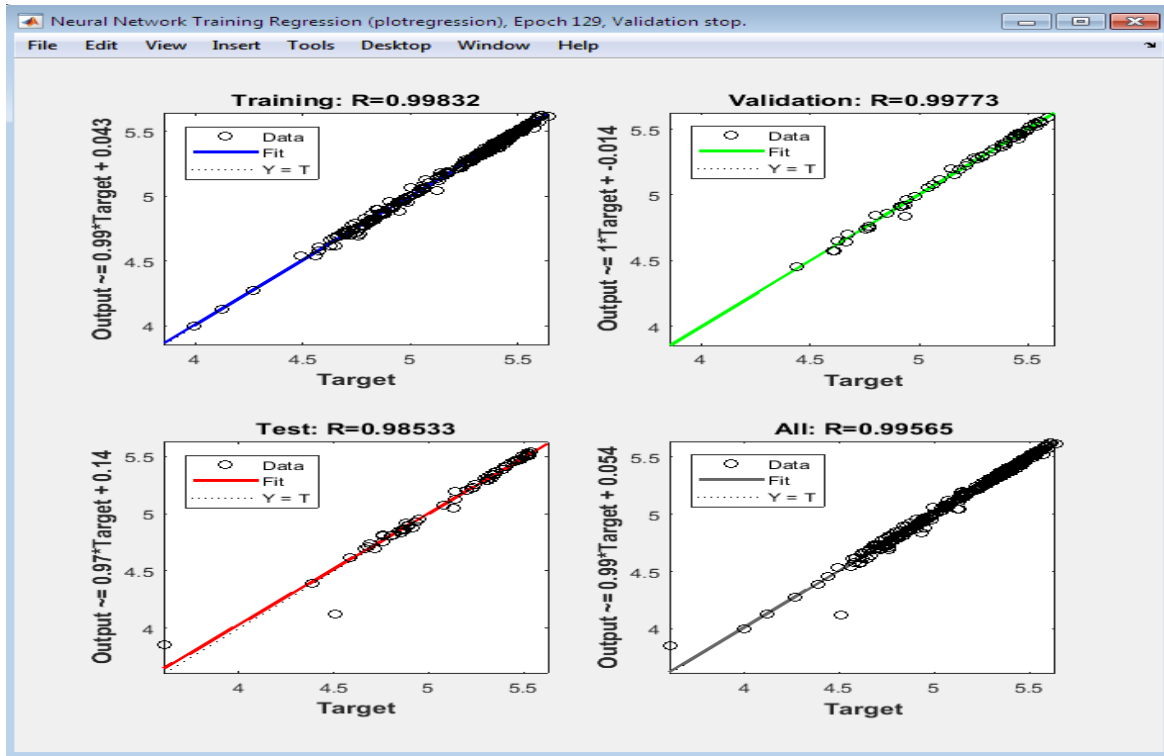


Correlation Coefficient for Network Performance, R (200 Data Samples)

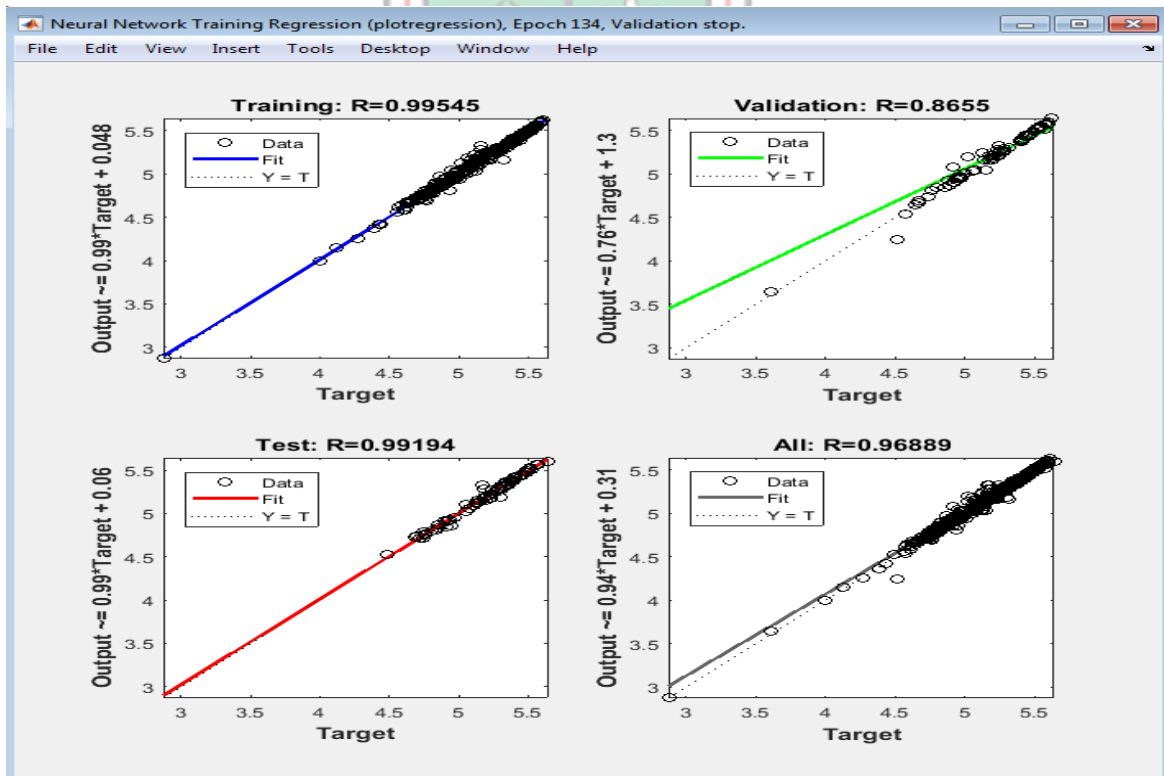


Correlation Coefficient for Network Performance, R (300 Data Samples)

MATLAB Results Using Levenberg-Marquardt/Logsigmoid Cont'd

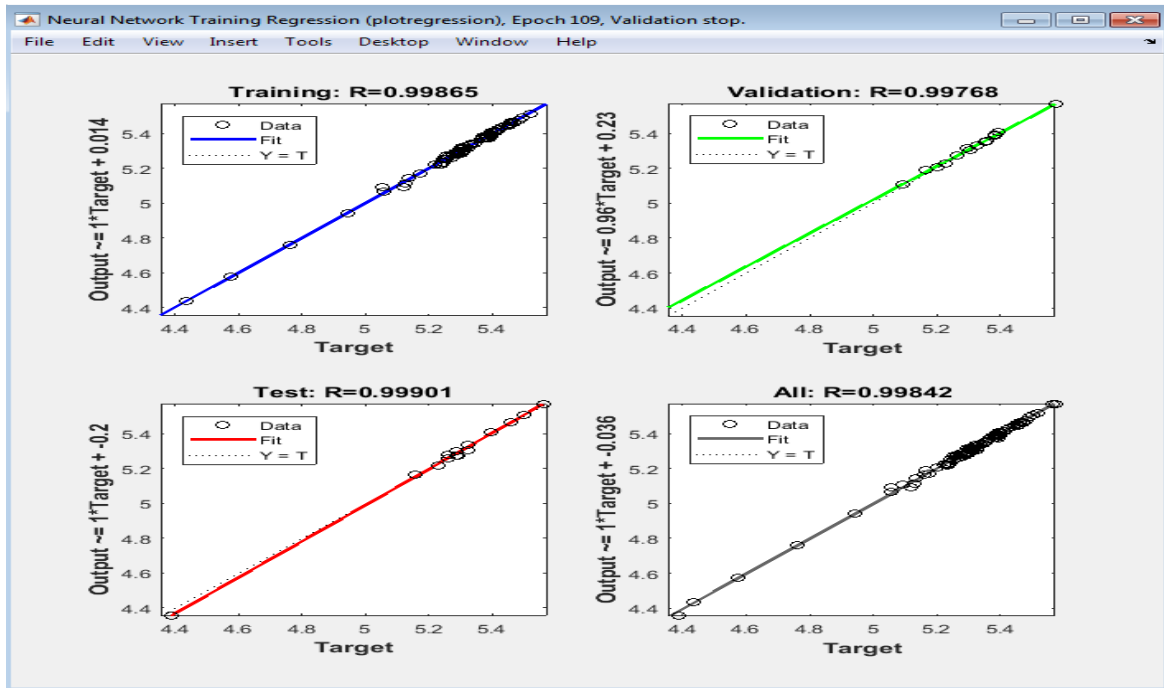


Correlation Coefficient for Network Performance, R (400 Data Samples)

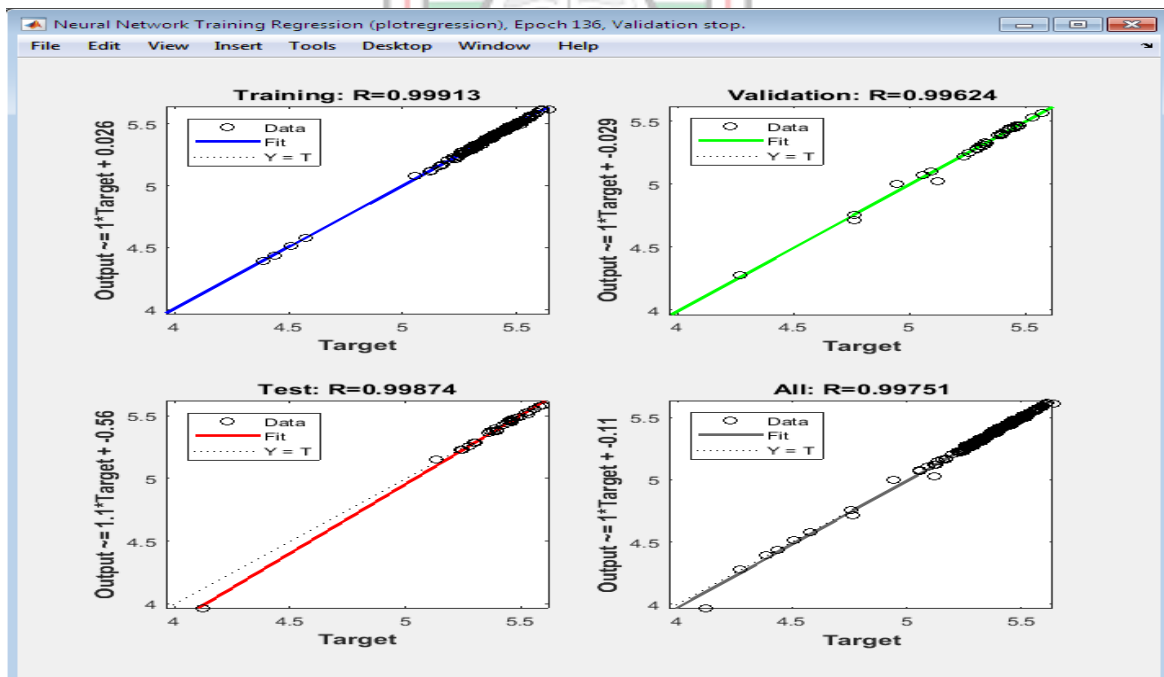


Correlation Coefficient for Network Performance, R (500 Data Samples)

MATLAB Results Using Levenberg-Marquardt/Tansigmoid

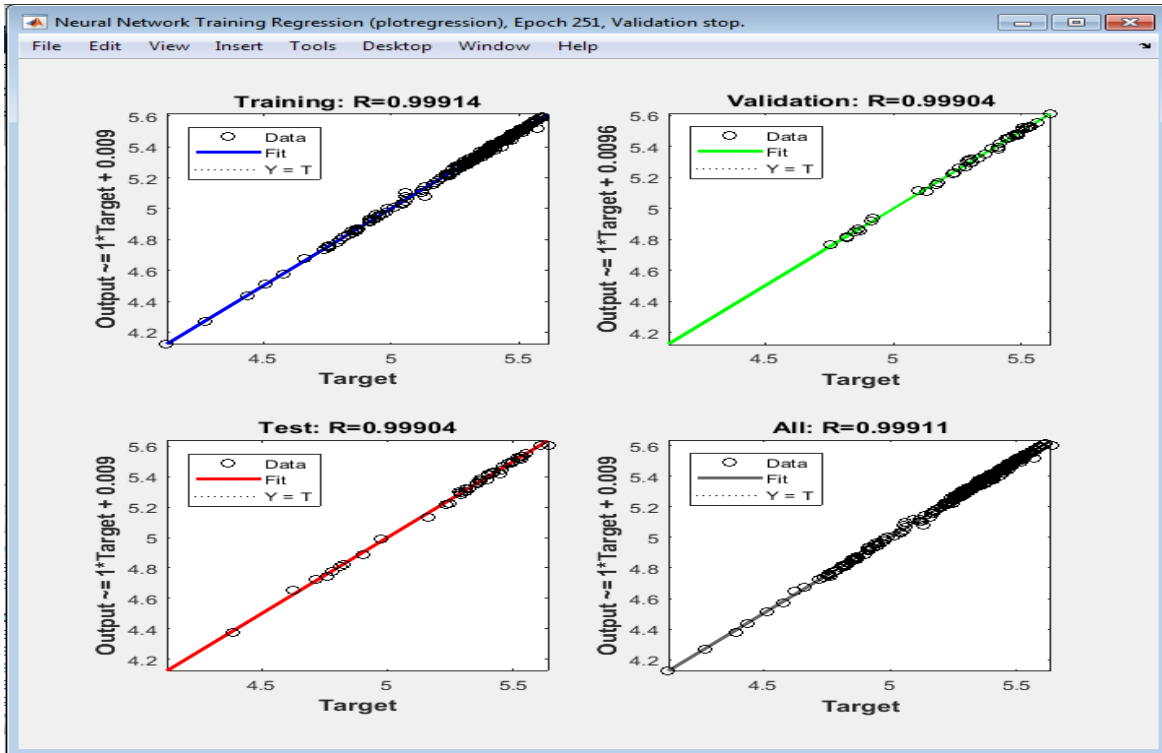


Correlation Coefficient for Network Performance, R (100 Data Samples)

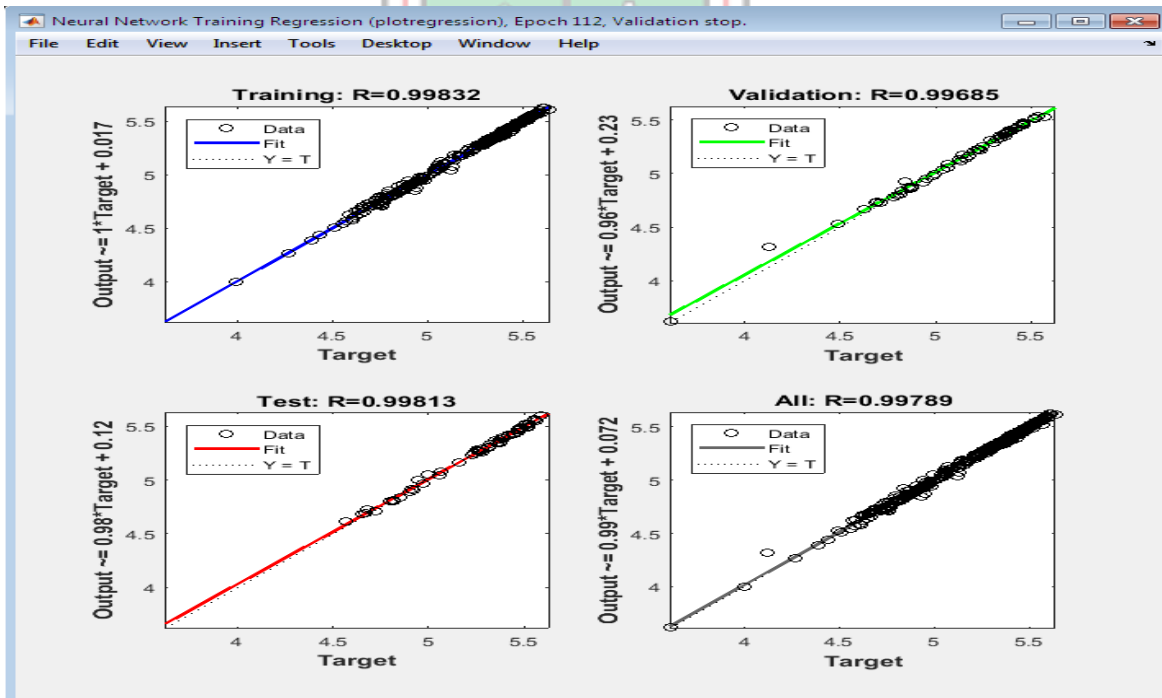


Correlation Coefficient for Network Performance, R (200 Data Samples)

MATLAB Results Using Levenberg-Marquardt/Tansigmoid Cont'd

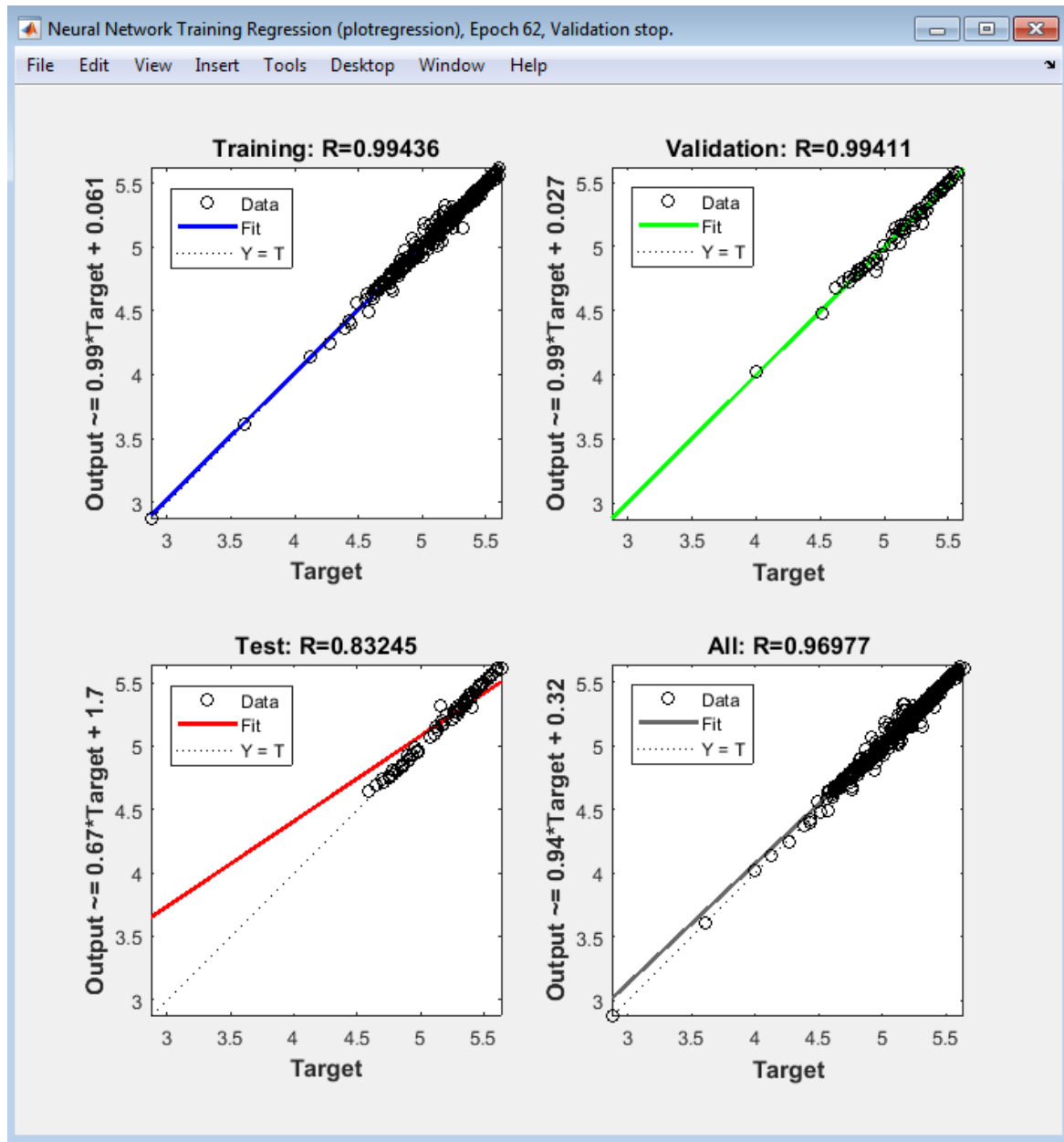


Correlation Coefficient for Network Performance, R (300 Data Samples)



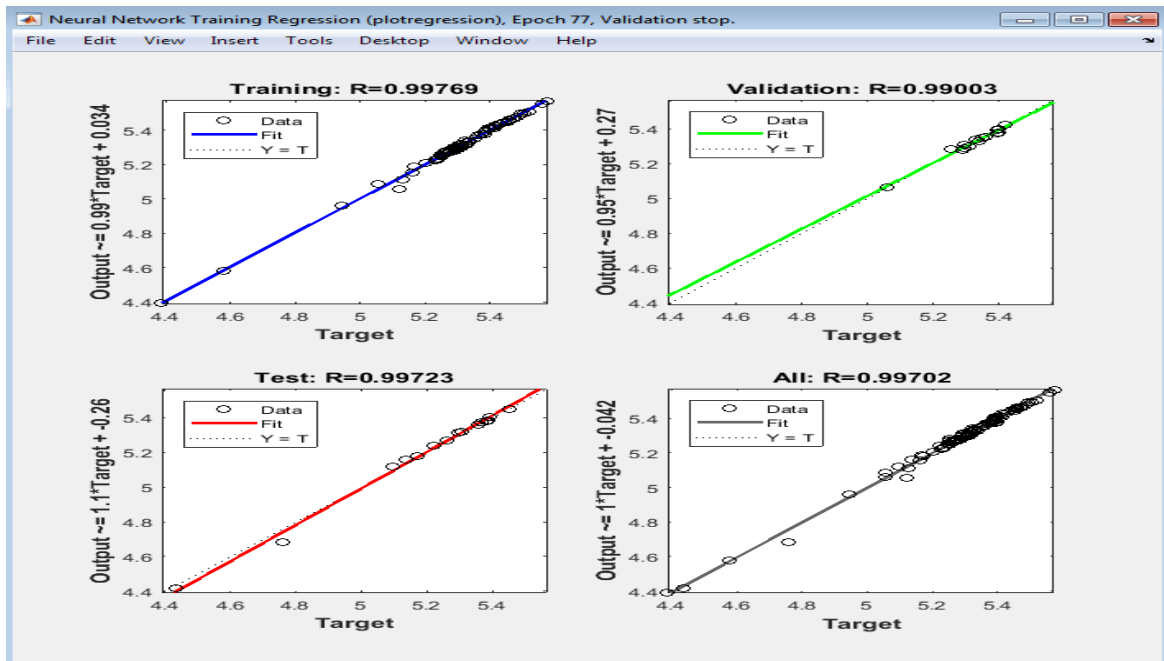
Correlation Coefficient for Network Performance, R (400 Data Samples)

MATLAB Results Using Levenberg-Marquardt/Tansigmoid Cont'd

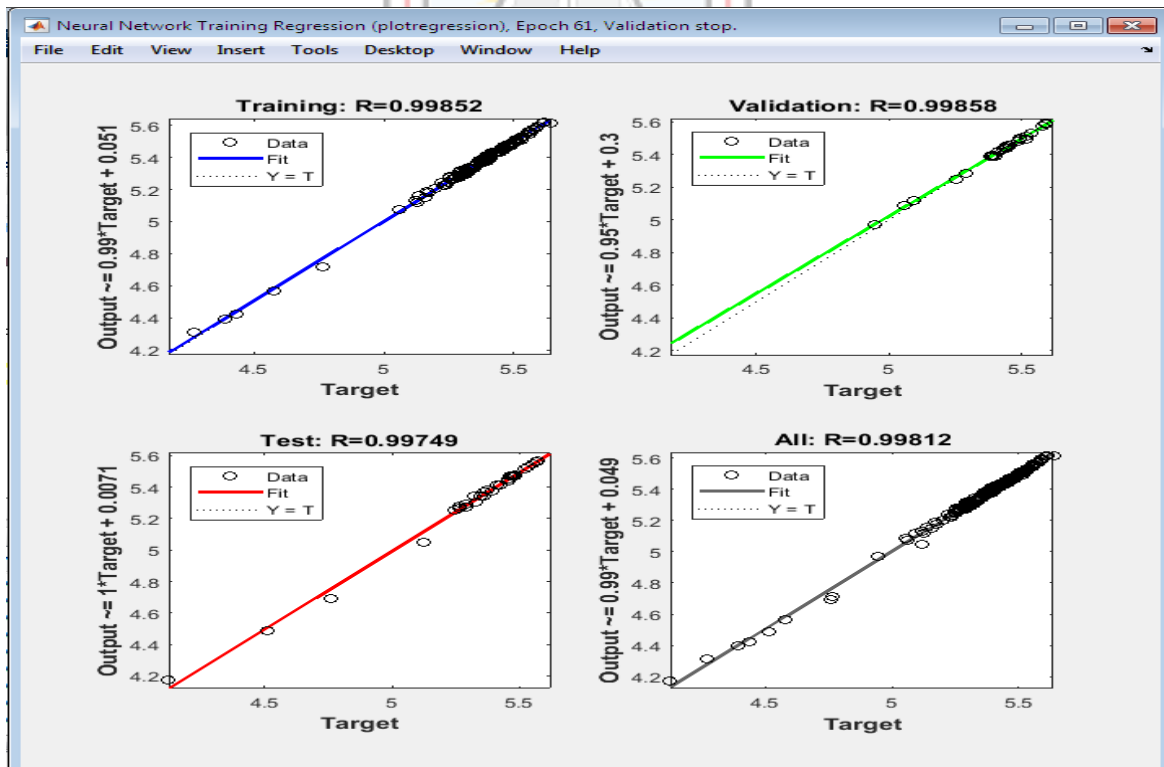


Correlation Coefficient for Network Performance, R (500 Data Samples)

MATLAB Results Using Bayesian Regularisation/Logsigmoid

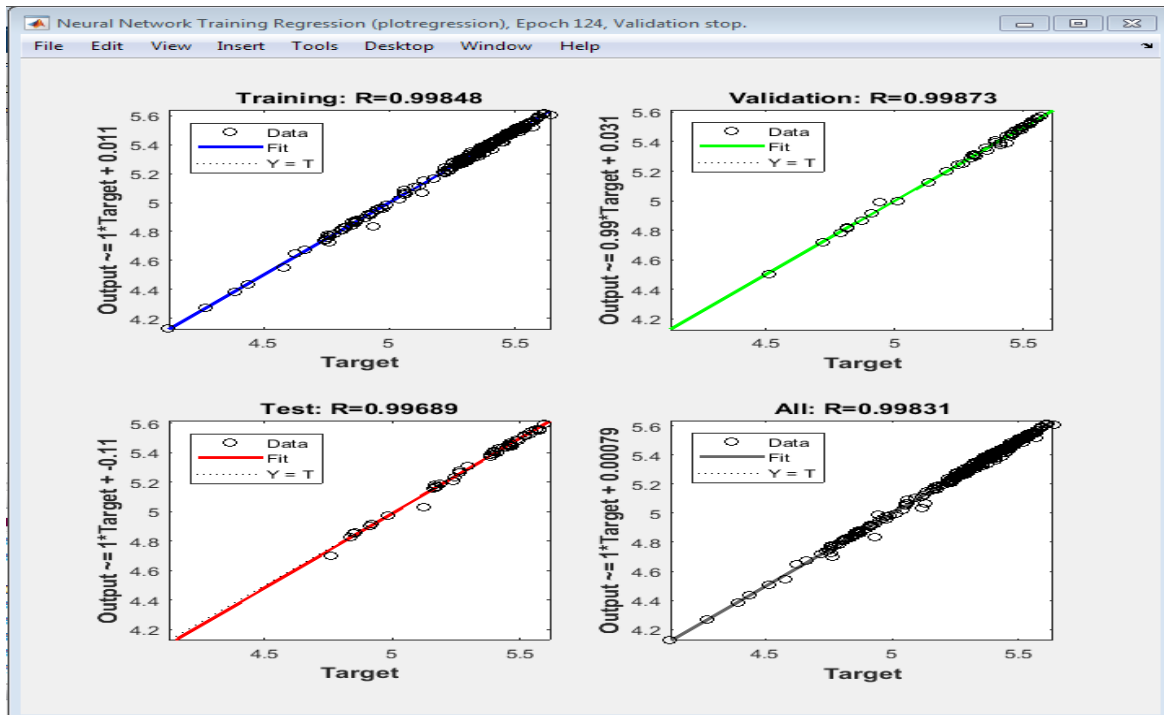


Correlation Coefficient for Network Performance, R (100 Data Samples)

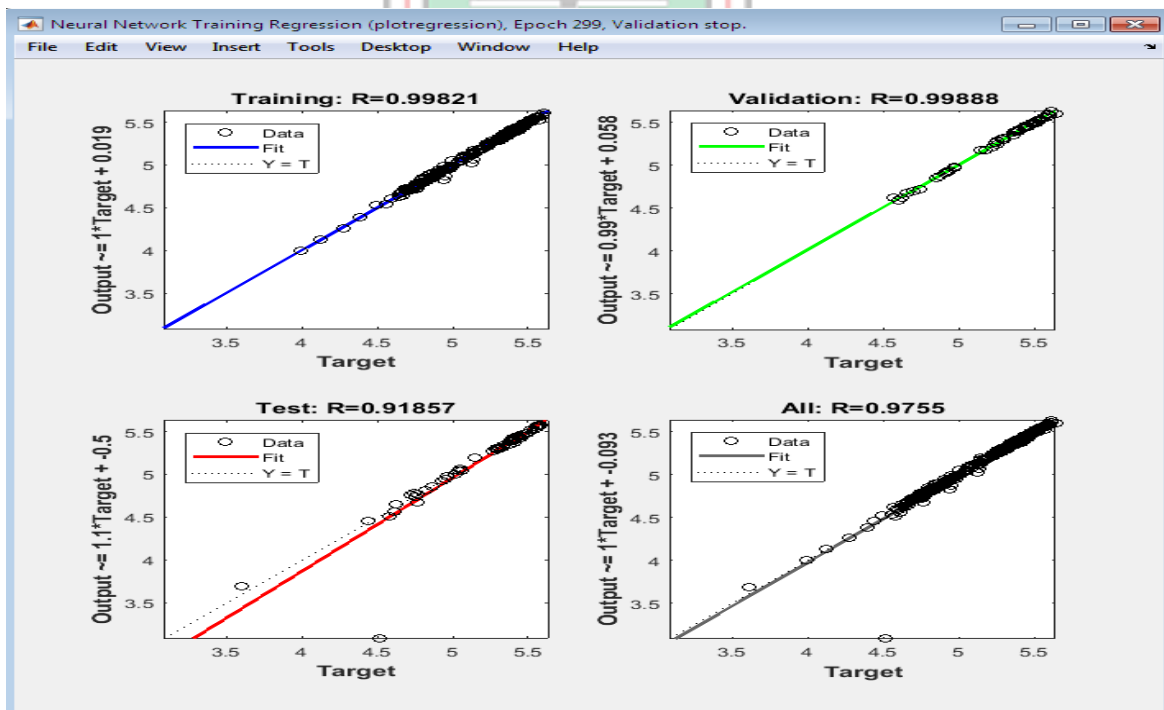


Correlation Coefficient for Network Performance, R (200 Data Samples)

MATLAB Results Using Bayesian Regularisation/Logsigmoid Cont'd

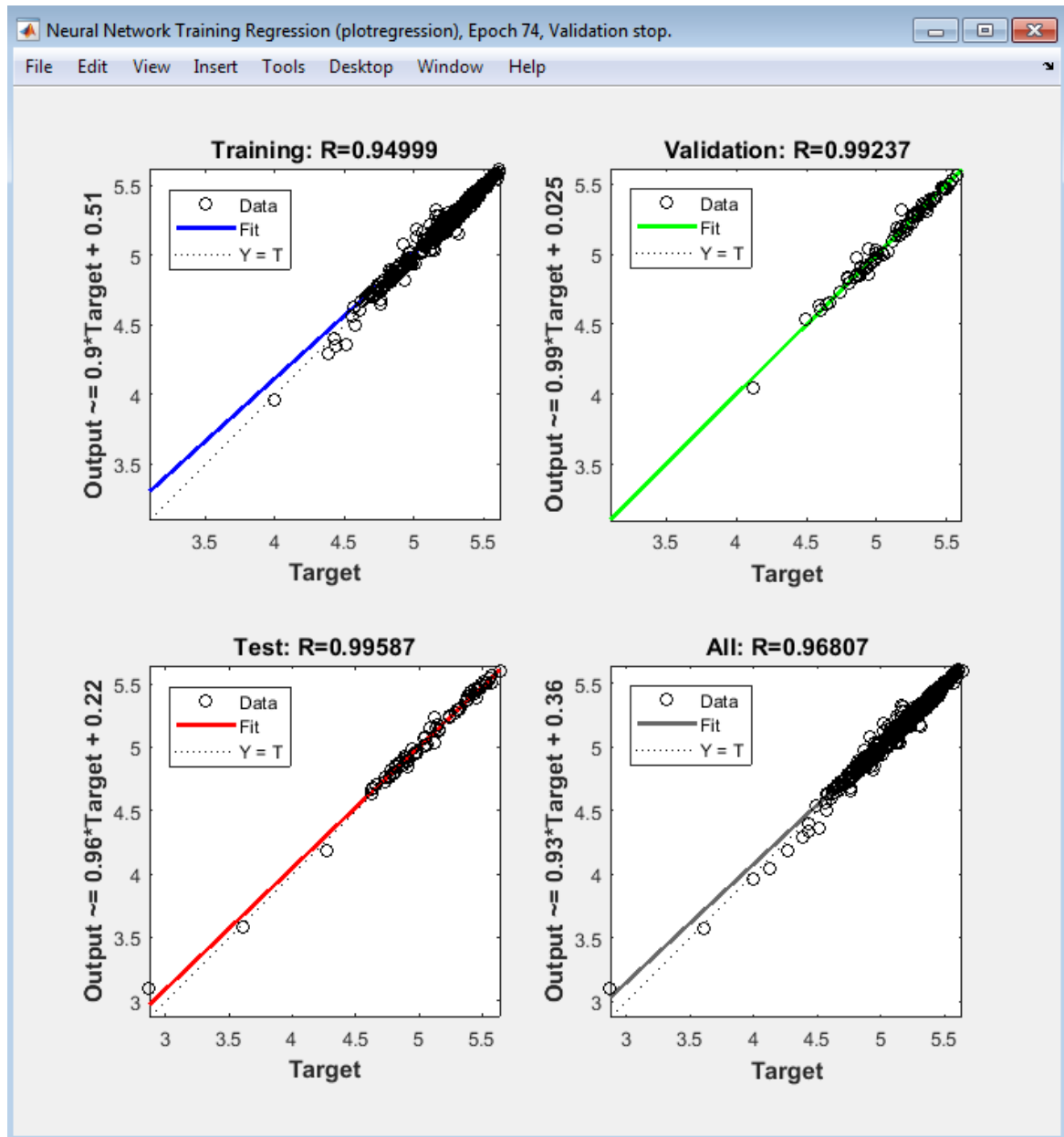


Correlation Coefficient for Network Performance, R (300 Data Samples)



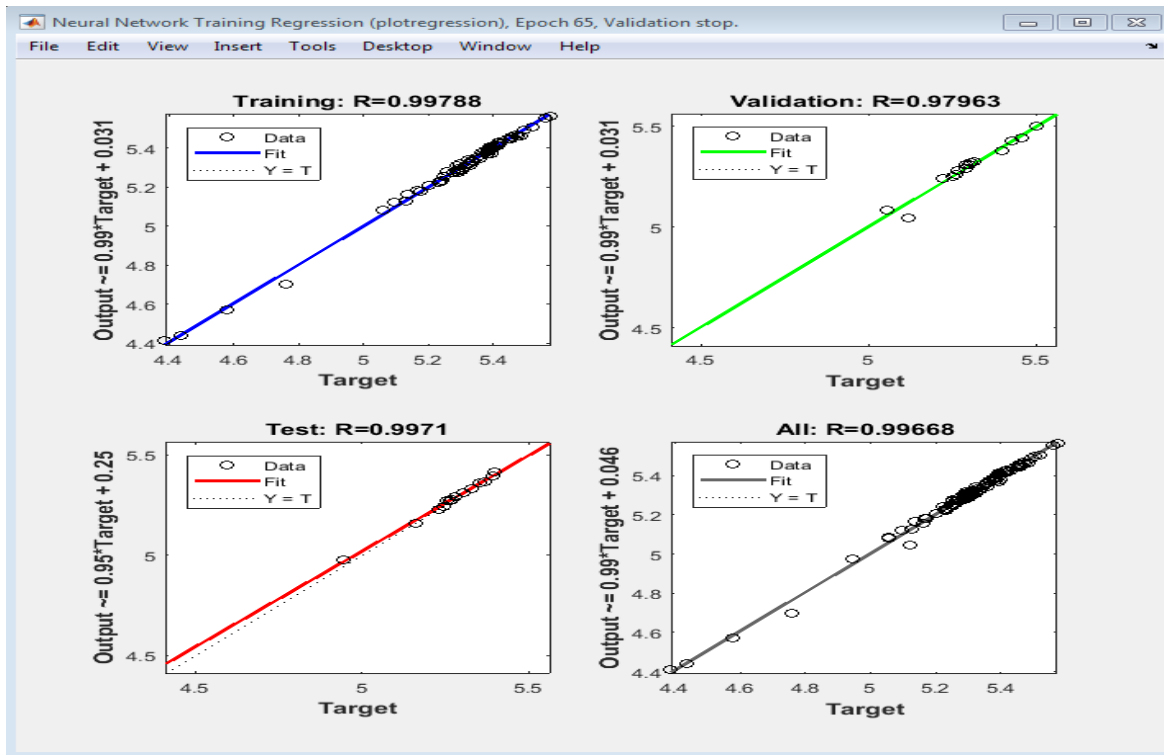
Correlation Coefficient for Network Performance, R (400 Data Samples)

MATLAB Results Using Bayesian Regularisation/Logsigmoid Cont'd

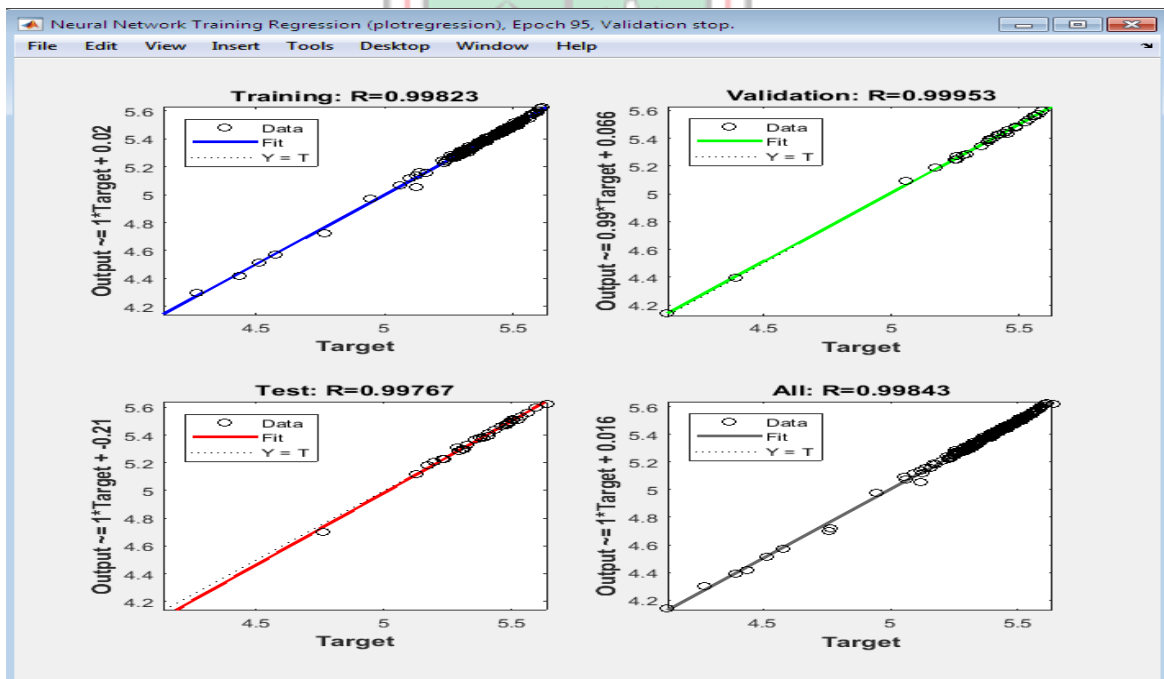


Correlation Coefficient for Network Performance, R (500 Data Samples)

MATLAB Results Using Bayesian Regularisation/Tansigmoid

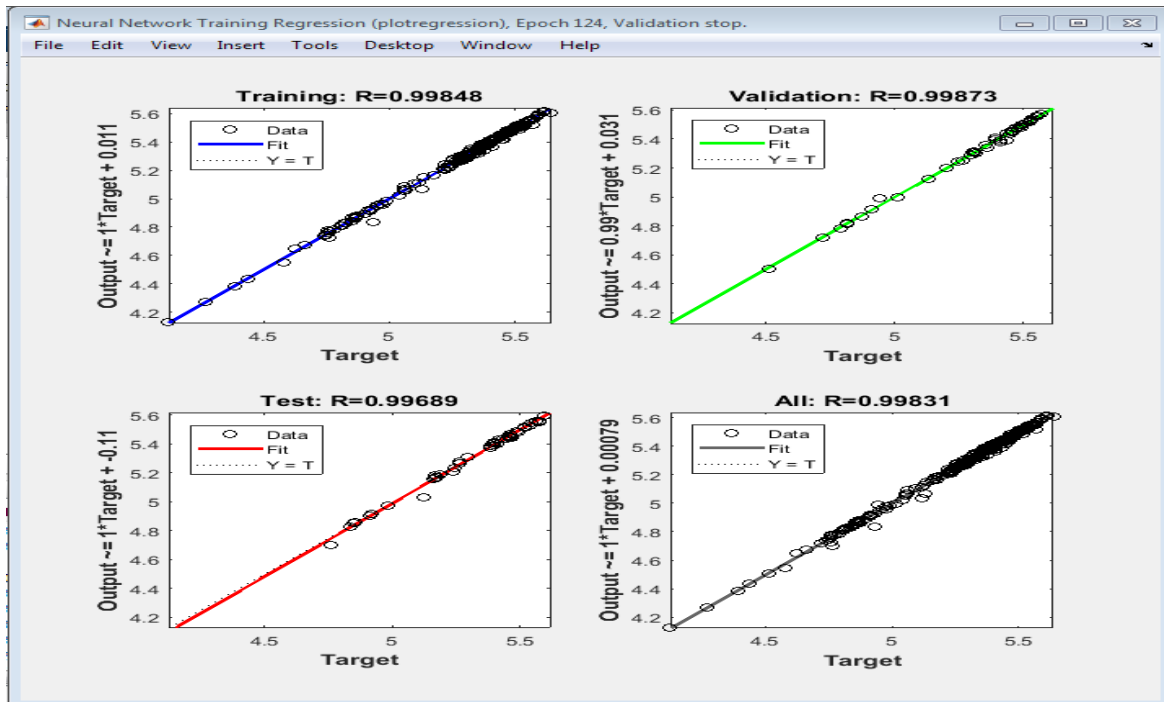


Correlation Coefficient for Network Performance, R (100 Data Samples)

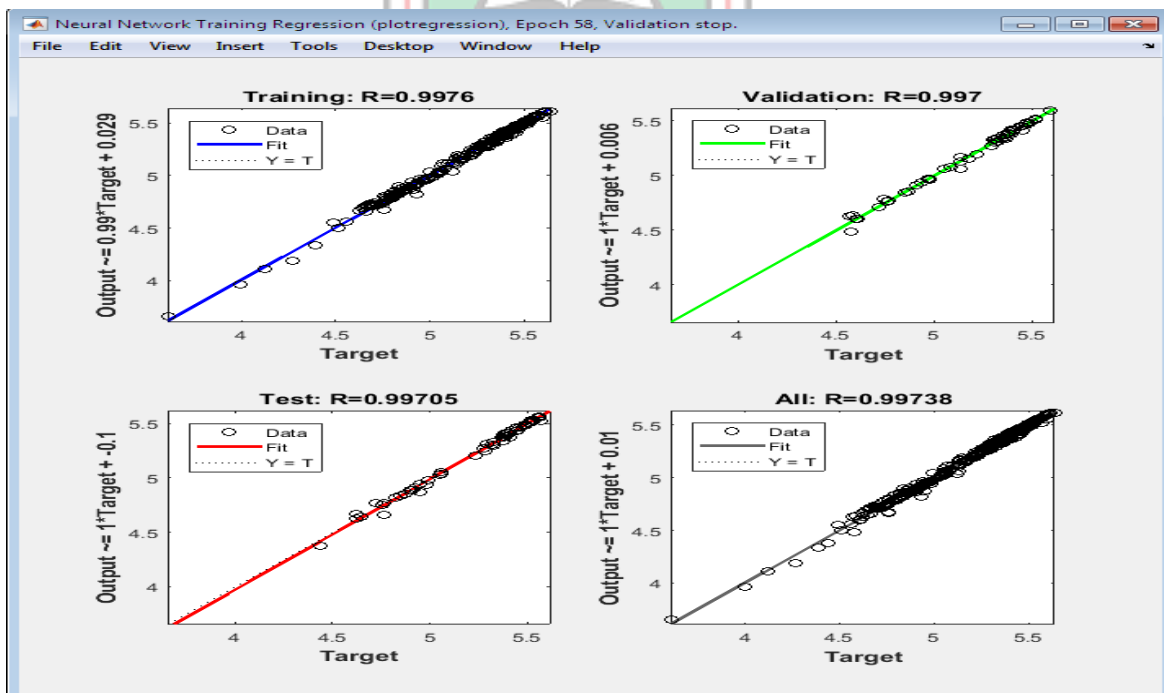


Correlation Coefficient for Network Performance, R (200 Data Samples)

MATLAB Results Using Bayesian Regularisation/Tansigmoid Cont'd

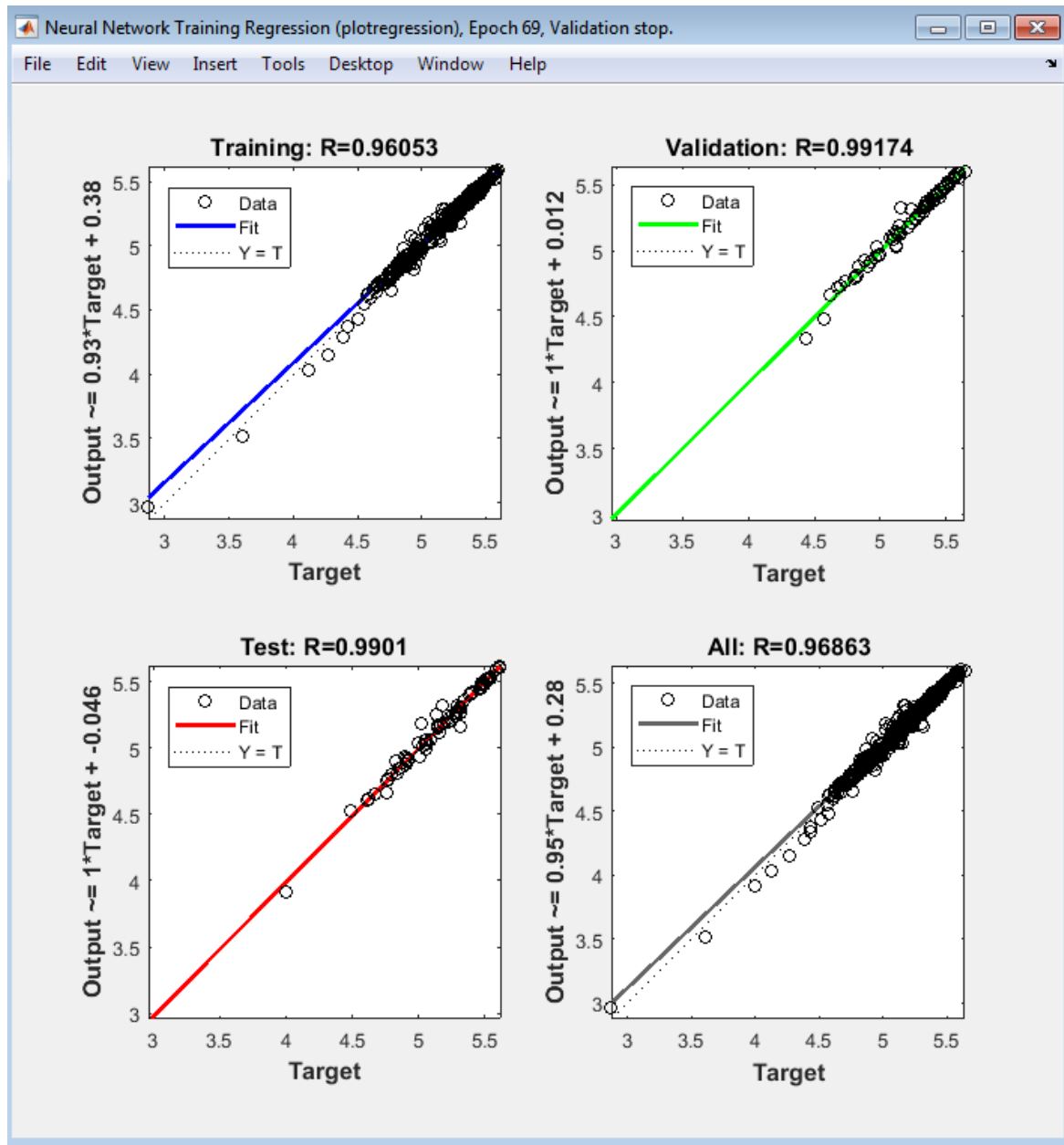


Correlation Coefficient for Network Performance, R (300 Data Samples)



Correlation Coefficient for Network Performance, R (400 Data Samples)

MATLAB Results Using Bayesian Regularisation/Tansigmoid Cont'd



Correlation Coefficient for Network Performance, R (500 Data Samples)

Index

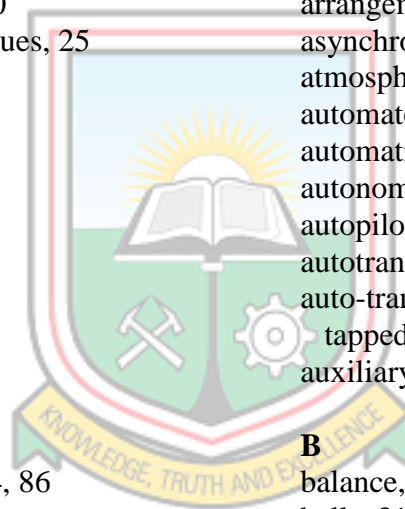
A

Abnormal heavy foaming, 76
AC (Alternating Current), 6–7, 11, 23, 35, 133, 135–40
 smooth progressive, 64
AC drive system, 48
AC induction motors, 48
action, breaking, 36
activation, 88
 applying, 88
activities, desired, 44
AC voltage controller, 20
adaptive channel equalizer, 45
adaptive nature, 42
addition, 1, 44, 48, 50, 79, 95
 non-symmetrical, 28, 30
Advanced control techniques, 25
agitator, 66, 133, 137–38
air circuit, 54
 external, 54
 internal, 54–55
 fundamental, 36
air gap flux density, 31
air gap length, 30–31
Air release capability, 73
alarm, 59, 62
alarm annunciation, 59
algorithms, 47–49, 91
 backpropagation, 42, 44, 86
 clustering, 42
 levenbergmarquardt, 50
 novel transform demodulation, 49
 propagation, 43
Alternating Current
 . *See* AC
 asynchronous, 6
amplitude, 24, 41
 first harmonic, 41
 variable-frequency-fixed, 23
analysis
 artificial neural network model, 106
 chemical product design, 46
 chip failure, 45
 computer chip quality, 46
 corporate financial, 46
 credit line use, 46
 external magnetic field, 41

 machine maintenance, 46
 regression, 101
 root-cause, 49
 spectral, 47
 statistical, 90
 welding quality, 46
anti-corrosion, 64
antifriction, 62
applications, 38, 42, 45, 49, 64, 66, 108, 110
 commercial, 6, 45
 real world, 49
 sensitive, 26
 speed, 19
 vapour compressor, 49
applied size, 106
applied voltage, 13, 17, 19–20, 22–24
approximation affairs, 101
arrangements, winding, 21
asynchronous machines, 11, 50, 109
atmospheric humidity, 58
automated information services, 46
automatic bond, 46
autonomous vehicles, 46
autopilot enhancements, 45
autotransformer, 15, 18
auto-transformer, 18
 tapped, 18
auxiliary limit switches, 65

B

balance, 22–23, 153
balls, 31–32
 dissected, 31
 lubricated, 62
 rotating, 31
ball tracks, 32
bar breakages, 48
bars, 10, 27, 64, 71
 aluminium, 9
 broken, 27
 insulated copper, 64
 multiple, 27
 short-circuited, 11
 side, 27
bearing components, 63
bearing damage, 26
bearing degradation, 39
bearing endshields, 77
bearing failure, 2, 31–32, 34, 50, 139

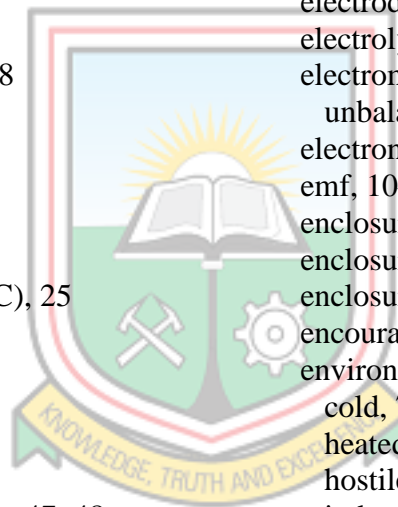


- bearing faults, 2, 27, 31, 40
 - bearing housings, 63, 76–77
 - bearing insulation, 77
 - bearing lubrication, 51
 - bearing material, 31
 - bearing oil, 73
 - bearing parts, 64
 - bearing pedestals, 77
 - bearings, 26, 31–32, 40, 51, 62–64, 70–71, 73, 76, 78, 138
 - roller type, 62
 - bearing seals, 63
 - bearing shells, 76
 - bearing shield, 49, 110
 - bearing temperature, 32, 48
 - bearing wear, 26
 - bearing wear faults, 48
 - biases, 87, 91
 - blast, strong, 58
 - block, decision-making, 95
 - blockage, accidental, 65
 - blocked air passages, 78
 - bolts, 58, 77
 - machine/bag, 51
 - BR (Bayesian Regularization), 50, 96, 98–99, 101–3, 105, 109
 - Breast cancer cell analysis, 46
 - broken rotor bar (BRBs), 26–27, 41, 47, 49–50, 108–9
 - broken rotor bars, 26–27, 41, 47, 49
 - broken rotor bars detection, 47
 - brush arrangement, 60
 - brushes, 6, 10, 56–60, 77–79
 - earth, 77
 - fixed, 55
 - new, 59
 - slip-ring, 21
 - brush gear, 57–58, 77
 - brush grade, 58
 - brush-holder frames, 60
 - brush-holders, 58–60, 79
 - brush pressure, 60
 - correct average, 60
 - brush pressure Quarterly, 77
 - brush removal, 58
 - brush wear, 57, 59
 - normal, 56
- C**
- cables, 68, 77, 79
 - cage, 9, 27
 - carbon blocks, 55
 - carbon brush, 55, 57, 59–60
 - carbon brush wear measurement, 57
 - carbon dust, 56, 58
 - Carbon in Leach. *See* CIL
 - cash forecasting, 45
 - cause damages, 34, 50
 - cause noise, 28
 - cause ripples, 28
 - cause turn-to-turn, 34
 - change, 1, 3, 10, 21, 37, 44, 72, 75, 77, 95, 136, 139
 - air gap flux, 21
 - speed, 18
 - state, 44
 - change AC, 136
 - circuit breakers, 34
 - circuit chip layout, integrated, 45
 - circuits, 1, 13, 23, 47, 71
 - electronic, 23
 - elution, 1
 - low pressure, 71–72
 - milling, 1, 51
 - solid-state, 20
 - stator magnetic, 10
 - tailings, 1
 - circular arc, complete, 60
 - circumference, 58
 - classes, main, 9
 - classification, 29, 39, 44–45, 50, 109
 - based fault, 80
 - vowel, 46
 - classifier, 49, 108
 - sonar, 45
 - clean oil-free cloths, 58
 - clean pumping, 70
 - cloths, small, 58
 - coil insulation, 34
 - coil movement, 34
 - coils, 7–8, 22–23, 33, 61
 - resulting, 34
 - combination, 22, 30, 33, 47
 - commercial success, 45
 - common-mode currents, 50
 - compartments, isolated, 64–65
 - complex post processing decision, 48
 - complex wavelets, 40–41
 - complicated problems, 101
 - components, 5, 7, 36, 39, 71

- current vector, 40
 - extracting signature frequency, 49
 - fault signature frequency, 49
 - main, 26, 79
 - winding, 61
 - compressed air, 58
 - computational models, 42
 - parallel, 42
 - concentric cylinders, 64
 - concomitant production losses, 6
 - condensation, 79
 - condition monitoring, 38–39
 - online, 39
 - on-line, 6
 - Condition monitoring and fault detection, 39
 - condition monitoring devices, 4
 - conditions, 11–12, 20, 24, 27, 35, 38, 63, 77
 - dynamic, 25
 - faulty, 102–3, 105
 - loaded, 20, 37
 - low error, 101
 - nominal, 47
 - normal, 40, 75
 - normal running, 17
 - site, 75
 - steady state, 50
 - surface roughness, 60
 - unloaded, 48
 - conductors, winding, 33
 - configuration, 92
 - confusion plot, 102
 - connection changes result, 21
 - connections, 10, 21, 23, 44, 77, 87
 - bolted, 63
 - constant horse-power, 23
 - constant torque, 23
 - constant-torque, 21
 - correct, 78
 - iron cascade, 48
 - series, 10
 - star, 17
 - terminal, 23
 - winding, 21, 78
 - connections result, 22
 - connection weights, 86
 - conservation measures, 79
 - constant, 7, 11, 18, 20–21, 24
 - maintained, 24
 - constant amplitude, 11
 - constant frequency source, 7
 - constant-horsepower type, 21
 - constant load torque, 51
 - constant torque, 20
 - constant torque type, 20
 - construction, 7–9, 19, 50, 52, 54–56, 66–67
 - consumables, replacing, 75
 - contamination, 32, 63
 - contamination display, 71–72
 - control cables, 69
 - control connections, 77
 - control scheme, 23
 - cooler tubes, 64
 - cooling, 51, 54, 66, 78
 - cooling air inlet, 79
 - cooling fan blades, 9
 - cooling fans, 54
 - copper, single, 9
 - copper conductor, 34
 - core, 8, 14
 - cylindrical iron, 8
 - dual, 48
 - core temperature, 39
 - corrosion, 32, 64
 - corrosive fluids, 32
 - Couple unbalance rotor, 29
 - coupling unbalance, 30
 - crawling, 26, 36–37
 - crawling effect, 37
 - credit application evaluators, 45
 - criterion, 101
 - important, 58
 - curable resin, 61
 - current density, 58
 - low, 65
 - curves, 18–19, 24
 - speed torque, 19
- D**
- damage, 27–28, 56, 61, 73
 - critical, 36
 - mechanical, 61
 - physical, 31
 - data division functions type, 154–59
 - data mining, 45
 - defects, 26, 40, 75
 - foundation, 26
 - delta, 17–18, 78



- desired output vectors, 45
 - detectability, 48
 - detection, 6, 48, 50, 106
 - false, 102
 - misfire, 45
 - online failure, 95
 - online half-broken-rotor, 48
 - detection efficiency, 102
 - deviations, 40, 75
 - possible, 75
 - devices, 45–46
 - rotating, 6
 - semiconductor, 20
 - diagnosis, 40, 47–48, 95, 108, 110
 - correct, 48
 - incipient BRB, 50
 - diagnosis procedure, 47
 - diagnostics, based, 49
 - dielectric, 61
 - lesser extent, 61
 - digital signal processor, 48
 - direction, 11, 36, 78
 - current, 23
 - given, 22
 - opposite, 36
 - single, 78
 - direct torque control (DTC), 25
 - dirt, 32, 73
 - dirt deposit, 58, 75, 77
 - dirt deposit Quarterly, 77
 - discolouring, 63
 - disconnect, 34, 76
 - discrete wavelet transform, 47–48
 - displacement, 64–65
 - dissipation, 20
 - heat, 35, 66
 - dividerand, 154–59
 - domain, wide, 43
 - downed line, 35
 - down important operating quantities, 75
 - downtime, 38–39
 - long, 38
 - unscheduled, 38
 - drive breakdown, total, 26
 - duty cycles, heavy, 6
- E**
- eccentricity, 29, 41
 - dynamic, 30
 - eccentricity faults, 40
 - edit network architectures, 91
 - effectiveness, 95
 - Effect of rotor mass unbalance, 30
 - effects
 - ageing, 61
 - small, 26
 - special, 46
 - electrical faults, 49, 107
 - electrical induction motors, 4–5
 - electrical interlock, 65
 - electrical motors, 1, 38
 - electric motor-Fuel Farm, 138
 - electric powers, instantaneous, 47
 - electrode arrangement, 65
 - electrodes, 64–65
 - fixed, 64
 - moving, 64–65
 - electrodes return, 65
 - electrode worm screw, 69
 - electrolyte, 64, 66
 - electromagnetic pull, 28
 - unbalanced, 28
 - electronic speed controller, 65
 - emf, 10–11, 23
 - enclosure, 68–69, 79
 - enclosure IP, 76
 - enclosure protection, 69
 - encouragement, iv
 - environment, 44
 - cold, 72
 - heated, 72
 - hostile, 35
 - industrial, 32
 - numerical computing, 91
 - working, 6
 - equilibrium, new, 44
 - equipment
 - auxiliary, 5, 79
 - portable measuring, 77
 - protective, 74
 - rotary, 6
 - special, 29
 - equipment failure, 35
 - equipment manual, 78
 - equipment set-up, 41
 - equivalent circuit, 13–14, 24
 - exact, 24
 - error minimisation, 81
 - estimation, 90, 110
 - fault severity, 41



- homogeneity, 50, 109
 - rotor flux, 47
 - estimation technique, 47
 - examination, bearing oil, 73
 - excessive line, 37
 - excitatory, 42
 - experience, 28, 75
 - explosion proof, 7
- F**
- failure avoidance schemes, 39
 - failure prediction, 3, 5, 39, 47, 80, 104
 - aided, 3
 - use of Artificial Neural Networks for, 5, 50
 - failure prediction methods, 39–40, 110
 - failure prediction networks, 106
 - failures, 2, 5, 27, 33, 38–39, 48–49
 - catastrophic, 4, 6
 - complete, 40
 - maximum validation, 92
 - premature, 38
 - recurring, 50
 - winding, 26
 - failures.The conclusion, identifying, 5
 - failure tracking, 39
 - false detection (FD), 102
 - fan rotation, 78
 - fans, 9, 18–19, 54, 73, 78, 140
 - installed, 51
 - fault conditions, 6, 39, 75, 102
 - fault detection, 39–41
 - incipient, 26, 41, 49
 - fault detection and diagnosis, 40, 110
 - fault detection range, 106
 - fault detection research, 49
 - fault diagnosis, 38, 40, 109
 - incorrect, 48
 - fault isolation, 49
 - fault prediction, 6
 - embedded systems, 48
 - faults, 2, 5–6, 25–26, 29–35, 37–41, 47–50, 74–76, 78, 106
 - air-gap eccentricity, 28
 - broken bar, 28
 - coil, 33
 - detecting, 49
 - diagnosing, 49
 - drive, 78
 - earth, 26
 - electromechanical, 36
 - experience, 26
 - external, 25–26
 - ground, 33–34
 - incipient, 38, 49
 - inter-turn, 47
 - open-circuit, 33–34
 - possible, 76
 - short circuit, 49
 - short-circuit, 26, 33
 - solving, 73
 - turn-to-ground, 34
 - turn-to-turn, 33
 - fault severity, 106
 - fault shaft rotational axis, 29
 - Faults in induction motors, 26
 - Faults in laminations and frame of stator, 32
 - FD (false detection), 102
 - feature, characteristic, 61
 - feature extraction, 45, 47, 81
 - feedback loops, 44
 - field, 6, 11–12, 45
 - four-pole, 23
 - pole air-gap, 23
 - rotating, 7, 10–12, 41
 - rotating stator, 11
 - filter, 71–73, 79
 - air, 71
 - filter element, 71, 73
 - filter monitor, 63
 - flow
 - generous, 59
 - restricted, 32
 - unidirectional, 43
 - flow-meter, 72
 - flux, 10–11, 22–24, 36
 - fundamental, 36
 - leakage, 39
 - peak, 23
 - rotating, 11
 - flux density, 11
 - flux level, 20, 24
 - flux lines, 22–23
 - emanating, 23
 - foaming, 73
 - forced circulation, 66
 - forces, 11–12, 34, 40, 74, 84
 - abnormal magneto motive, 37
 - brush-holder spring, 60

electromotive, 10
 high, 74
 induced electromotive, 23
 large centrifugal, 27
 foreign matter, 76
 forklift robot, 46
 formation, 43
 foundation blocks, 51
 four-pole arrangement, 23
 four-pole structure, 23
 fracture, 27, 32
 fault characteristics, 47
 sideband, 28
 switching, 75
 variable, 34
 frequency spectrum, 40
 fresh air, 59
 friction, 12, 31–32, 40
 friction surfaces, 40
 full load current (FLC), 16, 64
 Functional Location, 133–40
 functional relationships, 45
 functions, 40–43, 88–89, 91–92
 activation, 42–43, 88
 network train, 92
 sigmoid, 43
 threshold, 42
 trainParam train, 92
 weight/bias learning, 86
 weights/bias learning, 91

G

gear, motor shaft, 137
 gear pump, 71, 73
 gear teeth, 73
 generator, 55, 107
 genetic algorithm, 47, 108
 geometrical axis, 28
 glycerine, 71
 neutral, 71
 good power dissipation capability, 21
 gradient, 102, 105
 minimum performance, 92
 graphite forms, 58
 grease, 31–32, 62, 78
 fresh, 78
 grease chamber, 78
 grinding, 51, 58, 60
 grinding process, 60
 ground, 59–60

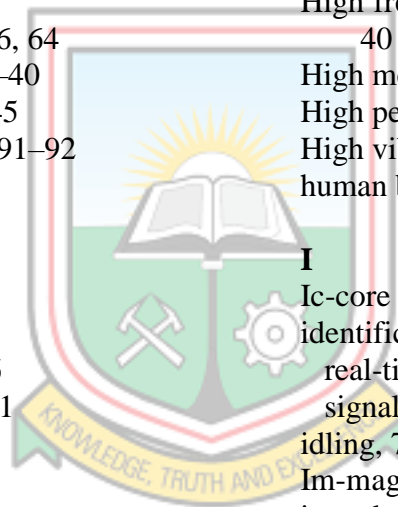
axial, 78

H

handstoning, 58
 hardlim, 158–59
 harmonic content, high, 37
 harmonic contents, 41
 harmonic fluxes, 36
 harmonic fluxes rotate, 36
 harmonics, 36–37, 41
 air gap flux density, 31
 predominant, 36
 harmonic vibration spectrum, 40
 heat, 35
 excess, 71
 heat exchanger, 66, 68, 71
 air-water, 76
 hidden layer size, 106
 High frequency components of vibration, 40
 High mechanical vibration, 34
 High performance aircraft autopilots, 45
 High vibration and wear, 32
 human brain, 42

I

Ic-core loss component, 14
 identification, 4, 106
 real-time particle, 46
 signal/image, 45
 idling, 78
 Im-magnetising component, 14
 impedances, 14
 implementation, 4, 91, 95
 implication, 5
 impregnation, 61
 Improvement, 39
 incipient, 49
 early, 50
 inclined fan blades, 78
 independent variables P_i , 86
 induced emf, 11, 23–24
 coiled, 22
 induction, 12, 108
 electromagnetic, 6, 10
 induction machines, 14–15, 18–19, 21, 23, 40, 48, 108
 line-operated, 47
 special three-phase, 47
 induction motor condition monitoring, 41



induction motor failures, 2–3, 25, 31, 38
 induction motor faults, 26
 induction motor model, 49
 induction motors, 1–2, 4–8, 10–18, 25–28, 30–32, 35–38, 41, 47–50, 79, 95, 104, 106–10
 based fault classification of, 80–81
 burnt, 1
 failure prediction of, 41, 50
 large, 10
 large three-phase, 10
 model based diagnostics and prognostics of three-phase, 49, 109
 operating, 2
 phase, 50
 polyphase, 6
 single phase, 105
 single-phase, 48–49
 slip-ring, 6, 9
 squirrel-cage, 6, 9, 47
 squirrel-cage type, 37
 starting three-phase, 15
 wound rotor, 56, 76
 induction motor stator, 49
 inductive reactance, 24
 industrial process, 38
 real, 50
 Industrial processes, 26
 industry, 6, 38, 50
 inefficient proposition, 20
 Inhibitor content, 73
 inhibitory, 42
 Initialization of weights, 81
 inlet pipe, 71
 input changes, 44
 input data, 39, 84, 91
 new independent, 42
 input excitation, 23
 input features, 49
 input function, 42
 input layer, 43
 input object, given, 43
 input parameters, 5
 measurable, 48
 baseline, 42
 obtained neural, 42
 rotor power, 14
 total, 44
 input units, 42
 input value, 88
 input variables, 43, 87
 input vector, 44, 86, 154–59
 input vectors, given, 44–45
 inspection, 38, 63, 75, 79
 extra non-scheduled, 75
 periodical, 64
 inspections, regular, 26, 79
 installation, 6, 32, 68
 installation defect, 26
 installations, heavy-current, 74
 Install New Mill Lube Pump Motor, 138
 instructions, 57, 78
 following, 76
 instrumentation devices, 5
 instruments, 75
 insulated shells, 63
 insulating paths, 57
 insulation, 33–35, 37, 58, 61
 bearing shell, 63
 best, 35
 carrier bolt, 58
 contaminate, 35
 stator inter-turn, 48
 insulation breakdown, 26
 insulation defects, 39
 insulation degradation, 49
 insulation life, 35
 Intelligent systems for motor failure predictions, 5
 INTERNAL AIR, 143
 Internal Faults, 25
 Intertank Screen Cil Tank, 135–36
 Intertank Screen Motor, 135
 inter-turn, winding, 49
 inter-turn failure, 105
 inter-turn fault detection, 50, 109
 intervals, 43, 57–58
 bounded, 43
 recommended maintenance, 75
 intervention, 75
 Inverse Approach for Interturn Fault Detection in Asynchronous Machines, 109
 Inverter-Driven Induction Motor, 107
 inverters, 23
 pulse width modulation, 50
 isolation, 64
 galvanic, 51
 Iterates gradient type of loop, 154–59
 iterations, 102, 105



K

knocking sounds, 77
knowledge, 47, 86
 expert, 47
knowledge discovery, 45
kV, 4, 80, 106
kV SAG Mill, 106
kW, 1, 52, 54–56, 66–67
KW Electrical Motor Change, 139
kW pebble crusher, 1

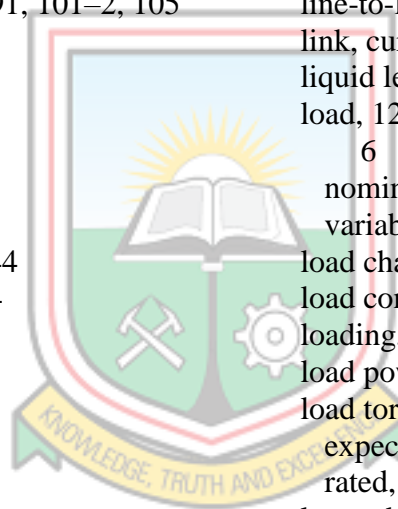
L

laminations, 32
 punched, 8
 stacked, 8
language, spoken, 46
Large currents flow, 11
layers, 42–44, 56, 86, 91
 hidden, 42–43, 86–87, 91, 101–2, 105
 lubrication, 40
leach, 1
leakage, 64, 71
leakage incl, 63
leakage paths, 56
leaks, 64, 72
learning, reinforced, 43–44
learning algorithm, 42, 84
 supervised, 44
learning by example, 42
learning rate, 92
Lenz's law, 11
level
 bearing vibration, 39
 electrode, 69
level switch, 72
Levenberg-Marquardt back-propagation, 92
Levenberg, 100–101, 109
levenberg-marquardt, 50, 96, 101, 103–4, 154–55
Levenberg Marquardt, 49
Levenberg-Marquardt (LM), 5, 50, 89, 92, 96–98, 101–6, 154–55, 158, 160–65
Levenberg Marquardt Algorithm, 109
Levenberg-Marquardt Algorithm, 89, 103, 106
Levenberg-Marquardt and Bayesian Regularisation, 5, 101
Levenberg-Marquardt and Bayesian Regularization algorithm, 102

Levenberg-Marquardt/Logsigmoid, 160–62
Levenberg-Marquardt/Tansigmoid, 163–65
Levenberg-Marquardt Training Algorithm, 96, 101–2, 105–6, 158
Levenberg-Marquardt training algorithm and tansigmoid activation function, 105
LH001-Liner Handler Hydraulic Pump Motor, 137
life
 limited, 62
 long electrode, 65
 long running, 70
life calculation, 62
life expectancy, 72
line-to-ground, 34
line-to-line, 34
link, current, 55
liquid levels, 75
load, 12, 19–20, 31, 35, 64, 78, 101, 105–6
 nominal, 50, 101
 variable resistance, 21
load changes, 18
load condition, 49, 102
loading, nominal, 60
load power, 102
load torque, 16, 19–20
 expected, 15
 rated, 51
loan advisor, 46
localisation, 48
locations, 27, 54, 59, 75
 exact, 106
locus, 40
logsig, 89, 100, 154, 156
loop, 154–59
low-cost Field-Programmable Gate Array, 48
low voltage (LV), 68
lubricant, 31–32
lubricant failure, 32
lubricants deteriorate, 32
LV enclosure, 69

M

machine, 6, 11, 17–20, 23–24, 26, 32, 38–40, 47–48, 50, 56, 58–59, 64, 74–79



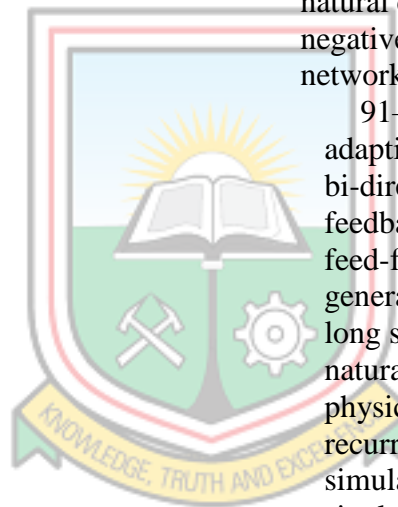
cage rotor, 20
 electrical, 40
 healthy, 48
 horizontal, 63
 large high-voltage, 61
 slip-ring, 20
 speed, 18
 machine behaviour, 50
 machine diagnosis, 46
 machine health, 32
 machine maintenance, 58, 63, 77
 machine manufacturer, 60
 machine noise, 77
 machine vision, 45
 magnetic field, 11
 revolving, 11
 magnetic flux, 11
 total rotating, 11
 magnetic flux linking, rotating, 10
 magnetic pole structure, 22
 magnetic valve, 71
 magnetizing, 15, 20
 magnetizing branch, 20, 24
 magnetizing inductance, 24
 magnitude, 10, 12, 28, 36, 84
 equal, 11
 magnitudes
 large, 84
 small, 84
 mains, 18, 76
 maintenance, 10, 32, 38, 63–64, 69, 72,
 74–76, 79
 breakdown, 38
 condition-based, 38
 engineering, 1
 fixed-time, 38
 low, 25, 38
 planned, 76
 preventive, 39
 maintenance action, 38
 maintenance cards, 74
 maintenance cost, 38–39
 current, 1
 high, 5
 maintenance department, 1
 maintenance investment, 74
 maintenance plan, 57–58, 63, 76
 maintenance plans, effective, 40
 maintenance schedule, 39
 maintenance work, 74
 actual, 75
 management, 40, 46
 manipulator controllers, 46
 manufacturing, 6, 46
 manufacturing defect, 27–28, 30
 unavoidable, 40
 manufacturing factors, 6
 manufacturing process control, 46
 market forecasting, 46
 mass unbalance, 26, 29–30
 induction motor rotor, 30
 matrix manipulation, 91
 maximum oil temperature, 71
 maximum temperature contact-
 thermometer, 71
 maximum torque capability, 24
 measured signal spectrum, 47
 Measure length of brushes, 57
 measure mains voltage, 78
 measures, special, 64, 78
 Measuring transducers, 51
 mechanical abnormality, 47
 Mechanical Faults Diagnostic, 108
 mechanical load, 38
 excessive, 38
 Mechanical-related faults, 26
 Medium & Heavy Medium, 73
 medium sizes, 48
 medium voltage (MV), 68
 method analyses, 40
 method of repair, 61
 microprocessor, 95
 microprocessor implementation, 95
 mode, 24
 learning, 88
 motoring, 18
 model, 4–5, 43, 47, 49, 80, 89, 101
 developed, 89
 neural network forecasting, 43
 neurobiology, 42
 new faulty, 47
 nonlinear, 47
 pretrained, 91
 statistical, 42
 statistical regression, 42
 model building, 43
 modelling
 computer, 4
 dynamic, 46
 function approximation/times series, 45

- nonlinear, 45
- reservoir, 46
- moisture, 76
 - external, 26
- money, 38, 46
- monitoring
 - short-circuit, 75
 - symptom, 39
- monitoring brushes, 59
- monitoring fault, 47
- monitor training progress, 91
- mortgage screening, 46
 - asynchronous, 26
 - burnt, 1, 136–37, 139–40
 - cage, 16
 - change burnt pump, 137
 - delta-connected, 35
 - electrode control, 65
 - faulty, 40–41, 95
 - geared, 65
 - healthy, 28, 40–41, 95
 - industrial, 6
 - noisy, 136
 - rotor-outer surface, 26
 - running, 74
 - servo, 65
 - slip-ring, 15
 - small, 16
 - squirrel-cage, 15
 - starter, 66
 - starter agitator, 66
 - switch fan, 74
- motor bearings, 50, 70
 - three-phase induction, 50
- motor condition, 82, 88, 95
 - faulty, 102
 - healthy, 102
- motor failure predictions, 5
- Motor failures, 26, 39
 - complete, 26
 - modelling induction, 101
 - predicting SAG Mill, 101
 - prediction of SAG Mill, 101, 104
- motor faults, 47
 - diagnose, 40
- motor hums, 78
- motor idles, 78
- motor intakes, 48
- motor manufacturers, 72
- motor operation, 26

- motor overheats, 78
- motor parts, 26
- motor performance, 14
- motor power, 82
 - mill, 96
- motors downtime, 39
- motor supply, 79
- Motor vibration and noise, 37
- movability, 73
- movement, 34, 58
 - free, 77
 - relative, 11
- multilayer perceptrons, 43, 86
- Multiple faults, 26
- multivariate, 101
- MV enclosures, 68–69

N

- natural convection, 66
- negative sequence, 35
- network, 5, 42, 49–50, 80, 82, 84, 86–89, 91–92, 96, 101–3, 105–6, 110
 - adaptive, 49
 - bi-directional, 44
 - feedback, 44
 - feed-forward back-propagation, 91
 - generalised feed-forward, 50
 - long short-term memory, 44
 - natural, 42
 - physical, 44
 - recurrent, 44
 - simulate, 92, 94
 - single-neuron, 45
 - stochastic, 44
 - train, 94, 154–59
 - trained, 43, 92
- network memorizes, 89
- network outputs, 92
- network performance function, 92
- network performance plot, 102
- network response, 101
- network structure, 43
- network validation, 89
- neural networks, 43–45, 48, 81, 87, 91, 94, 108, 154–59
 - feed-forward, 86
 - forward, 43, 49, 106
 - generalized feed-forward, 86
 - layered feed-forward, 86
 - use of artificial, 5, 50

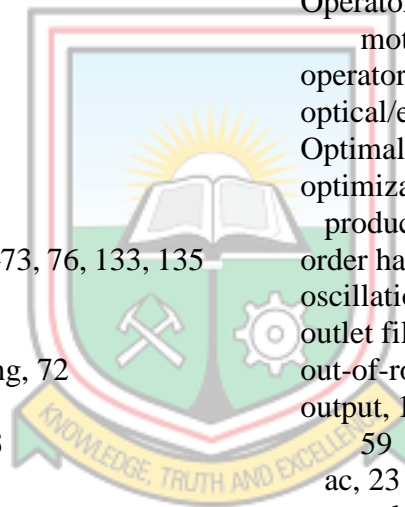


neural network software, 46
 neurons, 42–43, 86–88, 91, 101–2
 single, 86
 Neutralisation numbers, 73
 new start cycle, 65
 nodes, 42
 hidden, 43
 noise, 37, 48–49, 73, 77
 measurement, 50
 normal magnetic, 78
 noise level, 32
 noise suppression, 45
 non-linear elements, 43
 non-linear filters, 42
 non-linear mapping structure, 42
 non-parametric pattern classifiers, 42
 normalisation, 82, 84–85
 normalization, 84
 nylon slide, 65

O

object discrimination, 45
 obstructed ventilation, 34
 Occurrence of Faults, 40
 probability of, 2
 oil, 31, 46, 58, 62–63, 70–73, 76, 133, 135
 bearing lube, 76
 jacking, 63–64
 recommended lubricating, 72
 oil change, 62, 72
 oil change interval, 64, 73
 oil contamination, 62
 oil film, 76
 oil flow, 72
 oil gauge, 71
 Oil Ingress, 138
 oil leakage, 63
 oil level, 63, 71–73
 oil loss, 72
 oil rings, 63, 76
 oils, selected, 72
 oil stone, 60, 64
 oil supply system, 63, 70
 oil temperature, 71
 oil transport, 63
 Oil-water cooler, 64
 oil-water-heat exchanger, 71
 online approximators, 49
 On-line learning, 43
 Open-circuited rotor circuit, 78

operating, 18, 20, 25, 38, 47, 72, 74–75, 79
 operating characteristics, 40
 operating conditions, 38, 72, 75
 extraordinary, 75
 unloaded, 48
 operating hours, 72
 operating locations, 76
 operating personnel, 75
 operating pressure, 71
 permissible, 71
 operating reliability, 72
 operating temperatures, 62
 operational behaviour, 75
 normal, 75
 operational interruptions, critical, 74
 operation failures, 74
 operation phase, 43
 Operators and technicians of induction motors, 38
 operator/technician, 39
 optical/electrical, 63
 Optimal starting torque, 64
 optimization, 39, 46
 product, 46
 order harmonics, 36
 oscillations, 26, 30–31
 outlet filter frames, 79
 out-of-round, 60
 output, 11, 14, 42, 44, 87–88, 101–2, 154–59
 ac, 23
 actual, 88
 desired, 86, 88
 known, 43
 terminal, 68
 output data, 154–59
 output layer, 43, 87–88, 102
 output nodes, 43
 output object, 43
 output parameter, 5
 output shaft, 7
 output unit, 42, 44
 output value, 102
 overfitting, 89, 106
 overheating, 15, 26–27, 32
 overload, 26, 37–38, 75
 sustained, 34
 overloading, 76
 overload relay, 65



over/under voltage relays, 37
oxide ore, 1

P

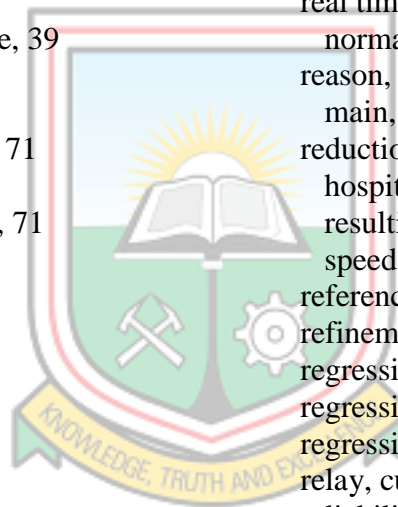
pair, 23
parameter estimation, 47
 unknown, 49
parameters, 14, 45, 47, 81, 108
 statistical, 48, 90
particles, 73
 foreign, 32
 metal, 64
 small discrete, 32
parts, 7, 27, 61
 bare, 79
 faulty, 38
 insulated, 77
 insulating, 77
 missing, 44
 necessary spare, 39
 vulnerable, 26, 61
 worn, 64
patent, initial, 6
patina, 55–56, 58
patrols, daily, 75
pattern completion, 44
pattern recognition, 44
pebble crusher crane, 137
performance, 26, 43, 50, 72, 89–90
 optimum, 104
 short-term, 90
 steady state, 25
performance function, 86, 91–92, 94
performFcn, 92
periodic inspections, 75
phase currents, 17, 40
phase fault, 33
phase-opposition, 74
phases, 4, 8, 10–11, 17, 23, 33–36, 51, 64,
 73, 80, 95, 104, 106
 healthy, 35
 learning, 43
 recall, 47
 single, 49
phase stator currents forms, 40
phase voltages, 17
phasing, single, 26, 35
Photograph, 27, 34, 51
piezoelectric accelerometer, 40
piping, 79
 associated, 79
 bearing oil, 63
 water, 64
piping flanges, 79
Plain Bearings, 63, 76
Plain bearings and oil supply unit for
 flood, 64
plant, 1, 4, 51, 74–75, 139
 metallurgical, 1
 processing, 5
plant component, 75
plant machinery, 1
plant operator, 38
plate, 69
 bearing lubrication, 62
 cable guide, 68
plotconfusion, 158–59
ploterrhist, 154–59
plotfit, 154–59
plotperform, 154–59
plotregression, 154–59
plottrainstate, 154–59
pointwise, 30, 39
pole configurations, 23
pole faces, 22
pole numbers, 21, 23
pole pairs, 21
poles, 9, 11, 18, 22–23, 36
 north, 23
pole structures, 23
Policy application evaluation, 46
polishing cloth, 77
Polypropylene compartmentalisation, 64
Polysius, 51
Portable Air Compressor, 136
position
 cracked, 27
 fitting, 70
 minimum resistance, 64
 running, 17
Position of limit mark on new brush, 59
possible aromatic content, lowest, 59
possible decision, best, 38
possible signs, 64
postprocessor, 95
power, 4–6, 8, 14, 23, 50, 80, 82–87, 95,
 101–2, 106, 113–32
 electric, 1
 electrical, 6
 measured, 90

predicted, 90
 total generated, 38
 power and temperatures, 84
 power cables entry, 68
 power factor, 20
 high, 14
 power failure, 65
 power inverter, 48
 power outputs, 7
 power supply, 25, 35, 37–38, 77, 95
 predicting failure, 4, 50
 predicting faulty conditions, 5
 Predicting Global Solar Radiation, 107
 predicting loan recovery rates, 45
 prediction, 6, 39, 43–44, 49, 101–2, 158–
 59
 currency price, 46
 paper quality, 46
 prediction method, 49
 Prediction of motor failure, 39
 pressure gauge, 71
 free glycerine, 71
 pressure gauge operation, 71
 pressure line, 71
 pressure line downstream, 71
 pressure relief valves, 71
 pressure switches, 72
 proactive recovery, 39
 procedure
 normalization, 84
 step-by-step, 73
 supervised, 43
 process, 1, 46, 74, 88
 brazing, 27
 learning, 42
 observed, 42
 testing simulation, 92
 process control, 45
 process monitor, 45
 process online, 95
 process problems, 42
 productivity, 38
 prognostics, 49, 109
 programme, common, 3
 project specifications, 79
 properties, 32, 73
 electrical, 61
 mechanical, 63
 protective measures, necessary, 74
 prototype, 106

experimental, 49
 pull, lower, 28
 pull direction, 28
 pump, 71–72, 133–34
 radial piston, 71
 pump aggregates, 71
 pump applications, 18
 pump unit, 71
 purpose System-On-a-Chip, special, 48
 pyrolysed products, 39

R

races, 31–32
 inner, 31
 races friction, 31
 rated flux levels, 20
 Real estate appraisal, 46
 real time, 101
 normal, 101
 reason, 35–37
 main, 34
 reduction, 20, 24, 26, 39
 hospital expense, 46
 resulting, 35
 speed, 23
 reference frame transformation theory, 49
 refinements, 95
 regression, 50, 90
 regression coefficient, 90
 regression line equation, 90
 relay, current, 38
 reliability, 6, 39, 48
 high, 6, 70
 repair break, 78
 representation, 41
 current vector, 41
 frequency domain, 40
 graphical, 82
 representative R-element input vectors,
 91
 representative SN-element target vectors,
 91
 resin results, 61
 resistance, 16, 20, 64
 chopper-controlled, 21
 eternal, 16
 measure insulation, 77
 residual, 65
 winding, 20



- resistance/phase, winding, 13
 resistance temperature detectors, 62
 resistance thermometer, 71
 resistors, 21
 external, 10
 external variable, 20
 respective technical data sheet, 72
 responsibility, 57
 Re-switching, 74
 return stroke, 60
 return valves, 71
 reverse phase sequence, 26
 rheostats, based, 21
 rings, 9–10, 27
 risk, 6
 increased, 56
 measuring credit, 45
 robustness, 49–50
 Rocha, 107
 rotating magnetic field, 7, 10–11
 rotation, 11, 27–28, 30, 78
 axis of, 28
 centre of, 28
 direction of, 52, 60, 78
 rotor, 2, 6, 8–13, 21, 23, 26–29, 31, 34–36, 38, 52, 55, 76–77
 blocked, 37–38
 centre of rotation of, 28, 30
 main, 62
 physical, 11
 result, 28
 revolving, 7
 secondary, 13
 slip-ring, 9
 squirrel cage, 9
 squirrel-cage, 9–11
 star-connected, 9
 stator or/and, 38
 unbalanced, 29
 weight distribution axis of, 29–30
 winding, 77
 winding Cooling air, 77
 wound, 9–10
 rotor bar failures, diagnosis of, 48, 107
 rotor bar metal fatigue, 28
 rotor bars, 9, 11–12, 26–27
 early broken, 50
 rotor body, 28
 rotor circuit, 10–11, 13, 16, 78
 rotor conductors, 10–12
 rotor construction, 8
 rotor copper losses, 14
 rotor currents, 27
 rotor eccentricity, 28, 49
 rotor faults, 2, 28, 40–41, 47
 bowed, 28
 rotor impedance, actual, 14
 rotor intersect, 29
 rotor mass unbalance, 28, 30
 rotor mass unbalance fault, 28
 rotor phase, 78
 rotor pullover, 28
 rotor resistance, 15–16, 20
 rotor resistance control, 20
 rotor result, 27
 rotor rubs, 28
 rotor side, 28
 rotor slots, 8–9, 37
 rotor starter, 74
 rotor supply, 78
 rotor terminals, 20
 rotor-to-stator misalignment, 34
 rotor type, 10
 wrapped, 6
 rotor windings, 8, 10
 rust, 64, 77
 possible, 64
S
 safety, 4, 26
 safety regulations, applicable, 74
 SAG Mill External Air Circuit Motor Rating, 54
 SAG Mill Fixed Bearing Rec Oil PumpMotor, 139
 Sag Mill Hp Pump, 138–39
 SAG Mill induction motor, 4, 80
 SAG Mill Internal Air Circuit Motor Rating, 55
 SAG Mill Liner Handler, 133
 SAG Mill Motor, 3, 5, 51–54, 61–62, 64, 70, 73–74, 76–79, 82, 84, 90, 96, 101–3, 105–6, 111–32
 healthy, 5
 kV, 5, 101, 104
 SAG Mill motor availability, increasing, 4
 SAG Mill motor condition, 86
 SAG Mill Motor Current, 83, 85
 SAG Mill Motor Current Vrs, 83, 85–86
 SAG Mill motor failures, 101, 104

Sag Mill Motor Lube System, 137
 SAG Mill Motor Rating, 52
 SAG Mill Motor Winding Temperatures, 84–85
 SAG Mill Slipring Compartment Motor Rating, 56
 SAG MOTOR, 111–32
 SAG MOTOR POWER, 111–12
 scheme, 20, 50

- neural-network based fault detection, 48

 screen captions, 92
 script files, 91
 seals, 63, 79
 secondary windings, 13
 security, 26, 71
 selection, 37, 81
 self-organising map, 44
 sensor, current, 41
 sensors, 45, 95

- smart, 46
- virtual emission, 45

 series inductor/autotransformer, 20
 series resistors, 20
 service, 56, 58, 76, 78, 138
 service cabinet, 51
 service downtime, 26
 shaft, 9–10, 26, 28, 30–31, 58, 62, 76–77, 79

- main motor, 62
- rotating, 31
- vertical drive, 51

 shaft deflection, 34
 shaft rotational axis, 29–30
 shaft surfaces, 79
 shaft train, 74
 shims, 79
 shock pulses, 40
 Short circuit, 33, 35, 38
 short-circuited contacts, 78

- faulty, 78

 Short-circuit winding fault, 33
 shorting contactor, 65, 68
 shorts/terminals, 55
 showed good agreement, 48
 sideband, lower, 28
 sight window, 63
 signal contact, 59
 signal processing, 95

- image, 45

 signals, 39, 44, 59

- electromagnetic, 47
- generating, 106
- measuring, 51
- stabilize voice, 45
- time domain, 40

 signal spectra, 48
 silky gloss, 58
 simulations, 4–5, 41, 80, 101, 104

- aircraft component, 45
- flight path, 45

 single-phase basis, 13
 single phasing fault, 35–36
 Single phasing fault motor windings, 35
 single-quadrant operation sufficing, 51
 Sleeve bearings, 62

- lubricated, 62

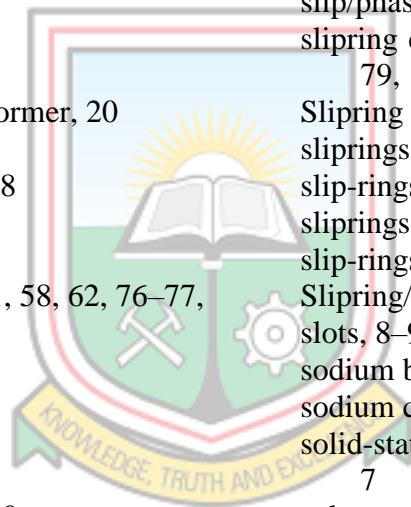
 sliding contact, 55
 sliding faces, 63
 slip/phase, 13
 slipring compartment, 54, 56, 58, 76–77, 79, 143
 Slipring Induction Motors, 51, 107
 sliprings, 55–61, 77, 79
 slip-rings, 6, 10
 sliprings, bronze, 55
 slip-rings, revolving, 10
 Slipring/Wound rotor, 74
 slots, 8–9, 61
 sodium borate, 66
 sodium carbonate, 66
 solid-state variable-frequency converter, 7
 solvents, 58–59
 solvent vapour, 58
 Source, 3, 52, 54–56, 64, 66–67, 73–74, 77–78, 89
 Sources of induction motor faults, 26
 spark-free commutation, 55
 spatial vector sum, instantaneous, 40
 specify target set, 154–59
 specify training set, 154–59
 speech compression, 46
 Speech recognition, 46
 speed control, 10, 21

- continuous, 7

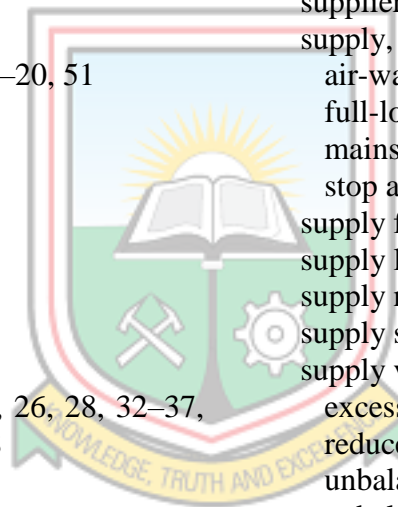
 speed control range, 20
 speed range, 19, 51–52, 54–56, 66–67

- wide, 7

 speed requirements, 18
 speeds



low, 15
 lower, 20
 speed torque characteristics, 24
 spiral grooving, 60
 spiral type grooving, 55
 squared error, 90, 92, 96–97, 99–100, 106
 squirrel cage induction motor, 16, 27
 squirrel-cage induction motor type, 6
 squirrel cage type, 19
 star, 17–18, 78
 star-delta, 15, 17
 start, 19–20, 36, 48, 65, 73, 78, 94
 new, 65
 starter, 64–66, 68, 78
 starting, 10, 15–18, 58, 64–65, 74, 78
 starting characteristics, 64
 starting currents, 15
 large, 16
 starting methods, 20
 starting period, 16, 28
 starting torque, 15–17, 19–20, 51
 generating high, 20
 good, 25
 start motor, 74
 start position, 65
 states, steady, 48
 stationary, 58, 64
 stationary brushes, 9, 55
 associated, 10
 stator, 2, 6, 8–15, 17, 21, 26, 28, 32–37, 40–41, 47–49, 77–78
 primary, 13
 special, 21
 stationary, 7
 switch rotor, 74
 stator coil, 34
 stator construction, 8
 stator copper losses, 14
 stator core, 33
 stator current/phase R1, 13
 stator faults, 2, 32–33, 40–41
 diagnose, 40
 stator frequency, 23
 stator laminations, 34
 stator magnetic field, 12
 stator magnetic flux, 11
 stator/phase, 13
 stator-phase, 47
 stator phases, 47
 stator switch, 76
 stator voltage, 24
 residual, 74
 stator windings, 17, 33, 95
 steel, 55, 71
 steel foundation, 77
 steel frame, 8
 steps, first, 43, 82
 stock trading, 46
 storage, 61, 76, 79
 story brass rods, 65
 stresses, 32–33, 35, 37
 extra, 27
 mechanical, 27, 34, 73
 non-uniform metallurgical, 27
 stresses stator faults, 32
 structure, actual, 47
 subject, 25, 74
 subtraction, 28, 30
 supplier, 76, 79
 supply, 7, 12, 15, 37, 65, 70, 73, 78
 air-water heat exchanger water, 74
 full-load, 36
 mains, 78
 stop air-water heat exchanger water, 74
 supply frequency, 11, 18, 36
 supply line, 36
 supply network, 15
 supply system, 35
 supply voltage, 16
 excessive, 16
 reduced, 16
 unbalance, 26
 unbalanced, 34
 supply voltage transient, 34
 surfaces, 28, 31–32, 58, 79, 110
 actual bearing, 76
 bare, 64, 76, 79
 contact, 58, 60
 gap, 8
 inner, 28, 64
 slipping contacts, 55
 smooth, 58
 stator-inner, 26
 switch, 17, 71, 74
 level limit, 66
 switch standstill heating, 74
 symptoms, 32, 39
 synchronous, 11–12, 15, 18, 20–21, 23–24, 36–37
 new, 21

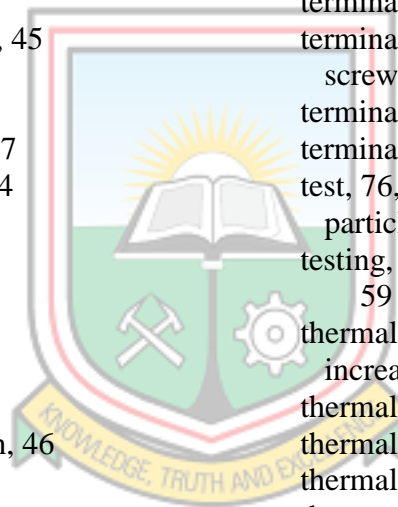


synchronous machines, 55
 Synchronous Speed, 21
 system, 5, 39–40, 45, 49, 64, 71, 73–74
 adaptive neural fuzzy inference, 48
 advisory, 46
 aircraft control, 45
 automatic guidance, 45
 based fuzzy inference, 49
 brush-lifting, 74
 cascade drive, 56
 chemical process, 46
 connected, 13
 customer payment processing, 46
 data acquisition, 39, 95
 electrode control, 66–67
 energy recovery, 51
 high availability, 39
 input parameter, 48
 installed, 72
 long distance telephone, 45
 moving electrode, 65
 new, 72
 online fault diagnosis, 47
 plain bearing cooling, 74
 risk analysis, 45
 routing, 46
 safe, 47
 supplying, 70
 utility, 35
 vision, 46
 visual quality inspection, 46
 winding insulation, 61
 systemic procedures, 80
 system monitoring, 39–40, 47
 System-On-a-Chip (SOC), 48
 system parameter degradation, 49
 system states, 39

T

tachogenerator, 51
 tank, 64, 71
 tansig, 89, 100, 155, 157–59
 tansigmoid activation function, 105
 tapping, correct, 18
 target outputs, 92
 target tracking, 45
 target value, 102
 technicians, 38
 techniques, 39–41, 47–48, 50
 advanced, 47

current signature analysis, 49
 deterministic, 50
 intelligent, 41
 isolated, 48
 magnetic pendulous oscillation, 50, 109
 power decomposition, 41
 signal processing, 41
 temperature detectors, 62
 temperatures, 32, 35, 58, 63, 65, 71, 75,
 84, 96, 101
 air circulation, 51
 ambient, 26, 34
 current increasing, 37
 excessive, 31–32
 high, 1
 measure, 77
 power and winding, 4, 83
 record, 63
 terminal boxes, 79
 terminals, 22, 78
 screw, 69
 terminals T1, 23
 termination, 81
 test, 76, 82, 89, 94, 133
 particle count, 73
 testing, 41, 43, 46, 89, 91–92, 100, 154–
 59
 thermal, 27, 32, 61
 increased, 73
 thermal damage, 61
 thermal overloading, 34
 thermal stresses, 27, 34
 thermometer, 63, 71
 three-phase, 17–18, 35, 47
 insulated, 9
 three-phase currents, 11
 three-phase fault, 34
 three-phase induction motor, 11, 15–16,
 35, 40, 48–49, 108–9
 three-phase motors, 35–36
 three-phase supply lines, 35
 three-phase voltage, 10
 threshold term, 42
 thumb rule, 34–35
 time domain, 50
 time phase, 36
 time schedule, 74
 top sticks, 34
 torque, 7, 11–12, 14, 18–20, 26, 28, 35–
 37



electromagnetic, 40, 47
 fundamental, 36
 harmonic, 36
 high, 16
 maximum, 16, 19–21, 24
 rated operating, 18
 running, 19
 stall, 18–19
 total motor, 36
 zero, 18
 torque control, 64
 direct, 25
 torque equation, 19
 torque fluctuations, 74
 torque production, 20
 torque requirement, 19
 track, 56, 59
 train, 80, 82, 84, 92, 94, 154–59
 train ANN, 5
 trainbr, 156–57, 159
 training, 42–43, 49, 86, 88, 91–92, 96,
 100, 102, 105, 154–59
 stops, 89, 102
 training algorithms, 5, 88, 96, 105
 training correlation coefficient, 102
 training data, 42–43, 89, 102
 training data set, 88
 training function, 86, 91–92
 training process, 88
 training set, 43–44
 trainlm, 92, 154–55, 158
 trainParam.epoch, 92
 trainParam.Ir, 92
 transferFcn, 158–59
 transfer function, 86, 89, 91, 101–2
 transformer, 6, 13, 135
 current, 41
 feedback converter, 51
 rotating, 6, 13
 transient, 34, 50
 translation, real-time, 46
 transportable measuring instrument, 63
 transportation, 6, 46
 TTF (Time To Failure), 49
 turbidity, strong, 63
 two-pole arrangement, 23
 two-pole structure, 23

U

unbalance, static, 30

unbalanced stator currents, 26
 undetected error auditing, 39
 units, 42, 44, 48, 72, 95
 computational, 42
 gear pump, 71
 hidden, 42
 interconnected adaptive processing, 42
 signal conditioning, 41
 unit volume, 73
 user interfaces, 91

V

vacuum, 58, 61
 vacuum tank, 61
 validating, 89
 validation, 50, 91, 100, 102, 107, 110,
 154–59
 validation performance, 102, 105
 validation sets, 43
 values, 14, 17–20, 24, 36, 43, 73, 87–88,
 100, 102
 computed, 100
 direct-on-line, 17
 initial, 64
 large, 14
 limit, 75
 low, 14
 measured, 101
 optimal, 45, 81
 outlying, 42
 possible, 95
 predicated, 90
 predicted, 101
 required, 18
 small, 14
 valve, reducing, 71
 variable selection, 43
 variable selection procedures, 43
 variation, 19, 31, 64, 90
 smooth, 23
 speed, 18, 64
 stepped, 21
 vector, current, 41
 vehicle scheduling, 46
 velocity, relative, 12
 vibration, 26, 28, 32, 40–41, 71, 75, 106
 excessive, 26
 measure, 77
 measure machine, 63
 vibration amplitude, 40

vibration analysis, 48
 vibration faults, 40
 vibration measurement, 77
 vibration parameters, 49
 vibration sensors, 63
 fitted, 77
 vibration spectrum, 40
 viscosity, 72
 kinetic, 73
 visualize activations, 91
 voltage, 10–12, 18, 20, 23–24, 26, 37, 39,
 52, 54–56, 66–67, 78, 95
 excessive, 15
 induced, 12, 31
 initial, 18
 low, 68
 lower, 19
 mains, 78
 medium, 68
 rated, 28, 35
 reduced, 18, 20
 transient, 34
 voltage control, 20
 voltage level, 37
 given, 19

voltage unbalance, 34

W

warranty activity analyzers, 45
 Wavelet techniques, 106
 wear, 28, 32, 57–59, 70, 73, 75, 77–78
 excessive, 32
 weights, 42, 44, 52, 54–56, 66, 76, 81, 86–
 88, 91
 network's, 44
 synaptic, 86
 weight updates, 81
 winding resistanc, low, 136
 winding resistance/phase X1, 13
 winding short circuit fault, 49
 winding temperature limit, 35
 winding temperature readings, 96
 winding temperatures, 4–5, 34–35, 48, 50,
 80, 82–83, 102
 winding temperature signals, 95
 winding temperature values, 102
 workhorse, main, 38
 wound, 6, 9–10, 22
 wound-rotor, 9

